THEORETICAL AND EXPERIMENTAL INVESTIGATION OF WALL-CONTROL BLASTING METHODS

SEYED HASSAN KHOSHROU

Department of Mining and Metallurgical Engineering

McGill University

Montreal, Canada.

A thesis submitted to the Faculty of Graduate Studies and Research
in partial fulfillment of the requirements for the degree of
Doctor of Philosophy.

February, 1996

ISBN 0-612-12401-0

In the name of God
the Compassionate, the Merciful

To the memory of my young mother
FATIMA ZAHRA,
Symbol of kindness and resistance against oppression

ABSTRACT

Overbreak and damage to rock walls is one of the most serious problems encountered in blasting operations. Several techniques have been developed to control the undesirable effects of rock blasting. These techniques are collectively known as wall-control blasting methods.

The stress distribution around pressurized holes has been numerically evaluated, in order to analyze the mechanism of wall-control blasting methods. The effect of blast geometry and the role of discontinuity on this stress field has also been studied in detail. The results obtained by numerical modelling have been verified by controlled blasting experiments, and further supported by analysis of existing roadcuts on a large scale.

It was found that the mechanism of wall-control blast can be explained by the collision and superposition of the stresses between the holes. A narrow fracture zone between the holes was produced by tensile stresses on the centreline. It is neither necessary nor realistic to assume onset of fractures at the midpoint between holes by reinforcement of the stresses from each hole.

The analysis shows that a burden can be defined as being infinite when the ratio of that to the spacing is greater than unity. For pre-split blasting (infinite burden) in an isotropic and homogeneous material the hole separation could range up to 15 borehole diameters. The decoupling ratio between the explosive charge and the borehole diameter should be smaller than 0.5. This ratio would generally be between 0.2 and 0.3 for pre-splitting (infinite burden), and between 0.3 and 0.4 in the presence of a free face.

A discontinuity parallel to the free face and located at the back of the holes causes high stress levels between the discontinuity and the boreholes, resulting is a shattered zone in this region. The presence of a similar discontinuity at the front of the holes leads to considerable overbreak and development of an undamaged "hump" of rock between holes. The effect of a discontinuity oriented normal to the centreline at the midpoint between holes has minimal effect on the blast results. As the angle of the discontinuity with the free face decreases from 90°, the damage zone between the holes and the discontinuity increases, and the shape of the final wall changes from a smooth face to a corrugated shape. A closed-discontinuity or an open discontinuity cemented with strong filling materials has little effect on the results of the blast. However, as the width of the discontinuity increases, the size of the damage zone also increases. An open discontinuity, 50 mm wide or more, plays a role similar to a free face.

In roadcut blast design, hole deviation is a key parameter in determining the quality of the face. However, consistent hole deviation in the same direction has minimal effect on the result of the blast. This type of deviation is usually associated with bedded rocks, with alternating bands of soft and hard rock on the face. The degree of deviation is dependent, amongst other factors, on orientation, thickness, frequency and the position of these bands.

RÉSUMÉ

Durant les opérations de dynamitage, les problèmes rencontrés les plus sérieux sont les dommages causés aux parois et le bris de profil. Plusieurs techniques ont été développées pour contrôler les effets indésirables du dynamitage des roches. Ces méthodes sont connues sous le terme "méthodes de sautage pourle contrôle de parois".

Une évaluation numérique de la distribution des contraintes autour de trous sous pressurion a été réalisée, dans le but d'analyser le mécanisme du sautage purle contrôle de parois. Une étude détaillée a été entreprise sur l'effet de la géométrie du dynamitage ainsi que le rôle de la discontinuité sur le champ de contraintes. Les résultats obtenus par modélisation numérique ont été vérifiés avec l'aide d'essais de dynamitage contrôlé et confirmés par une analyse à grande échelle des coupes de roc existants le leng des chemins.

Le mécanisme de dynamitage à contrôle de parois s'expligue par la collision et la superposition des contraintes entre les trous. Une zone de fissuration étroite entre les trous fut produite par les forces en tension sur la ligne centrale. Il n'est ni nécessaire ni réaliste de supposer un début de fissuration à mi-distance des trous causé par le renforcement des contraintes de chaque trou.

L'analyse démontre qu'un fardeau peut être considéré comme étant infini lorsque le ratio entre celui-ci et la distance est supérieur à l'unité. Dans le cas d'un dynamitage de tir à deux temps (pour un fardeau infini) dans un matériau isotropique et homogène, la séparation entre les trous de forage peut atteindre 15 fois le diamètre du trou. Le rapport de découplage entre le diamètre de charge explosive et le diamètre du trou de forage devrait être inférieur à 0.5. En général, ce ratio devrait se situer entre 0.2 et 0.3 pour le tir à deux temps (fardeau infini) et entre 0.3 et 0.4 en présence d'une face libre.

Une discontinuité parallèle à la face libre et située à l'arrière des trous cause des niveaux de contraintes élevées entre la discontinuité et les trous de forage. Une zone fragmentée en résulte dans cette région. La présence de discontinuités similaires à l'avant des trous de forage entraine des bris hors profile considérables et le développement d'un a'amas' de roche non endommagée entre les trous. L'effet sur les résultats de dynamitage d'une discontinuité normale à la ligne centrale et située à mi-distance des trous, est minimal. Lorsque l'angle de la discontinuité diminue (en partant d'un angle de 90° par rapport à la face libre), la superficie de la zone endommagée augmente entre les trous et la discontinuité. La forme finale du mur change d'une surface lisse à une forme ondulée. Une discontinuité fermée ou une discontinuité ouverte et cimentée avec des matériaux de remplissage rigides ont peu d'effets sur les résultats du dynamitage. Toutefois, si la largeur de la discontinuité augmente, la taille de la zone endommagée augmente aussi. Une discontinuité ouverte, de 50 mm de largeur ou plus, joue un rôle similaire à une face libre.

Lors de la conception par dynamitage des coupes de chemin, la déviation des trous est un paramètre important lorsqu'on détermine la qualité d'une face de roc. Toutefois, une déviation constante des trous dans la même direction a un effet minimal sur le résultat du dynamitage. Ce type de déviation est souvent associé aux litages de bandes alternantes de roches molles et dures sur la face. La déviation dépend, entre autres, de l'orientation, l'épaisseur, la fréquence et la position de ces bandes de roches.

ACKNOWLEDGMENTS

This research could not have been completed without help and contribution from many persons and organizations. I am specially indebted to my supervisor, Prof. B. Mohanty, for his most helpful criticisms, keen interest, continued guidance and many useful discussions and suggestions throughout the course of this work. I am also grateful to Prof. F.P. Hassani, Director of Mining Program for his valuable support and guidance during the conduct of this thesis.

Special thanks are due to ICI Explosives Canada, and the MacMasterville Technical Centre in particular, without whose support in site selection, measurement of the explosive properties, and the conduct of the experimental program, this work could not have been completed.

I wish to express my sincere and deep gratitude to Profs. H.S. Mitri, L. Lessard, J.A. Nemes and Mr. M.M. Shokrieh for sharing with me their knowledge on numerical modelling and allowing me to use the computer facilities, especially the *e-z tools* and *I-DEAS* codes.

The author wishes to express his deep appreciation to Prof. M. Scoble for encouraging me to examine existing large-scale wall-control blasts along roadcuts, and Y.C. Lizotte for his ideas on blast-induced damage in rocks.

The investigation on the roadcuts was made possible only through the active support of Mr. A. McBean, Geologist, Material and Research Division, and Mr. R.R. Keene, Traffic and System Engineer, Agency of Transportation, State of Vermont, U.S.A.

I would like to take this opportunity to thank my colleagues, especially A. Sadri, U. Prasad and P. Guevremont of the Department of Mining and Metallurgical engineering, and A. Kheyroddin, M. Shayanfar and M. Nassiri of the Department of

Civil Engineering. Thanks are also due to P. Mujumdar and M. Rosati, for facilitating administrative requirements and complying with my frequent requests in this regard, all these years.

I thank the Ministry of Higher Education of the Islamic Republic of Iran for financial support, and to Dr. S.R. Hosseini for his keen interest in the progress of my work.

Finally, I would like to acknowledge my indebtness to my family: my wife, Maryam Islamiat, my children Hossein, Mohammad and Zahra, and my parents and parents in-laws. Their understanding, support and patience sustained me throughout this work.

Table of Contents

CHAPTER 3 Wall-Control Blasting Methods

CHAPTER 4 Analysis of Wall-Control Blasting Methods

CHAPTER 5 Numerical Modelling

CHAPTER 6 Experimental Investigation

CHAPTER 7 Investigation of Wall-Control Blasts Along Roadcuts

CHAPTER 8 Conclusions

LIST OF FIGURES

Figure

Figure

Figure

Figure

Figure

Figure

Figure

Figure

Figure

Figure

LIST OF TABLES

Table

Table

CHAPTER 1

INTRODUCTION

1.1 GENERAL INTRODUCTION

Today, the use of wall-control blasting methods in mining and construction industry has become an integral practice in most excavation operations. Several techniques have been used to control overbreak at the limits of blasts. For many years, line drilling was the only method used to reduce overbreak. Cushion blasting, smooth blasting and pre-splitting are latter evolution of this method. This chapter gives a general overview of wall control blasting methods and the relative merits of these techniques. The objective and the structure of the thesis are also presented.

In recent years, the trend has been towards higher bench height, larger diameter blastholes and lower or cheaper explosives. Reduction in mining cost and increased production are the outcome of this approach. However, large diameter borehole blasts result is increased concentration of energy in the blast area which can create serious problems for final pit walls and damage the structures. Buildings around the mines, structures close to mining operations and final pit walls in open pit mines or in roadcuts must remain unaffected by a blast. The slope angle of an open pit has important economic consequences and is strongly linked to the stability of the slope and the geological characteristics of the rock. The stability of rock slope is affected directly by stresses induced by blasting operation. Overbreak and damage to structures and rock walls can also lead to safety problems.

In addition to safety problems and instability of rocks in the final pit walls, considerable losses can also be incurred from damaged structures and buildings in the vicinity. Any instability requires roof or wall support as well as face maintenance or back filling in the damaged regions. This may lead to a lowering of the slope angle, which would make certain mining operations not economically viable.

The best approach is to minimize or control this undesirable effects by accurate blast design, particularly close to vulnerable areas. This can be achieved by special techniques, which are known collectively as "wall-control blasting methods".

1.2 WALL-CONTROL BLASTING

Several wall-control blasting techniques have been developed to control fracturation of intact rock beyond the limits of excavation. These methods are based mainly on trial-and-error and field observations. The techniques employed are variously known as line drilling, cushion blasting, pre-splitting, buffer blasting and smooth blasting. Comprehensive pre-split blast designs were introduced on a large scale by Paine, Holmes and Clark in 1961. They presented a theoretical treatment of this phenomenon based on the superposition of stress wave at the midpoint of the centreline. Langefors and Kihlström (1978) described some of the principal parameters of pre-splitting and demonstrated the formation of cracks between holes in model scale blasting. Mathias (1965) studied the mechanism of pre-splitting in the laboratory with models of plexiglas and marble. The pre-splitting process based on the action of stress wave was investigated by Aso (1966). Kutter (1967) discussed the mechanism of pre-split blasting based on the interaction between stress wave and gas pressure. Sanden (1974) has attempted to explain the pre-splitting process theoretically on the basis of a simple pressurized borehole. Based on a series of tests on homogeneous materials and rock in the laboratory, Worsey (1984) has presented the effect of discontinuity orientation on pre-splitting. However, in spite of these series of research, the design of wall control-blasting still relies largely on empirical approaches. Even the various mechanism proposed do not always have a unifying physical basis.

1.3 OBJECTIVE OF THE STUDY

1) To analyze the theoretical bases of wall-control blasting method.
2) To evaluate the critical parameters of wall-control blasts, such as: borehole diameter, spacing, decoupling, explosive types, and properties of rockmass, and especially the role of discontinuities.
3) To verify the theoretical predictions in terms of fracture length, intensity and direction at selected sites.
4) To correlate theoretical predictions and experimental results with those observed in large-scale blasts along roadcuts.

1.4 STRUCTURE OF THE THESIS

This research program consists of two main parts. The first part deals with an investigation of the mechanism of wall-control blasting methods. This part analyzes the stress distribution around a single hole and between two holes in the presence of discontinuities. The second part consists of field investigations carried out to verify the theoretical predictions at two selected sites. This section is designed to study the length as well as intensity and direction of fracture in the presence of discontinuity, with different borehole pressure conditions and various blasting geometries. The relation between blast geometry, location of the final face and pre-existing fractures and the later effects on the blast results as seen on the final face, has also been investigated for a number of existing roadcuts.

This Thesis consists of seven chapters. The chapters have been structured somewhat independently, so as to enable the reader to study the topic of interest without having to refer extensively to other chapters. For this reason, there is some overlap in the content of some of the chapters.

Chapter one gives a general view of the development and the quality of various wall-control blasting methods. The objective and outline of the research program is also described.

Chapter two presents the important parameters in rock blasting and the process of rock breakage after initiation of an explosive charge in the borehole. The properties of rock, properties of explosive, and the process of the rock fragmentation are explained in detail.

Chapter three is a review of previous and current practices on wall-control blasting methods. Different methods of perimeter blasting are described in detail. The results of a survey of case studies from several mines in North America are discussed and compared with the results obtained in earlier studies.

Chapter four reviews the mechanism of wall-control blasting methods. The results of several research approaches are discussed in this chapter.

Chapter five presents the main theoretical thrust of the present work. The role of stress field around single and multiple pressurized holes in the presence of discontinuities is evaluated in this chapter. In the numerical study, a discontinuity is represented by a weak plane of finite width which is filled by a material of greatly reduced stiffness compared to the host rock. The various conditions investigated in this study are the following: i) the effect of a free face, ii) narrow weak plane parallel to the free face, iii) fixed weak plane for two different burdens, iv) weak plane of various widths, v) weak plane normal to the free face for a fixed burden, and vi) inclined weak plane.

Chapter six is devoted to the experimental part of this research. The main purpose of the chapter is to give an overview of how discontinuities and blast geometry affect the results of wall-control blasts. The emphasis is on highlighting the importance of orientation of the discontinuities relative to the centreline or the final rock surface as well as the width and the distance of these from borehole wall.

Chapter seven presents the results obtained from a field study on seventeen roadcuts along two highways. The relationship between the rock properties and rockmass structures with the results of blast as well as hole deviations are elucidated in this investigation.

Chapter eight presents overall conclusions, a claim for originality of the research and recommendations for future work.

CHAPTER 2

ROCK BLASTING

2.1 INTRODUCTION

Blasting process is complex because it involves many areas of science consisting of chemistry, physics, rock mechanics and material science. During past several decades, many blasting theories have been developed. Despite continuing effort of researchers, advancement in explosive science, numerous laboratory and field investigations, considerable gaps still exist in applying these theories to many practical blasting situations. The most important factors which influence blast results are: properties of the rock being blasted, properties of the explosive and the blast geometry.

2.2 ROCK

Rocks are classified and identified by their mineral components and the processes that formed the minerals. Three main types of rock are recognized:

a. Igneous: formed by solidification of molten magma.

b. Sedimentary: formed by alteration and compression of old rock debris or sediments on earth's surface.

c. Metamorphic: formed by alteration of existing rock by intense heat or pressure.

These three types of rock can be divided into various categories based on their strength properties, Jumikis (1983), Table 2.1.

2.2.1 Properties of Rock

The properties of rock are key parameters in rock fragmentation by explosives. These parameters vary from one mine to another and also in different parts of the same mine. Geology, material strength, seismic properties, frequency and orientat . of structural discontinuities must be considered and evaluated by suitable field or laboratory tests. In situ rock properties depend on the characteristics of each mineral component and the presence of interstices, joints, faults and bedding planes. Consequently, laboratory results on rock samples are considered only the first line of description of in situ rock. The principal rock properties that influence blasting are shown in Table 2.2.

2.2.1.1 Strength

Strength is the resistance of a material to applied force. The strength of rock largely depends on the nature of mineral composition. It can be defined only when all strength-factors such as, intensity and duration of load, size of rock samples, pressure and temperature, pore-water pressure, and failure criteria are known. Compressive, tensile and shear strength are three types of rock strength which can be measured in a variety of ways under static and dynamic conditions. Generally, rocks have very low tensile strength, moderate shear strength and high compressive strength. The tensile strength of rock is about 10 to 15% of its compressive strength (Jaeger and Cook, 1979). Table 2.3 shows compressive and tensile strength for different rocks (Szechy, 1966; Framer, 1968).

It should be noted that rocks have different behaviour under dynamic loading compared to static loading. The idealized behaviour of rock under different rates of loading is illustrated in Fig. 2.1. It can be concluded that the behaviour of rock under dynamic load is more elastic than static load, and the dynamic strength of rocks is greater than the static strength. The area between loading and unloading curves is proportional to the amount of energy which is dissipated in the body during a cycle of loading and unloading. This energy is utilized to produce plastic deformation and internal friction during loading. The dynamic strength of a material is a function of the loading rate, the duration and the magnitude of the load, therefore, it is very difficult to calculate an exact dynamic strength value for a material. Rinehart (1965) have shown that for most rocks the dynamic tensile strength is about 6 to 10 times greater than the static value (Table 2.4).

2.2.1.2 Modulus of Elasticity

Young's modulus is defined as the ratio of stress to strain in simple compression or tension. If a body is compressed equally from all direction, its original volume will be decreased. The ratio of stress to the fractional change in volume, is defined as *bulk modulus*. The reverse of bulk modulus is described as compressibility. *Shear modulus* is defined as the ratio of shear stress to shearing strain. Weathered and fractured rocks have a low modulus of elasticity, while, rocks with a higher modulus of elasticity are stronger (Table 2.5).

2.2.1.3 Stress waves

Several types of waves are generated when an elastic material is suddenly deformed by explosive action. For a spherical explosive source, these waves propagate spherically outward with diminishing amplitudes from the source point. They can be divided into two categories: Body waves and Surface waves.

Table 2.1 : Classification of rocks based on the uniaxial compressive strength.

Description	Uniaxial Compressive Strength (MPa)	Rock type
Very high strength	> 220	Quartzite, diabase and dense basalt.
High strength	≈110 to ≈220	Majority of igneous rocks; Strong metamorphic rocks; Weakly cemented sandstone; Hard shales; Majority of limestone; Dolomite.
Medium strength	≈55 to ≈110	Many shale; Porous sandstone and limestone; Schistose varieties of metamorphic rocks.
Low strength	≈28 to ≈55	Porous low-density rocks; Friable sandstone; tuff; Clay shales; weathered and chemically altered rocks of any lithology.
very low strength	< 28	

Table 2.2 : The primary properties of rock which affect blasting results.

Strength	Compressive, Tensile and Shear
Structure	Dip, Strike, Jointing systems, bedding planes, Grain size and Orientation
Elastic modulus	Young's, Shear and Bulk
Seismic velocities	P and S waves

Table 2.3 : Compressive, tensile and shear strength for different rocks.

Type of Rock	Compressive Strength (MPa)	Tensile Strength (MPa)	Shear Strength (MPa)
Igneous:			
Basalt	78 - 412	5.9 - 29.4	5.9 - 49.0
Diabase	118 - 245	5.9 - 12.7	5.9 - 9.8
Gabbro	147 - 294	4.9 - 29.4	3.9 - 8.3
Granite	98 - 275	3.9 - 24.5	4.9 - 49.0
Sedimentary:			
Dolomite	14.7 - 245	2.5 - 24.5	2.5 - 6.9
Limestone	3.9 - 245	1.0 - 24.9	1.5 - 49.0
Sandstone	49.0 - 167	19.6 - 24.5	2.9
Shale	9.8 - 160	2.0 - 9.8	2.9 - 29.4
Metamorphic:			
Gneiss	78.0 - 245	3.9 - 19.6	-
Quartzite	85.0 - 353	2.9 - 4.9	-
Slate	24.5 - 196	6.9 - 19.6	-

Table 2.4 : Dynamic and static tensile strengths of different rocks.

Type of Rock	Tensile Strengths of Rocks		
	Static (MPa)	Dynamic (MPa)	Ratio
Bedford Limestone	4.1	26.9	6.5
Yule Marble, "perpendicular to bedding"	2	18.6	9.0
Yule Marble, "parallel to bedding"	6.2	48.3	7.8
Granite	6.9	39.3	5.7
Taconite	4.8 - 7	91	13.0

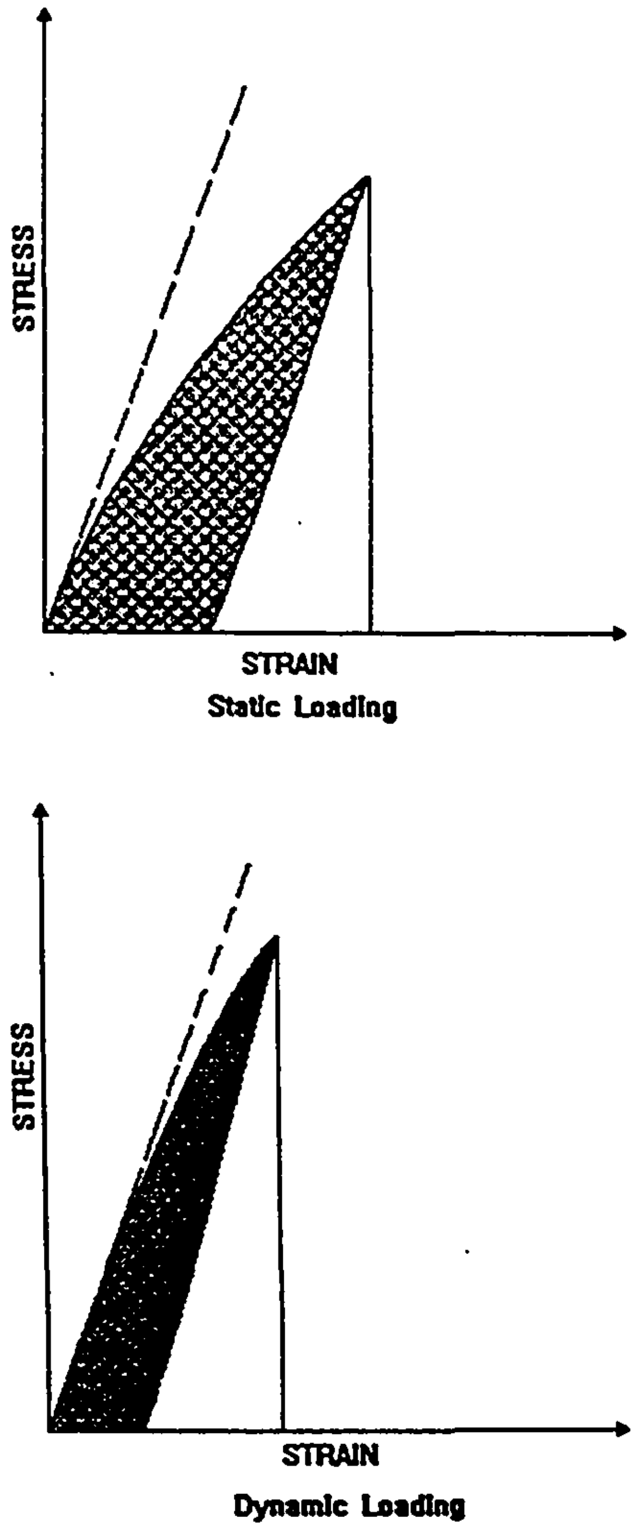

Figure 2.1 : Effect of loading rate on stress-strain behaviour.

Body waves propagate through the solid medium, and are divided into longitudinal and transverse waves. Surface waves travel along the surface or the interface between the individual layers. The most important surface waves are Raleigh waves and Love waves.

The longitudinal, transverse and surface waves travel with different velocities. In rock blasting the body waves are important at near distance while the surface waves become important at far distance from the centre of explosion.

If the direction of particle motion is parallel to the direction of propagation, the wave is called 'longitudinal'. The particles in the path of such waves move backward and forward along the line of propagation. Longitudinal waves are also referred to as compressional (compression/tension), dilatational, primary or P waves. The speed of propagation of the longitudinal waves is higher than the other waves, and can be determined by:

$$V_p = \left(\frac{\lambda + \mu}{\rho}\right)^{\frac{1}{2}} \tag{2.1}$$

In which V_p is the velocity of P wave, ρ is density of rock and λ and μ are Lame's constant and defined as:

$$\lambda = \frac{\nu E}{(1+\nu)(1-2\nu)} \qquad \mu = \frac{E}{2(1+\nu)} \tag{2.2}$$

Where E is the modulus of elasticity and ν is Poisson's ratio.

Modulus of elasticity is an important parameter which control the velocity of seismic waves in rocks.

Table 2.5 : Dynamic and static Young's and bulk modulus of several rocks (Sutherland, 1963).

Rock Type	E, "Dynamic" (GPa)	E, "Static" (GPa)	G, "Dynamic" (GPa)	G, "Static" (GPa)
Quartzite	87.5	66.2	40.4	29.9
Conglomerate	78.0	71.0	38.1	31.0
Conglomerate	70.3	73.4	34.6	30.3
Schist	87.4	67.6	37.0	26.9
Quartz carbonate with Sulphide bands	111.5	84.1	48.6	35.9
Quartz-sericite-carbonate	90.0	93.8	40.9	35.2
Conglomerate	86.0	74.5	37.1	31.7
Sandstone	26.3	25.5	11.6	9.7

If the direction of particle motion is normal to the direction of propagation, the wave is called 'transverse'. These waves are also known as distortional, shear, secondary or S waves. Transverse waves tend to change the shape of material while also compressing it. The velocity of propagation of S waves is slower than that of P waves, and can be expressed as:

$$V_s = \left(\frac{\mu}{\rho}\right)^{\frac{1}{2}} \tag{2.3}$$

In which V_s is the velocity of S wave and μ is the rigidity or shear modulus.
P and S waves are also called body waves, because they travel through the body of solid materials. The relationship between the velocity of primary, shear wave and Poisson's ratio can be described as:

$$\frac{V_p}{V_s} = \sqrt{\frac{2(1-\nu)}{1-2\nu}} \tag{2.4}$$

2.2.2 Rockmass Classifications

Many attempts have been made to classify rockmass and quantify experimental results from rock excavation. Consequently, several rockmass classification systems have been developed to assess rockmass conditions (Terzaghi, 1946; Deere 1964; Wickham et al., 1979; Bieniawski, 1979, 1978, 1976; Barton, 1974).

The Q classification system, Barton (1974), is based on the study of more than 2000 tunnels in Scandinavia. The value of Q is defined by:

$$Q = \frac{RQD}{J_n} \times \frac{J_r}{J_a} \times \frac{J_w}{SRF} \tag{2.5}$$

in which

RQD/J_n = block size

J_r/J_a = inter-block shear strength ($\approx \tan\phi$)

J_w/SRF = active stress

Where RQD is rock quality design, J_n is joint set number, J_r is joint roughness number, J_a is joint alteration, J_w is existence of water in the joint and SRF is stress reduction factor.

In the Geomechanics Classification System, RMR, the following six parameters are considered most significant in the behaviour of rockmass, Bieniawski (1976). The value of RMR is calculated by the algebraic sum of these six properties' rating, i.e. uniaxial compressive strength of intact rock, RQD, rock quality design, spacing of joints and bedding, orientation of joints, condition of joints and ground water inflow. However, these rockmass classification systems, if not all, are basically developed to quantify rockmass behaviour for preliminary design of support requirements for underground excavations or slope stability. There is no quantitative classification system which defines the ease with which rocks are fragmented in blasting and any relation between the properties of rockmass and blast geometry or energy of explosives.

2.3 EXPLOSIVES

2.3.1 Elements of Explosives

The use of explosives has a long history in the development of Chinese fireworks, about 2000 years ago. Gunpowder or black powder was described by Roger Bacon, but in thirteenth century Schwarz rediscovered it. It consists of a mixture of potassium nitrate, charcoal and sulphur, intimately ground together. For a safe method of ignition the first safety fuse was invented by William Bickford in 1831.

Nitrocellulose (NC; $C_{12}H_{14}N_6O_{22}$) the first high explosive, was discovered by Pelouze in 1838. Schonbein of Basel discovered guncotton, a mixture of nitric and sulphuric acid on cotton, in 1845-46. After the discovery of Nitroglycerine (NG; $C_3H_5(NO3)_3$) in 1846 by Sobrero, trinitrotoluene (TNT; $C_7H_5N_3O_6$) was discovered by Wilbrand in 1863. The handling of liquid nitroglycerine was very dangerous due to premature detonations.

In 1864, Alfred Nobel found that kieselguhr (diatomaceous earth) absorbed three times its weight in nitroglycerin. This mixture (75 parts of nitroglycerin with 25 parts of kieselguhr) was packed in a paper cartridge by Alfred Nobel and called dynamite. In 1875, "Blasting Gelatine" the first gelatinous explosive, a mixture of 92 percent nitroglycerin and 8 percent nitrocellulose, was invented by Nobel. A wide range of explosives based on these substances has since been developed.

Ammonium nitrate (AN; NH_4NO^3) explosives was discovered by the Swedish chemists Ohlssen and Norrbin, and were first used by Alfred Nobel in replacing some of the nitroglycerin in dynamite. Fertilizer-grade ammonium nitrate with a solid carbonaceous fuel was patented by H. B. Lee and R. L. Akre in 1955. During 1960's, a new composition of ammonium nitrate and fuel oil, ANFO, started to replace dynamite in dry conditions mainly because of its low cost, ease of loading and safety reasons.

In early 1960's, Cook introduced the slurry explosives consisting of ammonium nitrate, water, a high-explosives component and a gelling agent. Slurries were made with a wide range of chemical sensitisers such as: Amine nitrates, TNT, RDX, etc, depending on application, particularly borehole diameters.

In 1970's, emulsion explosives, which consist of oxidizer and fuel, were introduced. These products do not require a chemical sensitiser, and can be used in small diameter boreholes when sensitised with air or microballoons. Mixing emulsion with AN prills or ANFO was a natural evolution which led to the development of Heavy ANFO and AN-doped emulsion (Bauer et al., 1984). These explosives promise to be the most dominant explosives in mining industry in future. Table 2.6 shows the outline of history of industrial explosives (Cook, 1974, 1971; Gregory, 1984; Clark, 1987).

2.3.2 Properties of Explosives

On detonation of a charge the explosive converts into a glowing gas with an enormous pressure within a few microsecond. A detonation wave is a very rapid wave of chemical reaction which travels through an explosive column at supersonic speed, called the detonation velocity. The pressure immediately behind the detonation front range from 5 to 30 GPa. This pressure is called the Chapman-Jouguet (C-J) pressure, which is the stable detonation pressure of the explosive. Due to high temperatures and pressure within the reaction zone the measurement of detonation parameters is very difficult, therefore the conditions prevailing in this zone are not always known in detail. As detonation front progresses, a high intensity shock wave is sent out into the rock.

Fragmentation of rock is influenced by different factors such as blasting pattern, charge geometry, explosive type, delay design, etc . Explosive type is one of the most important factors affecting the quantity as well as the quality of broken rocks (Berry and Dantini, 1981; Mohanty, 1981) . Explosives are defined and classified according to different properties, such as energy, detonation velocity, detonation pressure, density, sensitivity, water resistance, and fumes.

2.3.2.1 Energy

The terms energy, strength and power are usually used in the explosives industry to rate the commercial explosives. Energy can be measured directly calorimetrically or determined theoretically from the composition of the explosive. The theoretical estimation

Table 2.6 : The outline history of industrial explosives.

No	Name	Year
1.	Black powder or Gun powder	before 12th century AD
2.	Mercury fulminate	1800 AD
3.	Nitroglycerin	1845
4.	Nitrocellulose	1846
5.	Dynamite & Blasting cap	1860's
6.	Boosters	1923, 1930
7.	Blasting agents, "Nitramon"	1931
8.	Millisecond delay and MS delay EB caps	1945
9.	Fertilizer-grade AN "FGAN"	1955
10.	ANFO	1960
11.	Slurry	1960's
12.	Emulsion	1970's
13.	Heavy ANFO	1980's

of explosive energy is usually done by computer codes. They are based on the thermodynamics of explosion products. Energy can be expressed on the basis of weight or the volume of explosive based on absolute or relative number. The explosive energy can be described in either absolute or relative terms (e.g. absolute weight strength, AWS; absolute bulk strength, ABS; relative weight strength, RWS and relative bulk strength, RBS).

The absolute amount of available energy per kg of explosive or per cubic meter are given as AWS and ABS respectively. The ratio of the AWS and ABS of an explosive to the AWS and ABS of some standard explosive such as, ANFO, are called relative weight strength and relative bulk strength respectively. Several methods such as, Ballistic mortar, Trauzl lead block test, Cylinder test and Underwater test are used to evaluate experimentally the energy of explosives.

Trauzl test is the oldest form of measuring the strength of explosives. In this test, the explosive is placed in an axial hole in a block of specially cast lead. The explosive energy is determined by comparing the cavity volume before and after detonation of charge (Fordham, 1966).

The ballistic mortar consists of a 3 meter high aluminum pendulum and steel mortar weighing about 360 kg. Ten grams of explosive is detonated in a firing chamber within the mortar, and its energy is measured by the recoil deflection of the ballistic pendulum. This energy is usually compared relative to a standard explosive.

In the cylinder test, the explosive energy is measured by radial motion of the detonated cylinder wall with a streak camera and usually expressed relative to some standard explosive. A 50 mm diameter standard copper cylinder, 30 cm long and 2.5 mm thick, is used for this test. For commercial explosives large-diameter cylinders are usually used at a constant ratio of the weight of explosive to metal.

Another method to calculate the explosive energy is by mean of the Underwater Test. A spherical or short cylindrical charge, usually up to 10 kg, is detonated at a relatively shallow depth, less than 10 m. When an explosive detonates underwater, the surrounding water is strongly compressed and an intense shock wave propagates outward. The water is heated very rapidly to a few hundred degrees. The water close to gas bubble has a large outward velocity and the diameter of the bubble increases rapidly. The high-temperature high-pressure explosion gases continue to expand, but at a slower rate, and the internal bubble pressure decreases. When the gas pressure drops below the equilibrium hydrostatic pressure, the process is reversed and the gas bubble begins to collapse. The time between the detonation and the re-expansion of the bubble (i.e. the bubble period) is a measure of the energy in the explosion gases.

2.3.2.2 Detonation Velocity

The velocity of detonation is the speed of explosive decomposition or the speed of detonation wave which travels through a column of explosive. Commercial explosives have velocities varying from 2000 m/s to 7,800 m/s. The velocity of detonation depends on density and grain size of explosives, its composition and borehole diameter. Detonation velocity usually increases with decreasing particle size and increasing density of explosives.

In commercial explosives, a minium charge diameter is required to detonate the explosives. This diameter is called the critical diameter. When the diameter approaches infinity the limit value is called the ideal detonation velocity. Consequently, the diameter of the borehole affects the reaction rate of commercial explosives. The relationship between charge diameter and detonation velocity is shown in Fig. 2.2.

For ideal explosives the width of the reaction zone is very small; the explosive converts into gas in a very short time and a detonation wave moves through the charge with constant velocity. Most commercial explosives are non-ideal explosives; ideal reaction can be obtained only in very large borehole diameters.

For many explosives the value of curvature radius, R, is about 3.5 times the charge diameter, d, (Johansson and Persson, 1970). With decreasing charge diameter the ratio of R/d falls close to the critical diameter, i.e. R/d=1. As shown in Fig. 2.3, the following equation can be written for the axial detonation velocity, V, and the local detonation velocity at a distance x from the axis, V_x:

$$V_x = V Cos\alpha = V(1 - \frac{x^2}{R^2})^{1/2} \tag{2.6}$$

The velocity of detonation increases with increasing charge diameter. The following relation can be written for the ideal detonation velocity and detonation velocity close to it:

$$V = V_i(1 - \frac{a}{d}) \tag{2.7}$$

Where V is detonation velocity, V_i is ideal detonation velocity, d is charge diameter and a is a constant. For each explosive a and V_i are determined from a diagram of V as a function of 1/d.

Therefore, ideal detonation can be obtained only when the reaction of all materials takes place within a value of R/d less than 1. Several methods such as, continuous resistance wire method, D'Autriche method and streak camera method are used to measure the velocity of detonation.

2.3.2.3 Detonation Pressure

On detonation of explosive, a dynamic pressure is generated in the reaction zone behind the detonation front. The value of this pressure depends on the density and detonation velocity of explosive (Hunter et al., 1993). According to the hydrodynamic theory, the detonation pressure can be calculated by the following equation (Anon, 1987).

$$P_d = P_1 + VOD \times v_p \times \rho \tag{2.8}$$

In which P_1 is initial pressure, P_d is detonation pressure, VOD is the velocity of detonation, v_p is particle velocity developed by explosive reaction and ρ is density of explosive.

The particle velocity is equal to one fourth of detonation velocity and the initial pressure is almost negligible. Therefore, equation 2.8 can be written as:

$$P_d \approx \rho \times \frac{VOD^2}{4} \tag{2.9}$$

A definite relationship exists between adiabatic pressure and detonation pressure (Cook, 1971). The former is defined as the hypothetical pressure that would be generated at a constant volume without heat loss to the surrounding. In most explosives, this relationship is approximately:

$$P_a = \frac{1}{2} P_d \tag{2.10}$$

The "borehole pressure", P_b can be approximated as:

$$P_b = P_a \tag{2.11}$$

Therefore, the borehole pressure can be defined as:

$$P_b = \frac{1}{2} P_d = \frac{VOD^2}{8} \times \rho \tag{2.12}$$

As seen above, for a given explosive with the same composition the energy and detonation velocity increase with increasing density. In bench blasting, when large diameter and deep boreholes (≥ 200 mm and ≥ 10 m) are used, the density at the top and the bottom of the explosive column may not be the same.

Sensitivity is also an important parameter when a borehole is loaded with several cartridges, because a piece of rock, dust or air gap can separate the cartridges from each other. Propagation of steady detonation reaction may be adversely affected by these gaps. The other relevant properties of the explosive are its water resistance and fumes characteristics. Both of these are essentially reflections of proper use of the explosive.

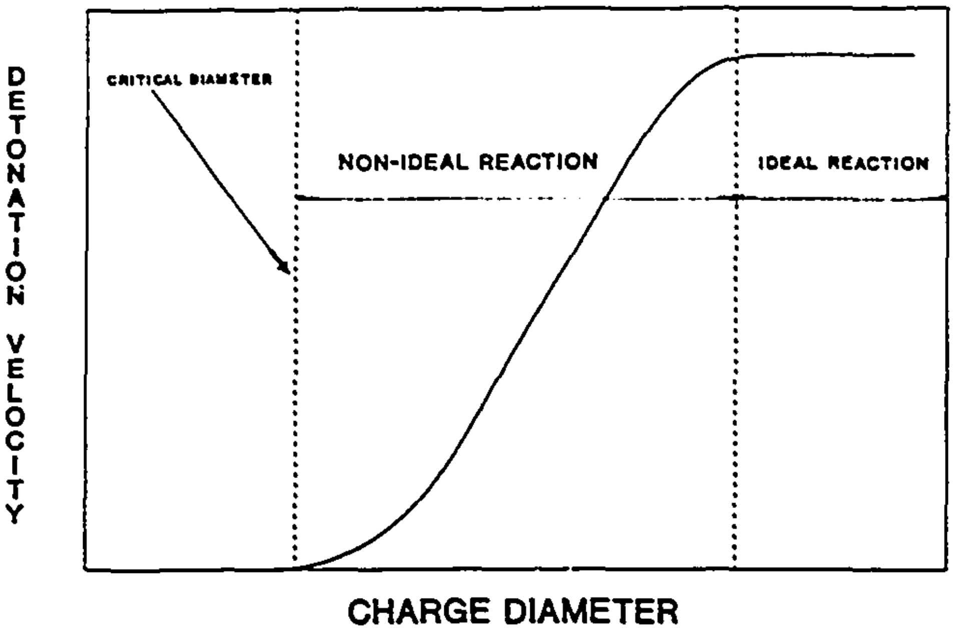

Figure 2.2 : Charge diameter versus detonation velocity for non-ideal explosives.

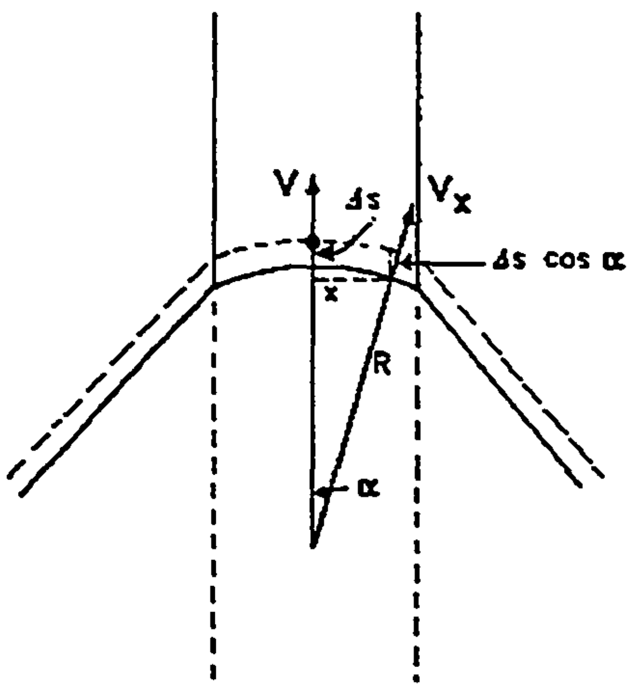

Figure 2.3 : Detonation propagation with curved front (Johansson and Persson, 1970).

2.4 FRAGMENTATION

The fragmentation process is started by the detonation of an explosive in the borehole. The chemical energy of the explosive is liberated, over a very short time, in the form of shock and gas under high temperature (3000° C) and pressure (about 10 GPa). The detonation wave starts at the initiation point and travels through the charge at supersonic speeds accompanied by a very high dynamic pressure (Barker et al., 1984). The velocity of detonation, as stated earlier, depends on density, particle size and composition of explosive, degree of confinement and borehole diameter. The pressure of gases are about 1 to 5 GPa, while temperatures are approximately 2000° to 3000° C.

When the explosive-rock interface is reached by the detonation front, a high intensity shock wave is propagated in the rock. The transfer of energy to the rock is a function of both characteristics of the explosive and the rock, depending on the acoustic impedance of the explosive and rock. In transferring the shock energy to the rock, the relationship between hole diameter and charge diameter (i.e. coupling ratio) plays an important role. The shock pressure on the hole wall decreases rapidly when the charge is decoupled.

Shock wave propagating into the rock crushes the rock in the immediate vicinity of the borehole. The extent of crushing depends on the dynamic properties of the medium, as the magnitude of shock pressure is many times higher than the strength of rock. Compressive, tensile and shear failures result from the energy of wave near the borehole wall. In the area close to the crushed zone the rock behaves as a non-linear elastic solid. The material is compressed by the stress wave front, and radial cracks are propagated from the centre of hole by the tangential component of the stress wave. The resistance of rock to tension is less than compression, therefore, the primary or radial cracks will propagate under the influence of tensile forces. Radial fracture can be created around the borehole up to a distance of about 2 to 6 times the borehole diameter from

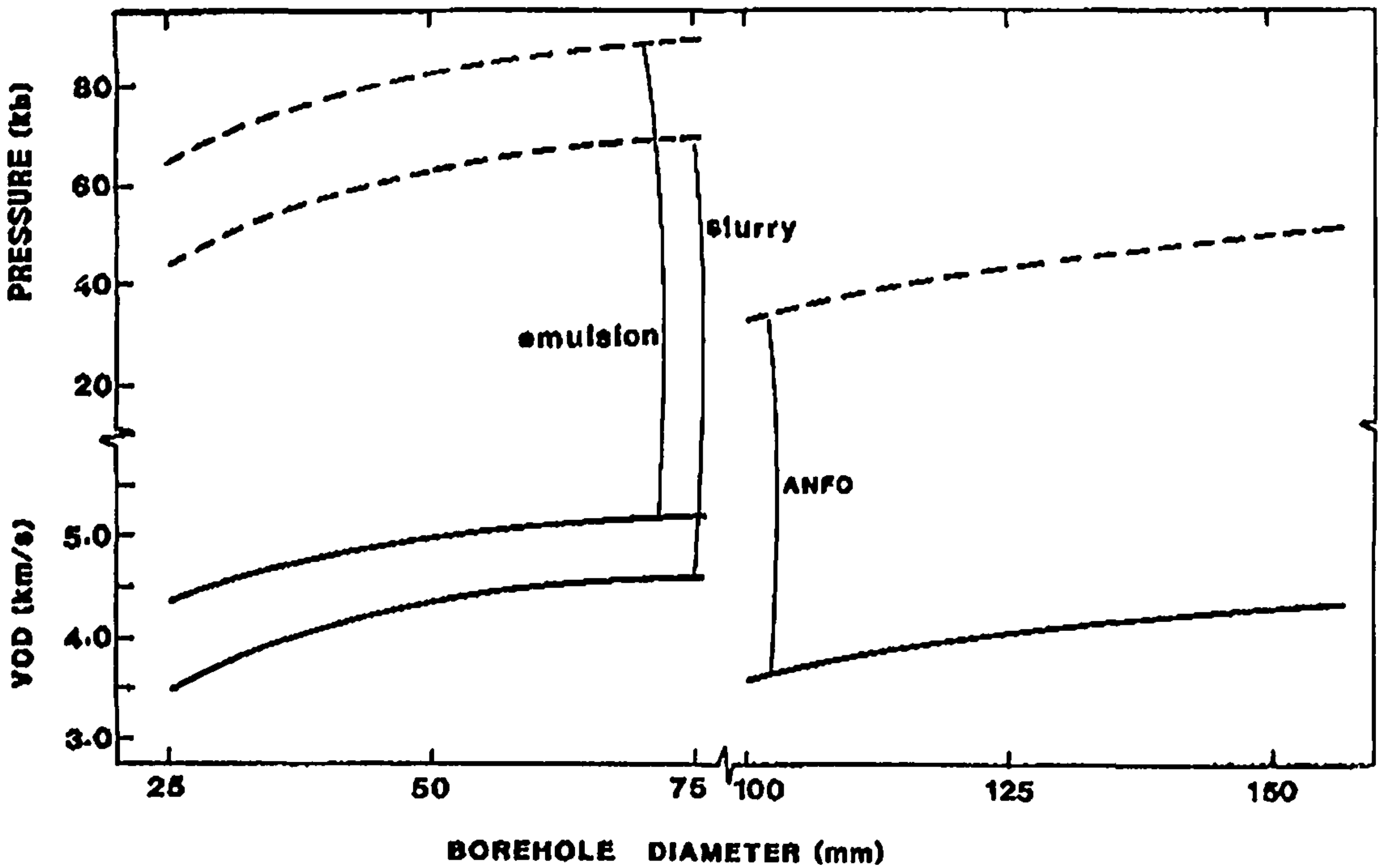

Figure 2.4 : Relationship between borehole diameter, detonation velocity and detonation pressure (Mohanty, 1988).

the centre of the charge (Harries, 1973; Susanszky, 1978; Hagan, 1979; Anon, 1987; Song and Kim, 1995). At a greater distance the stress wave decays to the point where it is transmitted through the rock as an ordinary stress wave.

When the compressive wave reaches a free face or a discontinuity, some part of the energy is reflected back into the media and some is transferred across the discontinuity. The case of reflection is of particular importance. Where a compressive wave meets a boundary the wave is reflected from the interface as a tensile wave. However, when the medium and boundary have similar acoustic impedance properties the wave propagates across the boundary without reflection.

In the fragmentation process these reflections and transmissions depend on the ratio of the acoustic impedance of the material on either side of the interface. The acoustic impedance for the material is defined as:

$$Z = \rho \times V_s \tag{2.13}$$

In which Z is the acoustic impedance, ρ is density and V_s is velocity of stress wave. Where the acoustic impedance of the medium is greater than the acoustic impedance of the boundary, some part of energy is reflected as tensile wave and the remaining transferred across the boundary. In the case of a free face most of the energy will be reflected back as tensile wave. The tensile stress wave can give rise to spalling at the free surface and can also create additional cracks and extend existing ones. In most explosives, the shock wave energy is theoretically limited to only 5 to 15 percent of the total energy of the explosive (Langfors and Kihlstrom, 1978).

The third phase, in the fragmentation process constitutes work done by the high pressure gases in the borehole. In this phase the actual breakage of rock proceeds at a slower pace. Under the influence of the high pressure, high temperature of the explosion gasses, the original borehole expands, radial cracks extended and the gasses penetrate into discontinuity. A pressurized borehole with radius r_b may be considered as a pressurized thick-wall cylinder with infinite thickness without external pressure (Obert, 1966). The radial and tangential stresses at any point on thick-walled cylinder are shown in Fig. 2.5. The theory of elasticity and equilibrium are used to solve the equations, given below:

$$\sigma_r = P_o \frac{(\frac{r_o}{r_i})^2 - (\frac{r_o}{r})^2}{(\frac{r_o}{r_i})^2 - 1} + P_i \frac{(\frac{r_o}{r})^2 - 1}{(\frac{r_o}{r_i})^2 - 1} \tag{2.14}$$

$$\sigma_t = P_o \frac{(\frac{r_o}{r_i})^2 + (\frac{r_o}{r})^2}{(\frac{r_o}{r_i})^2 - 1} - P_i \frac{(\frac{r_o}{r})^2 + 1}{(\frac{r_o}{r_i})^2 - 1} \tag{2.15}$$

In which σ_r is the radial stress, σ_t is the tangential stress, r_i is the inside radius of the cylinder, r_o is outside radius, r is distance from the centre of the cavity, P_i is the internal pressure and P_o is the external pressure.

Where P_o is equal zero and r_o approaches infinity equations 2.14 and 2.15 become:

$$\sigma_r = + P_i \frac{(r_i)^2}{(r)^2} \tag{2.16}$$

$$\sigma_t = - P_i \frac{(r_i)^2}{(r)^2} \tag{2.17}$$

In the case where the borehole with radius r_b is pressurized (Fig. 2.6), the above equations become:

$$\sigma_r = + P_b \frac{(r_b)^2}{(r)^2} \qquad (2.18)$$

$$\sigma_t = - P_b \frac{(r_b)^2}{(r)^2} \qquad (2.19)$$

P_b: Borehole pressure

The borehole boundary stresses are given by:

$$\sigma_r = P_i \qquad \sigma_t = -P_i \qquad (2.20)$$

In the case where the gases penetrate into the cracks, if the volume of cracks is negligible, the stresses at the boundary of crack zone are given by:

$$\sigma_r = P_i \qquad \sigma_t = -P_i \qquad (2.21)$$

The propagation of radial cracks to the surface and the time for generation of these fractures has been found to be about 3 ms per each meter of burden from high-speed photographs (Brady and Brown, 1985). The bulk of fragmentation is the gas pressure. The fragmentation process terminates after yielding and moving the front of holes forward. Some further breakage may occur by in-flight collisions and impact with the ground.

Thus, the breakage of rock occurs under two processes, one due to dynamic pressure and the other due to gas pressure. The rate of useful work in these two phases depends on the rock conditions, explosive properties and blasting geometry. The

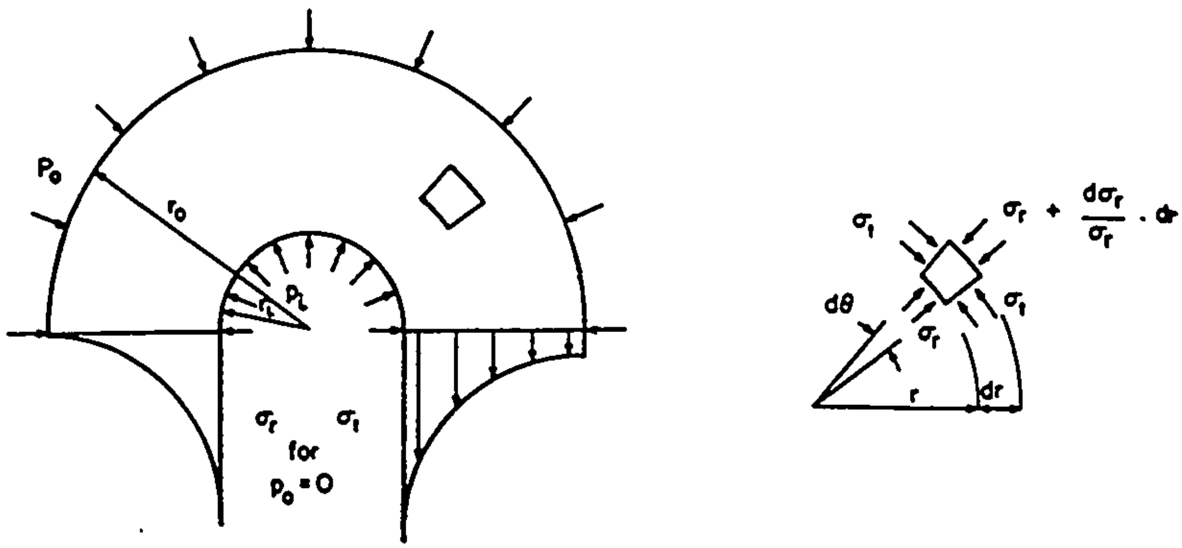

Figure 2.5 : Radial and tangential stress around a thick-wall cylinder (Coates, 1965).

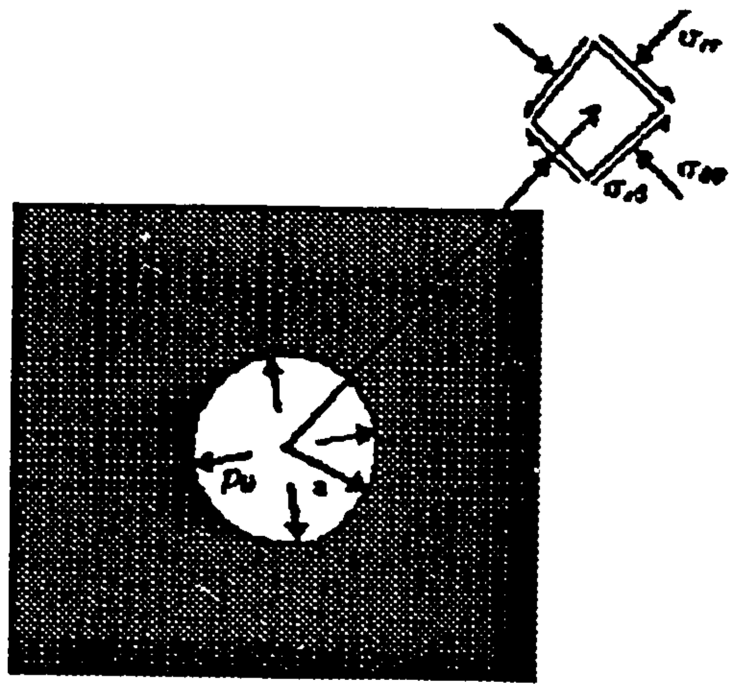

Figure 2.6 : Condition of quasi-static loading around a blasthole (Brady and Brown, 1985).

breakage of a given volume of rock to suitable size and movement of this volume to a certain distance normally consumes only a fraction of total explosive energy. The balance of the energy is used up in producing some of undesirable effect such as over crushing, fly rock, overbreak, vibration and airblast.

2.5 CONCLUSIONS

All materials deform under the action of loads. The behaviour of a material under an applied load depends on the nature of the material, the intensity and duration of loads and test conditions. Rocks are composed of crystals and grains in a fabric which includes cracks, fissures or other types of discontinuities. Strength and modulus of elasticity of rocks depend on the degree of crystallinity, the size and orientation of crystal axis, the elasticity of crystals and the matrix of the rock.

In blasting, rockburst and earthquakes, the applied load has a dynamic nature. The results of experiments show the value of dynamic strength of rock is many times greater than its static strength. The measured properties in laboratory under static conditions cannot always be applied for dynamic conditions.

In a rockmass where the direct measurement is not possible, the rock properties and conditions can be obtained by measuring the velocity of propagation of seismic waves. If the density is known, the value of elastic properties can be calculated from the velocity of P and S waves. The velocity of seismic waves is extremely sensitive to the degree of porosity, weathering and fracturing of the rock as well as the degree of discontinuity. Young's modulus, bulk modulus and shear modulus can be derived from the velocity of seismic waves. The dynamic modulus of elasticity is normally greater than the static one.

The properties of explosive play a dominant role in rock breakage. On detonation of the charge, the shock front compresses the explosive to a high density within a few microseconds, the explosive material converts into a gas at very high temperature and pressure. The chemical reaction develops a very narrow boundary between the explosive material and the explosion product, which is called the detonation wave. This wave transfers throughout the charge with a velocity of several thousand meters per second, and is known as detonation velocity. The amount of energy developed per unit of time exceeds 25,000 MW. It is noted that the explosive energy is very large, but not more than 1/5 of coal and 1/10 of gasoline energy on a weight basis, however, its rate of release is extremely high.

Energy or strength, velocity of detonation and density are the three important parameters which must be considered in the selection of an explosive. On the other hand, the best explosive for a given condition is not necessarily the highest strength, density, or detonation velocity. Most commercial explosives exhibit non-ideal reaction behaviour, whereas energy and pressure are usually calculated on the basis of ideal reaction. The calculation of various explosive energies and their selection on the basis of energy or strength are therefore not always realistic, because these values are not always indicative of field conditions. The energy of explosives depend on particle size, reaction rate and field conditions, such as loading conditions and confinement, and borehole diameter.

The fragmentation process is started by the detonation of an explosive in the borehole. The transfer of energy to the rock is a function of the characteristics of both explosive and rock. The initial shock wave crushes the rock around the borehole up to a few borehole diameters, depending on the dynamic properties of the rock. Radial cracks issue from the perimeter of the hole by the tangential component of the stress wave. The pressure in the shock wave falls off rapidly as it approaches the free face. The strength of rock being much lower in tension than compression, the primary or radial cracks are initiated under the influence of tensile forces. The initial fractures around the borehole extend to a distance of about 2 to 6 times the borehole diameter. When the compressive wave reaches a free face or a discontinuity some part of the energy is reflected back into the medium and the next is transferred across the discontinuity. These reflections and transmissions depend on the ratio of the respective acoustic impedances of the material on either side of the interface. In the presence of a free face most of the energy will be reflected as a tensile wave. The tensile stress wave can give rise to spalling at the free surface and can also create additional cracks and extend existing ones. The third phase is related to expansion of explosion gases in the borehole. In this phase, the actual breakage of rock proceeds at a relatively slower pace. The high pressure gases penetrate into cracks and extend them, and thereby create the bulk of the fragmentation. The pressure of gases ranges from about 1 GPa to 5 GPa. Some further breakage may occur by in-flight collisions and impact with the ground.

CHAPTER 3

WALL-CONTROL BLASTING METHODS

3.1 INTRODUCTION

Several blasting techniques have been developed to control overbreak beyond the limits of production shots. These techniques are applied to preserve the natural strength of rock walls, to avoid rockfalls or rockslides and to leave the remaining rock, practically undamaged. These methods have been called by various names such as "cautious blasting", "control blasting", "perimeter blasting" and "smooth blasting".

The objective of all wall-control blasting techniques is, to better distribute the explosive energy in the rock mass and reduce fracturing and backbreak of the remaining rock. In these techniques, the perimeter shots are different from the production shots. They are arranged, loaded and blasted in a specific way. Closer spacing, decoupling and decking of explosive charge, commonly smaller diameter boreholes, lower load and simultaneous firing are the main characteristics of these shots.

3.2 WALL-CONTROL BLASTING PARAMETERS

In control blasting, the major factors one must be considered are:

- Geology.
- Accuracy of drilling.
- Explosive type
- Hole diameter, charge diameter, spacing and loading of perimeter holes.
- Burden, spacing and loading of holes adjacent to perimeter row.

The geology should be investigated very carefully. All geotechnical data must be analyzed, and any potential problem must be evaluated as much as possible. Rock strength, degree of weathering and fracturing, nature, frequency, spacing and orientation of discontinuity must be investigated by suitable field and laboratory tests.

A very important point in perimeter blasting is that all of perimeter holes should be drilled in the same plane. The final production row should be parallel in order to create a constant burden from the top to the bottom of adjacent perimeter row.

The selection of a suitable explosive for perimeter blasting largely depends on properties of the in situ rock, strength, stability and lifetime of structure. The damage to final pit walls can be reduced by using a lower pressure explosives. The peak pressure of an explosive depends on its density and detonation velocity. Generally, the mines use similar explosives for production and wall-control blasts. However, the effects of explosion on final pit walls must be studied and evaluated thoroughly.

3.3 BLAST GEOMETRY

Several loading values and relationships between spacing, hole diameter, and diameter of charge and hole diameter have been proposed (Holmberg and Persson, 1978; Hoek and Bray, 1981; Mellor, 1976). These information can be used as a guide, but additional tests should be carried out to modify the proposed guidelines to suit specific conditions. Also, the results of control blasting must be constantly evaluated. It is important that the loading, spacing and burden of the last production row, before the perimeter row, be reduced to about 1/2 to 3/4 that of production holes. Otherwise, backbreak and damage to final wall may occur.

3.4 TYPE OF LOADING

The following three types of loading (Fig. 3.1) were usually employed in these blasts:

- Taping detonating cord to cartridged explosive and filling the hole with drill cuttings or fine gravel (intermittently loaded).
- Continuously loaded with an annular air gap or drill cuttings between charge and hole wall. Sometimes air bags are also used for stemming. "Air bag is a cylindrical plastic bag filled with of air which can be used as stemming or as air gap between charge and stemming.
- Loading holes with bulk explosives, such as ANFO, Emulsion or Slurry, at toe without stemming (toe loaded).

The holes were commonly loaded with cartridged explosive traced by a detonating cord or bulk explosives in a decoupled manner. The average ratio of explosive diameter to borehole diameter was roughly 0.5.

3.5 ROCK FAILURE

In discussing the wall-control blasting methods, it is important to bear in mind the different models of failure in rock. Three models of failure due to compressive stress, shear stress and tensile stress occur during the blasting process (Mohanty, 1982; Vutukuri and Bhandari, 1973).

As stated previously, the crushed zone is the result of shattering under high

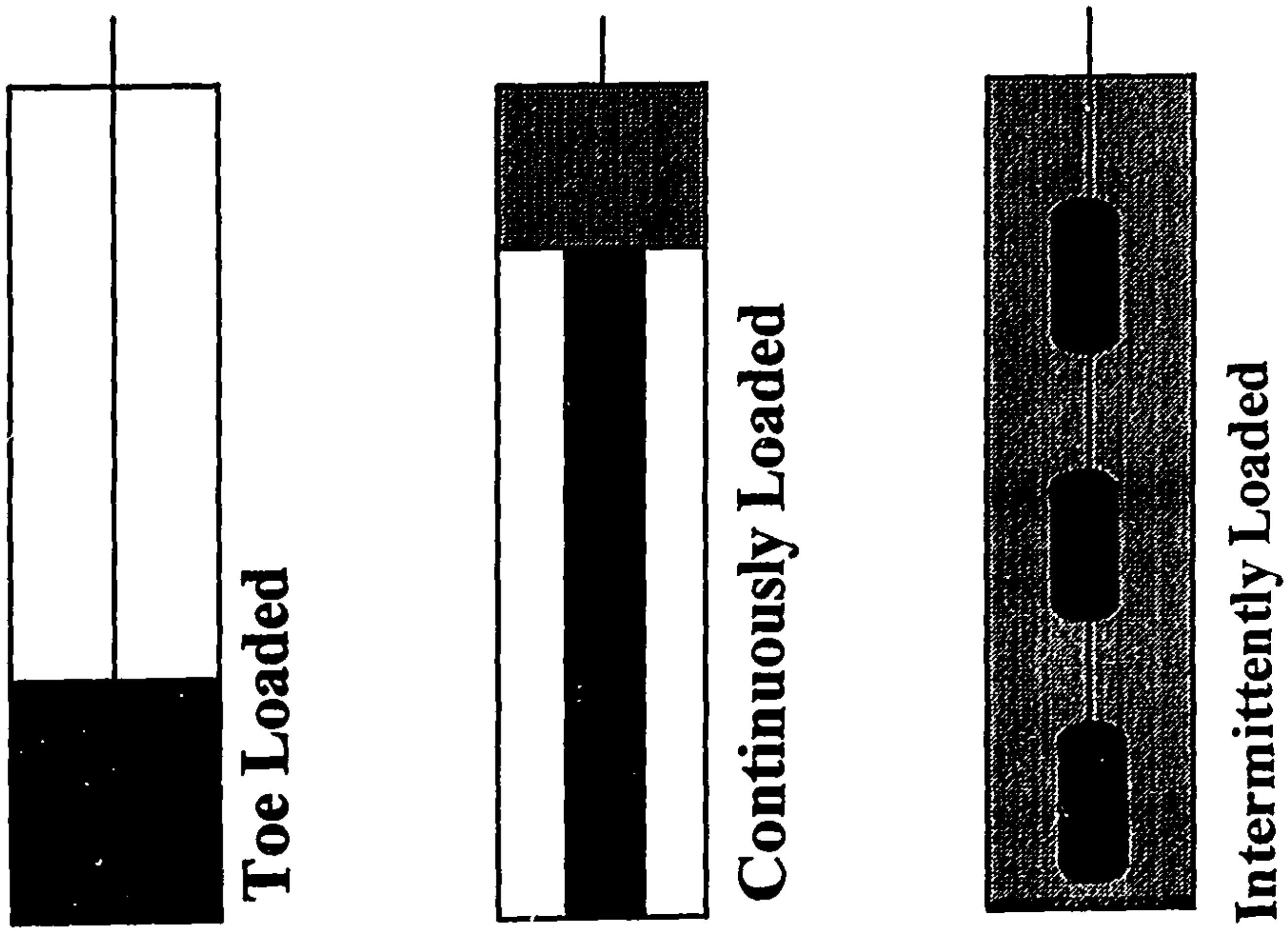

Figure 3.1 : Different types of loading for wall-control blasting methods.

explosion pressures. In this region the peak pressure of the outgoing waves exceed the dynamic compressive strength of the rock. The best result is obtained, when the peak pressure of the explosive does not exceed the dynamic compressive strength of the rock. In perimeter blasting, this can be achieved by using a decoupled charge. In the area close to crushed zone, the rock is compressed by the outgoing shock wave front and subjected to tangential tensile stress that creates the radial fracture around the hole.

When a stress wave encounters a free face or any discontinuity, it is reflected as a tensile waves. The tensile wave reflected back into the rock, and causes additional fracturing. The main reason is that the strength of rock in tension is lower than in compression or shear and the magnitude of tensile wave is much greater than the shear wave. On the surface spalling occurs if the tensile wave is sufficiently strong. Finally, under the influence of high pressure explosion gases radial cracks extend and gases penetrate into any discontinuity.

Shear failure occurs when the heaving effect of the blasthole gases causes relative movement of adjacent elements of burden along wave-induced, natural fractures and weakness planes, such as joints and bedding. Vertical shear fracture may also obtained when each segments of burden tends to be propelled outward before adjacent segment.

3.6 WALL-CONTROL BLASTING METHODS

The following six basic control blasting techniques are used in mine and construction excavation.

3.6.1. Line drilling.
3.6.2. Pre-splitting or Pre-shearing
3.6.3. Buffer blasting
3.6.4. Cushion blasting or Trim blasting

3.6.5. Smooth blasting

3.6.6. Fracture plane control blasting

The earlier survey of case studies in the Canadian Open Pit Mines (Calder, 1977) shows that pre-splitting method was used 46% of the times in all wall-control blasts. It was followed by cushion blasting (31%), buffer blasting (15%) and line drilling (8%). The results of this survey (henceforth referred to as survey 1) is illustrated in Fig. 3.2.

The result of the current survey (henceforth referred to as survey 2) carried out by writer, based on wall-control blasting methods employed in fourteen North American open pit mines are shown in Fig. 3.3 (Khoshrou, 1993). The result shows the following breakdown: Pre-splitting (66%), Cushion Blasting (17%), Buffer blasting (12%) and Line drilling (5%).

A comparison between these two figures shows that the extent of line drilling and buffer blasting has not changed significantly over the years. However, cushion blasting has gone down 17% and pre-splitting increased by 20%. The frequency of pre-splitting with a buffer row and without a buffer row represents 80% and 17% of the pre-splitting method in current and previous practices respectively.

3.6.1 Line Drilling

This method consists of drilling a single row of closely spaced holes along the excavation limit. The hole is carefully aligned on the same vertical plane. The holes are not loaded or some of them are loaded lightly and others are left empty. In some cases, all the shots are loaded by detonating cord. Detonating cord is a flexible cord which is made of a centre core of high explosive, commonly PETN, to initiate other explosives. These cords usually have core loads of approximately 4-13 grams per meter. The hole diameters are generally 50 to 75 mm with a spacing 2 to 4 times the hole diameter (D).

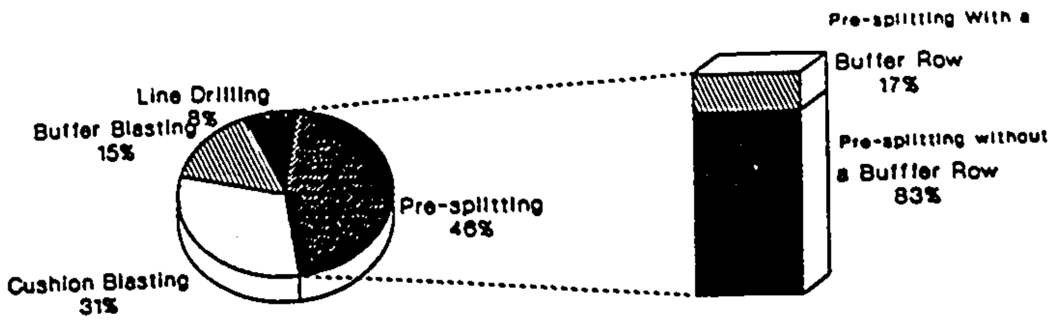

Figure 3.2 : Distribution of different types of wall-control blasting methods (survey 1).

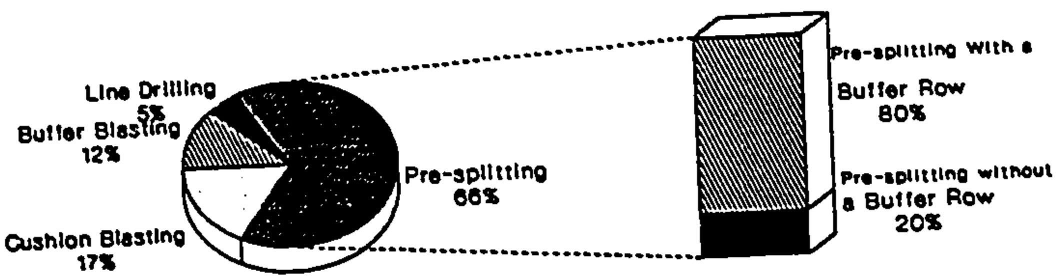

Figure 3.3 : Distribution of different types of wall-control blasting methods (survey 2).

$$S = (2 - 4) \times D \tag{3.1}$$

Empirical weighting factors have been proposed for different materials to estimate the hole spacing. These factors must be multiplied by the hole diameter (Table 3.1). The best results are obtained when the distance of the first-row-holes from the perimeter shots and the spacing of holes are reduced to 50 - 75% of the production holes burden and spacing. Also, deck charges with a 50% reduction in normal production holes loading and detonating cord for firing can be used in this row. Generally, the method is not used in open pit mines due to high costs of drilling. The advantage and disadvantage of line drilling method are shown in Table 3.2.

3.6.2 Pre-Splitting

Pre-splitting or pre-shearing is one of the most successful perimeter blasting methods. The aim is to create a narrow fracture zone at the perimeter of the excavation to isolate the explosion effects from the remaining rock. Several attempts have been made to explain the mechanism of generation of a weakness plane in pre-splitting blasting (Kutter and Fairhurst, 1968; Singh, 1990). But, no single theory has been developed that satisfactorily explains the mechanics of formation and extension of such a fracture zone.

The earlier works, attempted to explain the mechanism of pre-split zone based on interaction between stress waves, while new attempts emphasise on the quasi-static explosion pressure. These two hypothesis are:

- fracture zone occurs due to near-field stress waves.
- fracture zone occurs due to the nearly-static pressure.

Table 3.1 : Different factors for several types of rock to calculate the spacing.

Rock type	Factor
Taconite (Iron ore)	2.0
Copper ore	2.5
Asbestos ore	4.0
Coal overburden	5.0

Table 3.2 : Advantages and disadvantages of line drilling.

Advantages	* The method is simple. * No damage, vibration and airblast, because the method. requires a minimum amount of explosive.
Disadvantages	* Expensive due to high drilling cost. * Difficulty of maintaining hole alignment due to very close spacing. * Requires small diameter drills in comparison with the main production drills. * The shot must be drilled parallel to natural dip of rock.

Dynamic pressure

One school of thought proposes that when two boreholes are detonated simultaneously, it gives rise to a collision of shock waves between the holes which places the web in tension and causes a sheared zone between the holes (Du Pont, 1969). When the shock waves meet each other at the midpoint between two holes, the stresses at this point are doubled and fracturing ensues, if the tensile stress due to each hole is at least equal half dynamic tensile strength of the rock.

The stress wave transmitted in the rock, can be analyzed by examining its radial and tangential components. A fracture zone is developed around the cavity, because the peak pressure in the shock wave is higher than the compressive strength of rock. At the boundary between fractured zone and unfractured zone the tangential stress value is equal to dynamic tensile strength of rock. Both radial (compressive) and tangential stresses decrease rapidly with distance from the borehole.

Quasi-static pressure

The borehole pressure immediately after the passage of the detonation front, is the result of expansion of explosive gases against borehole wall. It is quasi-static in nature and approximately equal to one half the detonation pressure. The mechanism of creating a narrow fracture zone between two holes and stress distribution around the boreholes can be explained by a pressurized cylinder with infinite thickness without external pressure.

The calculation of radial and tangential stresses at any point on a thick-walled cylinder was presented in the previous chapter. In the case where the borehole with radius r_b is pressurized, the following equation hold,

$$\sigma_r = + P_b \frac{(r_b)^2}{(r)^2} \tag{3.2}$$

$$\sigma_t = - P_b \frac{(r_b)^2}{(r)^2} \tag{3.3}$$

Where σ_r is radial stress, σ_t is tangential stress, r_b is borehole radius, r is distance from the centre of the cavity and P_b is borehole pressure.

It is observed that rocks have very low tensile strengths, moderate shear strengths and high compressive strengths. Therefore, best results will be obtained when the tensile stress as are maximized while the compressive and shear stresses are minimized.

3.6.2.1 Decoupling

Since the borehole pressure is quite intense, the charge should be decoupled to minimize the extent of the crushed zone and encourage the growth of fewer radial cracks. This can be achieved by making the charge diameter smaller than the borehole diameter (Britton and Skidmore, 1988; Rollins, 1978). To generate a single predominant crack between any two perimeter holes the borehole pressure should be smaller than the compressive, but higher than the tensile strength of the rock. An annular air space is provided around the charge which absorbs part of the energy and therefore it reduces the peak pressure. Figure 3.4 shows the difference between fully coupled holes and decoupled holes by air and water (Day, 1982).

When a charge is decoupled, the borehole pressure can be calculated by the ideal gas law. The equation for ideal gas under adiabatic conditions is given by,

$$\frac{dp}{p} = -\gamma \frac{dV}{V} \tag{3.4}$$

On the assumption that γ is constant:

$$PV^{\gamma} = K \tag{3.5}$$

K is the integration constant and can take on a continuous range of values. Therefore,

$$PV^{\gamma} = P_1 V_1^{\gamma} \tag{3.6}$$

In which V is gas volume, P is gas pressure and $\gamma = C_p/C_v$.
Equation 3.6 can be written for explosive and borehole as:

$$P_b' = \frac{P_d}{2}\left(\frac{V_c}{V_b}\right)^{\gamma} \tag{3.7}$$

$$V_b = \pi r_b^2 h_b$$
$$V_c = \pi r_c^2 h_c$$

For unit height:

$$P_b = \frac{P_d}{2}\left(\frac{\pi r_c^2}{\pi r_b^2}\right)^{\gamma} = \frac{P_d}{2}\left(\frac{r_c}{r_b}\right)^{2\gamma} \tag{3.8}$$

Where γ is equal to C_p/C_v, C_p is specific heat at constant pressure, C_v is specific heat at constant volume, P_b is borehole pressure, P_d is detonation pressure, r_b is borehole radius and r_c is charge radius.

Different methods have been developed for measuring C_p, C_v and γ. One of the simplest methods is that of Clemeut and Sormes. A manometer and a large vessel fitted with a stopcock are used as shown in Fig. 3.5. The air in the vessel is pumped up to above atmospheric pressure, P_1. When the stopcock is opened, the pressure inside the vessel falls down to atmospheric pressure P_0. Then the stopcock is reclosed, and the final pressure, P_2, is read after the air has had time to come back to atmospheric temperature at constant volume. The P_1P_0 and P_1P_2 lines indicate adiabatic and isothermic states respectively. The results of this method are illustrated in Fig. 3.6. According to the relationship between P and V in Fig. 3.6., the ratio of specific heat can be calculated as:

$$\gamma = \frac{\dfrac{-(p_1 - p_o)}{\Delta v}}{\dfrac{-(p_1 - p_2)}{\Delta v}} \tag{3.9}$$

For explosion gas products, γ is determined by Cole (1965) and Crawford (1963) from 1.25 to 1.40 (Fig. 3.7. and Table 3.3).

Later, from controlled blasting experiments Bauer (1967) found the exponent of equation 3.8 to be equal to 2.4, $2\gamma = 2.4$. This value is very close to values found by Cole and Crawford for γ. Tests were carried out by decoupled spherical charges which were placed in the centre of 50-gal drums. The velocity of water shock was recorded with a streak camera, and then the pressure was determined from the velocity of shock.

In Fig. 3.8. the results of peak pressure in the water versus degree of coupling is illustrated for 46, 60 and 70 percent decoupling ratio. Therefore,

$$P_b = \frac{P_d}{2}\left(\frac{r_c}{r_b}\right)^{2.4} \tag{3.10}$$

In which P_b is borehole pressure, P_d is detonation pressure, r_b is borehole radius and r_c is charge radius.

3.6.2.2 Decking

Decking is used to distribute explosive energy along a specific section of the borehole, to avoid gas penetration in the soft seams and to reduce the weight of explosive per delay (Stachura and Cumerlato, 1995). Any number of decks within a blast hole is possible. The following relation for calculation of the deck thickness is recommended by Anon (1987):

$$T_d = 12 \times r_b \tag{3.11}$$

where, T_d is the length of the explosive deck and r_b the radius of borehole.
When a hole is decked the relationship between borehole volume and explosive volume is given by:

$$V_b = \pi r_b^2 h_b \qquad V_e = \pi r_e^2 h_e \qquad r_b = r_e$$
$$\frac{V_e}{V_b} = \frac{h_e}{h_b} \tag{3.12}$$

In which V_b is borehole volume, V_e is explosive volume, h_b is height of borehole and h_e is height of charge.

On substitution of equation 3.12 into 3.7 the borehole pressure for the decking charge can be calculated as:

$$P_b = \frac{P_d}{2} \cdot \left(\frac{h_e}{h_b}\right)^{\gamma} = \frac{P_d}{2} \cdot \left(\sqrt{\frac{h_e}{h_b}}\right)^{2\gamma} = \frac{P_d}{2} \cdot \left(\sqrt{\frac{h_e}{h_b}}\right)^{2.4} \tag{3.13}$$

Where P_b is borehole pressure, P_d is detonation pressure, h_b is height of borehole and h_e is height of charge.

If the borehole is decoupled and decked, the previous equation should be changed to the following (Chiappetta, 1991):

$$P_b = \frac{P_d}{2} \cdot \left(\frac{r_c}{r_b}\sqrt{\frac{h_e}{h_b}}\right)^{2.4} \tag{3.14}$$

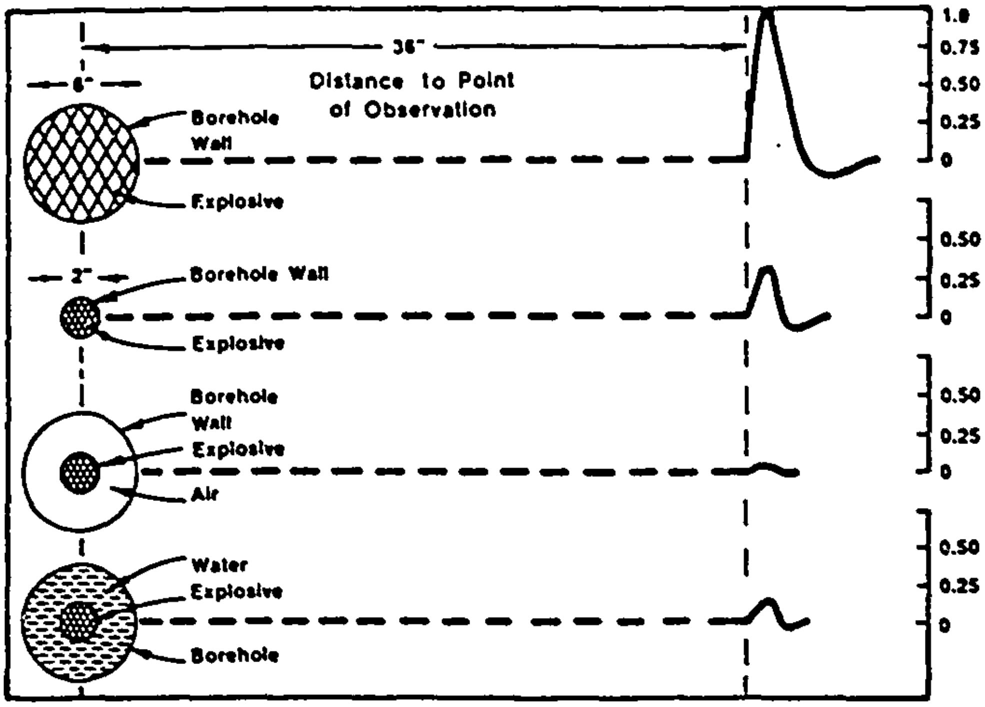

Figure 3.4 : Fully coupled holes and decoupled holes by air and water, Day (1982).

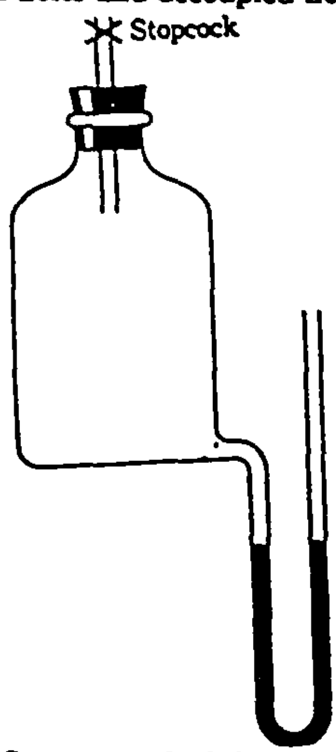

Figure 3.5. Clemeut and Sormes method for measuring C_p, C_v and γ (Crawford, 1963).

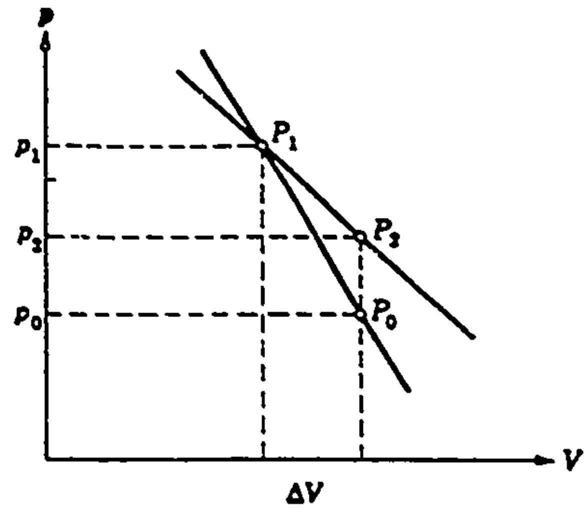

Figure 3.6. Relationship between pressure and volume for adiabatic and isothermic states (Crawford, 1963).

Table 3.3 : Ratios of C_p/C_v (γ) for different explosion gas products.

Name		Gases	γ
Cole	TNT	Mixture of: Hydrogen, Carbon dioxide, Carbon monoxide, Nitrogen, Nitric oxide and Methane	1.250
Crawford*	Diatomic gases	Hydrogen Carbon monoxide Nitrogen Nitric oxide	1.408 1.404 1.405 1.400
	Triatomic gases	Carbon dioxide Nitrous oxide	1.302 1.300
	Quintatomic gases	Methane	1.310
* Experimental values of γ for gases at 15° C and 1 atm.			

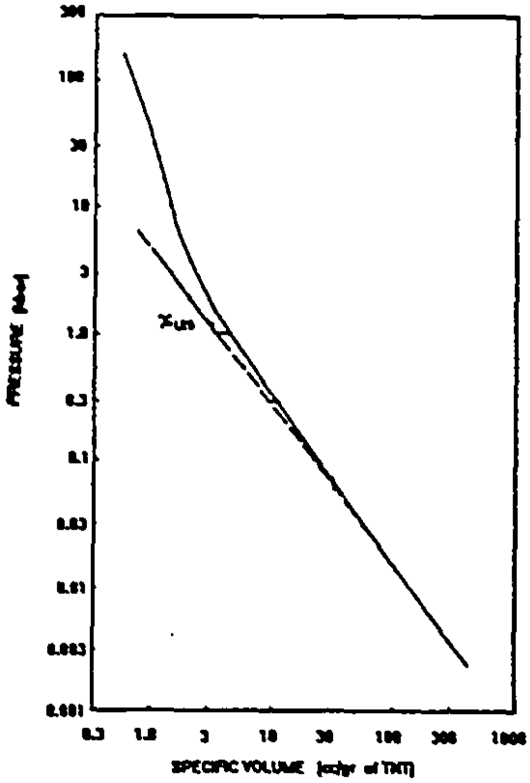

Figure 3.7 : Adiabatic pressure-volume relation for products of TNT (Cole 1965).

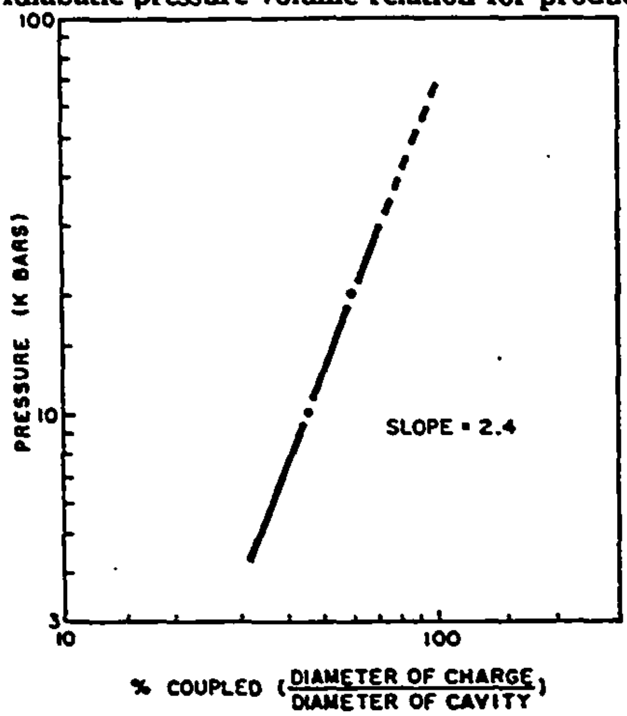

Figure 3.8 : Relationship between peak pressure and decoupling ratio for pentolite spheres fired in water (Bauer, 1976).

However, on pre-splitting a single row of closely spaced holes is drilled along the final excavation line. The holes are lightly loaded with suitable explosives and fired instantaneously or with millisecond delay. The pre-splitting row can be blasted separately from the production shots or with primary shots (Avey, 1990; Leinberger et al., 1992; Scoble, 1992; Owens, 1995).

If pre-splitting shots are fired with the production shots, there should be a minimum of 200 ms between the pre-splitting holes and the nearest production boreholes, Anon (1987). The distance between pre-splitting holes depends on rock condition and borehole diameter. Closer spacing will be required in weathered or jointed rocks.

Pre-splitting is often done with 50 mm to 150 mm diameter blasthole (Anon, 1987; Calder and Tuomi, 1980; Calder, 1977; Calder and Morash, 1971), and depths up to 12 to 18 m. Larger diameter blastholes, 230 mm to 313 mm, greater spacing and deeper holes, > 24 m, have been used successfully for pre-splitting in some operations. Typical spacings would be 0.6 m to 1.2 m with a hole depth limit of 15 m to 60 m. Table 3.4. lists some pre-splitting rules of thumb (Du Pont, 1969; Gustafsson, 1973; Anon, 1987).

The holes are charged between 55 to 75 percent of the hole depth, the lower value being applicable to soft, weathered and fractured. For best results, the row of holes immediately before pre-splitting holes is charged lighter than production holes.

An important point in pre-splitting is the effectiveness of stemming. A collar length of 7 to 10 blasthole diameter is usually sufficient (Hoek and Bray, 1981). A larger stemming length is used for frequent open joints and highly weathered rock. Table 3.5. shows the depth of collar for different rock types. It is noted that the length of stemming also depends on the borehole depth. Furthermore, in pre-splitting method the holes are sometimes lightly loaded in the toe without stemming. Therefore, this table, or similar tables, are commonly based on field experiments given conditions, and can only be used as approximate guide lines.

Pre-splitting method can be used successfully in horizontally bedded rocks, but has serious difficulties in discontinuous rocks. Where discontinuity is located between the holes, the gas pressure is reduced, due to venting of explosive gases. If the discontinuity is open, the cracks further extension will be impeded unless the hole is fully stemmed throughout the entire column charge. The crack can be propagated across a discontinuity when it is either closed or cemented by some materials. Table 3.6 shows the advantages and disadvantages of pre-splitting blasting.

3.6.3 Buffer Blasting

Buffer blasting method is directly employed near the excavation limits or in conjunction with some other control blasting such as pre-splitting and line drilling. The spacing and burden is smaller than production holes, generally 1/2 to 3/4 of that used in primary blasting. The buffer row burden is less than spacing to avoid over-size muck. Hole diameter and hole depth are the same as for production shots, but loaded lightly with explosives. The powder factor is reduced to 0.6 of the main blasting factor (Calder, 1977).

Depending on the collar length, which normally is 24 borehole diameter, the weight of explosive per hole can be calculated by (Calder, 1977):

$$W = (H_B + S_d - S_T) \times w \tag{3.15}$$

Where, H_B is the bench height, S_d the length of sub-drill, S_T the length of stemming and w the powder factor.

For a given spacing and burden of the buffer row, the charge per hole must be

Table 3.4 : Some pre-splitting rules of thumb.

Year	References	Hole Diam. (mm)	Hole Spacing (m)	Explosive (kg/m)
1969	Du Pont Blasters' Handbook	38 - 45	0.30 - 0.45	0.08 - 0.25
		51 - 63	0.45 - 0.60	0.08 - 0.25
		76.5 - 89	0.45 - 0.90	0.14 - 0.50
		102	0.60 - 1.20	0.25 - 0.75
1973	Swedish Blasting Technique	25 - 32	0.20 - 0.30	0.07
		25 -32	0.35 - 0.60	0.16
		40	0.35 - 0.50	0.16
		51	0.40 - 0.50	0.32
				0.16
		64	0.60 - 0.80	0.36
1987	Explosives and Rock Blasting .	38	0.3 - 0.5	0.13
		45	0.3 - 0.5	0.16
		51	0.5 - 0.6	0.25
		63	0.6 - 0.8	0.35
		76	0.6 - 0.9	0.52
		89	0.6 - 0.9	0.75
		102	0.9 - 1.2	0.90
		126	0.9 - 1.5	1.40
		153	1.2 - 1.1	2.00
		204	1.5 - 2.1	3.00

Table 3.5 : Depth of collar for different rock types in pre-splitting blast.

Rock Type	Compressive Strength	Compressive Strength	Length of Stemming
	(psi)	(GPa)	$\varnothing_c$: Charge Dia.
Hard Competent rock	< 30,000	< 210	$12 \times \varnothing_c$
Competent Rock	≈ 15,000	≈ 100	$22 \times \varnothing_c$
Incompetent Rock	≈ 5,000	≈ 34	$30 \times \varnothing_c$

Table 3.6 : Advantages and disadvantages of pre-splitting.

Advantages	* Reduce drilling cost, due to use larger spacing. * After blasting of the first section and before continuing operation for the main round, it is not necessary to move broken rocks. * It is not necessary to return to blast slopes or walls after primary excavation.
Disadvantages	* It is not possible to get information from the rock conditions because holes are fired before mine rounds. * Estimation of pre-splitting results can be done only completely after primary blasting and moving the broken rock.

reduced until the powder factor of the buffer holes becomes equal to about 0.6 times that of the production powder factor.

3.6.3.1 Staggered Hole Depth Technique

Another form of buffer blasting is called "Staggered Hole Depth Technique". In this technique, rows of blastholes are drilled at various depths close to an underlying structural plane without penetrating the plane. These rows have a reduced powder load, spacing and burden, but loaded with the same explosive as the buffer row. It is noted that, the structural plane must be known and the holes should be drilled within the correct distance from the plane.

3.6.4 Cushion Blasting

Cushion blasting, sometimes referred to as trim blasting, is a mean of trimming or slashing the excess material from the final walls. A single row of holes is drilled at the perimeter of the excavation, loaded lightly with explosive and fired after production blasting. In cushion blasting the explosive charges are decked with inert material, stemmed throughout the entire column and initiated with detonating cord or MS delay to minimize the delay between holes. Explosive is generally decoupled by 50% from borehole wall, and the collar length is 10 to 25 times the borehole diameter.

The spacing and loading of a cushion blasting row depends on the rock conditions, actual remaining burden and the results of primary blasting. Table 3.7. shows some typical values for spacing, burden and borehole diameter (Anon, 1987; Du Pont, 1969). Unloaded guide holes between cushion blast holes may be used to provide better results in weathered or fractured rock, particularly around corners or curved sections. To insure shearing at bottom of cushion blast holes, a bottom charge is usually used, which is 2-3 times the column charge per 0.3 meter, especially when the burden at the toe is greater than the burden at the top of bench.

The distance between the perimeter shots and the first-row-holes can be made equal or less than the primary blasting burden. Care should be given to spacing and loading of this row to create a constant burden for final row. Cushion blasting method also helps to prevent explosive gases from the opening discontinuities in the final wall. Table 3.8 shows the advantage and disadvantage of cushion blasting.

3.6.5 Smooth Blasting

In underground excavations, it is extremely important that the surrounding rock be free of cracks. Smooth wall blasting was first used in Sweden to control overbreak in underground headings and stopes, particularly in tunnelling. This method is similar to pre-splitting except that the perimeter row is fired after the main lifter shots. Smooth blasting involves drilling a number of closely spaced holes around the final excavation (Lizotte, 199[illegible]). The holes are loaded with light, well distributed charges and fired after the main production holes on the last delay, usually after the main lifter holes.

The best results are obtained when the charges in the contour row are fired simultaneously. It is difficult to manage because the perimeter row is fired as the last row, and it is necessary to use a high delay number. In underground excavations, blastholes range from 37 to 86 mm for horizontal holes in tunnels and 86 to 165 mm for downward holes, 64 to 127 mm for upward holes in stopes, drifts and shafts. The spacing between the holes is usually 15 to 16 times the hole diameter, and the ratio of burden to spacing about 1.5 to 1.0 (Du Pont, 1969). The holes are usually decoupled by an annular air space around the charge to reduce the magnitude of the initial high pressure. Maximum efficiency is obtained when the charge is centred in the holes.

A heavier bottom charge is used to insure breakage of the rock at the bottom of

Table 3.7 : Blast geometry for cushion blasting.

Hole Diam.	Spacing	Burden	Explosive Load
(mm)	(m)	(m)	(kg/m)
51 - 65	0.9	1.2	0.12 - 0.0.38
75 - 87	1.2	1.5	0.13 - 0.75
100 - 112	1.5	1.8	0.38 - 1.13
125 - 137	1.8	2.1	1.13 - 1.5
150 - 162	2.1	3.2	1.50 - 2.25

Table 3.8 : Advantages and disadvantages of cushion blasting.

Advantages	* Reduces drilling cost, due to use larger spacing. * Larger diameter borehole, generally the same as primary shots. * Deeper holes. * Can yield better results in fractured and weathered rocks. * Results can be viewed immediately after blasting buffer row.
Disadvantages	* Careful loading and stemming. * Additional set up which adds time and therefore cost. * Delays production. * Overbreak from the first-row-in holes can break into cushion holes, and presents redrilling and loading problems. * Not suitable for blasting around the corner and curved sections.

hole. The first-row-in holes from the perimeter must be controlled by spacing, burden and loading to avoid overbreak beyond the perimeter holes. In smooth blasting, the drilling precision is extremely important for good results. In tunnels, the holes should be looked-out to get room for next round drilling. The value of looking-out depends on the application and arrangement of holes, and the size of drilling equipment.

In principle, smooth wall blasting is identical to cushion blasting. The major difference is that the holes are drilled horizontally, and they are not fully stemmed. Therefore, the holes could be stemmed by sand bags, water bags, clay or tamping plug to prevent the charge from detonating previous holes. Some parameters of smooth wall blasting are given in Table 3.9 (Du Point, 1969; Hoek and Brown, 1980). Table 3.10 shows the advantage and disadvantage of smooth blasting.

3.6.6 Fracture Control Blasting

In this method the growth of the crack can be controlled, and formation of undesirable cracks can be suppressed. In this technique the perimeter holes are grooved along the desired plane by a grooving tool, such as water jet, a linear shape charge or a special drill bit. Also, the notched holes can be replaced by a series of holes at the opposite sides of each central hole (Mohanty, 1990). The mechanics of fracture has been studied in some detail under static and quasi-static stress field, and to some extent under dynamic stress. The crack tip stress intensity factor, K, is one of the important factors in fracture mechanics. This parameter may be regarded as the intensity of load transmitted through the crack tip region caused by introducing the crack into the body of interest. This factor has units of *stress* $\times$ *(crack length)*$^{1/2}$ or *force* $\times$ *(crack length)*$^{-3/2}$. Failure or fragmentation can occur when K equals a critical value. This value is taken as a material property, and called the plane strain fracture toughness, K_{IC}. Thus, the fracture toughness of a material is defined as resistance of a material to crack extension.

Consequently, to initiate cracks at the notches the stress intensity factor must exceed the fracture toughness in the material. Several approaches are available to determine the fracture toughness and the intensity factor (Kim and Stout, 1978; Ouchterlony, 1988). Fracture toughness factor for different rock types is presented in Table 3.11 (Fourney et al., 1984). The aim of using of fracture mechanics in rock blasting is to analyze the fracture behaviour and crack growth around a pressurized borehole under dynamic and quasi-static pressure. This problem was analytically treated by Bowie (1956) and Kutter (1970) for any number of cracks around a pressurized borehole. Ouchteronly (1974) has discussed radial crack growth from a pressurized borehole for linear elastic materials, given the relationship between stress intensity factor values for the pressurized circular hole with radial cracks of equal length for various crack numbers, (Fig. 3.9). This figure shows, when the cracks around a borehole are very short, a = 0.05 × R, the critical pressure required to initiate cracks is independent of the cracks number around the hole. Therefore, the critical pressure can be calculated by (Fourney et al., 1984).

$$P_c = \frac{K_{IC}}{2.24\sqrt{\pi a}} \tag{3.16}$$

The results are plotted in figure 3.10.

As shown for several types of rock, cracks can be initiated at the notches with a relatively low pressure. The pressure range depends on the fracture toughness of the rock, the natural flaw size and the depth of the side notches. The relationship between the ratio of notched borehole pressure, P_{crit} and unnotched borehole pressure, P_t, for crack initiation and the length of the notches, a, in Bohus granite with K_{IC} equal 2 MN/m$^{3/2}$ and P_t equal 16 MPa as illustrated in Fig. 3.11 (Bjarnholt et al., 1983).

The spacing can be greater than in other control blasting methods, but depends on the degree of jointing and other discontinuities. Fracture control blasting can be utilized in both open pit mines and underground excavations. Table 3.12. shows the

Table 3.9 : Blast geometry for smooth blasting.

Year	References	Hole Diam.	Charge Diam.	Explosive	Spacing	Burden
		(mm)	(mm)	(kg/m)	(m)	(m)
1969	Du Pont Blasters' Handbook	51-64	-	0.12-0.38	0.90	1.20
		76-89	-	0.20-0.75	1.20	1.50
		102-114	-	0.38-1.13	1.50	1.80
		127-140	-	1.13-1.50	1.80	2.10
		152-165	-	1.50-1.75	2.10	2.70
1980	Underground excavation in rock	25-32	11	0.08	0.25-0.35	0.30-0.45
		25-48	17	0.20	0.50-0.70	0.70-0.90
		51-64	22	0.44	0.80-0.90	1.00-1.10

Table : 3.10 Advantages and disadvantages of smooth blasting.

Advantages	* Reduces overbreak. * Requires less wall and roof support.
Disadvantages	* Careful loading and stemming. * More drilling so more cost and time. * The method can not eliminate the ground support in highly fractured rock.

advantage and disadvantage of fracture plane control blasting.

Table 3.11 : Fracture toughness values for different rock types (Fourney et al., 1984).

Rock types	K_{IC} psi.(in)$^{1/2}$	Rock types	K_{IC} psi.(in)$^{1/2}$
Limestone	598 - 903	Salem Limestone	862 - 2390
Sandstone	164 - 180	Barre Granite	4660 - 6910
Grey Granite	2024	Sioux Quartzite	1280 - 5220
Red Granite	2021	Dresser Basalt	4880 - 17260

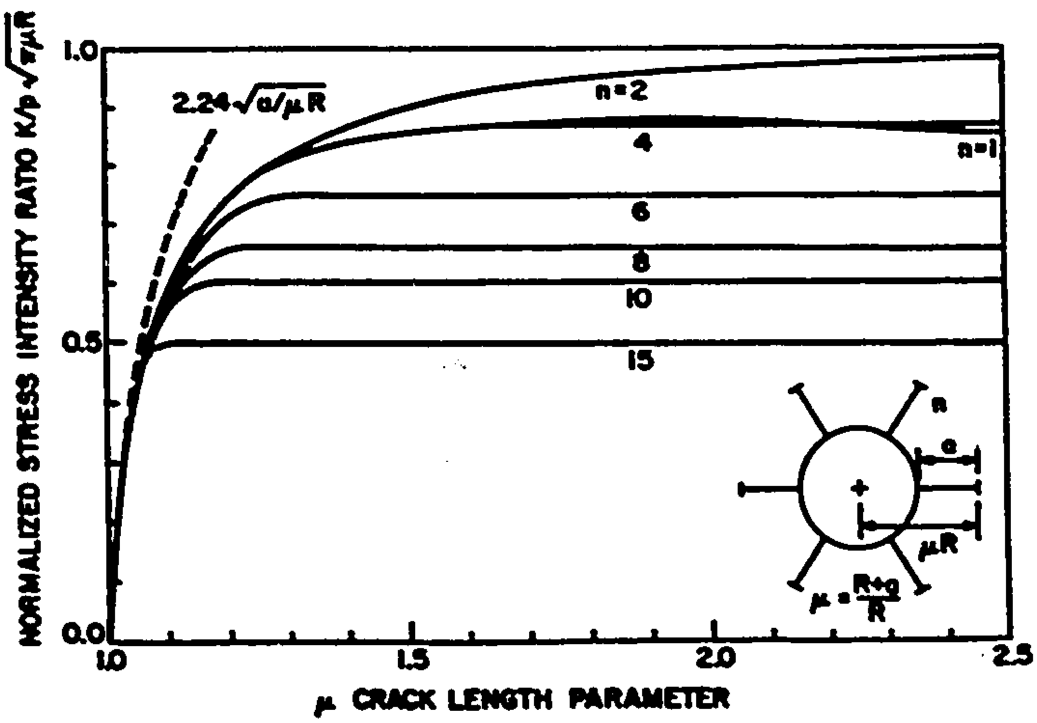

Figure 3.9 : Normalized stress intensity factor values for the pressurized circular hole with radial cracks as a function of crack length for various crack numbers (Ouchterlony, 1974).

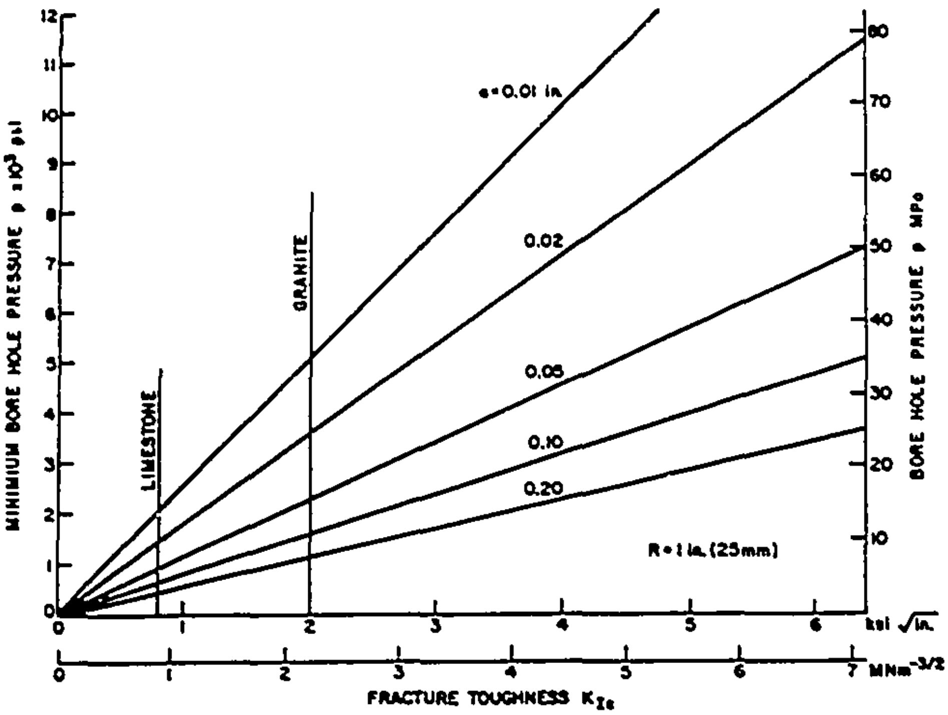

Figure 3.10. Pressure required to initiate cracks at the borehole (Fourney et al., 1984).

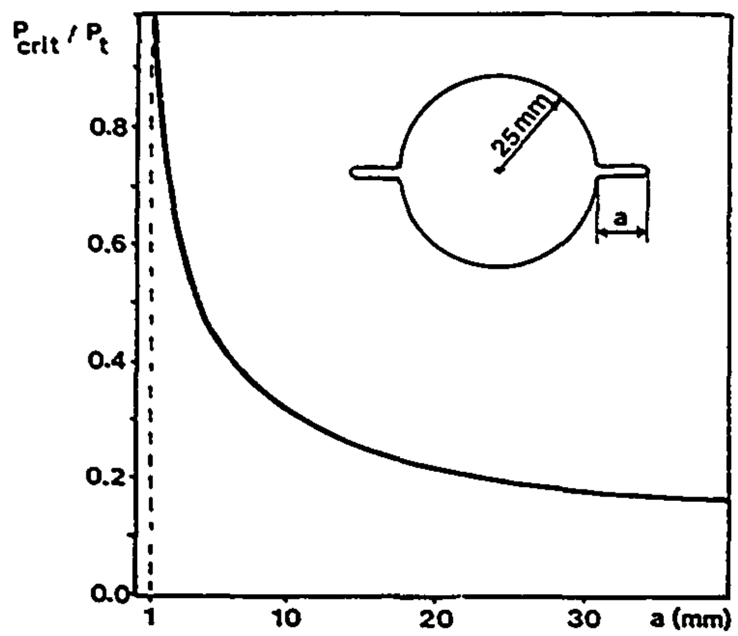

Figure 3.11. Ratio of necessary borehole pressure for crack initiation as a function of the length of notch (Bjarnholt et al., 1983).

Table 3.12 : Advantages and disadvantages of fracture control blasting.

Advantages	* Reduce the number and explosive loading of the perimeter holes. * Can yield very good results in highly jointed, fractured, weathered rocks which can not be achieved with the other control blasting methods. * Reduce drilling cost due to greater spacing, specially in homogenous rocks.
Disadvantages	* The installation of the notches on the side of a borehole is difficult and needs more time, additional equipment and additional step.

3.7 CURRENT PRACTICES

A survey (henceforth referred to as survey 2) of current wall-control blasting practice was carried out as part of this investigation. A brief questionnaire was sent to collect the following information from North American Mines:

- Wall-control blasting methods
- Geometry of production and perimeter blasting.
- Rock types and their properties.
- Explosives types and explosive properties.
- Type of initiation and delay design.
- Criteria of assessment of wall control blasts.

Despite the limited nature of responses, the survey did yield valuable trends, and information on current practices. Figures 3.12 and 3.13 illustrate borehole diameter versus spacing for various perimeter blasting practices. Based on survey 1, boreholes with diameter ranging from 64 to 250 mm and spacings from 1 to 5.5 m were used in most mines. In pre-splitting, the spacing increased with borehole diameter, and the data points show a linear trend between these two parameters. In cushion blasting the dispersion of data points indicate that spacing is increased as borehole diameter increased, but the agreement is only qualitative.

Figure 3.13 illustrates the current perimeter blasting practices (survey 2). As shown, the boreholes have a diameter of 165 to 380 mm and spacings of 1.5 to 5.5 m. However, boreholes of 250 and 275 mm diameters and spacings between 2.5 and 5.5 are most commonly used. A linear trend also exists between spacing and borehole diameter for pre-split holes when loaded with bulk explosives in a decoupled manner (avg. 0.3). In most cases, the toe loaded holes are used with bulk explosives without any stemming. The weight of charges varies from 40 to 200 kg per hole, and depends on the properties of rock, spacing, borehole diameter and type of loading.

The scatter of toe loaded data points does not indicate that any positive correlation between spacing and borehole diameter. For example, Table 3.13 shows the relation between spacing and borehole diameter for toe-only loaded holes.

Figures 3.14 and 3.15 show the borehole diameter over decoupling ratio versus spacing in past and current practices. Decoupling is usually used to minimize overbreak to final pit walls. An annular air gap around the charge absorbs some of the energy and significantly reduces the peak pressure. These figures also show a linear trend between spacing and borehole diameter over decoupling ratio for pre-split holes when loaded with cartridge or bulk explosives. However, no correlation can be established for toe-only loaded holes. The dispersion of cushion blasting data points indicate that less linear trend exists between spacing and borehole diameter over a range of decoupling ratios.

Table 3.13 : Relation between spacing and borehole diameter for toe loaded holes.

Borehole diameter	Spacing
(mm)	(m)
250	3.7, 4.6 and 5.5
270	3.5 and 3.7
350	2.5
380	4

The assessment of results from both survey 1 and survey 2 indicate that the final pit wall conditions varied from good to poor. The summery of current survey of wall control practices are shown in Table 3.14.

3.8 CONCLUSION

The most current survey (survey 2) unfortunately had limited response from the mines. Also, there appears to be a general lack of a quantified approach to wall-control blasting and characterization of blast-induced damage in mines. However, several valuable guidelines can be gleaned from these surveys.

Based on both surveys (survey 1 and 2), it is concluded that spacings and hole diameter have an approximately linear correlation for pre-split holes with a decoupled explosive column. It is clear that geology varies from one mine to another and also at different location in the same mine, and hence the lack of exact correlation.

The data do not show any positive correlation between spacing and borehole

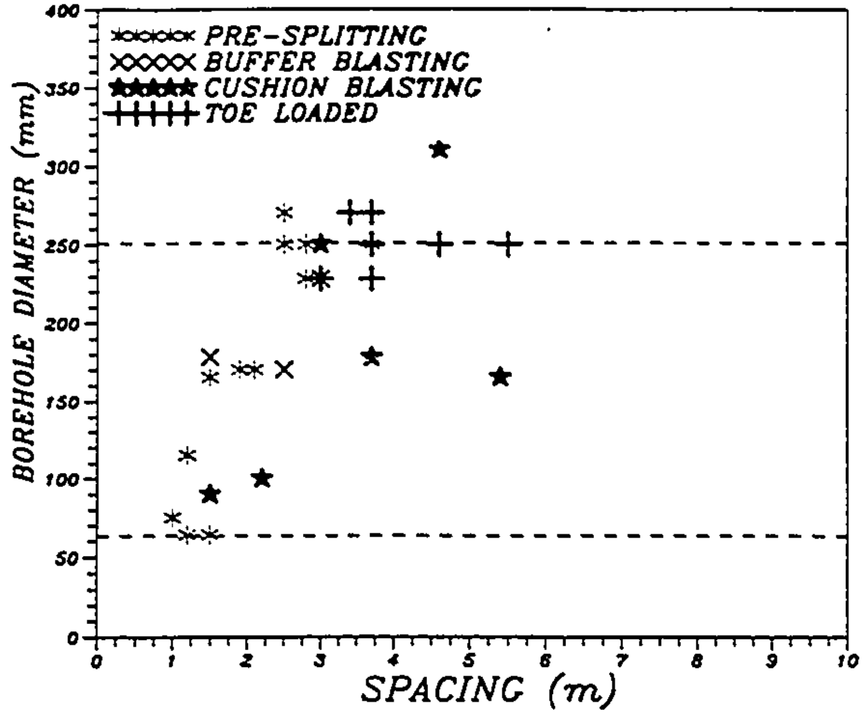

Figure 3.12 : Borehole diameter versus spacing (1977-survey).

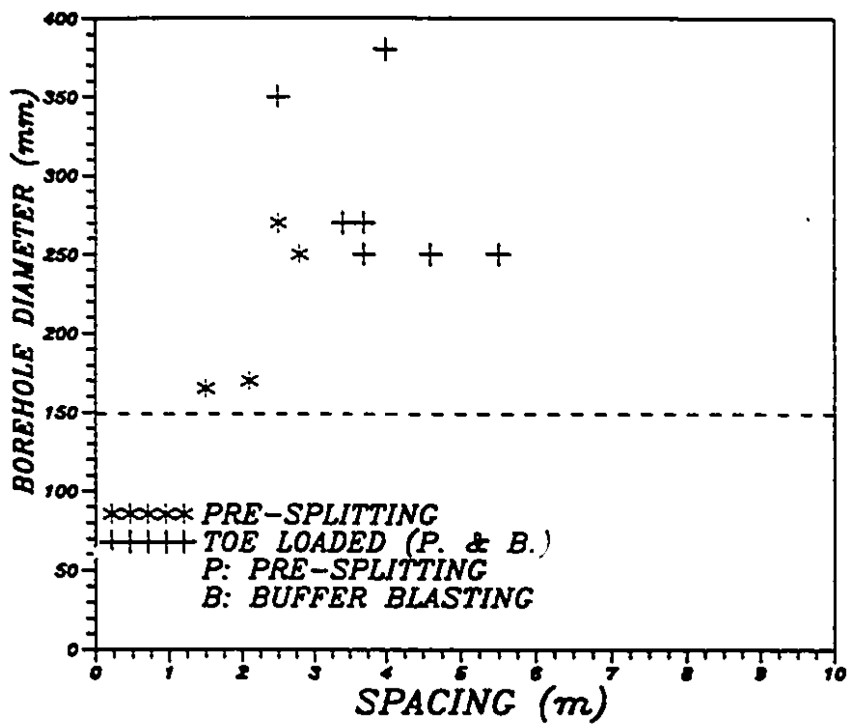

Figure 3.13 : Borehole diameter versus spacing (1992-survey).

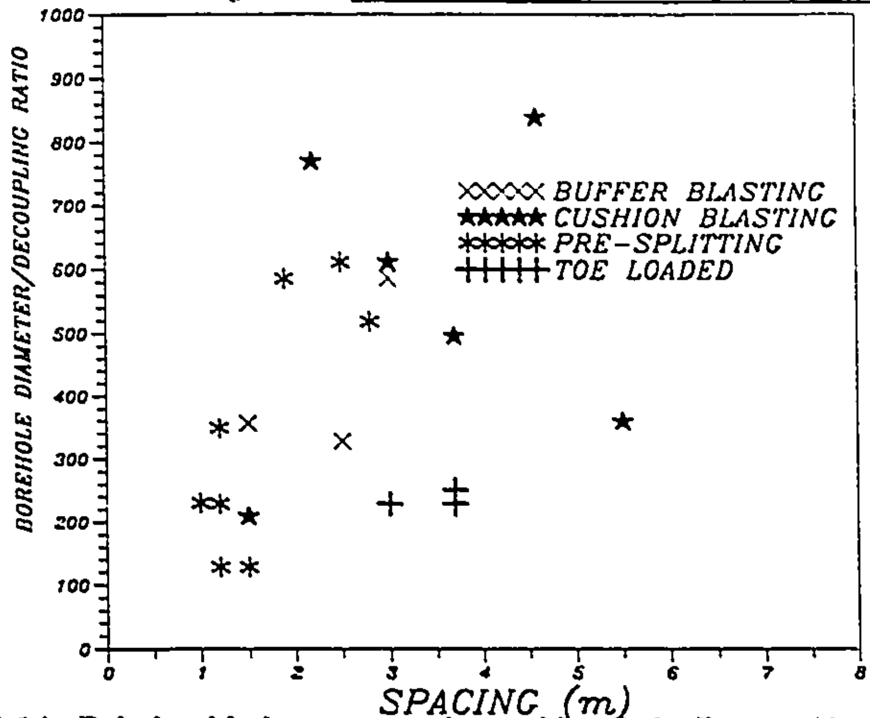

Figure 3.14 : Relationship between spacing and borehole diameter/decoupling ratio (1977-survey).

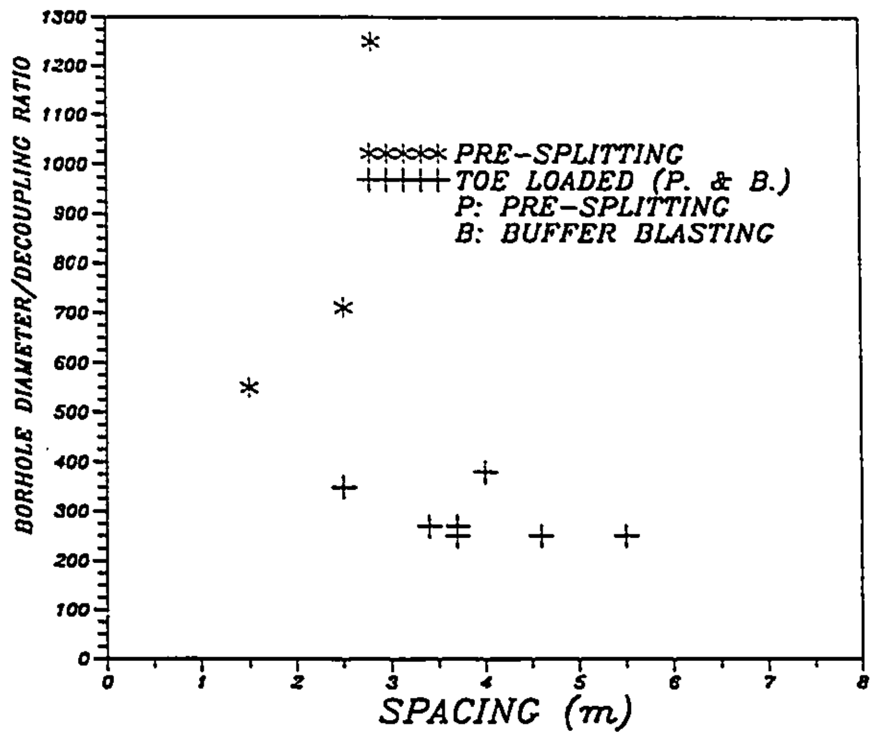

Figure 3.15 : Relationship between spacing and borehole diameter/decoupling ratio (1992-survey).

diameter for toe loaded holes. This is attributed to non-uniform explosion pressure compared to that from a column charge of explosives with an approximately constant pressure from the toe to the top of the hole. In toe-loaded holes, the pressure in the toe region are greater than in the rest of the hole.

In cushion blasting, the burden in the toe is usually greater than that in the collar region. Also, the rocks is fractured more intensely in the latter due to blasting in the preceding level. These conditions affect the relationship between the spacing and borehole diameter, resulting in a less clear trend between spacing and borehole diameter, as shown in the figures.

Table 3.14 : Summary of current wall control blasting practices.

Borehole Diameter	Spacing	Decoupling Ratio	Charge Weight	Stemming	Stemming Materials	Wall-Control Blasting Method	Type of Ore	Assessment
(mm)	(m)	-	(kg/hole)	-	-	-	-	-
250	2.8	0.2	25	Full Length	Crushed Rock	Pre-splitting	Asbestos	Not listed
105	1.5	0.3	45	None	None	pre-splitting	Copper	Backbreak at crest
250	7.0	1	-	9 m	Drill Cuttings	Pre-splitting	Copper	Some backbreak
270	2.5	0.38	74	None	None	Pre-splitting	Copper	No loose material
270	6.0	1	272	Top: 6.6 m Between Deck:2.4	Drill Cuttings	Pre-splitting	Copper	Damage to backwall
350	2.5	1	-	11.4 - 12.6 m	Drill Cuttings	Cushion blasting	Copper	Damage to backwall
380	4	1	200	None	None	Pre-splitting	Iron	Damage to backwall
250	5.5	1	68	7.2 m	Air bag	Pre-splitting	Iron	Some backbreak
250	6	1	61	Variable	Crushed Rock	Pre-splitting	Iron	Not listed
270	4	0.74	50	10.5 m	Air bag	Pre-splitting	Sandstone	No damage
270	2.7	1	49	None	None	Pre-splitting	Sandstone	Not listed

CHAPTER 4

ANALYSIS OF WALL-CONTROL BLASTING METHODS

4.1 INTRODUCTION

Line drilling was the first method to be used to control overbreak. Later, modification in line drilling produced some new methods of wall-control blasting methods, such as cushion blasting, smooth wall blasting and pre-splitting. Cushion blasting and smooth wall blasting with spacing and borehole diameter larger than line drilling are used to reduce backbreak in open cuts and underground openings. Pre-splitting is used to provide a weakness plane between the primary shots and the perimeter of excavations. Today, line drilling is only used in a limited way in open pit mines and open cuts to isolate the final pit walls from the production shots. However, all these techniques have been developed in the field, commonly on trial-and-error basis with corresponding advantages and disadvantages.

4.2 INVESTIGATION OF PREVIOUS WORK

Pre-splitting is the only wall-control blasting method which has been studied in detail. The pre-split phenomena was described theoretically by *Paine et al.*, (1961). They presented the following equations to calculate the magnitude of peak pressure at any point and the magnitude of peak tensile stress for the middle position between two holes with radius a, distance D and simultaneous initiation.

$$P_o = P_b.\sqrt{(a/R)}.e^{-KT} \tag{4.1}$$

When two cylindrical holes are detonated simultaneously the tensile stress in the direction tangential to the wave front at the midpoint can be calculated as:

$$E.\varepsilon_o = -\sigma P_b\sqrt{(2a/D)}.e^{-KD/2U} \tag{4.2}$$

P_o : Compressive peak pressure at a point

P_b : Borehole pressure

a : Radius of borehole

R : Distance from the centre of hole

K : Attenuation constant

T : Time

E : Young's modulus

ε_o : Strain

$E\varepsilon_o$: Tensile stress

σ : Poisson's ratio

D : Spacing

U : Velocity of stress wave

They concluded that the radial fractures are generated by tensile stress and started from each hole. The cracks lengths are increased by superposition of the stress waves at the midpoint on the centreline because the collision of shock wave tends to produce particle displacements which are perpendicular to the centreline and in the opposite direction against this line. The results of the wave fronts reinforcing between holes will be to increase the length of cracks to the point where they actually meet between the holes.

Based on this theoretical investigation, the superposition of the stress wave between two holes at the midpoint was considered the major cause for pre-split fracture. As shown in equation 4.2, one dimensional stress-strain relation is used to discuss the case of cylindrical wave propagation. There is no reason to believe that the radial cracks are produced just along the proposed breakeline and only the length of these cracks increases by displacement forces.

Langefors and Kihlstrom (1978) demonstrated the formation of cracks between final holes in two-dimensional model-scale blasting. They described the important factors of perimeter blasting and illustrated the results of experimental tests in plexiglass models. The authors considered the major factors of perimeter blasting such as: borehole diameter spacing, burden, charge weight, and their relations. They did not explain the mechanism of smooth wall blasting or pre-splitting methods from a theoretical standpoint.

Mathias (1965) studied pre-splitting process empirically in the laboratory with models of plexiglas and marble. He investigated the effects of changes in various parameters such as, borehole diameter, spacing, decoupling, borehole length, external pressure on the fracture pattern in plexiglas blocks. A series of 2 in. thick plexiglas plate models, were tested by several types of Mild Detonation Fuse (MDF) in single and multiple holes, with various amount of explosives (1 grain to 20 grains of PETN per ft). Work was also carried out on 3 in. thick of marbles.

He showed that two systems of radial fractures are developed; cylindrical fractures around the hole in all directions due to shock wave propagation, and longer cracks beyond the shock-wave induced fractures due to gas expansion. The author concluded that pre-split fracturing results from the fractures at the first stage and from the joining of gas-expansion induced fractures between adjacent holes.

Based on these tests, the author stated that the compressive stress parallel to the pre-split line have beneficial effect on the quality of the pre-split fracture, while, a compressive stress perpendicular to this line has adverse effect on the quality of the pre-split fracture. Also, the compressive stress parallel to the hole axis has no effect on the formation of pre-split fractures. The major part of his study concentrated on the effects of changes in various parameters on pre-splitting in plexiglas models. The conclusions are based upon his observation, and no theory is given to explain the phenomenon.

Aso (1966) studied the mechanism of pre-splitting by both theoretical and experimental means. He concentrated on the theoretical phase of his study using a model consisting of two infinitely long boreholes in an infinite elastic medium. The two holes were loaded with the same amount of explosive and detonated simultaneously. The diffraction effect at the boundaries of the holes was ignored. The author calculated the stresses and strains from various pressure-time curves for a single hole and then repeated for two simultaneous holes. He concluded that the decay of the compressive radial stress depend upon the rise time of the borehole pressure (times from the initiations of the borehole pressure to the development of peak pressure), and the decay of the tensile tangential stress depends upon the shape of the borehole pressure-time records. In the case of two boreholes, the author concluded that the pre-split weakness plane is caused by radial fracture around each hole and the interaction between stress waves from the holes at midpoint.

The validity of this postulate was checked experimentally on a small scale laboratory scale-model. But the experimental results did not validate all the theoretical predications. Cement-mortar blocks (30 in long, 20 in wide and 10 in high) were tested in the experimental phase. A 50 grain/ft detonation cords served as the explosive source.

Based on the experimental results, the following breakage process was proposed: 1) an incipient crack opens and closes at 2.5 inch from the centre of holes, 2) the opening of a large crack at the midpoint due to collision between stress waves and 3) spreading of this large crack towards the holes. The author concluded that the pre-splitting phenomena depends mainly upon stress wave, and the role of gas pressure was negligible.

In a parallel investigation, *Kutter* (1967) studied the interaction between stress wave and gas pressure in the fracture process, then applied the results of this consideration to pre-splitting. He investigated the fracture process around the cavity under dynamic and quasi-static pressure separately. Laboratory scale-models of glass, plexiglass and four rock types (charcoal, Tennessece marble, basalt and salt) were used to analyze the experimental phase under dynamic pressure. Based on the experimental and theoretical investigation under dynamic pressure, he concluded that the very dense radial fractures zone are caused by tensile hoop stresses around the cavity and close to this zone; radial fractures in the second zone were extension of the some of the cracks of the first zone.

Fracture extension was studied under quasi-static pressure. He analyzed a pressurized star-cracked hole in an infinite plate. The author assumed that the gas does not penetrate into the small fissures and pores of the rock, but it stays within the large radial cracks and the cavity. Also, the gas pressure is assumed to remain constant during crack extension and all the radial cracks arranged symmetrically around the cylindrical cavity with equal lengths.

In the third phase, the roles of stress waves and gas pressure were investigated for pre-splitting as functions of delay between the holes. He concluded that, i) the stress wave itself is unable to complete the full fracture process and, gas pressure plays a vital role in pre-splitting, ii) the most complete generation of pre-split plane can be expected, with zero delay interval, and iii) the success of pre-split depends strongly on in situ geological structure.

Despite many key findings, the work suffered because it was limited to plexiglass and rock models in the laboratory. The mechanism of pre-splitting was based on a theoretical approach, and the author did not verify the theoretical predictions experimentally.

Sanden (1974) equated the pre-splitting process with pressurized thick-wall cylinder. He derived several equations to calculate the spacing between perimeter holes and borehole pressure. He showed that the maximum spacing between pre-split holes can be calculated by:

$$S = \frac{2 \times D \times P_b}{T} \tag{4.3}$$

Where S is the spacing between boreholes (in), D is the borehole diameter (in), P_b is the borehole pressure (psi), and T is the tensile strength of the rock (psi).

The validity of the theoretical equations was checked experimentally on rectangular limestone blocks and in the field with small diameter holes (45 mm), and in a skarn-magnetite rock formation with large diameter holes (175 mm). A 50 grain per foot detonating cord (PETN) and 400 grain per foot (TNT-PETN) were used in limestone blocks and in the field tests respectively. He concluded that the experimental program validated his theoretical prediction.

However, the effect of geology and rock properties, type of explosive, length and direction of fractures was not deal with in his work. The author did not explain the major parameters of perimeter blasting and their relationship. Equation 4.3 can not be applied under all conditions to calculate the distance between pre-splitting shots, and under certain conditions, leads to absurd results.

Worsey (1984) Studies the mechanism of pre-splitting method and the effects of discontinuities on the blast results in model blasting in blocks of plexiglas, concrete and rock. In the first part of his study, the role of the dynamic and quasi-static pressures are discussed separately on pre-split blast. A series of single and multiple holes were tested in blocks of polyester resin with detonating cords.

He concluded that the pre-split fracture is caused by both dynamic and quasi-static pressures. In normal pre-split practices, no fracturing was initiated at the midpoint between two holes by the superposition of the dynamic shock waves. He stated that the pre-split fractures formed primarily by the overlapping of the fracture zones from the neighbouring boreholes.

He also discussed the influence of single and multiple discontinuity(ies) as well as the orientation of discontinuities with the final face on the results of blast in blocks of plexiglas, concrete and rock. The validity of the experimental results were checked with results obtained from field observations on roadcuts.

Based on these series of tests, he concluded that the orientation of the discontinuity with the final face is the most important factor which influenced the success of pre-split blasts. From the field observation, he showed that the drilling accuracy is the most important non-geotechnical factor affecting the success of the pre-split blast.

4.3 CONCLUSIONS

Despite of many studies in this area in the past, an entirely satisfactory theory has not been developed to explain the mechanism of pre-splitting. In fact, mechanism of generating a weakness plane is still a complex process in pre-splitting. The relative roles of stress waves and gas expansion still remain a matter of considerable interest. Some researchers emphasize on the action of stress waves, whereas others emphasize the gas pressure. Aso (1966), for example, postulated that fracture starts at the midpoint due to the effect of the interaction of shock waves, whereas Kutter (1967) demonstrated that cracks begin to form at the boundary of each hole by shock wave and propagated by the quasi-static pressure. In view of these, it is clear that no unifying theory currently exist which can be used to describe all aspects of pre-split and related blasts.

Laboratory and field investigations are necessary to understand clearly all basic mechanisms which govern the creation of a weakness plane between production blasts and final pit walls or any other structure. The purpose of this research is to make a comprehensive study of wall-control blasting techniques so as to correlate theory with empirical practice on a more sound basis.

CHAPTER 5

NUMERICAL MODELLING

5.1 INTRODUCTION

Analytical solutions are among the best methods to investigate stress fields around pressurized holes, but they are unable to answer all the practical questions. In engineering, many existing problems are extremely difficult or impossible to solve by analytical methods. One possibility is to simplify the problems to the point where analytical solutions can be used effectively. In some cases this procedure works, but in many cases it is not possible to obtain closed-form solutions; however, the emphasis in engineering analysis moves towards more versatile numerical solutions. One class of these methods is called the finite element method.

A number of studies has been carried out to analyze the stress distribution around a loaded hole with explosive in the presence of a horizontal free face (infinite burden). Most of these studies discussed and modeled the in-situ fragmentation for oil shale fragmentation (Trent, et al., 1981; Young, et al., 1985; McHugh et al., 1985; Shaffer et al., 1987). The stress distribution through the hole in a vertical section by two dimensional finite element program and the effect of bench height and burden in a three dimensional bench have been studied by Ash (1973) and Smith (1976) respectively. The effect of burden on the free face movement has been discussed by the Haghigh and Konya (1985) under quasi-static pressure. Sunu et al. (1988) have studied the stress and displacement in the burden region in a vertical section in a single hole by two-dimensional dynamic finite element program. The effect of borehole diameter at constant burden on the distribution around a pressurize' hole was discussed by Bhandari (1979), Ghosh (1990), Ghosh and Daemen (1995), and Carbonell and Detournay (1995). Song and Kim (1995) have also attempted to model the Smooth blasting process.

These studies largely deal with the condition of stresses in normal production blasting, except for Song and Kim (1995). None of these studies however consider the effect of free face or discontinuities on the stress field around pressurized holes, especially on the centreline between the holes which is a critical line for wall-control blasting methods.

However, as mentioned earlier, a simple analytical expression is available to describe the mechanism of the wall control blasting method with infinite burden. In this analysis, the stresses depend only upon the borehole pressure and the width of the material surrounding the borehole. The strength properties of the latter, the influence of free face and any type of discontinuity are ignored in this approach. However, treatment of the latter is crucial to understand the mechanism of fracturation in rock under realistic conditions. The effects of these parameters on the stress distribution can be studied by numerical approach and field investigations. To illustrate this case, a two-dimensional finite element modelling has been carried out to determine the effect of the presence of a free face, and a parallel, normal and inclined joint or weak plane to the free face on the stress field around a pressurized hole, and between two and three pressurized boreholes.

5.2 FINITE ELEMENT METHOD

The finite element method is a numerical procedure to obtain approximate solutions to complicated problems which engineers and scientists are called upon to solve. This method was introduced in 1956 by Turner et al. to analyze aircraft structure. Since 1960, the finite element method has been successfully applied to a large number of problems in such widely different fields as: structural mechanics, soil mechanics, rock mechanics, fluid mechanics, heat conduction, and blasting (Rao, 1989; Huebner, 1975).

In all finite element analysis, a given problem is modelled by dividing it into a mesh of small subregions. The body or solution region is called the domain, and each part of mesh area is called an element. These elements are considered to be connected at specified points which are called nodes or nodal points. An element may also have a few interior nodes. The choice of mesh is arbitrary. The configuration, shape, size and number of the elements in a model depend upon the desired accuracy of the results.

The size of the elements has a direct influence upon the final solution, and they have to be chosen carefully. In a mesh configuration, the elements need not be the same size. The general rule is to have a finer mesh where sharp changes in the stress are expected. Although increasing the number of elements generally gives a better approximation of the solution; for any given problem there will be an optimum number of elements beyond which the accuracy cannot be improved by further refinement of the mesh, (Fig. 5.1). The aspect ratio of the elements, the ratio of the largest dimension to the smallest dimension of each of two-dimensional elements, also affects the final solution.

The boundary conditions of the analysis domain should be chosen carefully. In most problems, such as beam, plate and shell analysis, the boundaries of the solution region are clearly defined. These boundary conditions should be satisfied on the nodes along the boundary of the structures. Depending on the finite element, a different number of degrees of freedom can be considered per node. The nodes on the boundary can be either completely or partially fixed or moved and rotated in x, y or z directions freely. For example, in a two-dimensional plane strain analysis each node has two degrees of freedom.

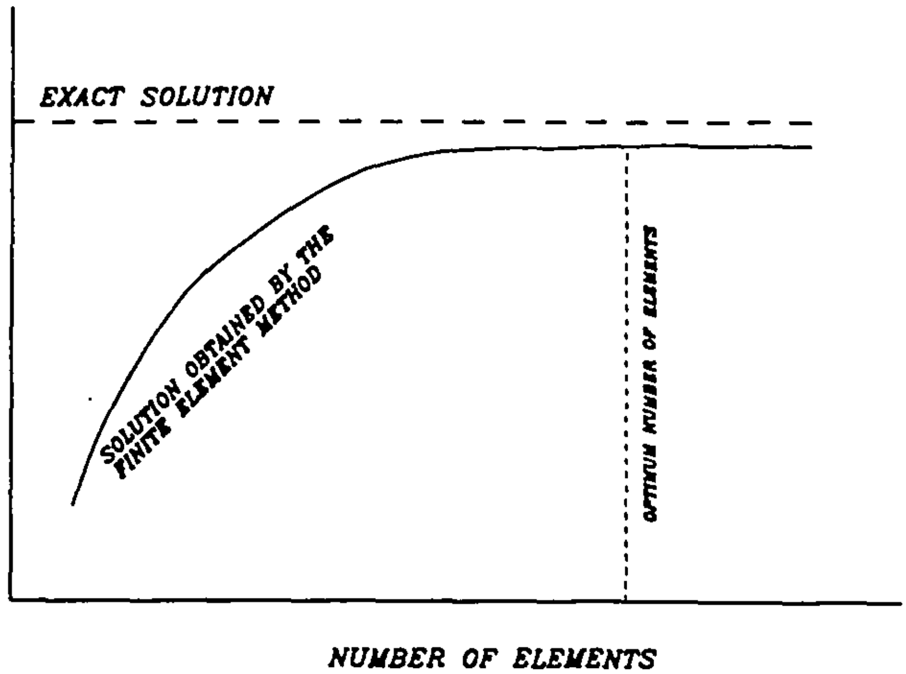

Figure 5.1 : Relation between the number of elements and convergence results obtained by the finite element method.

As stated before, in the finite element method, the body or domain is divided into smaller subdivisions, known as elements. These elements are connected to each other at specific points (called nodes) within or on the boundary of the element. Displacements at these nodes are treated as unknowns and should be calculated during the analysis. The nodal displacements are related to the external forces through the equilibrium equations as will be discussed later in this section. The resulting system of simultaneous equations can be solved to obtain the nodal displacement. Displacement at any point within an element are related to displacement at nodes using the shape functions. Therefore, strain can be determined from the displacement field within an element using the strain-displacement relationship. Based on the governing strain-stress relation, stresses at any point of the element can be calculated from the corresponding strains.

In the finite element procedure, the coordinate values of nodal points of each element (element nodal displacement) are arranged into a matrix $\{D\}_n$, and the elastic properties of the material set up into the constitutive matrix [E]. The element stiffness matrix in a local coordinate system $[K_m]_n$ is obtained from

$$[K_m]_n = \int_{v^e} [B]^T [E] [B] \, dv^e \tag{5.1}$$

in which [B] is the strain-displacement matrix, [E] is the constitutive matrix and v^e is the element volume.

The above integration is evaluated using one of the numerical integration schemes such as the Gauss-quadrature procedure. The transformation of the element stiffness matrix from the local to the global axes is performed by:

$$[K]_n = [T]^T [K_m]_n [T] \tag{5.2}$$

in which $[K]_n$ is the element stiffness matrix in the global coordinate system and [T] is the transformation matrix. The global stiffness matrix of the whole structure [K] is obtained using the summation of the element stiffness matrices. This process can be represented symbolically by:

$$[K] = \sum_{n=1}^{N} [k]_n \tag{5.3}$$

where N is number of elements in the domain.

For linear analysis, equilibrium equations can be expressed as:

$$\{F\} = [K] \{D\} \tag{5.4}$$

where [K] is the stiffness matrix of the structure, {F} is the total force vector due to in situ stress, gravity and boundary pressure, and {D} is the nodal displacement vector, all in the global coordinate system. The displacement at any point of the element can be evaluated in terms of the displacements of the nodal points on the boundaries, or within the element as:

$$\{u\} = [N]\,\{U\}_n \tag{5.5}$$

where {u} is the displacement at any point of the element, [N] is the matrix of shape function and $\{U\}_n$ is the element nodal displacement vector in the element local coordinate system.

The strain at any point of the element, $\{\varepsilon\}$, is related to the element nodal displacement, $\{U\}_n$, by the following equation:

$$\{\varepsilon\} = [B]\,\{U\}_n \tag{5.6}$$

where [B] is the strain-displacement matrix and can be obtained as:

$$\{B\} = [L]\,[N] \tag{5.7}$$

in which [L] is the differential operator matrix and defined such that:

$$\{\varepsilon\} = [L]\,\{U\} \tag{5.8}$$

In two-dimensional problems, the strain vector, differential-operator matrix and the displacement vector are defined as:

$$\begin{Bmatrix} \varepsilon_x \\ \varepsilon_y \\ \gamma_{xy} \end{Bmatrix} = \begin{bmatrix} \dfrac{\partial}{\partial x} & 0 \\ 0 & \dfrac{\partial}{\partial y} \\ \dfrac{\partial}{\partial y} & \dfrac{\partial}{\partial x} \end{bmatrix} \begin{Bmatrix} u \\ v \end{Bmatrix} \tag{5.9}$$

Based on the stress-strain relations, stress at any point of the element can be found as:

$$\{\sigma\} = [D]\,(\{\varepsilon\} - \{\varepsilon^{\circ}\}) + \{\sigma^{\circ}\} \tag{5.10}$$

where $\{\varepsilon^{\circ}\}$ is the vector of initial strain, [D] is the material property or material stiffness matrix and σ° is the in situ stress.

If the problem is in plane strain, for an isotropic material, matrix [D] is defined as

$$[D] = \frac{E}{(\nu + 1)(1 - 2\nu)} \begin{bmatrix} 1 - \nu & \nu & 0 \\ \nu & 1 - \nu & 0 \\ 0 & 0 & \frac{1 - 2\nu}{2} \end{bmatrix} \tag{5.11}$$

In summary, the solution of a problem by the finite element method can be stated as follows:

a. The structure or solution region must be divided into an adequate number of subdivisions or elements to obtain the global stiffness matrix, [K], and the total force vector, {F}, of the structure. These elements are assumed to be connected at specified points which are known as nodes. The displacements of these nodal points will be the basic unknown parameters of the problem. Type, number and size of the elements affect the final results and will depend upon the structure, loading conditions and accuracy required.

b. The element stiffness matrices must be derived for each element in the local coordinate system. This local coordinate system usually changes from element to element.

c. The element stiffness matrix must be transformed from the local coordinate system to the global coordinate system using a matrix which is called the transformation matrix.

d. The global stiffness matrix and global element nodal force vector must be assembled in a suitable manner, as outlined in any elementary text book on finite elements. The equilibrium equations have to be formulated as [K] {D} = {F} for the complete structure.

e. The equilibrium equations must be solved for the unknown nodal displacements.

f. Finally, the element results, such as strains, stresses and internal forces, can be computed from the nodal displacements using the corresponding equations.

5.3 FINITE ELEMENT PROGRAMS

Two finite element programs have been used to analyze the stress distributions in the regions of interest. These programmes are named *e-z tools* and *I-DEAS*.

5.3.1 Finite Element Program, *e-z tools*

This is a linear elastic program for stress and stability analysis of two-dimensional models on surface and underground excavation in rock and soil materials (Mitri, 1993). The program consists of three models: preprocessor, core program and postprocessor which are named, EZPRE, EZCOR and EZPOST respectively.

The preprocessor displays the model layout, boundary conditions, and types of material structures. The layout of the problem domain is divided into quadrilateral areas known as "zones" (Fig. 5.2). It reads a prepared data file (file.DAT) to create the required data file for the core program (file.COR). It then displays the finite element "mesh" as well as the proposed sequence of excavation. The core program reads the created data file by preprocessor. It calculates the nodal displacement and stresses within the elements and stores complete results in a file called file.DOC. It also produces three output files for processing by postprocessor which are called: file.NDE, file.DIS and file.STS.

The postprocessor reads the output files and transforms them into graphical nodal displacements and the principal stresses at the element's centroidal point. All the graphic

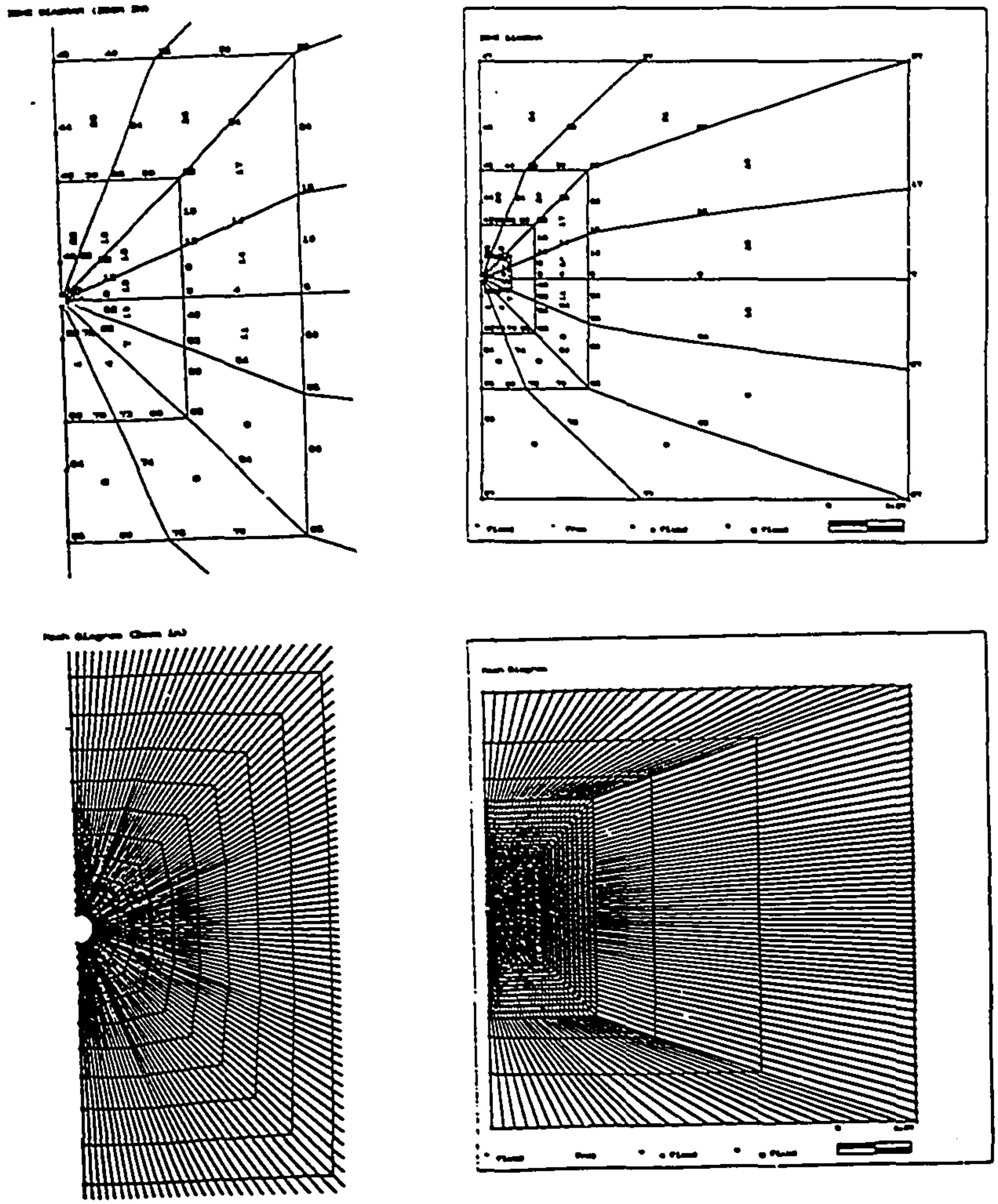

Figure 5.2 : Finite element mesh around a pressurized hole model by *e-z tools*.

results can be viewed on the monitor or relayed to a printer. The *e-z tools* program has been developed to calculate the stresses in x, y and z directions as well as the principal stresses and their orientation at each point.

5.3.2 Integrated Design Engineering Analysis Software, *I-DEAS*

I-DEAS is an integrated mechanical engineering software tool which has been developed by Structural Dynamic Research Corporation, SDRC (Lawry, 1991; I-DEAS, 1990). The program is made up from a number of "families" of software models. The main families are: solid modelling, drafting, finite element modelling and analysis, system dynamics, test data analysis and manufacturing. A complete finite element model can be built by *I-DEAS*, including physical and material properties, loads and boundary conditions. The finite element analysis consists of three steps: preprocessing, solution and postprocessing.

Preprocessing is graphically complete. It includes the process of developing the geometry of a model, creating of mesh, entering three physical and material properties, describing the boundary conditions and loads, and checking the model (Fig. 5.3). The triangular and quadrilateral elements are available in the library of element types. These elements have two or three nodes along each edge and are known as linear and parabolic elements, respectively. The *I-DEAS* model solution can solve linear statics, dynamics, heat transfer, and potential flow analysis. Postprocessing tasks display and interpret the results of an analysis after the solution is completed. It can generate a display of deformed geometry, as well as the other plots.

5.4 FINITE ELEMENT MODELLING

e-z tools is designed to serve as a useful analytical tool for mining engineers. The *I-DEAS* program is used to complement it for generating a symmetrical mesh for

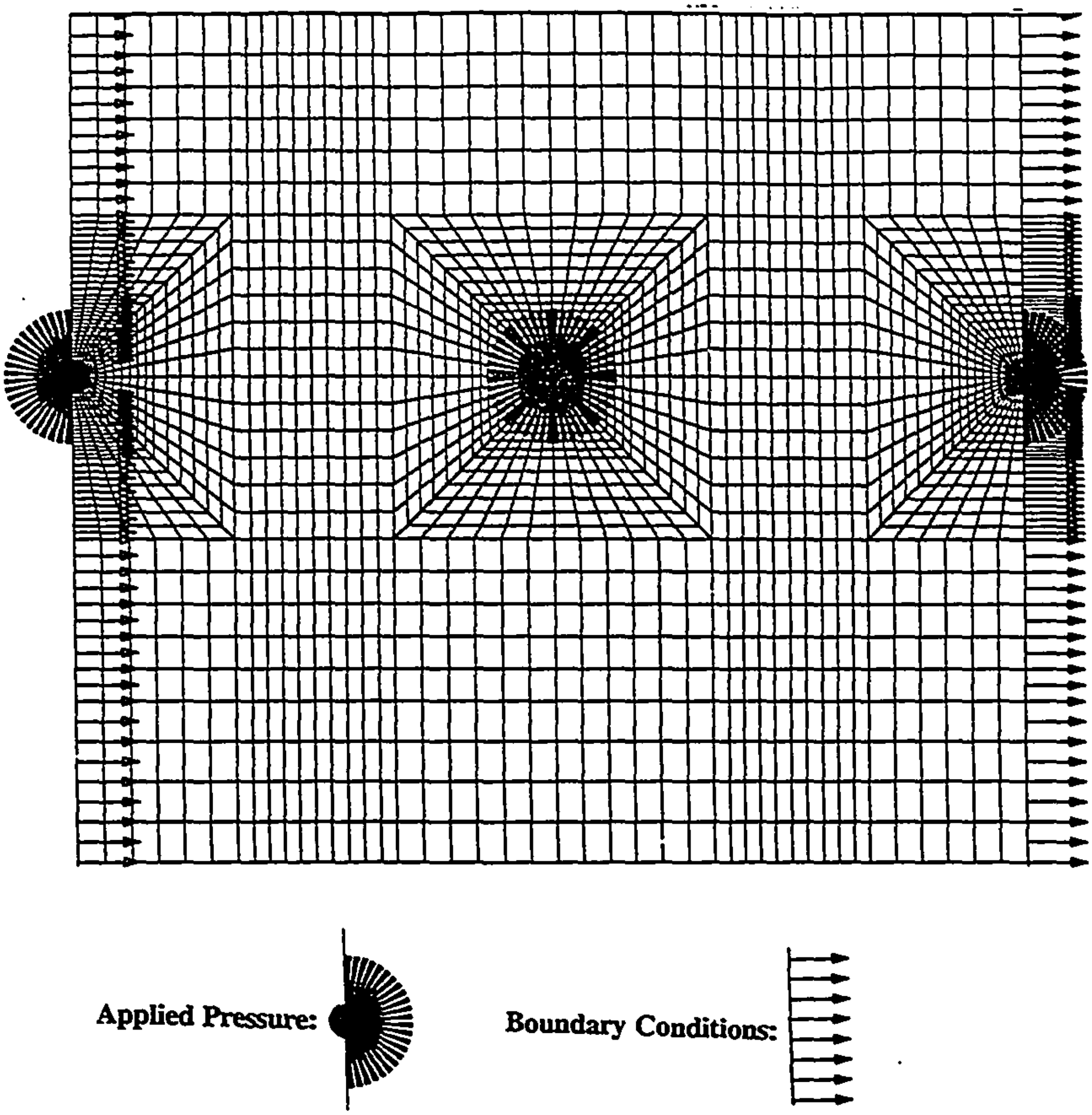

Figure 5.3 : Finite element mesh around and between three pressurized holes model by *I-DEAS*.

multiple or triple circular shapes in the solution region. The *I-DEAS* program is used to analyze the stresses between two and three pressurized holes. Therefore, the numerical investigation in this chapter is divided into the following steps:

1. Analysis of stress field around a pressurized hole by *e-z tools* program.
2. Analysis of stress field for two and three pressurized holes by *I-DEAS* program.

In both models, the five following cases have been analyzed: a) effect of a free face, b) effect of a narrow weak plane parallel to a free face at constant burden, c) effect of a fixed weak plane with two different burdens, d) effect of a weak plane of various width, e) effect of a weak plane normal to a free face at constant burden and f) effect of inclined weak plane.

The concept of weak planes with varying compliances is used to simulate joints, faults and foliation planes in rock and their effect on the stress field.The material properties of the rock and weak plane are presented in Table 5.1. The properties of the two media chosen represent an average rock and a weak cementing or gouge material for a weak plane. The results are normalized in terms of borehole pressure and radius to facilitate extrapolation of the results to other geometries and explosives.

Table 5.1 : Material properties of the rock and weak plane.

Material Properties	Unit	Rock	Weak Plane
Modulus of Elasticity	(GPa)	40	0.4
Poisson's Ratio	-	0.15	0.4
Density	(g/cm^3)	2.5	2.1

In all cases, a 100 mm diameter borehole is pressurized at 2000 MPa. This corresponds approximately to the explosion pressure generated by detonation of a fully-coupled ANFO explosive charge. It should be noted that a simple case is modeled first by these two programs before modelling the more complex problems. The results obtained are compared to each other as well as to the analytical solution.

5.4.1 Simulated Models By *e-z tools* Program

For the present investigation, a horizontal section normal to the axis of the pressurized hole has been modeled using the above program. The zone of interest lies on lines which are normal to the free face and straddle the hole centre. The models utilize the symmetry of the y-axis. This approach reduces the number of elements required to model the problem and the size of the matrix formed to solve the equations. For the single hole case the three geometries investigated are effects of a) a free face, b) a weak plane between borehole and the free face and c) a weak plane normal to the free face at the side of hole.

5.4.1.1 Free Face

The dimension of burden in the simulations is 5 to 20 times the hole diameter. These values are realistic for different types of wall control blasting methods used in mines, quarries and road cuts. The boundaries are fixed in the x-direction at the right and left sides of the models and in the y-direction at the back of the holes. For each burden, radial and tangential stresses have been calculated around the pressurized borehole.

5.4.1.2 Weak Plane Parallel to Free Face at Constant Burden

In this case, the effect of the presence of a weak plane, such as clay-filled joints, on the stress field is analyzed. It consists of placing a weak plane parallel to the free face but at varying distances from the borehole. The distance of weak plane from the borehole wall ranges from 5 to 12.5 borehole diameters, and the burden is fixed at 15 borehole diameters.

5.4.1.3 Fixed Weak Plane Parallel to Free Face

The converse case of a variable weak plane is modeled in this section. The weak plane is fixed at seven and half times the borehole diameter for various burdens. The radial and tangential stresses are calculated around the hole for two burden distances, (10 and 15 times borehole diameters), and compared with the same model but in the absence of any weak planes.

5.4.1.4 Weak Plane with Various Widths

The effect of weak planes of varying widths is analyzed at constant burden. The width of the weak plane (located at a distance of ten borehole diameters) is varied from 1 mm to 40 mm, for a constant burden (15 $\times$ borehole diameter).

5.4.1.5 Weak Plane Normal to Free Face

In the last case, the effect of a weak plane normal to the free face on the stress field is discussed. This plane is also perpendicular to the line which connect the centres of two holes. In the mechanism of wall control blasting methods the stresses on the centreline between two holes play a very important role creating a fracture zone between the holes (centreline). The distance of the weak plane from the hole centre in different simulations is 5 to 15 times the hole diameter at constant burden.

5.4.2 Simulated Models by *I-DEAS*

In the second phase of analysis, the five earlier cases will be repeated, as well as an inclined weak plane. This weak plane is placed in the back and between the holes. A horizontal section normal to the axis of the pressurized holes has been modeled using the *I-DEAS* program. The zone of interest is divided into three and four different sections for two and three holes, respectively. These sections are located on the centreline, along directions normal to free face and connecting the pressurized boreholes, and midpoint between two holes, named C, N1, N2 and N3, (Fig. 5.4). All the normal lines are continued to the back of the holes. The models utilize the symmetry of the y-direction as far as possible.

5.4.2.1 Free Face

The spacing between two holes in the models is 10 and 15 times the hole diameter. These values are realistic for different types of wall control blasting methods used in mines, quarries and road cuts. The dimensions of burden are 2.5 to 20 times the borehole diameter, and that of spacing 15 and 10 times the borehole diameter respectively (Table 5.2). The boundaries of the models are fixed in the x-direction on the right and the left sides and in the y-direction at the back of the holes. For various burdens, stresses are calculated at x and y directions as well as principal stresses in the solution regions. Figure 5.5 schematically shows the simulated model for this analysis.

5.4.2.2 Weak Plane Parallel to Free Face

The effect of weak planes such as open clay-filled joints or thin clay-layers, parallel to the free face on the stress field is analyzed. It consists of placing a weak plane parallel to the free face but at varying distances from the boreholes at a constant burden and spacing. These weak planes are located in the front of two and three holes configurations (Fig. 5.6). The distance of weak planes from the borehole wall, dimensions of burden and spacing between holes are shown in Table 5.3.

5.4.2.3 Fixed Weak Plane Parallel to Free Face

In this case, the weak plane is fixed at 2.5 and 5 times the borehole diameter. The dimension of burden ranges from 5 to 15 times the borehole diameter (Table 5.4). Holes have a spacing of 10 and 15 times the borehole diameter. Compressive, tensile and principal stresses are calculated for each model. The schematic model is illustrated in figure 5.7.

5.4.2.4 Weak Plane Normal to Free Face

A weak plane is placed between the holes normal to free face for two burden distances. The principal, compression and tensile stresses are calculated between the holes. The final results are compared with the same model but in the absence of any weak planes. The geometry of the models for different cases is shown in Table 5.5. Figure 5.8 schematically shows the simulated model for this analysis.

5.4.2.5 Weak Planes of Varying Widths

The discontinuities in the rock may be filled or open. The width of discontinuities in a rock mass differs. In this section, the effect of weak planes of varying width will be discussed. As mentioned before, an open discontinuity cannot be simulated by these two programs. Therefore, in all models the discontinuities are filled by gouge materials and named weak planes. These materials are much weaker than the rock. The width of the weak plane is varied from 1 to 20 mm, as shown in figure 5.9. The location of weak planes parallel to the free face and the geometry of blast simulation is shown in Table 5.6. The effect of similar weak planes normal to free face (located at 2.5 and 5 $\times$ borehole diameters) on the stress distribution is investigated for constant burden and spacing (10 $\times$ borehole diameter).

Table 5.2 : Geometry of models for different burdens.

Spacing	Burden
15 * D	2.5 * D 5.0 * D 7.5 * D 10.0 * D 15.0 * D 20.0 * D
10 * D	2.5 * D 5.0 * D 7.5 * D 10.0 * D 15.0 * D 20.0 * D
D : Borehole Diameter, Figure 5.5.	

Table 5.3 : Geometry of models for weak plane parallel to the free face.

Spacing	Burden	Distance of weak plane from the hole centre
15 * D	15 * D	2.5 * D 5.0 * D 7.5 * D 12.5 * D
	10 * D	2.5 * D 5.0 * D 7.5 * D
10 * D	10 * D	2.5 * D 5.0 * D 7.5 * D
	15 * D	2.5 * D 5.0 * D 7.5 * D
D : Borehole Diameter, Figure 5.6.		

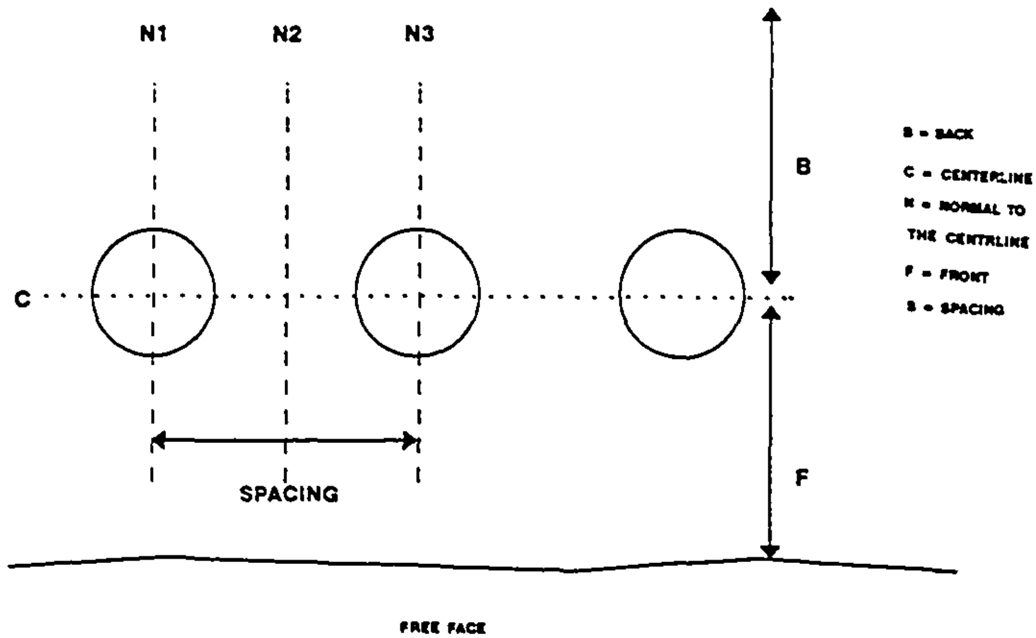

Figure 5.4 : Imaginary lines for plotting stresses around boreholes.

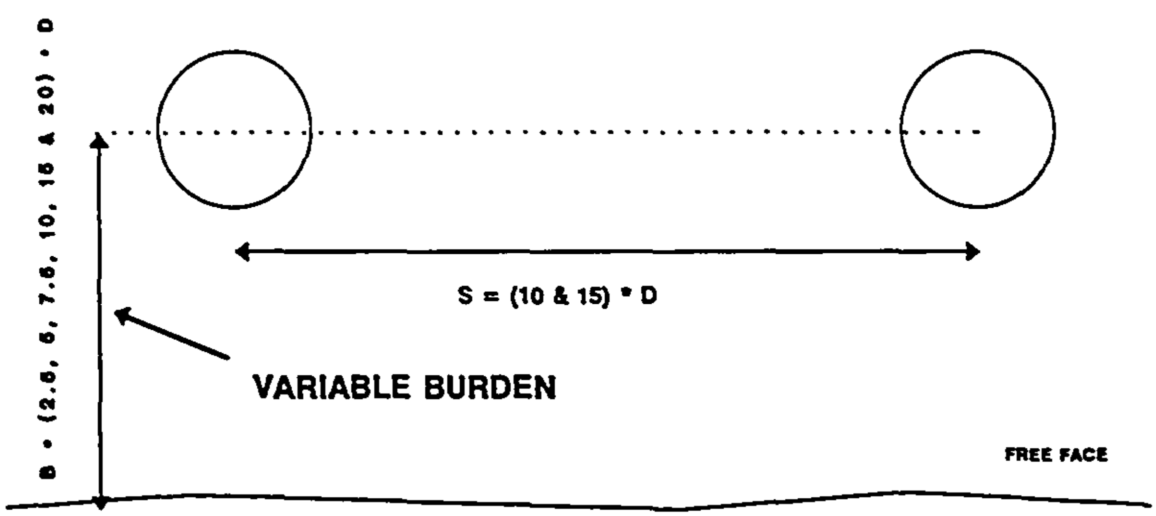

Figure 5.5 : Variable burdens for two different spacings.

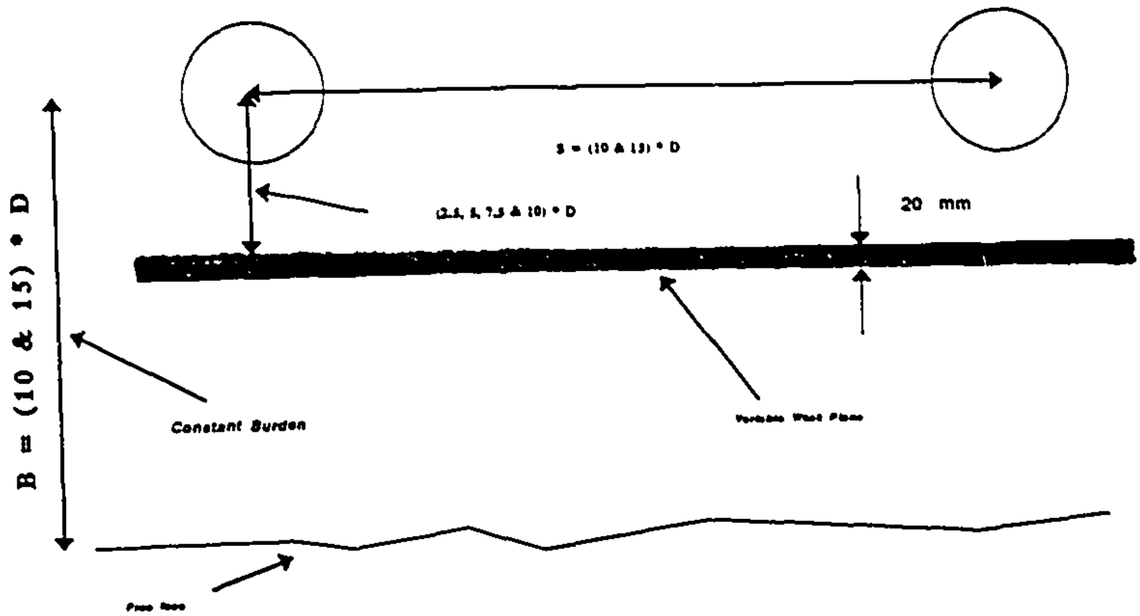

Figure 5.6 : Variable weak plane parallel to free face at constant burden.

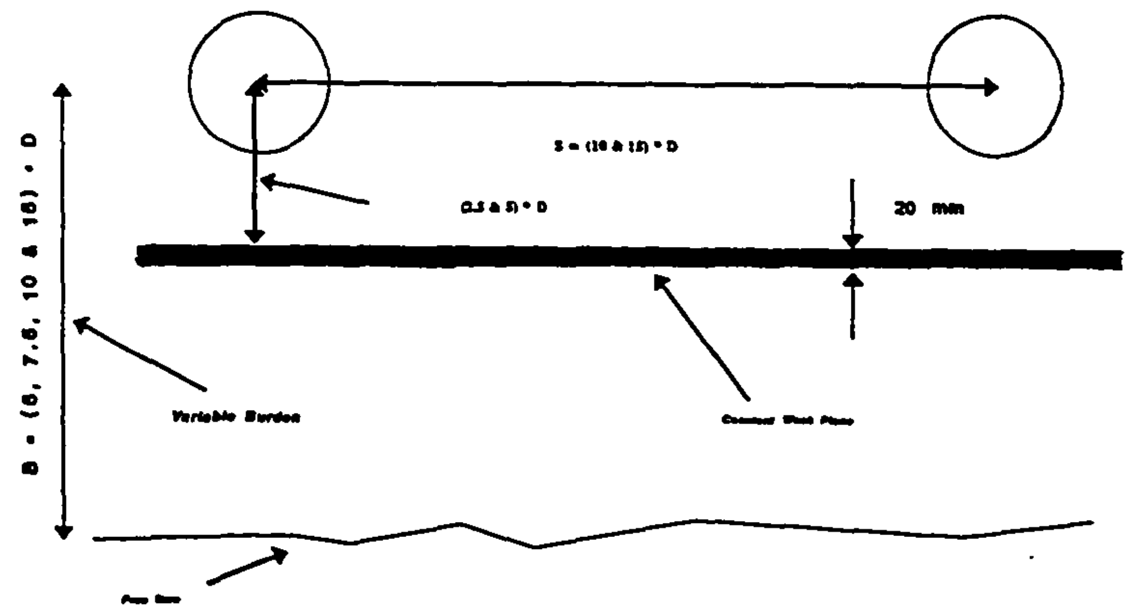

Figure 5.7 : A fixed weak plane parallel to free face with various burdens.

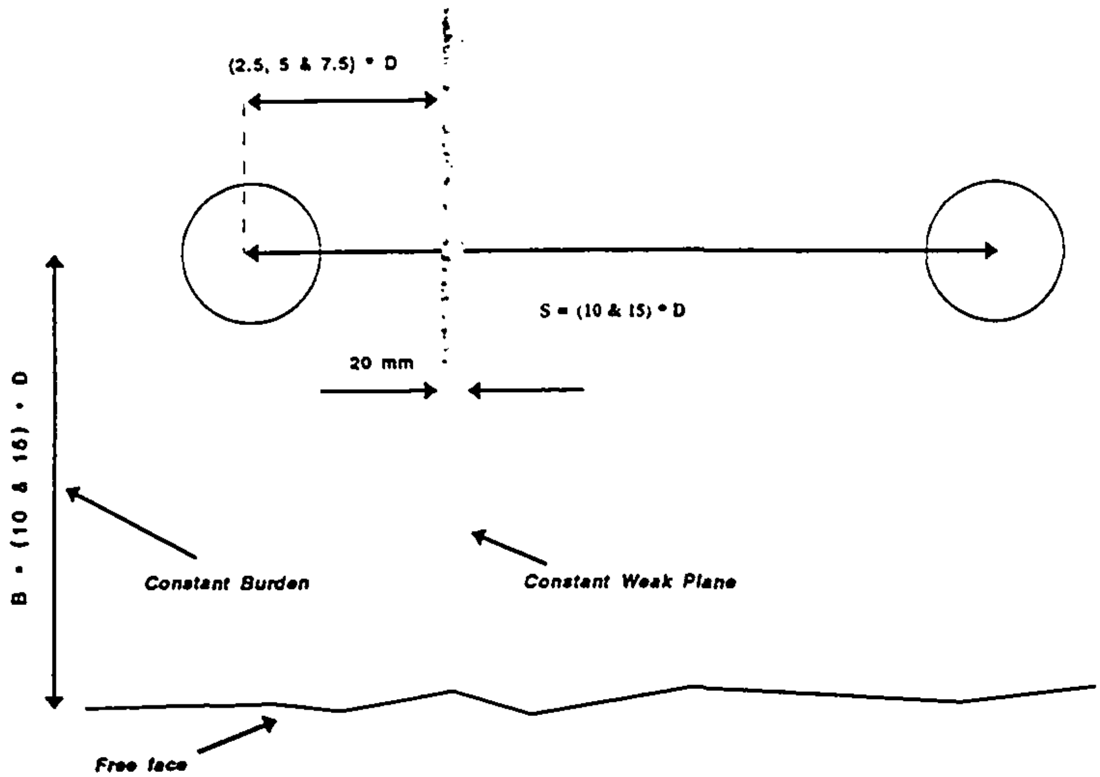

Figure 5.8 : Variable weak plane perpendicular to free face at constant burden.

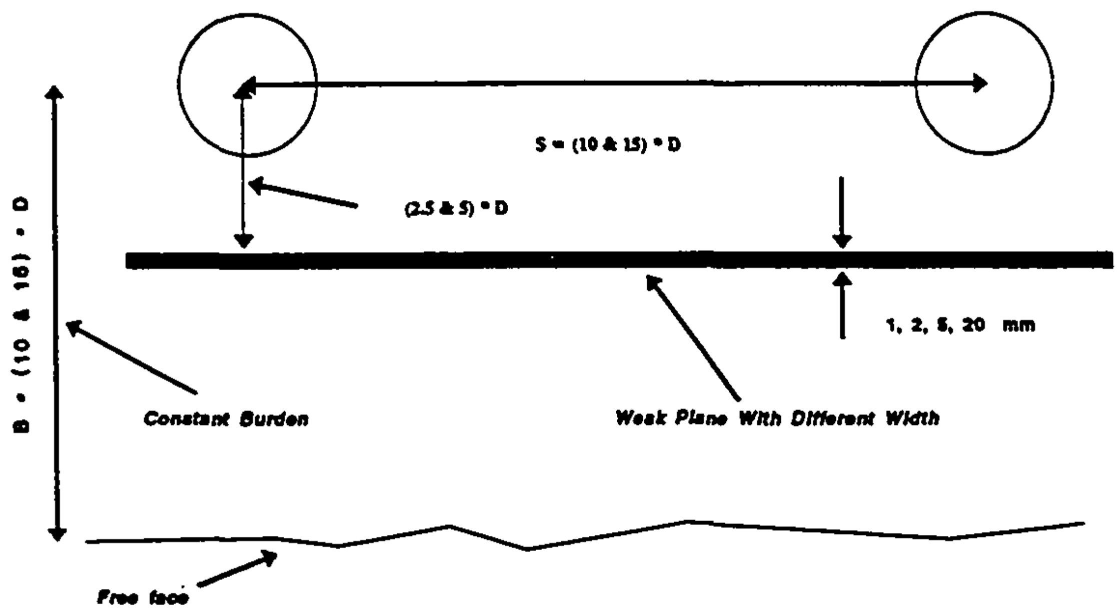

Figure 5.9 : A fixed weak plane parallel to free face of varying widths at constant burden.

Table 5.4 : Geometry of models for a fixed weak plane parallel to the free face.

Distance of weak plane from the hole centre	Spacing	Burden
2.5 * D 5.0 * D	15 * D	5.0 * D 7.5 * D 10 * D 15 * D
2.5 * D 5.0 * D	10 * D	5.0 * D 7.5 * D 10 * D 15 * D

D : Borehole Diameter, Figure 5.7.

Table 5.5 : Geometry of models for weak plane normal to the free face.

Spacing	Burden	Distance of weak plane from the hole centre
15 * D	15 * D	2.5 * D 5.0 * D 7.5 * D
10 * D	10 * D	2.5 * D 5.0 * D
	15 * D	2.5 * D 5.0 * D 7.5 * D

D : Borehole Diameter, Figure 5.8.

Table 5.6 : Geometry of models for parallel weak plane to the free face with various width.

Spacing	Burden	Distance of weak plane from the hole centre	Width of Weak Plane (mm)
15 * D	10 * D	2.5 * D 5.0 * D	1, 2, 3
10 * D	5 * D	2.5 * D	1, 2, 3
	7.5 * D	2.5 * D 5.0 * D	1, 2, 3
	15 * D	2.5 * D 5.0 * D	1, 2, 3
D : Borehole Diameter, Figure 5.9.			

5.4.2.6 Inclined Weak Planes of Varying Widths

In this case, the effect of a weak plane inclined to the free face on the stress distribution is analyzed. In the first step, a weak plane is fixed at the back of three holes for constant burden and spacing. The distance of the plane from the first and the third holes is 2.5 and 5 times borehole diameter respectively, as shown in figure 5.10. The width of the weak plane in different simulations is 1, 2 and 20 mm. All other parameters are kept constant.

In the second step, a weak plane is placed between the first and the second hole, so that; one end is located on the front of the first hole and the other placed at the back of the third hole (Fig. 5.11). The distance of the weak plane from the front of the first hole and the back of the third hole is 2.5 and 5 times the hole diameter respectively.

5.5 Results and Discussions

As mentioned in chapter three, during the second phase of rock fragmentation due

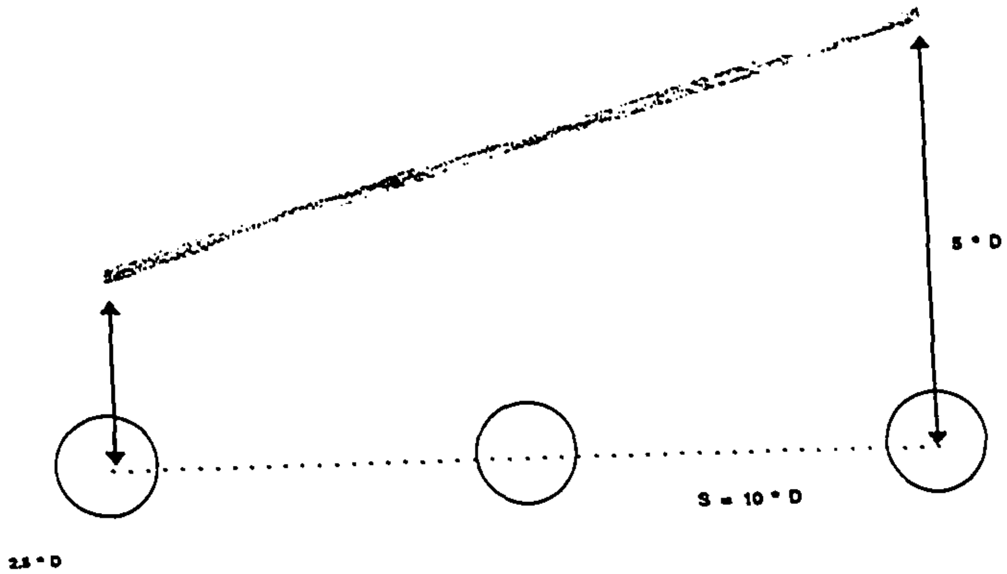

Figure 5.10 : Inclined weak plane fixed at back of holes.

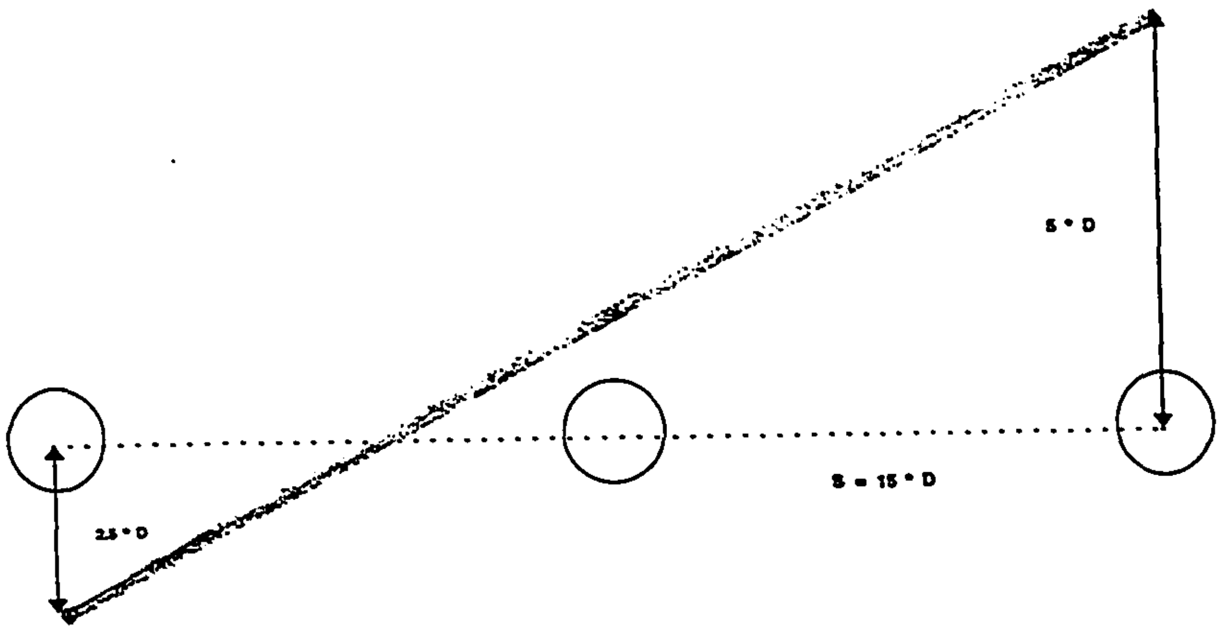

Figure 5.11 : Inclined weak plane crossing centreline between holes.

to action of high pressure gases in the borehole, cracks extend as the gases penetrate into discontinuity. This process can be considered as analog of a pressurized thick-wall cylinder with infinite thickness without external pressure. Therefore, in very simple analytical solution both radial and tangential stresses can be calculated by the following equations:

$$\sigma_t = P_b \frac{r_b^2}{r^2} \qquad \sigma_r = -P_b \frac{r_b^2}{r^2} \tag{5.12}$$

The stresses calculated by this analytical solution are compared to the final results of the simplest models of numerical analysis. The results obtained from numerical analysis will be discussed in two separate sections.

In the first part, radial and tangential stresses for a pressurized hole are analyzed. Both radial and tangential stresses are calculated at the centroid of each element of the models. The final results on the lines parallel and perpendicular to the free face from the hole centre are discussed . In the second case, the *I-DEAS* program has been used to calculate the stress field for two and three pressurized holes. The principal stresses as well as stresses in the co-linear and perpendicular directions are calculated at each node of the elements. These stresses have been plotted along the direction normal to free face from the centre of the hole and the midpoint, as well as on the centreline.

5.5.1 Stress around a pressurized hole

Figures 5.12 through 5.16 show the characteristics of stress distribution induced by a pressurized hole in an elastic medium for five different cases. The calculated tangential and radial stresses for various burdens (in terms of borehole diameters) are shown in Figs. 5.12(a) and 5.12(b), along a direction normal to the free face and connecting the pressurized borehole. The corresponding results from an analytical solution of a thick wall (20 diameters) cylinder case are also shown for comparison. As expected, for large burdens the results from the numerical and analytical solutions are equivalent. The decay rate of stress with distance from the borehole is similar for both tangential and radial components.

As the dimension of burden decreases, the tangential stress increases in the front of the hole. When the burden is decreased to 2.5 times the borehole diameter, the value of this stress on the normal line (N1), near the free face, is 2.7 times higher than the stress on the line parallel to the free face from the hole centre at similar point; whereas, this value is about 1.04, when the burden increases from 2.5 to 10 times the borehole diameter. However, as one reduces the distance to the free face the tangential component begins to predominate. It nearly triples its value when the burden is reduced by half (i.e. from 20 × diameter to 10 × diameter). For ANFO under fully-coupled conditions in the borehole (i.e. borehole pressure: 2000 MPa), this implies that the tangential stress at a burden ten diameters wide would be in excess of 60 MPa. This would cause tensile failure under this loading conditions, even without taking into account the explosion gas penetration effect in the extending of the cracks.

As shown in Figs. 5.13 through 5.16, the presence of a weak plane causes the stress to drop immediately to zero at the boundary of the plane. It does recover, however, to its normal value without the weak plane, but at considerable distance from the plane in question. The recovery distance is found to be inversely proportional to the proximity of the weak plane to the borehole. The tangential stresses increase as the distance between the plane and the borehole wall decreases. It is shown that the weak plane or open discontinuity, parallel and perpendicular to the face, play a role similar to a free face. The stresses calculated from the models are compared with the tangential stress from the same model without any weak planes. The data illustrate the variation of tangential stresses along the radial direction perpendicular to the free face for a weak plane 2 cm wide.

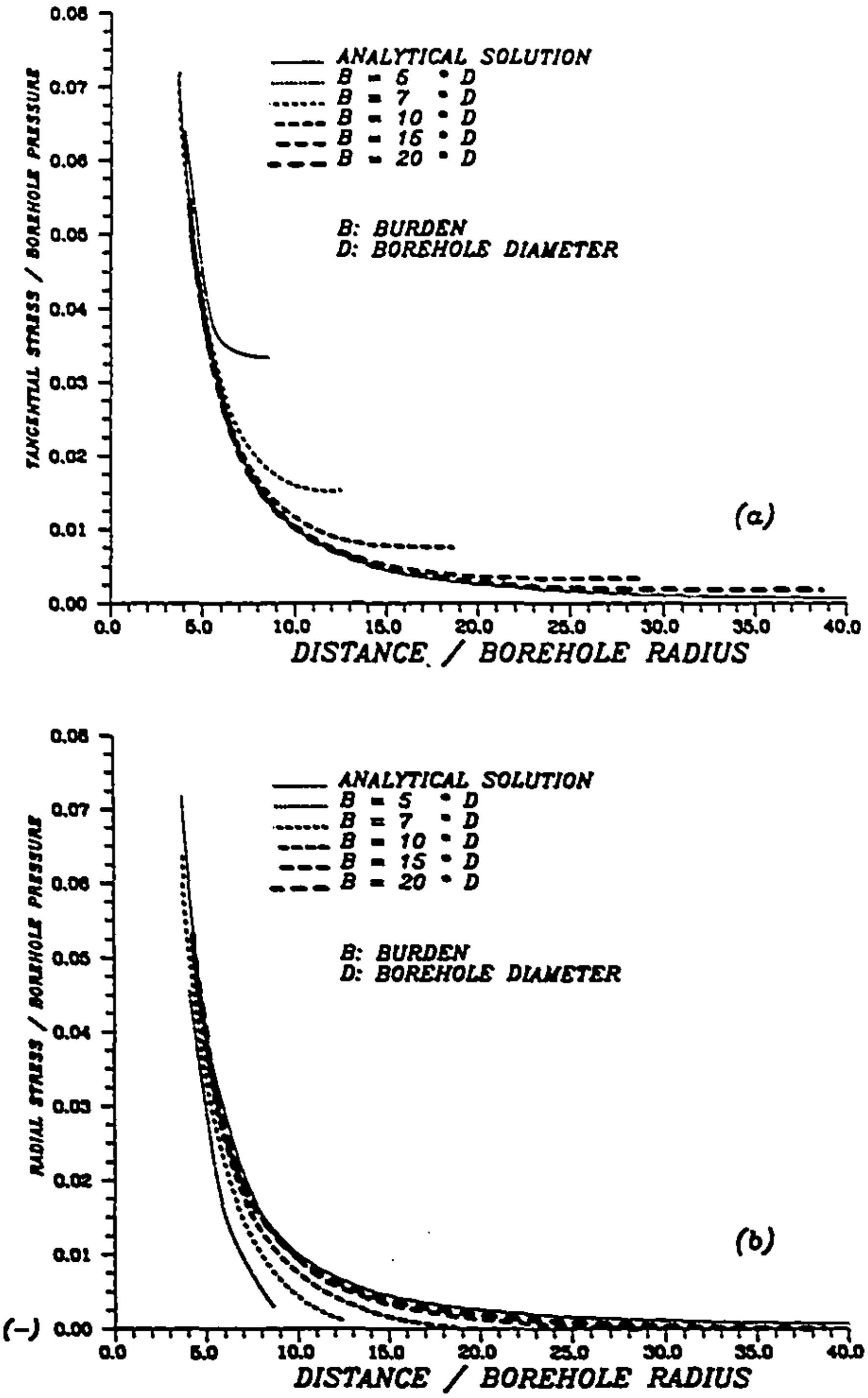

Figure 5.12 : Tangential and radial stresses for various burdens from numerical solution, and for the largest burden by analytical solution.

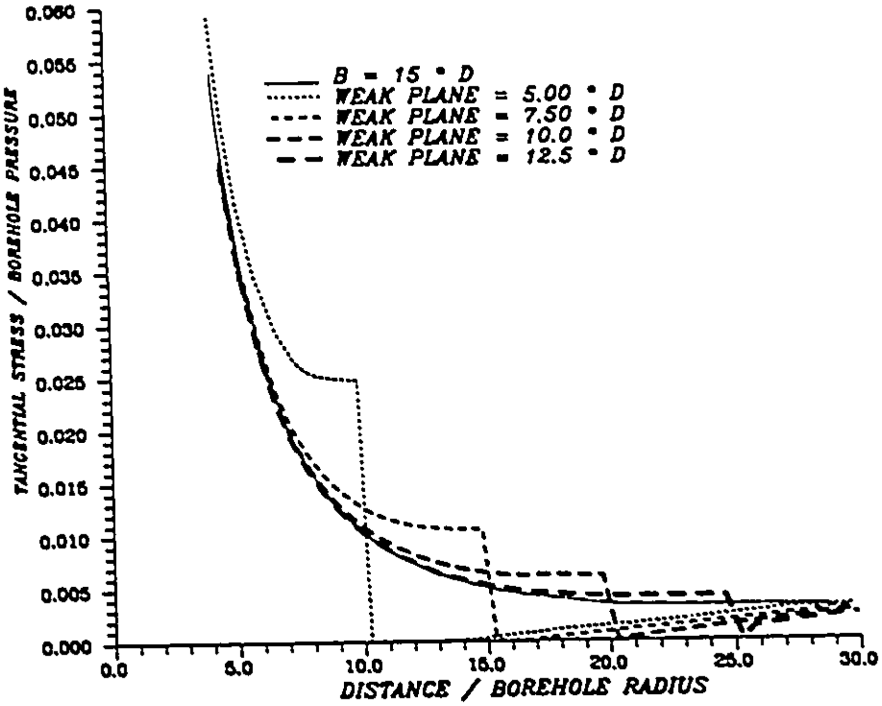

Figure 5.13 : Tangential stresses for different weak planes parallel to free face at constant burden, solid line representing the same without any weak plane.

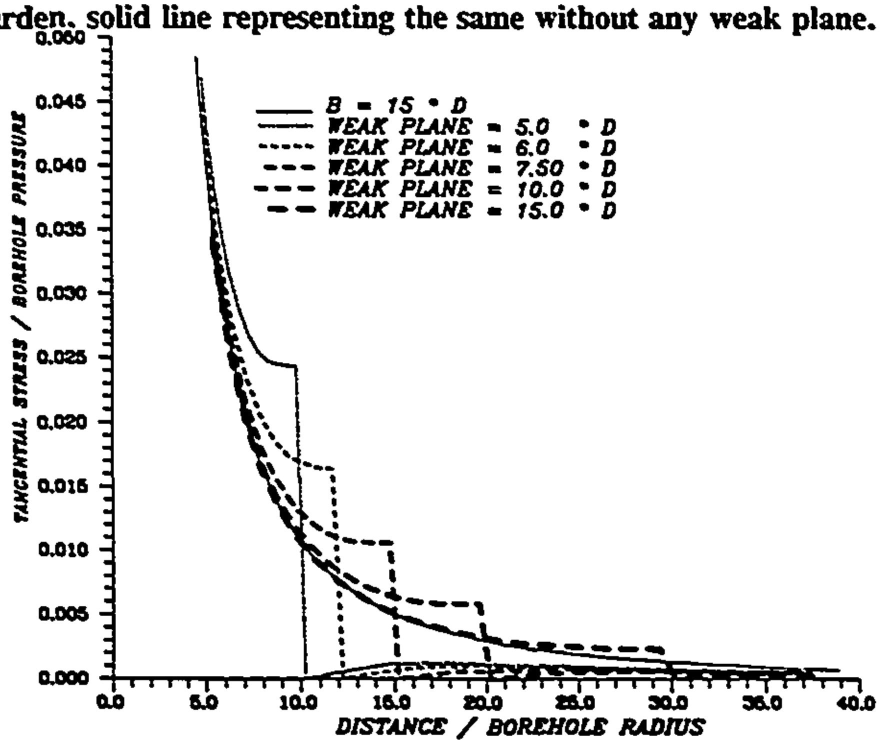

Figure 5.14 : Tangential stresses for different weak planes perpendicular to free face from the numerical analysis, solid line showing the same without weak plane.

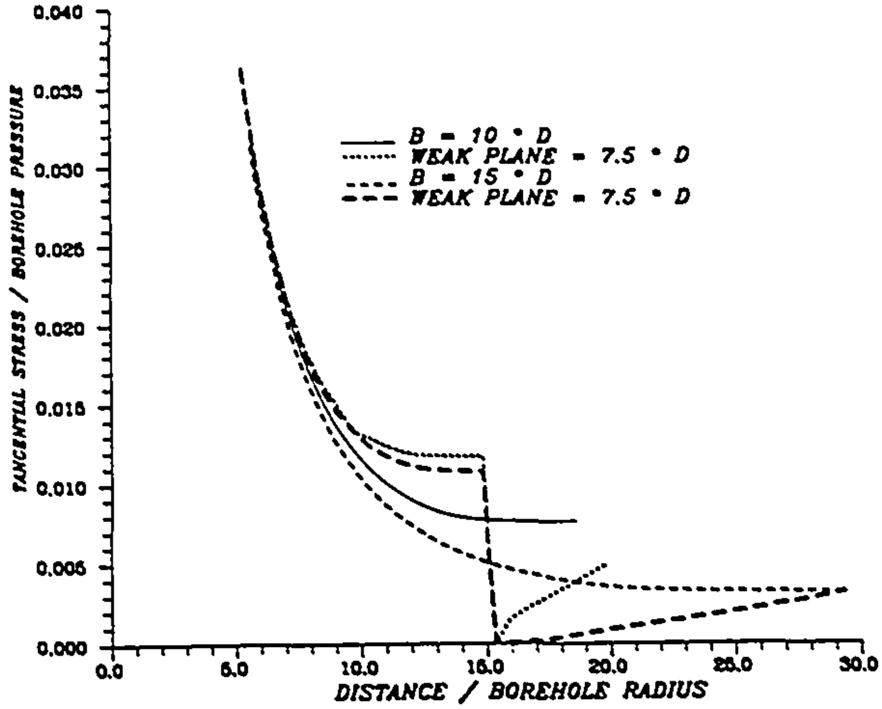

Figure 5.15 : Tangential stresses for two different burdens with a constant weak plane parallel to free face.

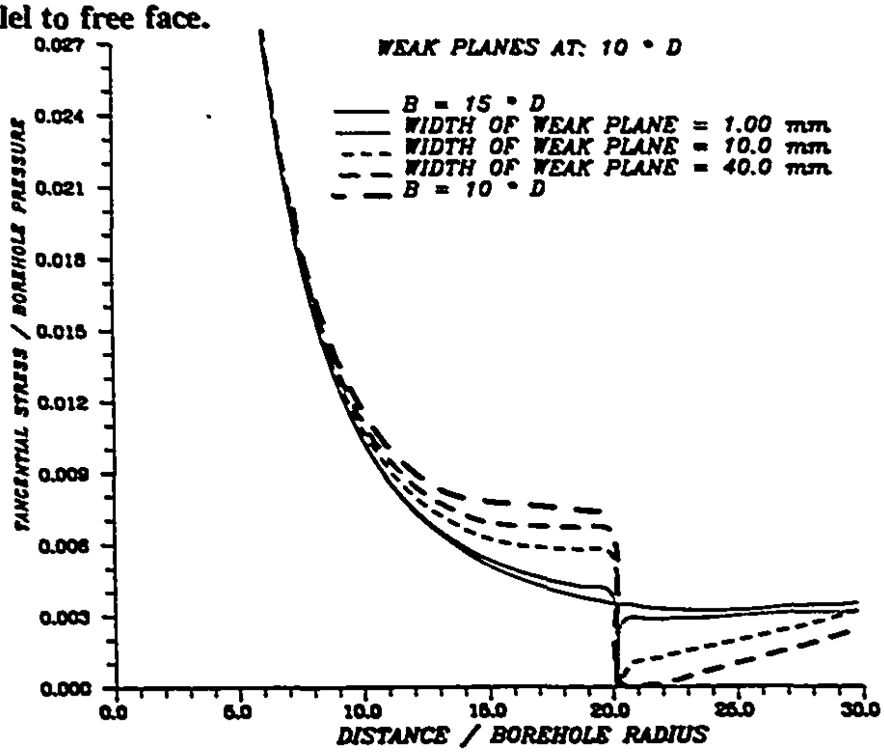

Figure 5.16 : Tangential stresses for weak planes of varying widths parallel to free face from numerical analysis.

The width of discontinuity has a direct effect on the stresses in the region between the weak plane and the borehole wall. The results show that the stresses drop to a negligible value at the boundary of the weak plane, and their amplitude depending on the width of the weak plane. Also, a very narrow weak plane causes the stress to recover almost immediately. As shown in figure 5.16, the tangential stress for a discontinuity with 1 mm width is very close to the value obtained from the same model without a weak plane. This value increases as the width of weak plane increases. For widths greater than 60 mm, the results obtained are similar to those for a free face in the presence of a free face located at the same distance as the weak plane. The stress field for the case without the weak plane is also shown for comparison.

5.5.2 Analysis Of Stress Field Between Two Pressurized Holes By *I-DEAS*

In this approach, the effect of a free face and a discontinuity on the stress field is discussed around two and three pressurized holes.

5.5.2.1 Effect of a free face

Figures 5.17(a), 5.18(a) and 4.19(a) show the calculated maximum principal stress for different burdens at constant spacing (15 × borehole diameter). The maximum principal stress at the midpoint for an infinite burden is 2 times greater than the stress at the same point for a burden 5 times the borehole diameter. When the spacing is reduced to 10 diameter the effect of the free face at 2.5 times borehole diameter is approximately comparable to a burden and spacing 5 and 15 times the borehole diameter respectively (Fig. 5.20). The tensile stresses and maximum principal stresses are identical along a direction normal to the free face and connecting the midpoints and centres of holes (N1 and N2). These stresses are reduced as the burden is decreased, and are about zero for a simulated model for a burden and spacing equal to 2.5 and 15 times the borehole diameter, respectively.

On the other hand, the tensile stress increases dramatically in the burden region which is close to the face at smallest distance, along a direction normal to free face and connecting the pressurized boreholes. The maximum principal stress for a small burden (2.5 × borehole diameter) is 4 to 6 times greater than the infinite burden for two different spacings (10 and 15 × borehole diameter), (Fig. 5.18). The influence of a free face on the stress field for a burden greater than 15 times the borehole diameter is negligible. From the view of quasi-static pressure, for normal wall-control practices the free face does not have any effect upon the stresses at a distance of greater than 10 and 15 times the borehole diameter for the same spacings (10 and 15 times borehole diameter) (Figs. 5.17 through 5.19). Therefore, a burden can be characterized as an infinite burden when the ratio of that to the spacing exceeds unit, and the critical size of the burden for pre-splitting is defined as a distance equal to spacing. In an isotropic and homogeneous media, a spacing between 10 and 15 times the borehole diameter should be acceptable, but the exact value would depend on the rock properties. As the dimension of the critical burden decreases, the tension zone starts to collapse in the front of holes, and the tensile stresses decrease on the centreline from the midpoint to the centre of holes as well as on the line normal to the free face from the midpoint (Figs. 5.17 and 5.19). Conversely, the stresses on the line normal to the free face from the hole centre increase as the burden decreases. Consequently, the form of the fracture zone changes from elliptical to an approximately circular shape for each hole (Fig. 5.21). It should be noted that the shape of this fracture zone is similar to an ellipse for an optimum spacing in an infinite burden.

For a ratio of burden to spacing of about 0.8, a fracture zone can be achieved between the holes, and to a lesser extent, in the burden regions. The effect of a fixed free face at a distance equal to 0.8 times spacing from the hole centre on the stresses along the centreline and the line normal to it through the midpoint is almost negligible, whereas, the stresses in front of each hole is increased (Figs. 5.17-19). This description is analogous to the concept of cushion blasting method. As stated before, in this technique

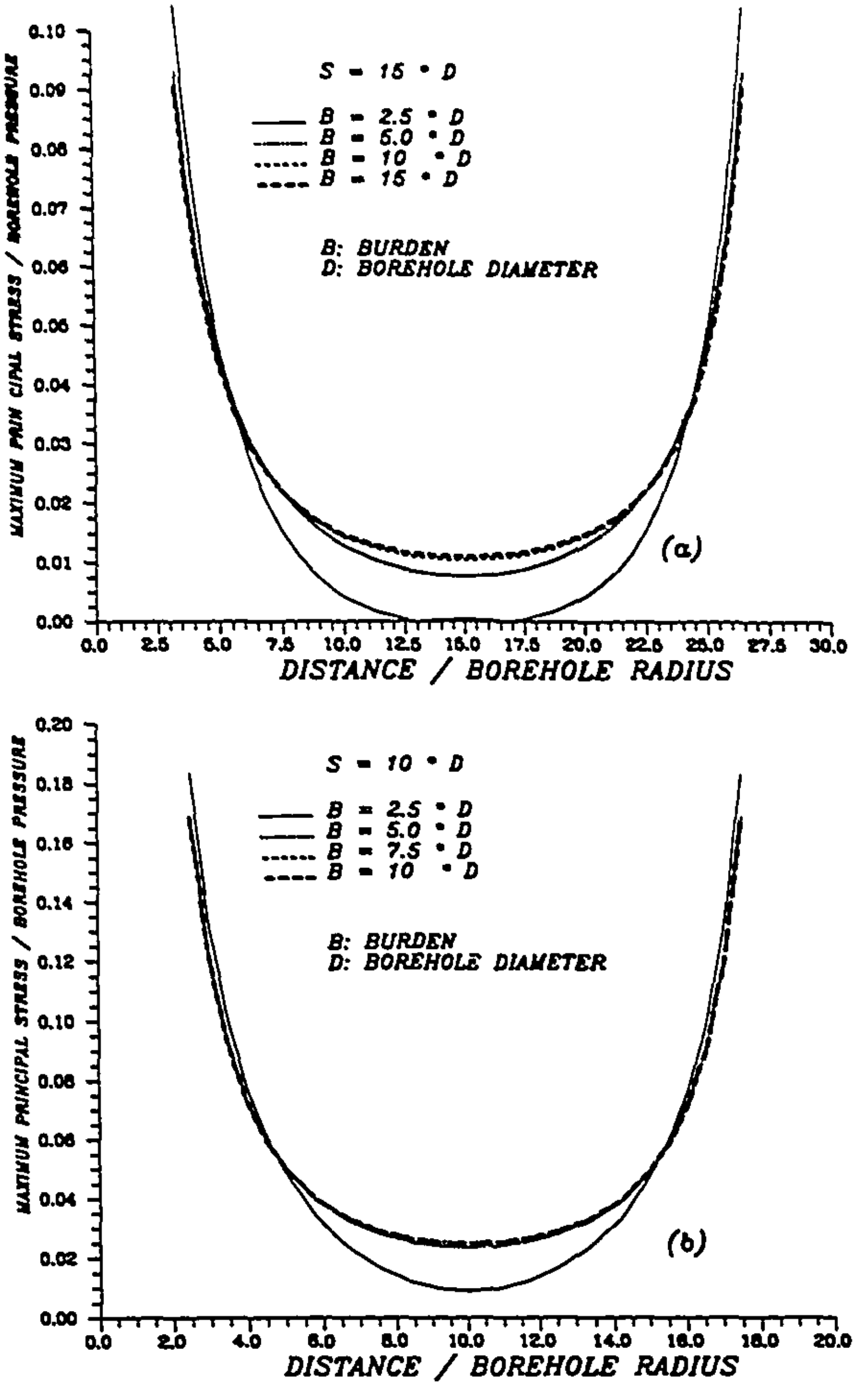

Figure 5.17 : Maximum principal stresses along the centreline for different burdens with two constant spacings, 15 and 10 times borehole diameter.

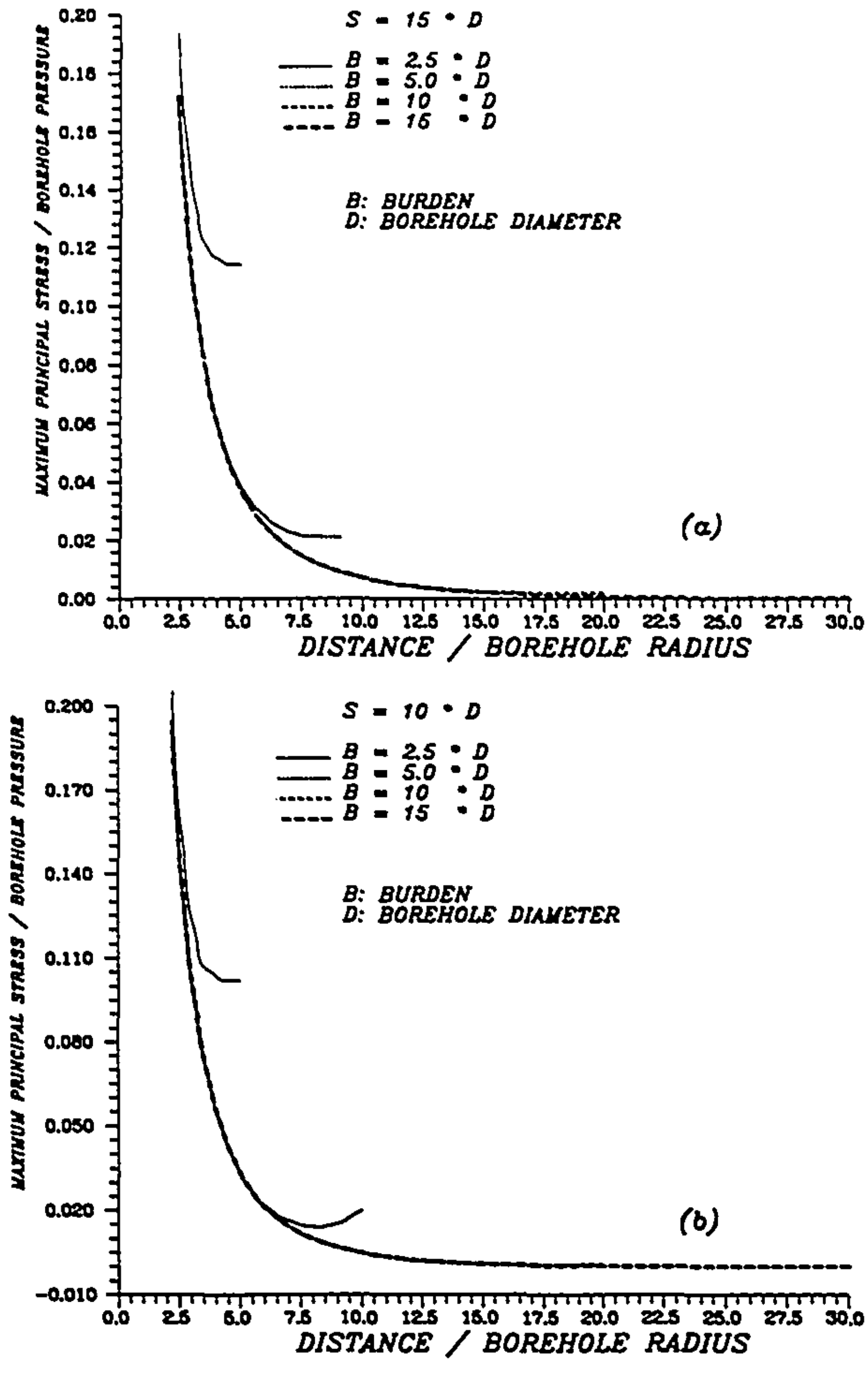

Figure 5.18 : Maximum principal stresses along line normal to face from hole centre for different burdens with two constant spacings, 15 and 10 times borehole diameter.

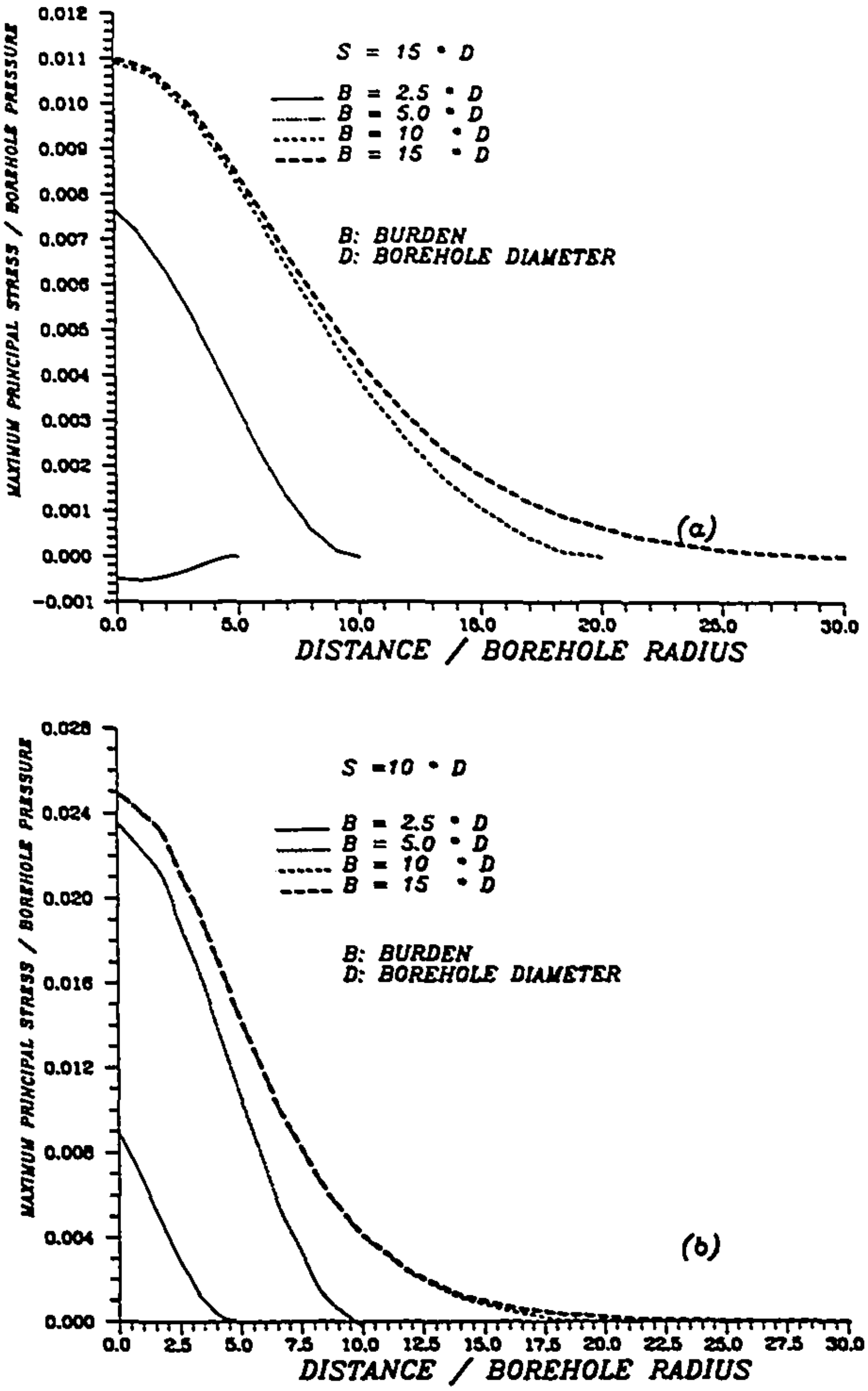

Figure 5.19 : Maximum principal stresses along line normal to face from midpoint for different burdens with two constant spacings, 15 and 10 times borehole diameter.

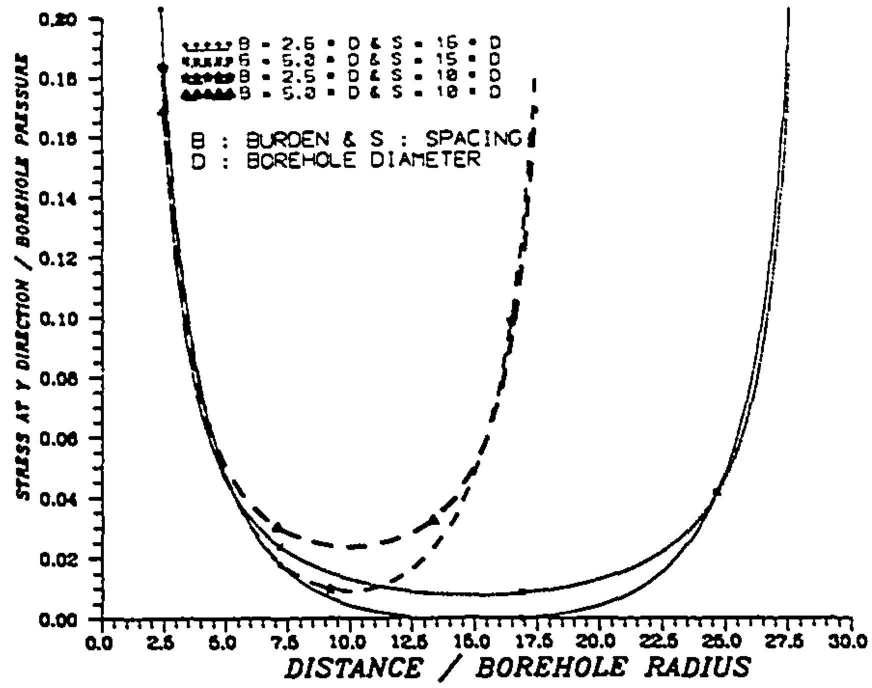

Figure 5.20 : Comparison between calculated maximum principal stresses along centreline for two different spacings and various burdens.

Figure 5.21 : Shape of tensile zones around two pressurized holes for small burden (B/S = 0.2).

the aim is to create a narrow fracture zone at the perimeter of the excavation, trimming or slashing the excess material from the final walls. The ratio obtained by numerical analysis (B/S=0.8) is also similar to the recommended ratio by the blasting engineer for cushion blasting.

Furthermore, the mechanism of buffer blasting can also be analyzed by means of this investigation. Base on trial-and- error, the recommended ratio of the burden to spacing ranges from 0.8 to 1.2 in buffer blasting. For ratio smaller than 0.8, an irregular face (hump left between the holes) is predicted; for ratios greater than 1.2 large muck and cratering can be expected.

5.5.2.2 Effect of a Weak plane

In this section, the effect of distance of a weak plane (with 20 mm width) from the borehole wall is analyzed for multiple pressurized holes. The weak plane is fixed at 2.5, 7.5, and 12.5 borehole diameters for a constant burden and two different spacings (15 × borehole diameter). As shown in figure 5.22, a weak plane with a distance greater than 7.5 times the borehole diameter does not affect the distribution of stresses on the centreline at a constant burden. This value has a direct relationship to the spacing, and decreases to 5 times borehole diameter, where the borehole separation decreases to 10 times borehole diameter with the same burden. Therefore, the influence of a fixed weak plane parallel to the face at 2.5 and 5 borehole diameters from the hole centre on the stress field should be the same if the spacing is decreased to 5 borehole diameters. As a result a fixed discontinuity parallel to the free face at half spacing should not have any effect on the stresses along the centreline.

For a constant burden and spacing, the value obtained for maximum principal stresses near the weak plane, on the lines normal to the face from the hole's centre and the midpoint, are respectively 3 times greater and about 2 times smaller than the stresses at the same points for similar models without the weak plane (Figs. 5.23 and 5.24).

The role of a filled discontinuity parallel to the centreline at a constant burden and spacing is approximately analogous to a free face which is located at the same distance from the hole wall. Overbreak around holes and hump between holes are thus predicted by numerical analysis for a weak plane (20 mm wide) parallel to the free face with a distance smaller than half the spacing from boreholes wall (Fig. 5.25). In all cases, the presence of a wide weak plane causes the tensile stress to drop immediately to zero on the weak plane. The recovery distance is found to be inversely proportional to the proximity of the weak plane to the borehole. Therefore, fractures should not pass the wide weak plane (over 20 mm) or an open discontinuity.

In the next case, a 5 mm wide weak plane parallel to the free face is fixed at 2.5 times the borehole distance for various burdens at constant spacing. As shown in Figs. 5.26, 5.27 and 5.28, the stresses on the centreline and along the direction normal to free face and connecting the borehole (critical distance) are found to be independent of the width of the burdens. The smallest burden causes a reduction in the stresses on the line normal to the free face from the midpoint. The values of maximum principal stresses along the critical distance are very close to that obtained from the simulated model with a free face at a similar distance from the borehole. On the centreline and on the line normal to the face from the midpoint, the value of this stress is about equal to the average of stresses from the smallest and largest burden (2.5 and 10 times borehole diameter). Consequently, the influence of the dimensions of the burden on the stresses between the weak plane and the pressurized holes is negligible.

In all cases, fractures will start to develop from the borehole wall and extend to the parallel weak plane along the direction normal to the latter. The rock should remain intact between the holes, especially around the mid-region.

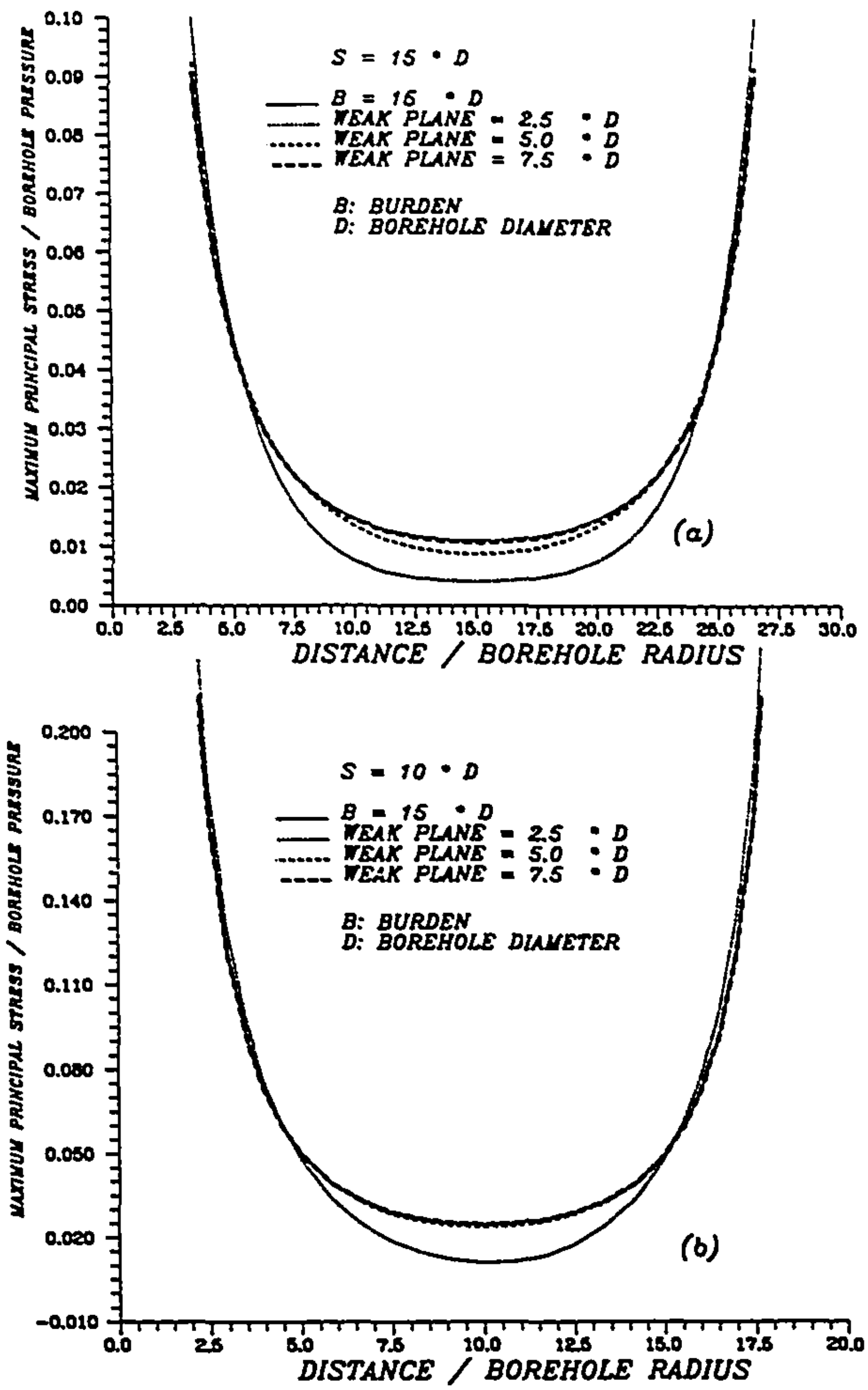

Figure 5.22 : Maximum principal stresses for different weak planes parallel to free face along centreline for two different spacings at constant burden.

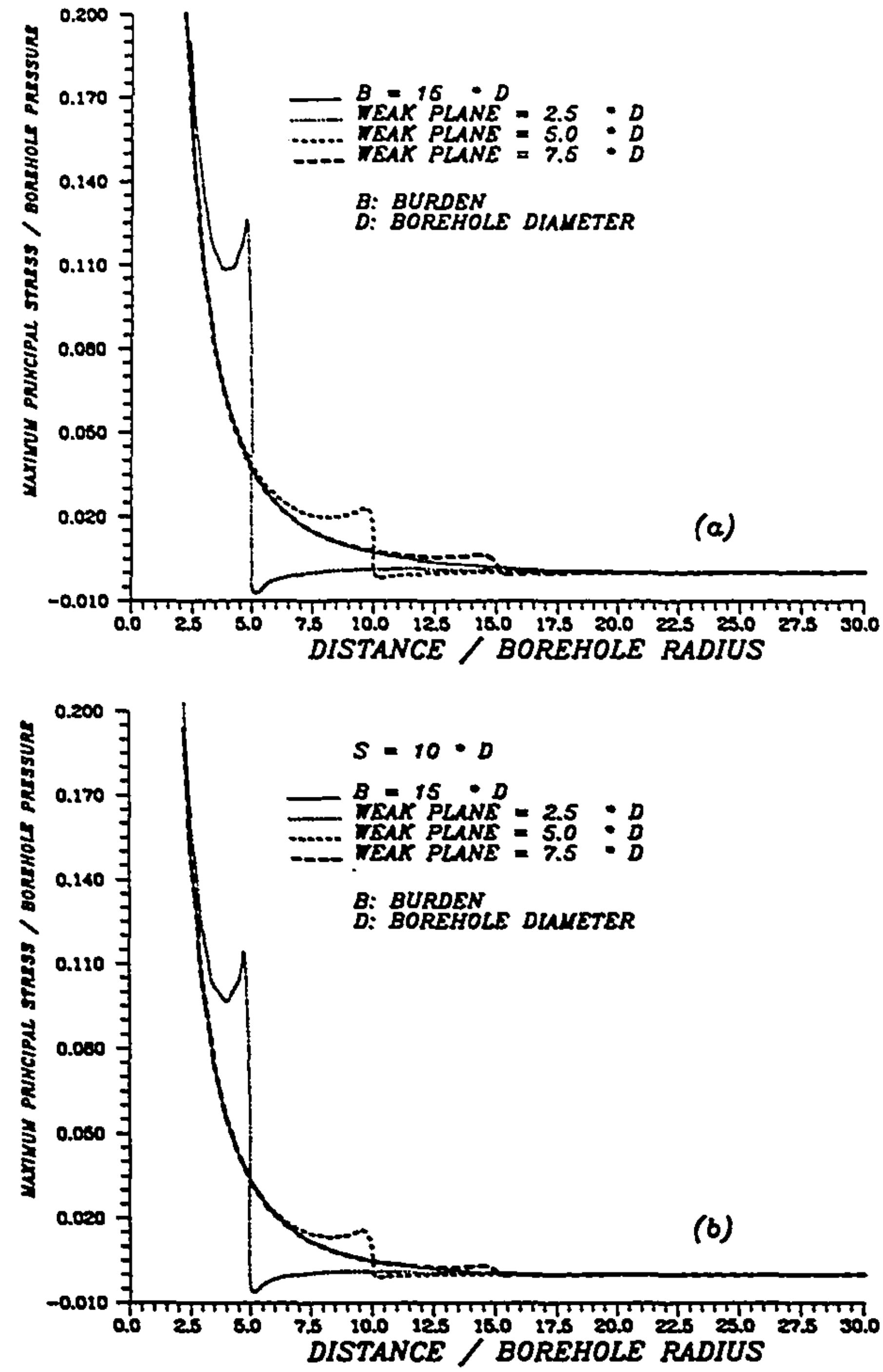

Figure 5.23 : Maximum principal stresses for different weak planes parallel to free face along a direction normal to free face and connecting the pressurized borehole for two different spacings and a constant burden.

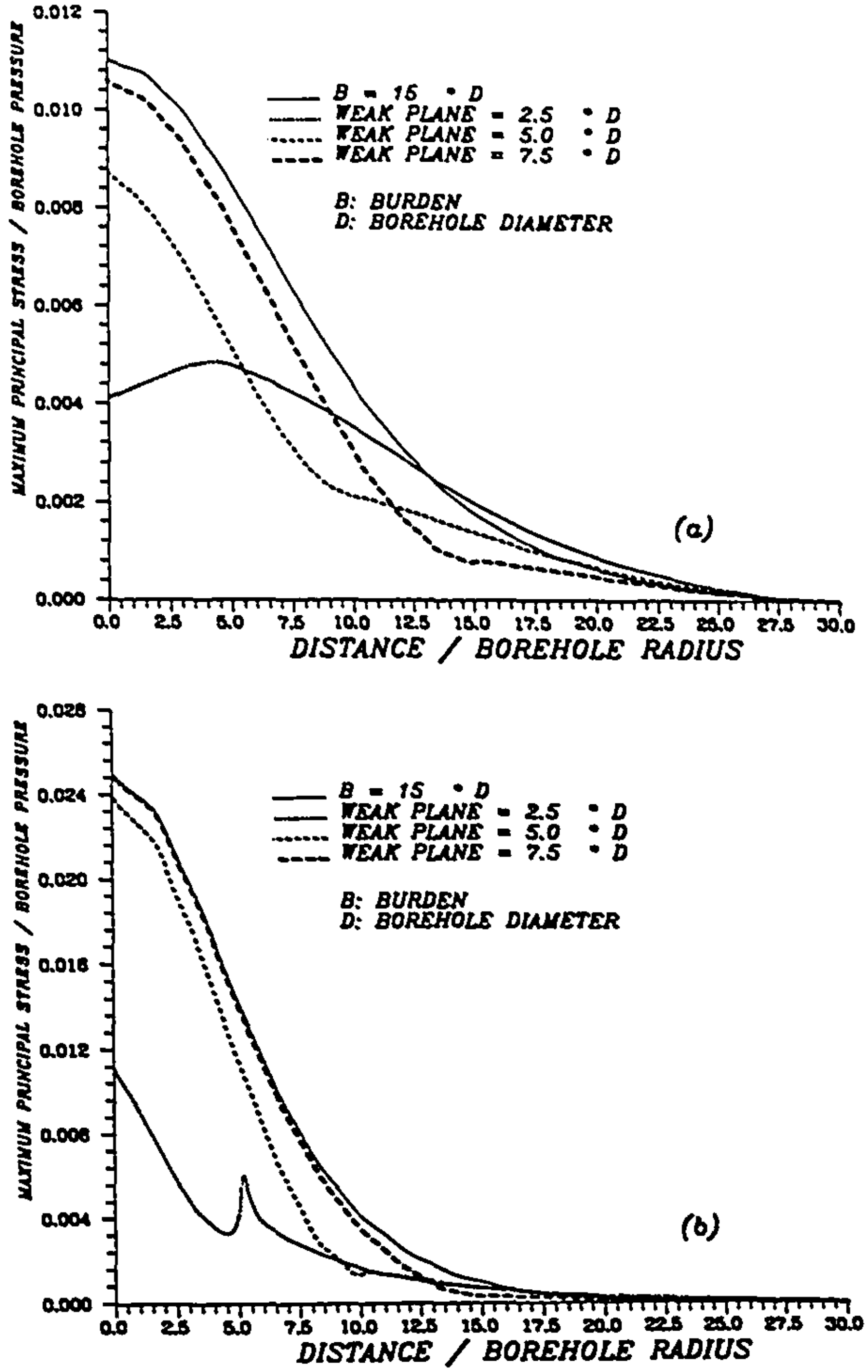

Figure 5.24 : Maximum principal stresses for different weak planes parallel to free face along a direction normal to free face and connecting the midpoint for two different spacings and a constant burden.

Figure 5.25 : Stress distribution around three pressurized holes in the presence of a weak plane.

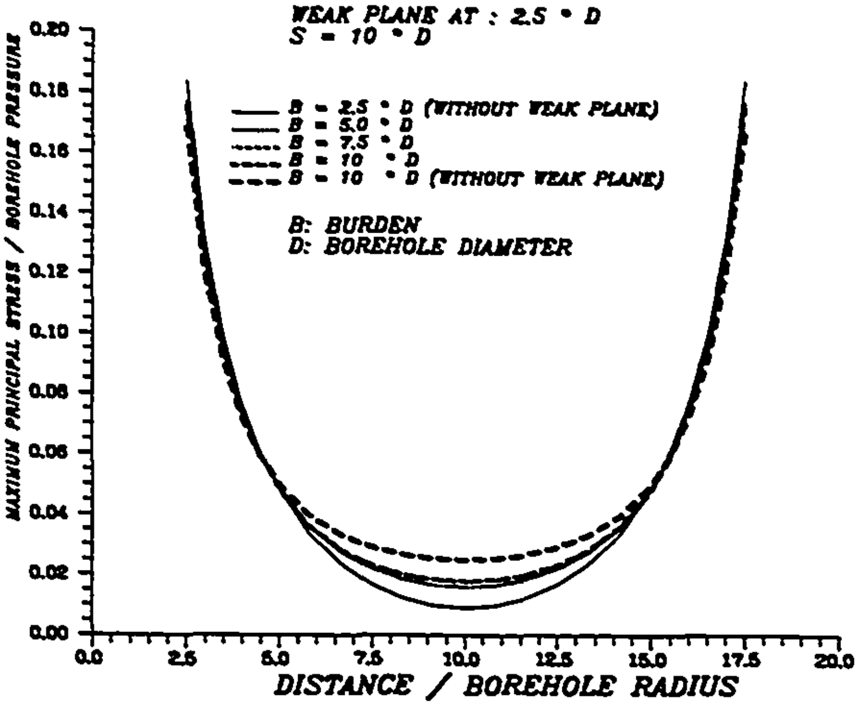

Figure 5.26 : Maximum principal stresses for three different burdens with a weak plane parallel to free face along centreline.

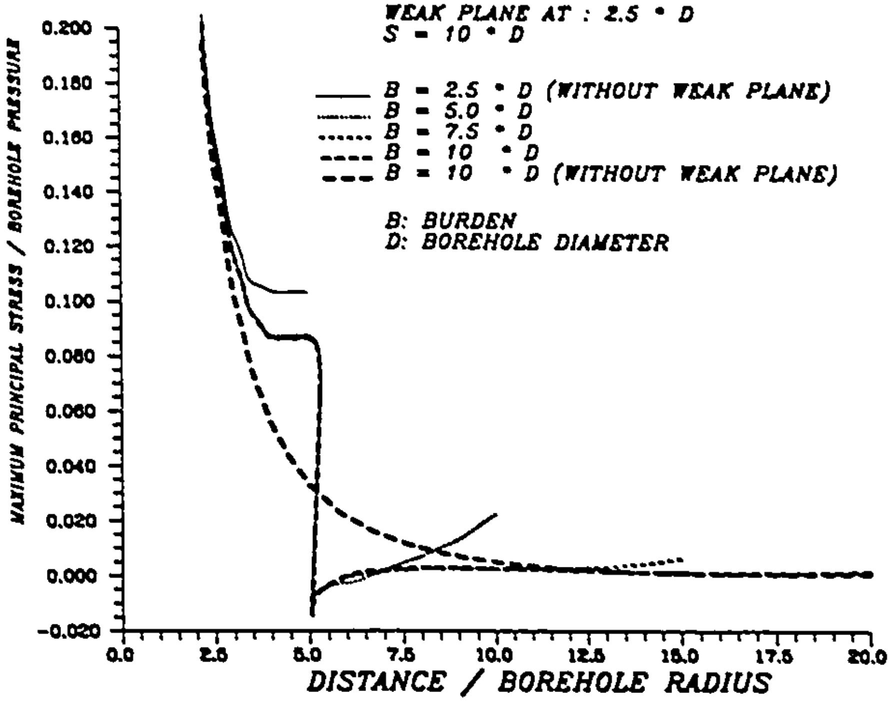

Figure 5.27 : Maximum principal stresses for three different burdens with a constant weak plane parallel to free face along a direction normal to free face and connecting the pressurized borehole.

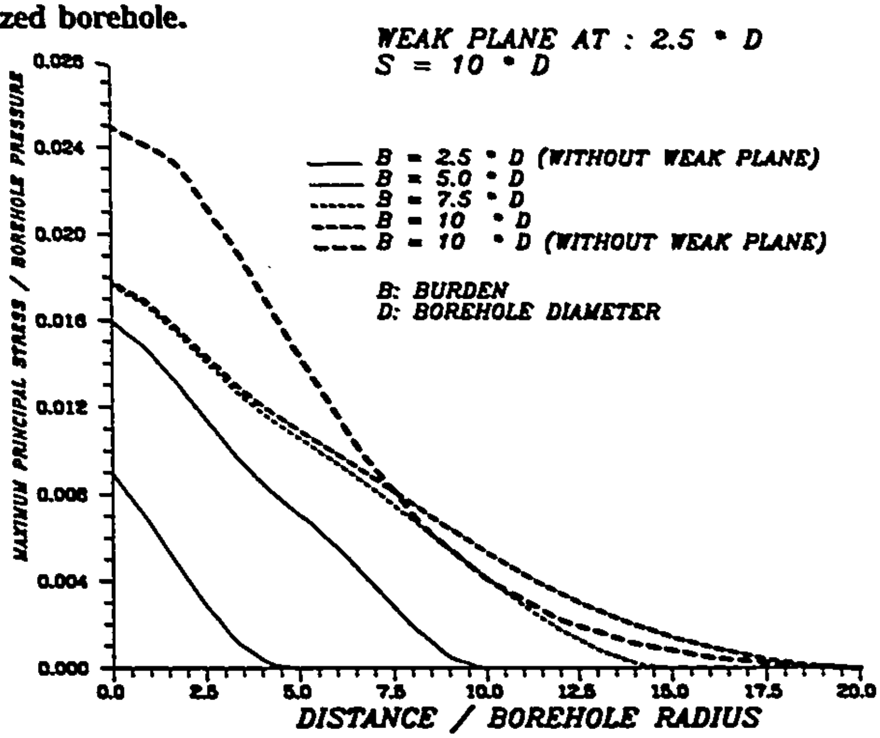

Figure 5.28: Maximum principal stresses for three different burdens with a constant weak plane parallel to free face, on line normal to the face from midpoint.

Several models have been simulated to examine the effects of weak planes normal to the free face on the stress distribution. The conditions of these models are exactly similar to that parallel weak plane used for two pressurized holes. In this case, the parallel weak plane is rotated 90 degrees, and fixed at 2.5, 5 and 7.5 times hole diameter at constant spacing equal to 15 times borehole diameter with two different burdens (10 and 15 × borehole diameters). Next, the spacing is reduced to 10 times borehole diameter, and the plane is located at 2.5 and 5 times borehole diameter from the hole with a burden equal to spacing.

Analysis of stress distribution using the model with normal weak planes shows characteristics which are considered very important to the degree of success of wall control blasts. Normalized maximum principal stresses on the centreline are shown in Fig. 5.29. The magnitude of the maximum principal stresses increases as the distance of the weak plane to the borehole wall decreases. A circular tensile zone is developed between the weak plane and the nearest borehole wall, when the distance of the weak plane from the hole centre is smaller than 5 borehole diameters. This zone is approximately similar for all simulated models. The value of tensile stresses reaches its maximum near the boundary of the weak plane and presents the same condition for all models. As shown in Figs. 5.29(a and b), the calculated maximum principal stress for a model with a fixed plane at 2.5 times borehole diameter is about 2.5 times greater than the real value for spacings equal to 10 and 15 times hole diameter. Therefore, it can be concluded that the value of tensile stresses between the hole and the normal discontinuity is independent of the spacing. The presence of a weak plane perpendicular to the centreline causes the stress immediately to drop to zero at the boundary of the plane. The stresses start to recover quickly after the weak plane, but the recovery rate depends on the distance of the weak plane from the borehole wall as well as the width of the discontinuity. It reaches its real value at half spacing and continues to the other holes normally.

As figure 5.29 show, the influences of the weak plane normal to the free face from the middle of the centreline on the stress distribution is negligible. The results illustrate that the plots for two different cases, simulated models with weak planes at the middle of the spacing and models without weak plane, correspond to each other. A comparison between the final results of finite element models and the experimental results (Belland, 1966; Worsey, 1984) shows that the numerical results are in good agreement with the field results. In a field study at Carol Lake Mine, Belland observed that blasting across the major joint close to vertical has caused a vertical face in the back of blastholes. Based on laboratory investigation and field observation, Worsey had concluded that the normal discontinuity to the final line of pre-split has little effect on the blast results.

The calculated stresses for different spacings and burdens are shown in Figs. 5.30 and 5.31, along directions normal to the free face and connecting the borehole as well as the midpoint on the centreline. The results illustrate that the tensile stress at midpoint is a function of weak plane distance from the borehole wall. As the distance is reduced, the stresses also decrease, and the optimum results can be obtained when the weak plane is located at mid-point between two holes.

To summarize, a weak plane with an intersection angle equal to 90 degrees to the line of pre-split at half spacing has minimal effect on the results of the blast. The presence of a perpendicular weak plane with a distance greater than 2.5 times hole diameter from the borehole hardly influences the stresses along a radial direction normal to the free face from the hole. Where the distance of the plane form the hole centre is smaller than 2.5, the tensile stresses start to increase in a circular region between the hole and the weak plane. After this stretch, the stresses decrease along the normal line to the face from the hole centre corresponding to the models without a weak plane. The media between the holes and the weak plane and at the back of the holes is liable to be extensively fractured by this tensile zone. Therefore, backbreak and loss of half barrel

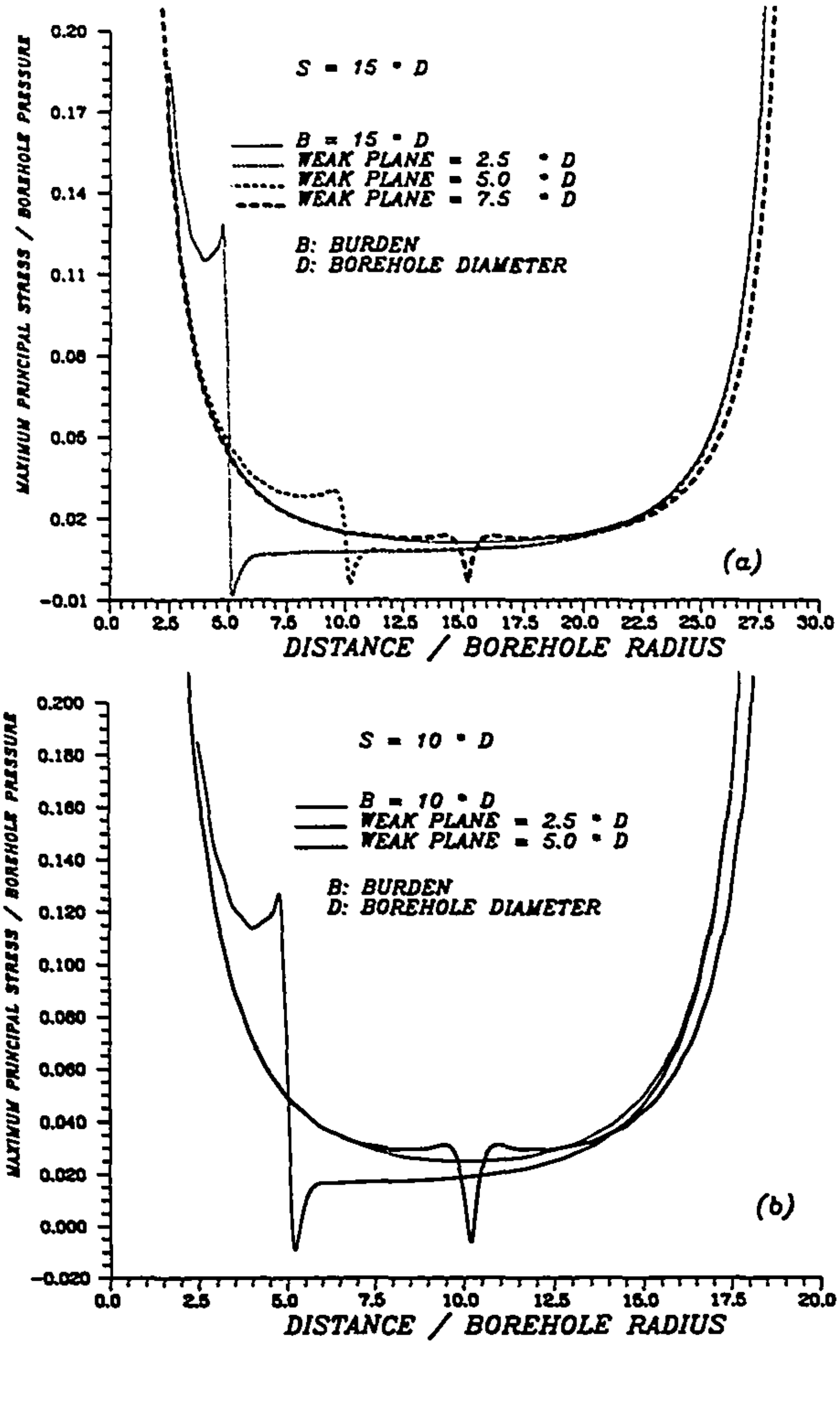

Figure 5.29 : Maximum principal stresses for weak planes normal to free face for different burdens and spacings, along centreline.

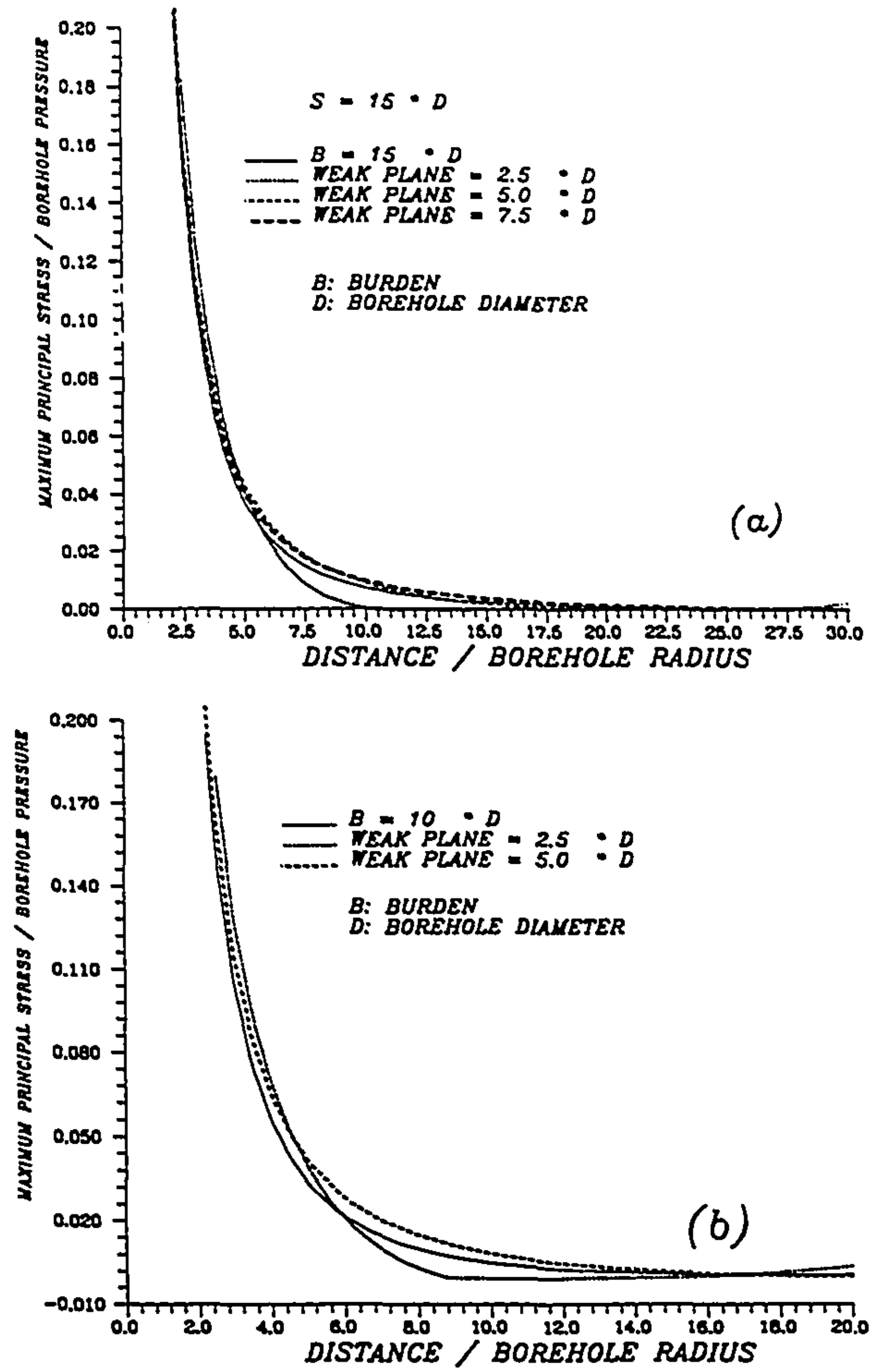

Figure 5.30 : Maximum principal stresses for weak planes normal to free face for different burdens and spacings, along line normal to free face from the hole centre.

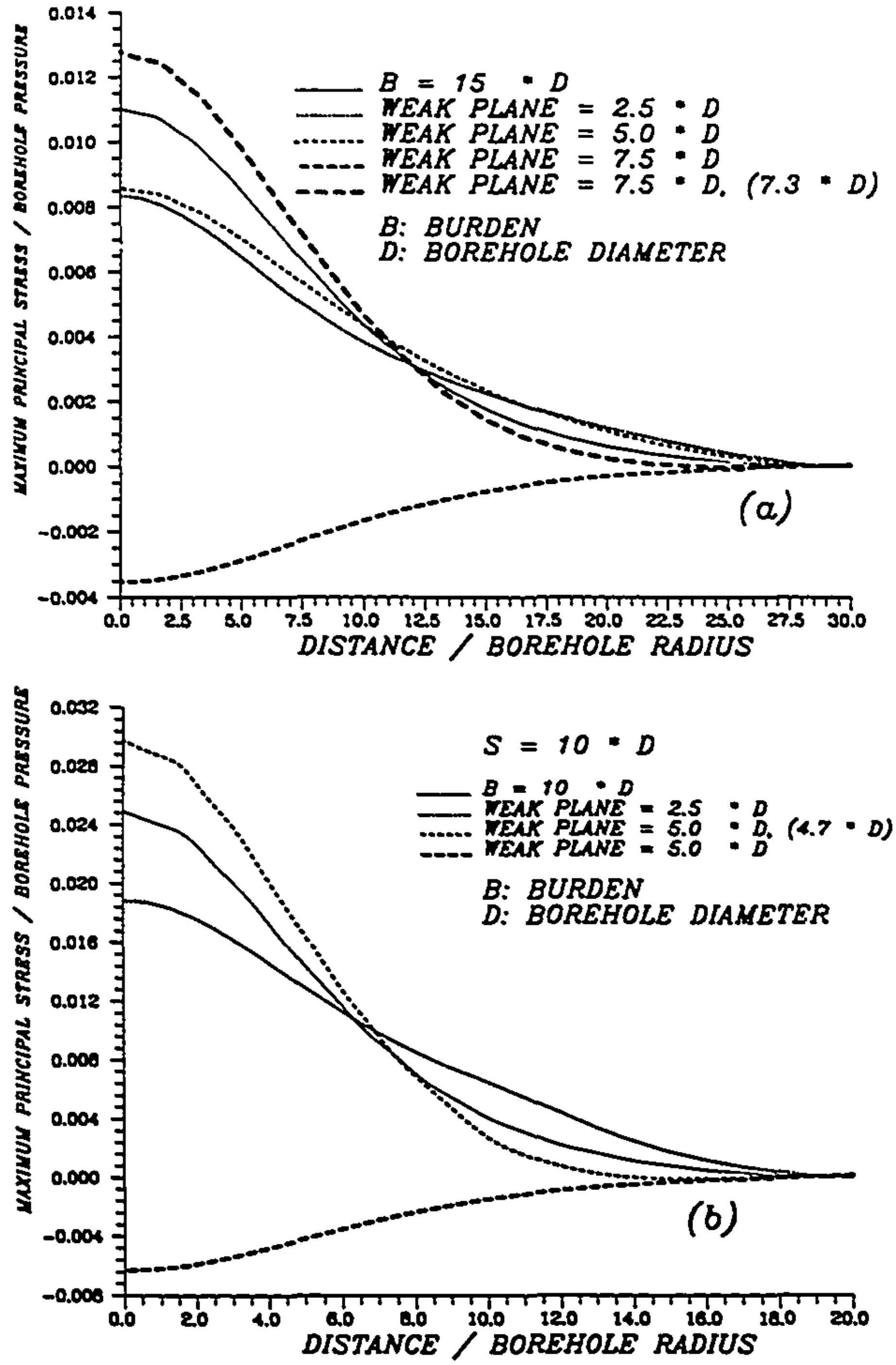

Figure 5.31 : Maximum principal stresses for weak planes normal to free face for different burdens and spacings, along line normal to free face from midpoint.

of hole should be the final results of such blast.

In all cases, the effect of a normal weak plane on the compressive stresses is almost negligible.

5.5.2.3 Effect of the Width of a Weak Plane

The influence of the width of the discontinuity is analyzed next for planes both parallel and perpendicular to the face. For each case, stresses in x and y directions and maximum principal stresses have been calculated, and the final results plotted along the centreline and along directions normal to the free face and connecting the pressurized boreholes and the midpoint (N1 and N2). The width of the weak plane has been varied keeping the burden and spacing constant to discuss stress distribution around the pressurized holes for a weak plane with a fixed distance to the hole. The effect of the width of a weak plane parallel to the free face on the tensile stresses along the centreline for various burdens at constant spacings is illustrated in Fig. 5.32. As shown, the dimension of burden does not have any effect on the stresses. For a fixed plane close to the hole centre (2.5 × borehole diameter), the maximum principal stresses are augmented as the width of weak plane increases, and is close to the real value for a narrow weak plane (1 mm).

As stated before, the parallel weak plane near the hole causes a higher tensile stress between the plane and the holes, but the values of stresses are proportional to the width of weak plane. The stresses reach the maximum value near the boundary of the weak plane and drop to zero on the discontinuity. This value approaches the real one (without weak plane) for a narrow plane (1 mm). The amplitude of stress, immediately before the boundary, varies directly with the width of the weak plane. Also, a very narrow weak plane causes an immediate recovery from the stress. The recovery distance depends on the width of the weak plane for a fixed weak plane, and it is much greater

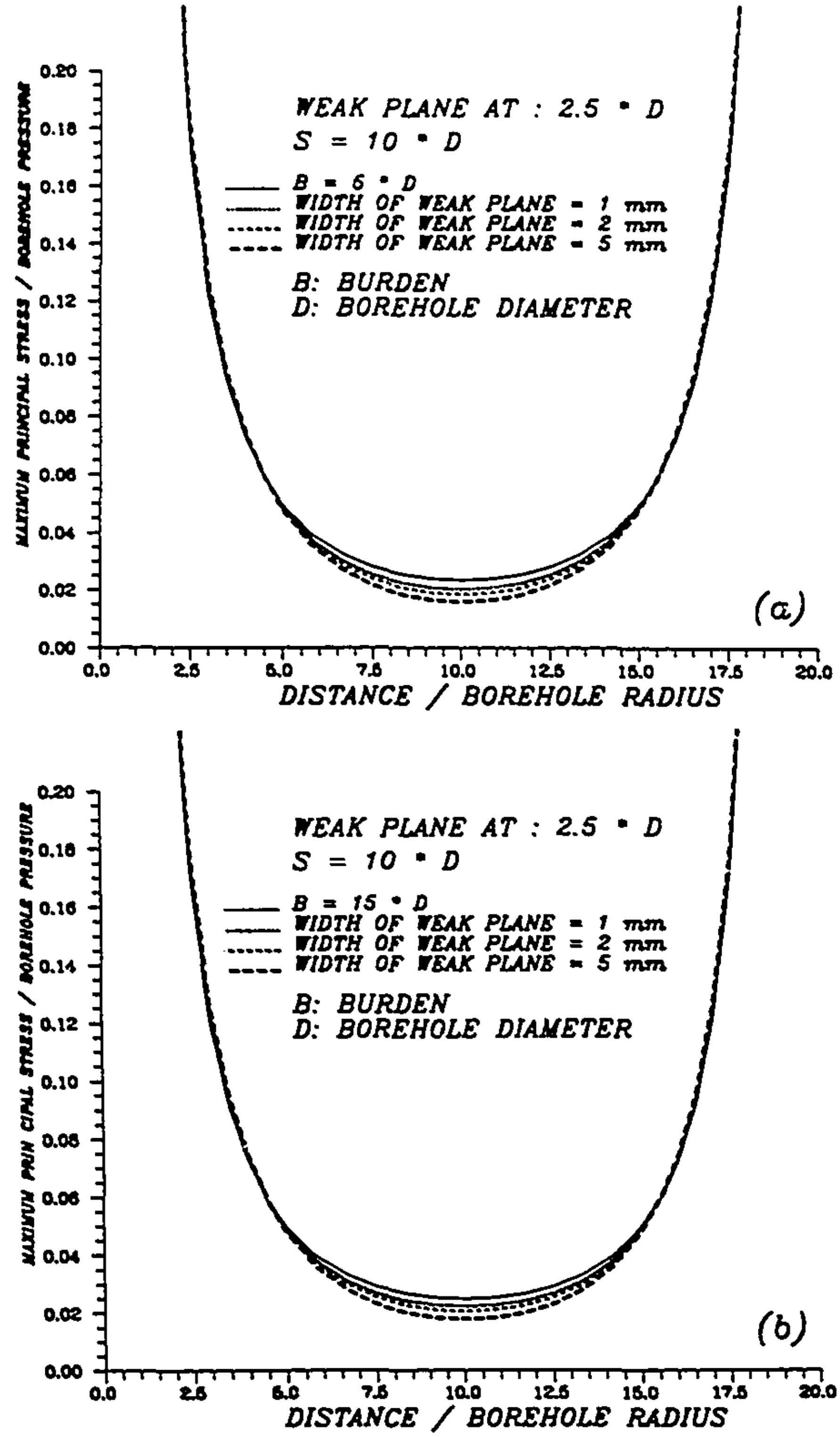

Figure 5.32 : Maximum principal stresses for weak planes of varying widths parallel to free face for different burdens at constant spacing, along centreline.

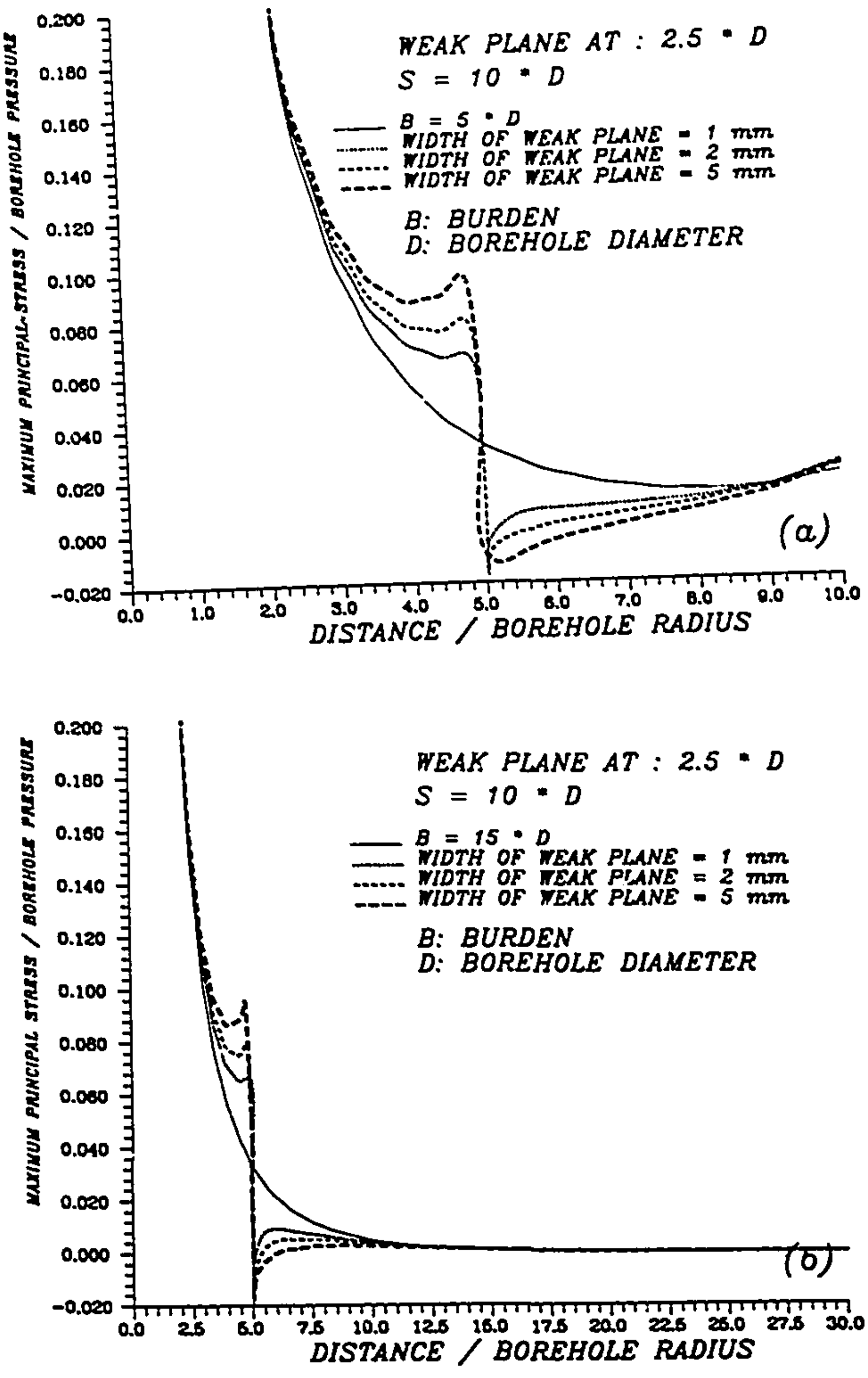

Figure 5.33 : Maximum principal stresses for weak planes of varying widths parallel to free face for different burdens at constant spacing, along line normal to free face from hole centre.

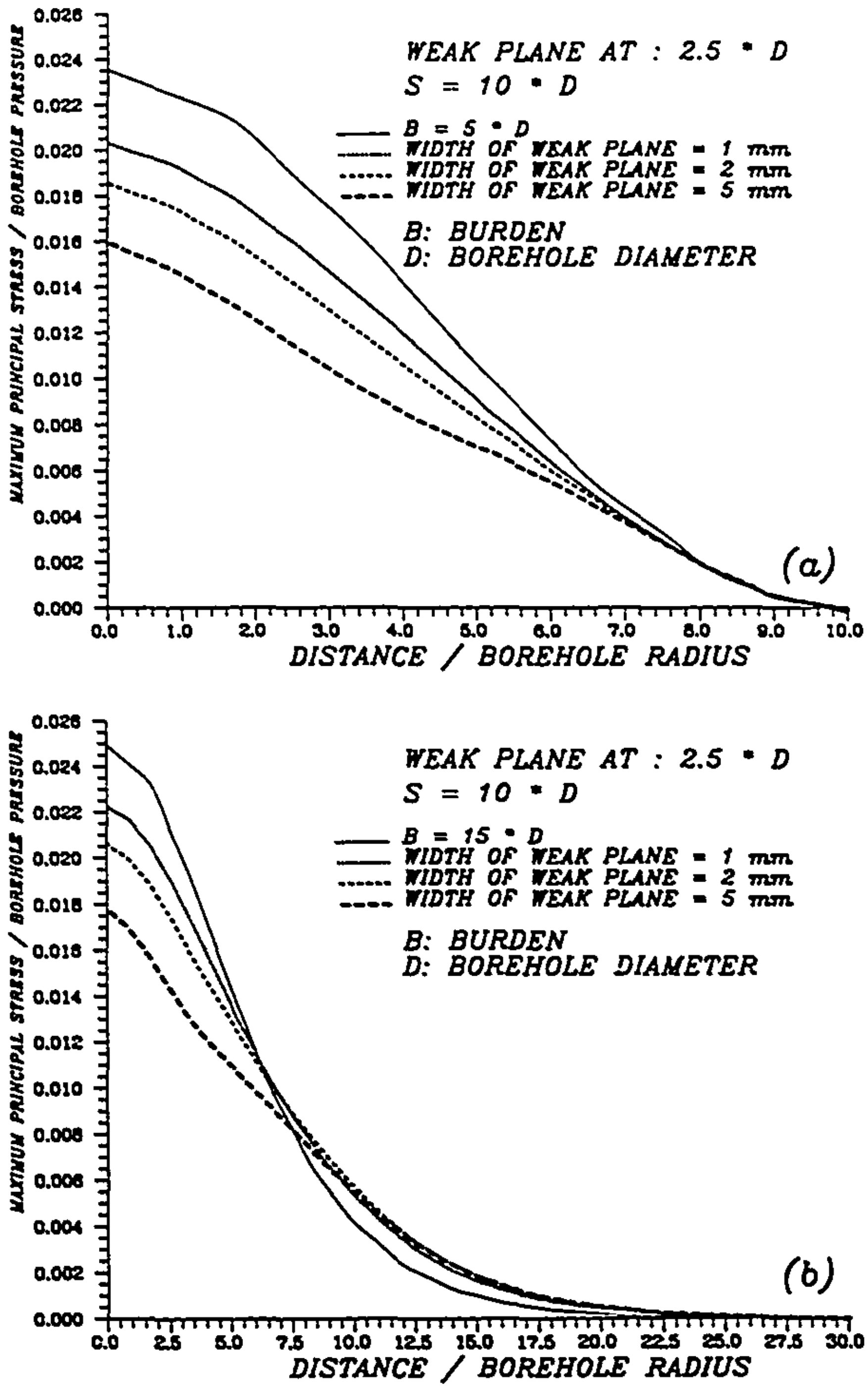

Figure 5.34 : Maximum principal stresses for weak planes of varying widths parallel to free face for different burdens at constant spacing, along line normal to free face from midpoint.

for a larger width. The results are shown in Fig. 5.33.

At the midpoint, both tensile and compressive stresses are functions of the width of the weak plane. For an infinite burden, the magnitude of tensile stresses for a 1 mm wide weak plane is 1.25 times greater than the stresses for the similar model with a 5mm wide weak plane. The results predict that the difference between the magnitude of stresses for varying widths (1, 2 and 5 mm) at constant spacing and various burden will be almost equal (Fig. 5.34).

For distances greater than half the spacing, a narrow weak plane does not have any effect on the stress distribution on the centreline, and it is almost negligible along the direction normal to the free face at the midpoint (Fig. 5.35). When the separation of holes is increased from 10 to 15 borehole diameters, the effect of the weak plane also increases. This separation is an inverse function of weak plane width (Fig. 5.36).

The effect of a parallel weak plane with various widths on the compressive stresses along the centreline is also found to be negligible. These stresses increase between the weak plane and the centreline, along the direction normal to the free face, and immediately reverse to the tensile on the weak plane. The results predict some fractures close to the weak plane, due to this conversion of the stresses. The stresses begin to recuperate quickly after the plane, but the rate of recovery is varied for different widths of weak plane. Consequently, a very narrow discontinuity or an open discontinuity cemented with a strong material would have little effect on the final results of wall control blasting.

According to the results, the weak planes with width smaller than 5 mm, and a distance greater than 5 borehole diameters do not have any effect on the stress distribution. For distances smaller than this, the rate of stress increase largely depends upon the width of the weak plane, and for a very narrow discontinuity (less than 1 mm)

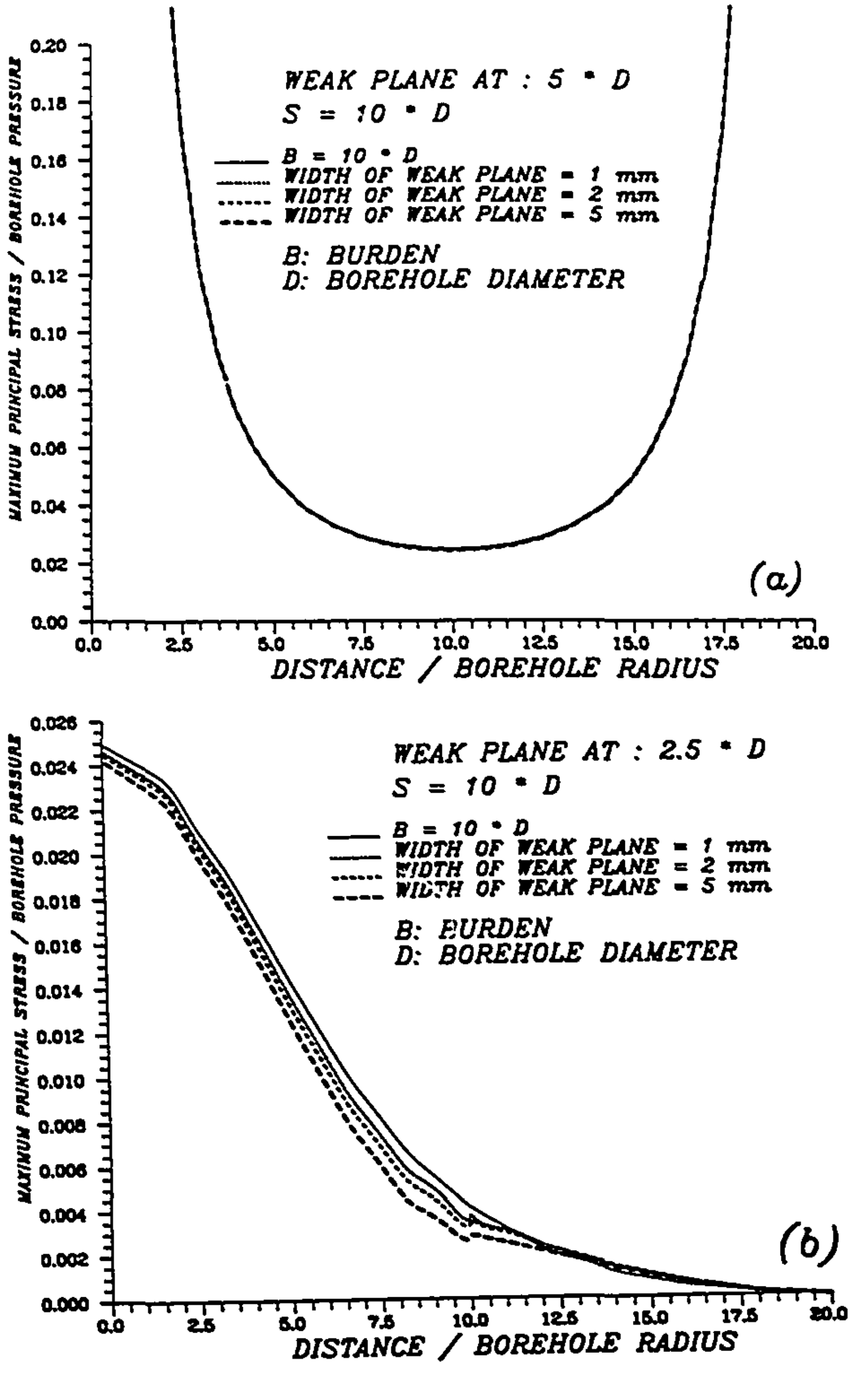

Figure 5.35 : Maximum principal stresses for a weak plane of varying widths parallel to free face constant burden (10 × B) and spacing (10 × B), along centreline, and along line normal to free face from midpoint.

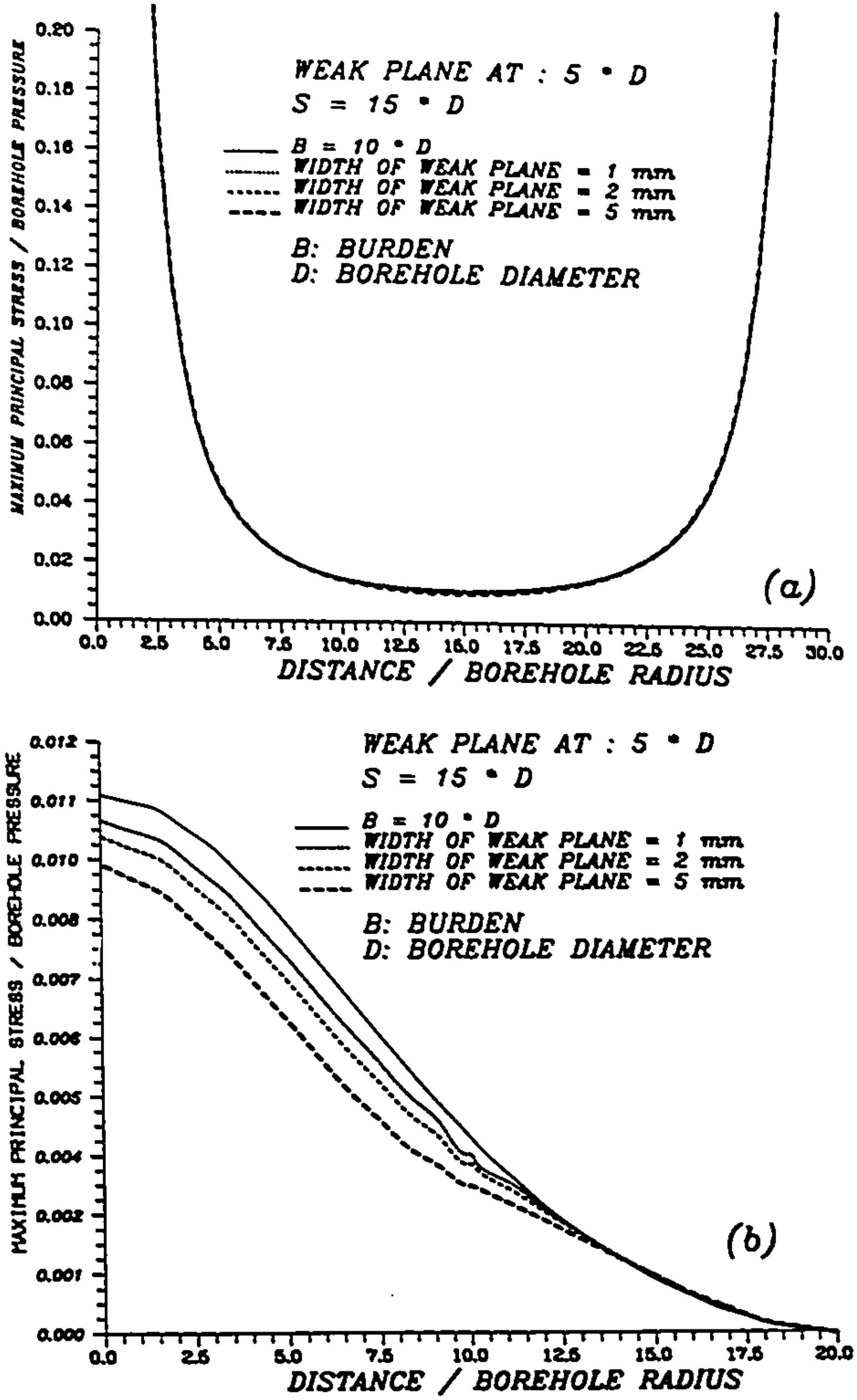

Figure 5.36 : Maximum principal stresses for a weak plane of varying widths parallel to free face constant burden (10 × B) and spacing (15 × B), along centreline, and along line normal to free face from midpoint.

it approaches the value calculated from the same model without any weak plane.

The maximum principal stress between the holes and the boundary of a normal weak plane with various widths is equal, when the plane is located at middle of spacing between two holes. The magnitude of the stresses are variable close to the boundary of weak plane, the narrowest weak plane, but the difference between them is not significant. Similarly, a parallel plane (1 mm width) does not have any effect on the stress distribution, and the influence of a weak plane width smaller than the 5 mm on the stresses is negligible (Fig. 5.37).

As the distance of a perpendicular discontinuity to the borehole decreases, the magnitude of tensile stresses increases close to the boundary of the weak plane. For a weak plane 5 mm wide and located at 2.5 times hole diameter, this value is 2 times greater than that calculated for similar models without a weak plane (Fig. 5.38). This reduces to 1.5 times when the width of the weak plane is decreased to 1 mm. However, a discontinuity with a distance smaller than 5 times the borehole diameter always produces higher stresses in a zone between the borehole and the discontinuity. The magnitude of the stresses in this zone depends on the weak plane width and its distance from the borehole wall. It is expected that several tensile fractures would form in this zone. Consequently, backbreak and rock losses should be resulted in the area between the plane and the pressurized hole. The extent of overbreak in the field should be higher than those numerically calculated, due to the penetration of the explosion gases into the fractures and finally along the discontinuity.

5.5.2.4 Effect of an Inclined Weak Plane

The presence of a single inclined discontinuity in the back of the hole greatly influences the final line of perimeter blasting. The degree of success depends on the critical distance (the smallest distance from each holes to the weak plane). If the

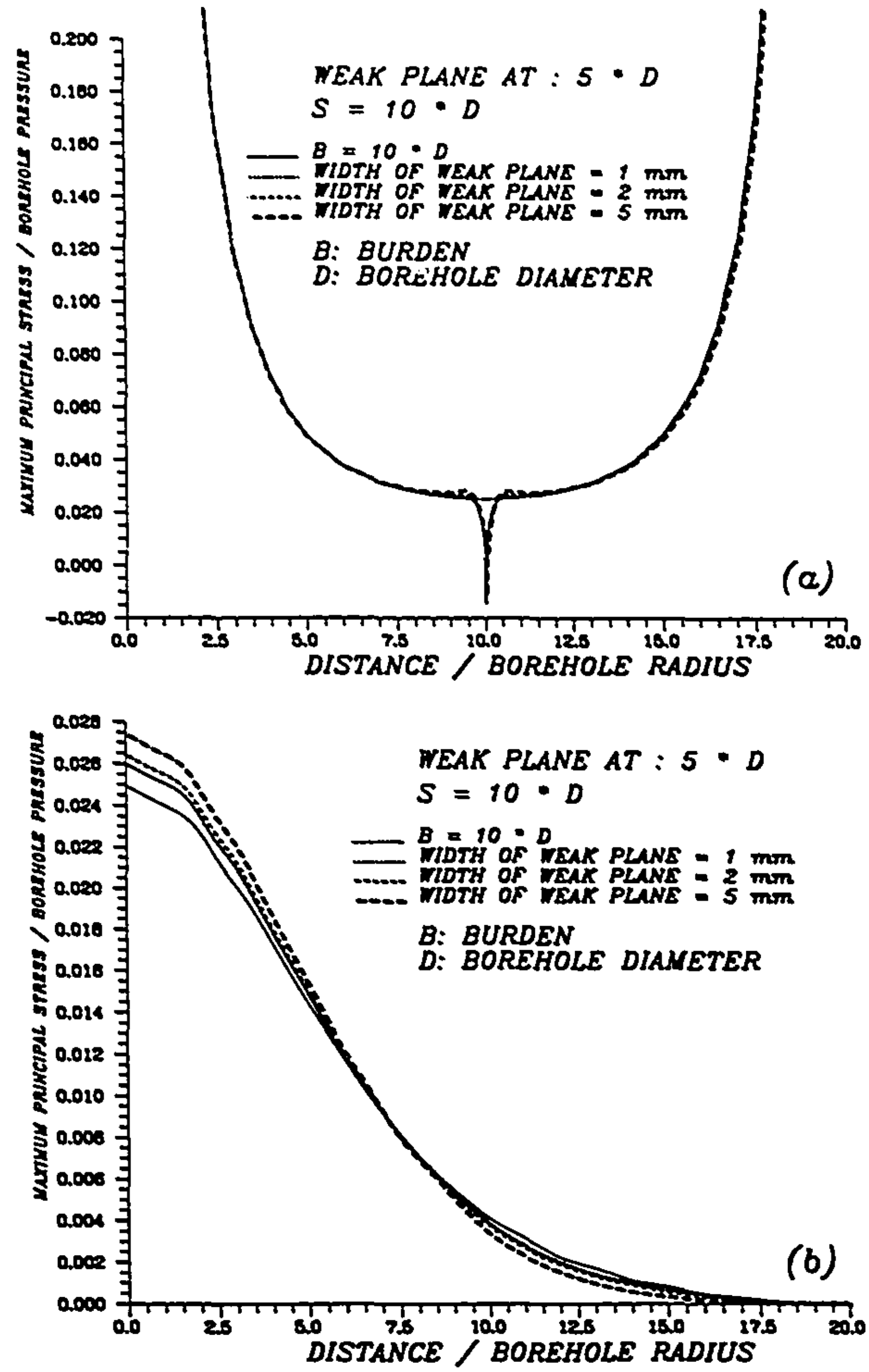

Figure 5.37 : Maximum principal stresses for a weak plane of varying widths normal to free face at the middle of spacing, along the centreline, and along line normal to free face from midpoint.

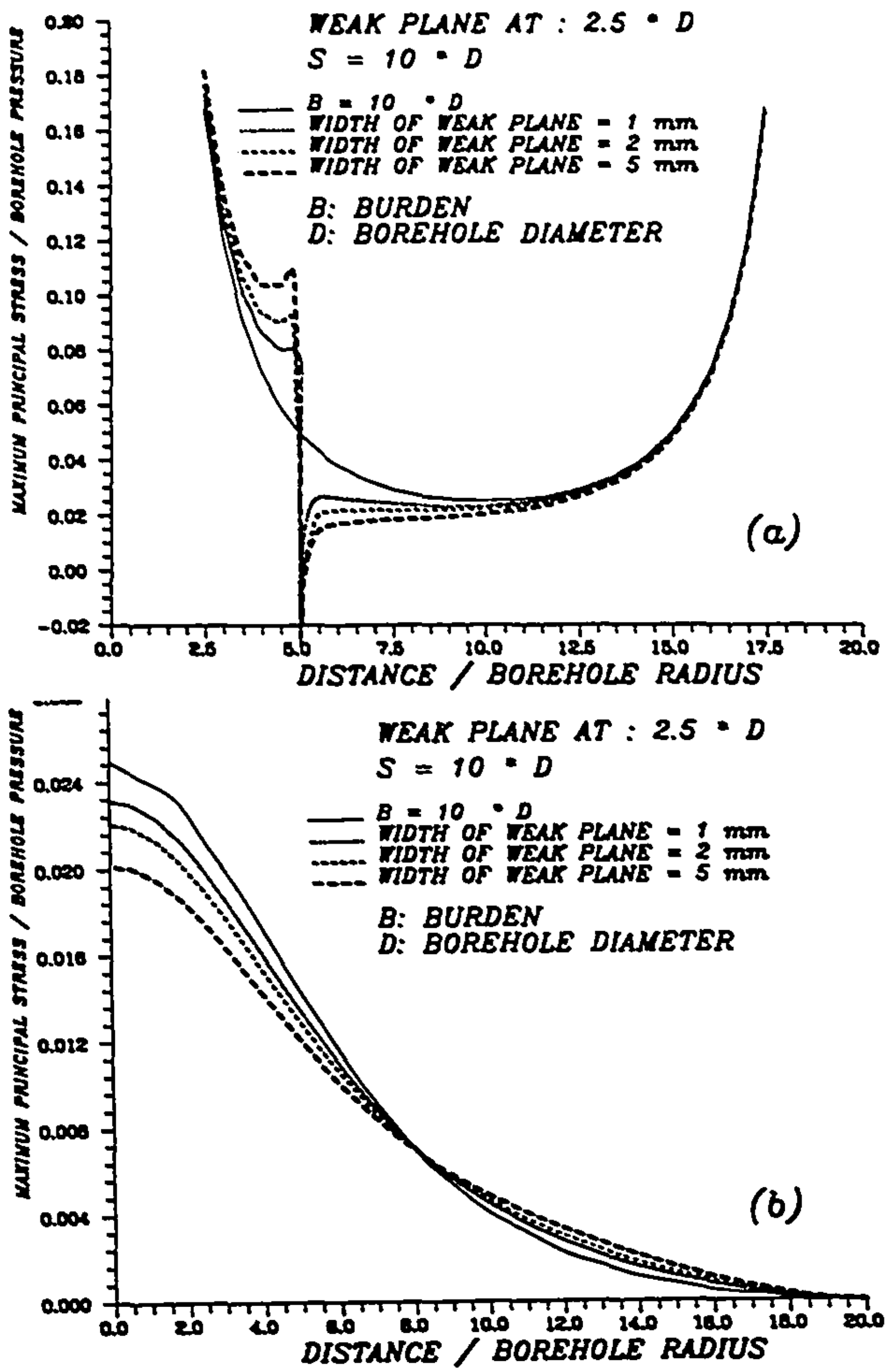

Figure 5.38 : Maximum principal stresses for a weak plane of varying widths normal to free face at 2.5 times borehole diameter from the hole centre, along the centreline, and along line normal to free face from midpoint.

perpendicular distance from the hole to the discontinuity is equal to 2.5 times the borehole diameter, the spacing should not exceed 5 times the borehole diameter.

For distances less than the critical distance, the dominant fracture will be generated normal to the discontinuity from the hole wall. The subsequent gases opens the discontinuity to where the neighbouring hole has fractured it. Therefore, the final face will be changed from the centreline to a line from the first hole to the discontinuity, then along it, and finally to the second hole over the shortest distance. The area between the weak plane and centre line would be completely removed, due to the fractures and rock losses. The distribution of the principal stresses on the line normal to the free face from the holes centre and the midpoints is illustrated in Fig. 5.39.

As shown, the magnitude of the stresses depends on the distance of the weak plane from the borehole walls. These are about two times greater than the stresses obtained from the same without a weak plane, along a direction normal to the free face directly in front of the pressurized hole. However, the magnitude of the stresses would be lower than the case containing no weak plane. The graphs show a tensile zone between the holes and the discontinuity which would be responsible for high backbreak.

The role of an inclined weak plane, which crosses the centreline, on the stress distribution depends on its alignment with the perimeter line. As mentioned earlier, a weak plane normal to the centreline at the middle of holes ($\beta = 90°$) has no effect on the stresses around the pressurized holes. It means that the perpendicular distance between the holes and the discontinuity is exactly located on the centreline. As the angle of the weak plane decreases (from 90°) the perpendicular distance between the holes and the weak plane makes an angle with the centreline. The fracture zone between the discontinuity and the perimeter line depends on the value this angle and the intersection point of the weak plane with the centreline.

Thus, numerical analysis predicts that a weak plane with an angle close to 90° or 0° would cause minimum backbreak and overbreak at perimeter row, and the final face would be smoother. Maximum backbreak and irregular face would result where the angle of discontinuity reaches 45°. It should be noted that, if the discontinuity crosses the borehole wall, the borehole pressure reduces rapidly, due to the penetration of gas inside this discontinuity.

5.6 SIMPLIFIED MATHEMATICAL ANALYSIS

As mentioned in the numerical analysis, after simultaneous detonation of two blast holes in infinite burden under a proper geometry, the superposition of stresses between two holes produces a tensile zone around the centreline. The tensile stresses along the direction normal to the centreline from the hole centre are much higher than the stresses along the two parallel lines crossing the holes. The fracture zones would therefore assume approximately elliptical shape for each hole, with major axis of the ellipse being coincident with the centreline.

The geometry of blast, burden, spacing and borehole diameter, and any type of discontinuity close to the borehole walls can influence the shape of these elliptical fracture zones. As the burden or spacing decreases, the tensile stress increases on the line normal to the free face from the hole centre. Consequently, these fracture zones would change shape from elliptical to circular. The rate of variation depends on the position of the burden and spacing between holes. The role of a single discontinuity (parallel, perpendicular or inclined to the perimeter line) on the fracture zone is approximately similar to that of a free face. The degree of backbreak and smoothness of the final face depends on the position of the discontinuity and the angle between it and the centreline. The results obtained from the simulated models by finite element analysis in the presence of a weak plane show the elliptical shapes of tensile zones between the pressurized holes change. The new zones have a more circular shape and are located between the borehole wall and the discontinuity.

Based on these analyses, it is postulated that maximum rock breakage would occur in the region between the holes and the discontinuity which has an approximately triangular shape (Fig. 5.40). The maximum backbreak or overbreak would occur when H reaches the highest value. In the right-angled triangle **OPH$_1$**, OP can be calculated by

$$= \quad {}_1 \times \ IN$$

In the right-angled triangle **OMH$_1$**, OH$_1$ is equal to

$${}_1 = \quad {}_1M \times \ IN$$

$$\begin{aligned} OP &= \ {}_1M \times \ IN \ \times \ O \\ &= \frac{1}{2}\times \ {}_1M \times \ IN2 \end{aligned}$$

Therefore, H is equal to

$$H = \frac{1}{2} \times K \times SIN 2\beta$$

where H is the height of the triangle, K is distance between the hole and the discontinuity on the centre line, and the β is the angle between the perimeter line and the discontinuity. For a constant K the value of H reaches the maximum when SIN 2β is equal to one, or $2\beta = 90°$ and $\beta = 45°$. For each hole the maximum backbreak would occur when the angle of discontinuity and the perimeter line is equal to 45°. Conversely, for a constant angle the maximum rock breakage would be produced where K reaches its maximum value. It means that the weak plane crosses the centreline at the midpoint.

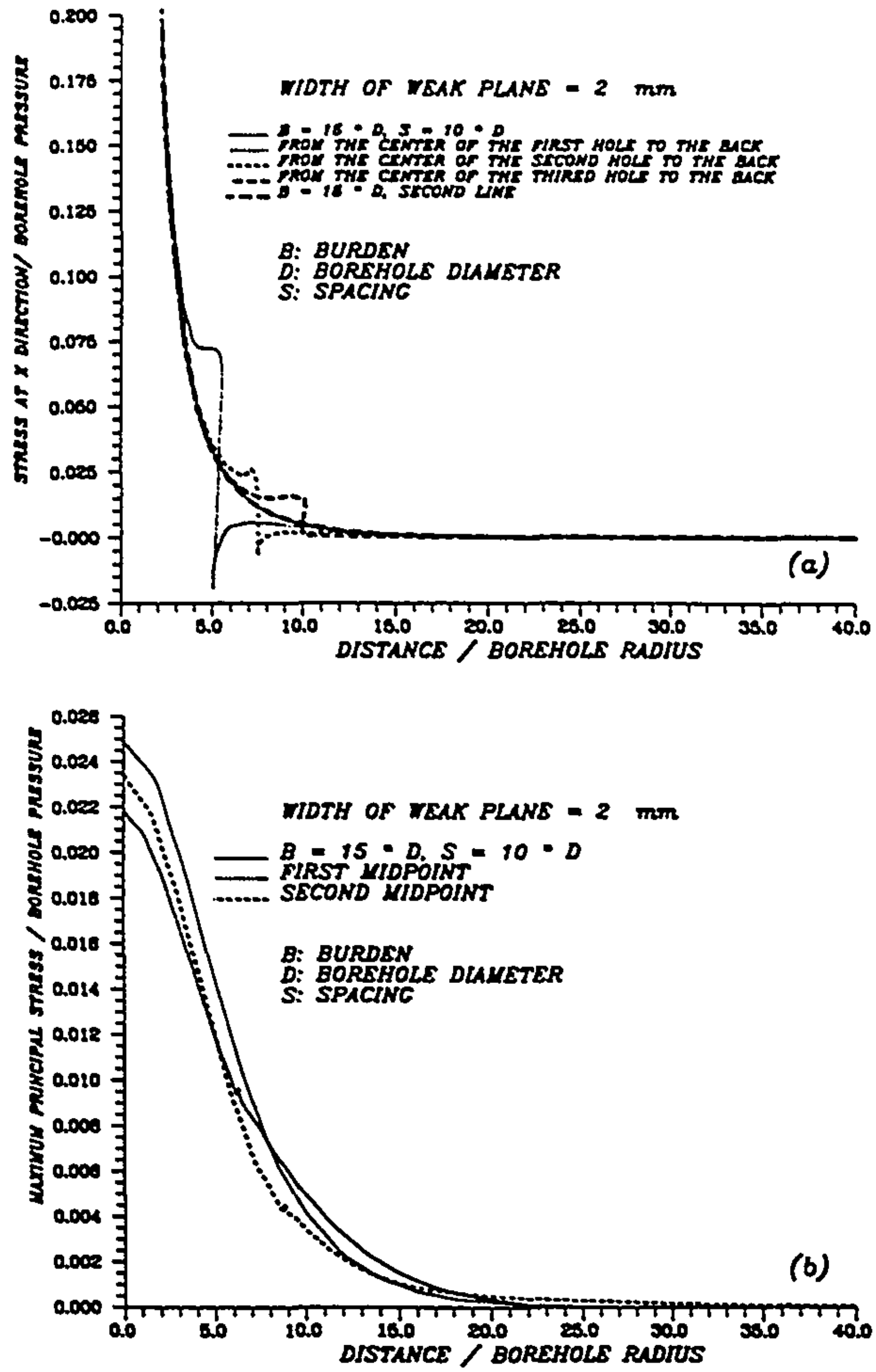

Figure 5.39 : Maximum principal stresses for an inclined weak plane (2 mm wide), along lines normal to free face from holes centre and from midpoints.

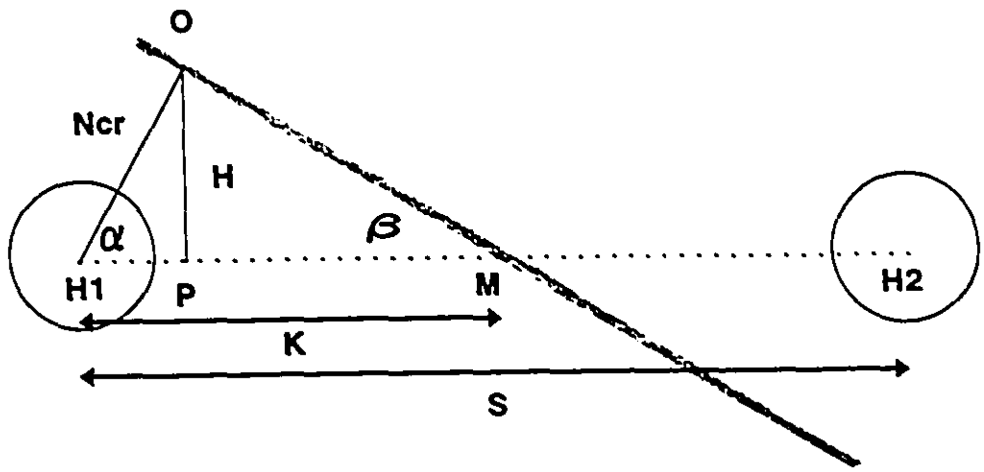

Figure 5.40 : Two dimensional triangular fracture zones between two pressurized holes.

In the other words, K should be equal half spacing. Therefore maximum backbreak or overbreak (and the resulting irregular face) would develop where the discontinuity is located at the midpoint with a angle equal to 45°. Based on the following relations:

$$H = N_{cr} \times COS\,\beta$$

For a constant N_{cr}, the maximum backbreak would also occur where H is at maximum (i.e. $\beta = 0°$). Similarly,

$$K = \frac{N_{cr}}{SIN\,\beta}$$

Thus, when $\beta \rightarrow 0$, $K \rightarrow \infty$, and as a result, maximum backbreak would occur when the discontinuity is parallel to the centreline. It corresponds exactly to results obtained from the numerical analysis.

For a constant N_{cr}, the minimum backbreak would develop between two pressurized holes where **COS** β is equal to 0. Therefore, β must be 90°, H must be equal to zero, and N_{cr} becomes K (i.e. a weak plane normal to the centreline). As mentioned earlier, the maximum value of the critical distance (N_{cr}) is equal to K, or half spacing (S/2). Another result is that, the maximum effective distance between the hole and the discontinuity is equal to half spacing, and for a distance equal or greater than this the role of the weak plane on the stress distribution is negligible. This result also is agreement with the calculated values from numerical analysis.

The area of the broken rock can be calculated by the following relation:

$$A = \frac{1}{2} \times N_{cr}^{2} \times \frac{COS\,\beta}{SIN\,\beta}$$

Maximum backbreak would therefore occur for a N_{cr} equal to the half spacing (N_{cr} = S/2). The maximum fractured area (A_{max}) would therefore be equal to

$$A_{max} = \frac{1}{8 \times TAN\beta} \times S^{2}$$

The above relations would of course apply to idealized cases. In actual blasting, the usual field variables would render these equations somewhat approximate. Nevertheless, they represent useful guidelines in estimating the extent of fracture zones.

5.7 ANALYSIS OF FRACTURE FORMATION WITH MULTIPLE HOLES

When the blast holes are detonated simultaneously, the pressure on each borehole wall generates the radial and tangential stresses which create the fractures. As shown in

Fig. 5.41 at infinite burden, at location L1 the stresses generated by the holes oppose each other, whereas these stresses are reinforced at location L2. Therefore, on the lines which connect the hole centre to the free face, the stresses are not adequate to develop the cracks. On the centrelines, the stresses are enhanced by each other, but compressive stresses are not sufficient to create the crack because rock is much stronger in compression than tension. Therefore, the rock starts to fail between the holes, and the fractures diminish in other directions. As illustrated in Fig. 5.42, the tensile stresses at the midpoint of the centre line, (the line at which stresses reinforce each other), are six times greater than the stresses at similar points on the line normal to the free face from the centre of the second hole.

In addition, the area between each of the two holes is under tension, which would tend to pull the rock apart along the centreline from both sides. This zone will be developed by the collision and support of the tensile stresses in the region between each of the two holes. The results obtained by the numerical analysis clearly show this tensile area between the three pressurized holes (Fig. 5.43). By this process, a tensile crack would be created and opened between two holes, for very large burden. Of course, all fractures must originate from the borehole wall, because the stresses at the borehole wall are much higher than at other points. However, only radial cracks along the co-linear direction (connecting the holes) would grow preferentially over others, due to the nature of stress distribution.

In summary, co-linear crack formation, can be explained by simultaneous detonation of holes, and collision of the stresses generated between the holes (in the dynamic case) and reinforcement of stresses (in the quasi-static case) in order to obtain a narrow fracture zone between them. The fractures are produced by tensile stresses on the centreline, augmented by a tension area between the holes which pull the rock against the centreline. The final outcome would be a narrow fracture zone between multiple blastholes, suitably spaced, loaded and timed.

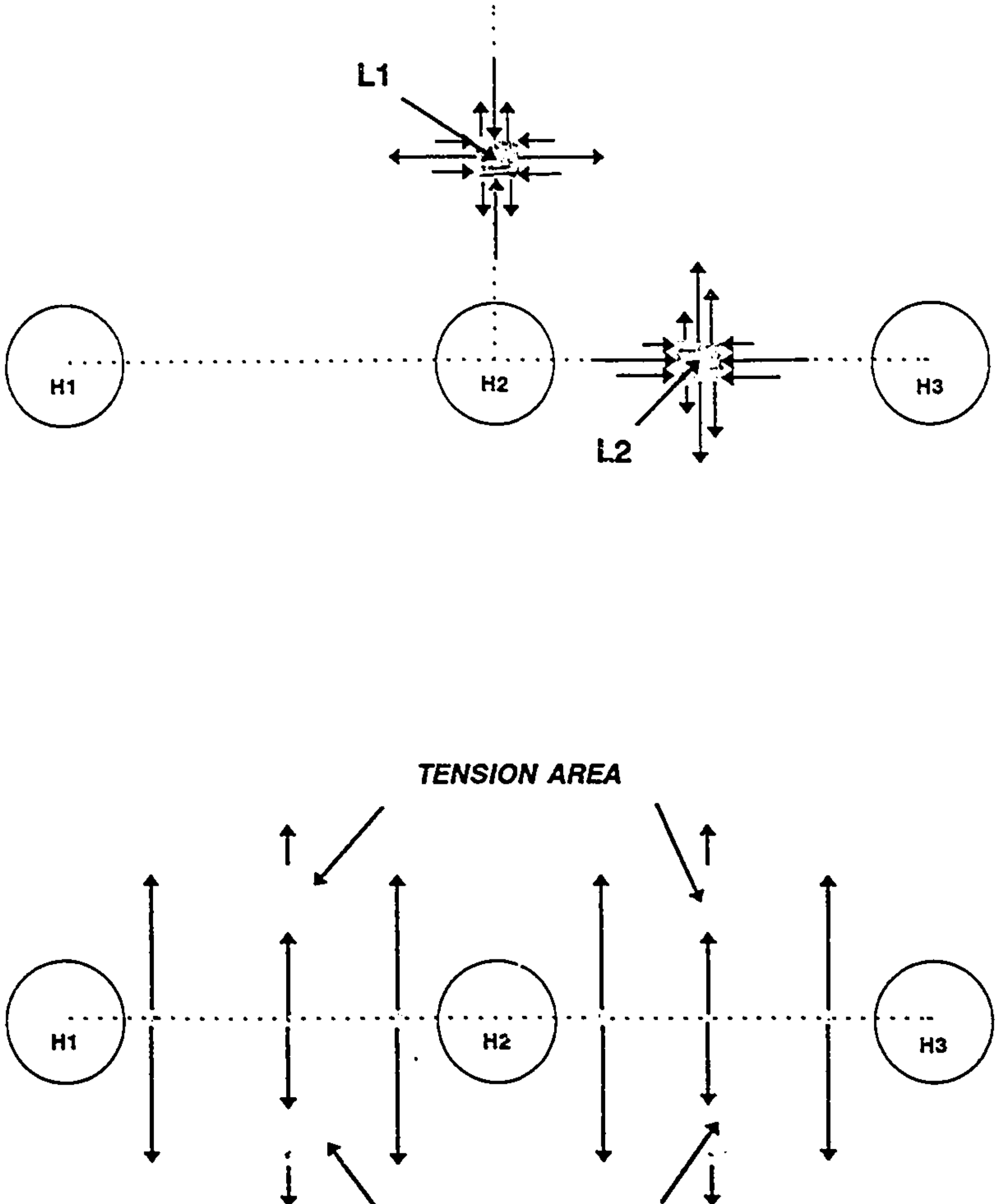

Figure 5.41 : Stress analysis around three pressurized holes.

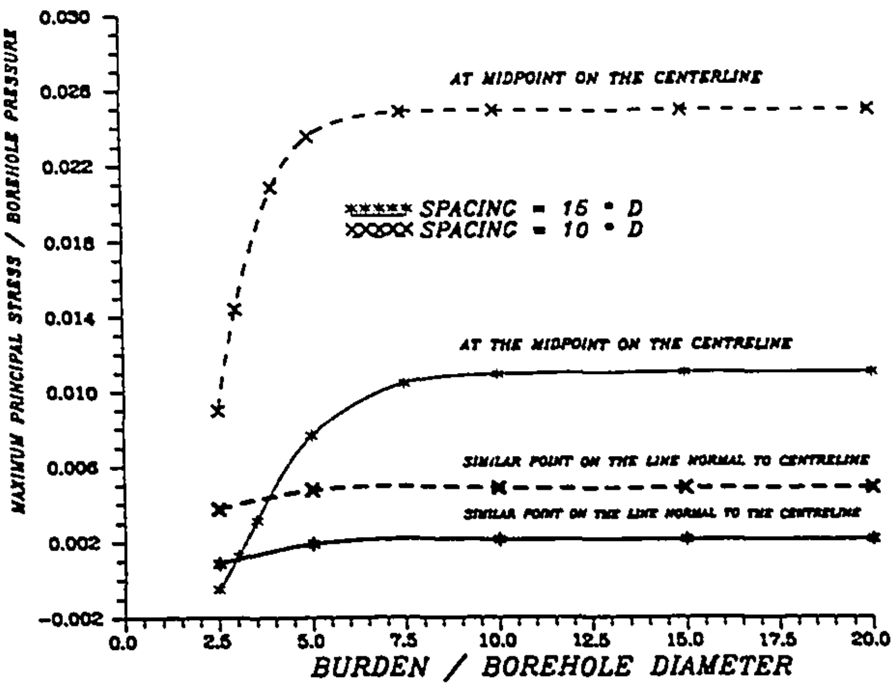

Figure 5.42 : Calculated maximum principal stresses at midpoint and similar point on the line normal to the free face for various burdens.

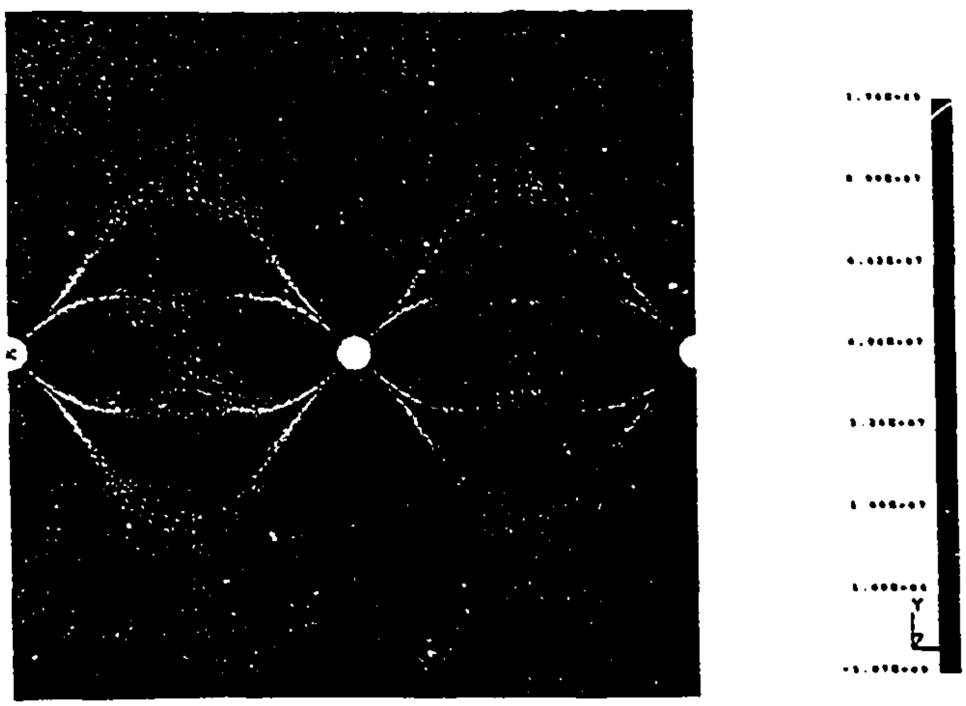

Figure 5.43 : Tensile zones between three holes from numerical analysis.

5.8 CONCLUSIONS

The mechanism of creating a narrow fracture zone between two holes and the stress distribution around one and two pressurized hole(s) has been analyzed from the view point of the quasi-static explosion pressure. An analytical solution has been used to determine the radial and tangential stresses around a pressurized hole in an infinite medium. In this simple analysis, the stresses depend only on the borehole pressure. The reliability of the finite element models has been tested by comparing the results with these obtained with an analytical solution for the simple case of a pressurized hole in an infinite medium.

Two-dimensional finite element modelling has been carried out to determine the effect of a free face and weak planes oriented at various angles to the free face on the stress field around and between the pressurised holes. Maximum principal stress and stresses in the co-linear and perpendicular directions, on the front and back of the holes, have been calculated using two established finite element programs. The stress fields have been calculated along the direction normal to free face from the centre of the hole and the midpoint, as well as on the centreline. Both burden and spacing have been varied keeping the borehole diameter constant to analyze the stresses in the burden region and behind the holes. The effects of a weak plane of varying widths as a function of burden and spacing and a fixed weak plane for different burdens on the stresses around the pressurized holes have also been discussed .

Based on numerical modelling, for normal wall-control practices a burden can be defined as an infinite burden, when the ratio of that to spacing is greater than unity. With an infinite burden, the stresses are maximum at the borehole wall and decrease symmetrically and monotonically with distance around the hole. The rate of decay is inversely proportional to the square of the distance. When the burden region is smaller than some critical burden, the rate of decay diverges significantly from the infinite burden analysis, but only close to the free face. This rate depends on the distanc of the free face from the borehole wall.

Numerical analysis shows that hole separation would range up to 15 borehole diameter for pre-split blast (infinite burden) in an isotropic and homogeneous material. For an optimum spacing, the form of the fracture zone for each hole is approximately elliptical shape. The major axes of these ellipses coincide with the centreline between the holes. As the burden or spacing decreases, the fracture zones change from elliptical to circular or conical shape. The degree of change depends on the dimension of the burden and the separation distance between the holes.

The analysis also shows that a ratio of burden to spacing up to 0.8 for cushion blasting and between 0.8 and 1.2 for buffer blasting would be applicable. With these ratios, a dominant fracture plane would be created between the holes, along with some fractures in the burden region. The analysis predicts "humps" between the holes when the ratio is less than 0.8, and large blocks and extensive backbreak when the ratio is greater than 1.2. These ratios are similar to the ratios recommended by blasting engineers for cushion and buffer blasting, which have been obtained by trial-and-error and field observations.

In all simulated models, for a distance more than two borehole diameter away, the stresses become very small compared to the applied pressure on the borehole wall. Therefore, onset of fractures at the midpoint between two holes would be highly unlikely.

As the results of numerical modelling show, the mechanism of wall-control blast can be explained by the collision and/or superposition of the stresses between the holes, in order to obtain a narrow fracture zone between them. This fracture is produced by tensile stresses on the centreline, which is greater than at any other directions, and a tension area between the holes which pulls the rock against the centreline.

The presence of a wide (parallel, normal and inclined) weak plane (of the order of 10 mm) causes the tensile stress to reach the maximum value at the boundary of the weak plane; the stress drops immediately to zero on the weak plane. It does recover, however, to its original without the weak plane, but only at a considerable distance from the weak plane. The recovery distance is found to be inversely proportional to the distance of the weak plane to the borehole. In this case, a wide weak plane represents essentially the effective burden and therefore acts as a fracture terminator.

Excessive overbreak in the direction of the centreline and humps between the holes are also predicted by model for a wide weak plane parallel to the free face with a distance smaller than half the spacing from the borehole wall. The tensile stresses increase close to the weak plane as the distance of that to the borehole wall decreases. A fracture would start to develop from the borehole wall to the parallel weak plane along the perpendicular direction. In the presence of a weak plane behind the boreholes, this weak plane will present the final wall provided the distance of the weak plane is less than the half spacing. For the same reason, in the presence of a wide parallel weak plane the stress field around the pressurized holes would be independent of the location of the free face.

A weak plane located at the midpoint between the holes and lying normal to the centreline is shown to have only minimal effect on the results of the wall-control blast. It is also seen that when the distance of the perpendicular weak plane is changed by moving it closer to one of the holes, the tensile stress at this plane not only increases, as would be expected, but also considerable overbreak would be seen to ensue near the closer hole. The model shows that at 1/4 the spacing, the presence of this weak plane would cause the stress field between it and the borehole to assume a more circular shape. Therefore, more intense fracturing would take place around this hole, which would adversely affect the degree of fracture-plane control.

In case of perpendicular weak planes, on the other hand, planes < 5 mm wide and located at a distance greater than five borehole diameters have negligible effect on the stress distribution. Therefore, a very narrow discontinuity or wide discontinuity which is filled with a strong material would have negligible effect on the final results of a wall control blast.

The results show that the tensile stresses and maximum principal stresses are identical along the centreline, and along the direction of the three lines normal to the free face from the hole's centre and centreline's midpoint

The amplitude of maximum principal stresses, immediately before the boundary, varies directly with the width of the weak plane. The stresses drop to zero on the discontinuity, and a very narrow weak plane causes an immediate recovery from the stress drop. The recovery distance depends on the width of the weak plane as well as the distance of that to the borehole wall. The effect of a weak plane wider than the 60 mm is virtually identical to that due to a free face.

Finally, some parameters are either ignored or over-simplified in the modelling of the process, due to the limitations of the finite element codes. For example, two-dimensional finite element programs have been used to analyze the stress distribution around the pressurized holes. Isotropic and homogenous materials are selected as the media, and an elastic solution is used to calculate the stresses in the regions of interest. A concept of a weak plane is used to present any type of discontinuity in the rock mass, because the programs can not handle an open joint in the simulated models. The role of explosion gases inside the opened cracks are also ignored, which may significantly affect the final out-come, resulting in rather conservative estimates of burden and spacing.

CHAPTER 6

EXPERIMENTAL INVESTIGATION

6.1 INTRODUCTION

In analytical solutions and in most cases of numerical analysis, as described in previous chapter, rock is assumed to be homogeneous and isotropic, presenting a simplified model for rock excavation using explosives. These models can only analyze the influence of one or two practical processes at a time, separate from the other processes. However, rock is really a continuous medium, and no accurate mathematical solution is available to analyze the complex process representative of explosive-rock interactions.

Rock is generally divided into segments by natural breaks, such as joints, faults bedding planes, foliation and schistosity planes etc. Each of these segments is approximately intact and comprises a block of rock. Therefore, the same mineralogical rock types may have differing mechanical properties. Since, most rocks are neither homogenous nor isotropic, in designing a blast pattern in rock, unlike other engineering material, the designer conforms with blocks of rock material separated by various types of discontinuities. Therefore, the best approach is to carry out controlled experiments based on the results obtained by simplified mathematical or numerical analysis, and previous investigations.

The term discontinuity has been recommended by the International Society for Rock Mechanics (ISRM) to describe collectively joints, weak planes, schistosity planes, weakness zones and faults. The ten following parameters have been selected to describe the discontinuities in the rock mass: orientation, spacing, persistence, roughness, wall strength, perture, filling, seepage, number of sets and block size. The relation between blast geometry and these parameters should be more important than the numerical value of Q or RMR. Certainly, these parameters do not have equal influence on the results of perimeter blasting. The primary factors that influence the final results of the perimeter blasting and the degree of smoothness of the face could be described as follows:

1. Orientation of the discontinuity with the final face or blast geometry.
2. Distance between fractures and the borehole wall.
3. Width of discontinuities.

The orientation of the discontinuity can be defined by dip angle and dip direction or stick and dip. Spacing is described as a perpendicular distance between adjacent discontinuities which controls the size of the blocks making up the rock mass. Spacing can also be defined by the number of discontinuities per meter (frequency).

The perpendicular distance between two adjacent rock walls of a discontinuity is defined as the width of the discontinuity. This discontinuity can be opened or filled by several types of materials, such as; clay, silt, sand, gouge, breccia, mylonite, calcite and quartz. With the exception of those filled with strong vein materials (calcite, quartz, etc), filling materials usually are weaker than the parent rock. The filled discontinuities display a wide range of physical behaviour.

In production blasting, rock fragmentation characteristics vary with the orientation of the discontinuities relative to the blast direction, the spacing of the discontinuities and the filling materials. But in wall-control blasting methods, the degree of success largely depends on the orientation of discontinuities relative to the final rock surface, the distance of the discontinuities to the wall of boreholes, and the width of the discontinuities. The main purpose of this chapter is to analyze the influence of discontinuities on the results of perimeter blasting in situ blast in two different rock types with completely disparate rock structure as well as explosive type and blast geometry.

There have been a number of studies in this area over the last three decades (e.g. Belland, 1966; Ash, 1973; Burkle, 1979; Lande, 1983; Bhandari, 1983). The effects of discontinuity on the results of production blasting and their control over fragmentation size have been discussed by these authors. The results obtained are still somewhat qualitative. They conclude that a strong correlation exists between the direction of blasting and orientation of discontinuities, spacing of the joint sets and the dominant discontinuity in terms of blast results. These have been thoroughly reviewed by Lizotte and Scoble (1993). Mckown (1984), Worsey (1984), and Tariq and Worsey (1995) have studied the influence of discontinuities on the results of perimeter blast. These were based on laboratory investigation in plexiglass, concrete and blocks of rock, coupled with some field observations in quarries, mines and roadcuts.

The main purpose of this chapter is to give an overview of how discontinuities and blast geometry affect the results of wall-control blasts. The emphasis is on highlighting the importance of orientation of the discontinuities relative to the centreline or the final rock surface as well as the width and the distance of these from the borehole wall. This experimental investigation has been carried out at two different sites. Three different borehole diameters, three different types of explosives and various blast geometries have been used in two different rock types in the presence of several discontinuities. The results obtained from the first site have been analyzed by direct observation of crack formation on the surface. At the second site, the degree of success has been assessed by direct observation of crack formation on the surface as well as using half-cast factor (HCF) on the excavated face.

6.2 FIELD EXPERIMENTS

Blasting experiments have been carried out in two different rock types with different structures at two different sites. The Richmond site (Site 1), is located at about 150 km from east of Montreal and 25 km from the town of Richmond. The Kingston site (Site 2), is located 30 km west of the town of Kingston in Ontario and about 360 km from Montreal.

6.2.1 Type of Explosives

Considerable attention was given to the selection of suitable explosives for this experimental investigation. Firstly, the explosives had to be reliable and give reproducible results. Secondly, due to the nature of the investigation, the charge had to be decoupled in the blastholes. Therefore, the explosive cartridges had to be available in a wide variety of diameters. The following three explosives were selected for the field tests: PRIMAFLEX[1], SUPERFRAC 4000 and MAGNAFRAC 3000. PRIMAFLEX is a special detonating cord with a core load of TNT/PETN (85 g/m), contained in a plastic tube with a wall thickness of 0.5 mm. SUPERFRAC is an emulsion explosive containing Ammonium nitrate (AN) prills. MAGNAFRAC is an aluminized emulsion. All are detonator sensitivitive, and are characterized by a high degree of reproducibility in terms of detonation properties (velocity of detonation, energy and pressure). Some of these properties are summarized in Table 6.1.

[1] : *PRIMAFLEX, SUPERFRAC and MAGNAFRAC are ICI trademarks.*

Table 6.1 : Properties of the explosives used for the field experiments.

Explosives	Diameter	RWS	RBS	Density	Velocity of Detonation	Calculated Detonation pressure
	(mm)	-	-	(g/cc)	(m/s)	(MPa)
PRIMAFLEX (Detonating Cord)	11	112	183	1.37	6500	7000
SUPERFRAC 4000 (Emulsion with AN prills)	25 32	89 89	125 125	1.17 1.17	4250 4510	2560 2880
MAGNAFRAC 3000 (Aluminized Emulsion)	25 32 40 50	93 93 93 93	125 125 125 125	1.13 1.13 1.13 1.13	4600 4750 4900 5150	2890 3090 3280 3630

RWS : Relative Weight Strength, (explosive energy relative to ANFO by weight).
RBS : Relative Bulk Strength, (explosive energy relative to ANFO by volume).

Each 25 - 32 diameter cartridge measures 300 mm in length.
Each 40 - 50 diameter cartridge measures 300 mm in length.

6.2.2 Rock and rock mass properties

At Site 1, the peridotite host rock contains relatively narrow asbestos veins. The joints, which dip about 80° towards N50E, are filled with the asbestos. The width of the filled material is about 2 mm, and the spacing of the joints are about 1 m. The foliation in the same rock has a dip angle of 52° with N340E direction (Marcotte, 1980; Marquis, 1985). In some places, serpentinization zones are visible in the rock mass. These probably represent the shear zones. The foliations are usually open to 0.3 m below the surface, presumably due to weathering.

The experimental area at the second site (Site 2), is comprised of massive bedded limestone with individual layers varying from 1 to 3 m thickness. It is oolite limestone ($CaCo_3$ rich up to 95%) which use for cement production (Sabina, 1983). The dominant joints are normal to the horizontal bedding planes, and are generally closed. The spacing between joints varies from 1 to 2.5 m, and in some places a few random joints cross these joint systems. Irregular discontinuities normal to the bedding planes are also found in the rock mass. These are opened and filled with soil. The width of the filled material varies from 10 to 20 mm. The rock mass is divided into different blocks by these weak planes and the joints.

Table 6.2 shows the properties of the rock in the experimental areas. These properties are obtained from the core samples with static test measurements, and from block samples with ultrasonic measurements. The dynamic properties of the rock samples are obtained from stress wave velocity (P-wave and S-wave) and density (see Equations 2.1 to 2.4).

The seismic properties were measured on blocks (~ 30 cm sides) whereas, static properties were measured on small core samples. This would explain the higher modulus values, fined under the static measurements.

6.2.3 Blast Geometry

Three different borehole diameters were employed at the two sites. The boreholes at Site 1 were 50 mm and 100 mm in diameter and were drilled to a depth of 2.5 m. The boreholes at Site 2 were 100 mm and 150 mm in diameter and drilled to a depth of 3 m. The burden and spacing at both sites varied from 10 to 30 times the borehole diameter. The major considerations in the design of the experiments were as follows: a.) blast geometry comparable to those obtained from the numerical analysis and these employed in wall-control blasts, b) decoupling ratio, relation between the charge diameter and the borehole diameter (Fig.6.1), and c) blast geometry and pre-existing discontinuity.

Based on the above parameters, the following observations and assessments were

Table 6.2 : Properties of rock at Site 1 and Site 2.

Rock type	Uniaxial Comp. Strength	Tensile Strength	Density	E_s	E_d	ν	C_1	C_2
	(MPa)	(MPa)	(g/cc)	(GPa)	(GPa)	-	(m/s)	(m/s)
Site 1: Peridotite	172	5.2	2.65	50.5	44.5	0.25	4510	2590
Site 2: Limestone	153	7.16	2.67	80.0	68.3	0.28	5755	3165

E_s : Static Modulus of Elasticity C_1 : Velocity of P-wave ν : Poisson's Ratio
E_d : Dynamic Modulus of Elasticity C_2 : Velocity of S-wave

made for each blasts.

1. Evidence of crushing in each hole
2. Extent of radial cracking around each hole
3. Influence of structure and type of discontinuity.
4. Resulting fracture (single or more) between holes on the surface and characteristics of the fracture.
5. Calculation of Half Cast Factor (HCF) where feasible.

6.2.4 Blast-Induced Damage and its Measurement

Wall-control blasting is a term that describes all techniques usually employed to reduce vibration and damage to unfragmented rock and other structures. The results obtained by these methods, or the extent of damage which is induced by these blasts, can be assessed by several techniques such as, blast vibration monitoring, half cast factor and comparison between velocities of P and S-waves before and after blast.

The term HCF (half cast factor) is defined as a ratio between the blasthole half-

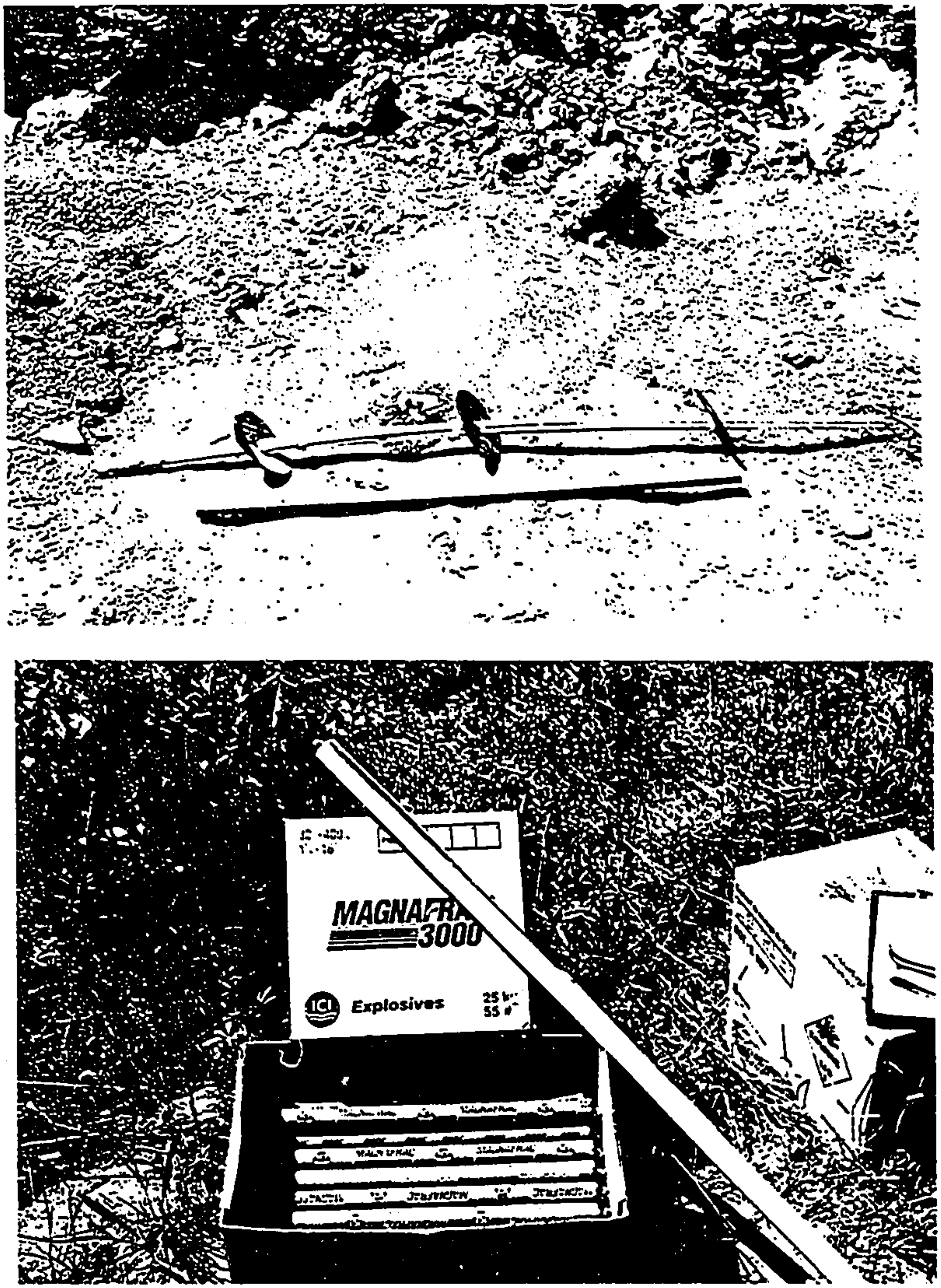

Figure 6.1 : Decoupling of explosive charges in the borehole.

barrels visible on the final face and original length of the borehole. Monitoring of ground vibrations offers an opportunity to evaluate the effects of blast design parameters and site characteristics on the final results of a blast. Vibration damage criteria are commonly related by the peak particle velocity (PPV), as measured or predicted in the ground surrounding a blast. It is related to charge wight and distance with a power function of following form (Langefors and Kihlstrom, 1978).

$$V = K \cdot \left(\frac{R}{Q^{\alpha}}\right)^{-\beta} \tag{6.1}$$

where V is peak particle velocity, Q is charge weight per delay, R is distance of monitoring point from the blast and K, α and β are constants based on site characteristics.

Several researches have made studies of damage and control of overbreak in underground mining and construction, (e.g. Free, 1973; Frantti, 1977; Coursen, 1978; Dowding, 1985; Gamble and Jow, 1985; Nand, 1988; Chitombo and Scott, 1990; Sanchidrian and Pesquero, 1992; Lizotte, 1995; Mohanty et al., 1995). Yang et al. (1993), Singh (1993), Singh and Lamond (1995), and Mojtabai and Beattie (1996) have studied the blast damage around the explosion point in small scale blasts, and in some cases, on the final face in open pit mines.

It should be noted however that in wall-control blasting, the damage area should be evaluated very close to the explosion point. The propagation of blast vibrations close-to the borehole is very complex and difficult to measure, due to much higher vibration levels and frequency ranges in the rock mass close to charge compared to far field condition. Also, in these investigations attempts have been made to relate the peak particle velocity with structural damage around the blasting area; none is related to the damage zone adjacent to the explosion source. In wall-control blasts, as will be shown, the half cast factor is not always an accurate measure of the extent of the damage around the perimeter holes. The length and the width of pre-existing fractures can significantly affect the overall quality of the wall. As the results of the tests in this chapter show, in many cases in spite of the presence of half barrels on the face, the damage zone behind the face was found to be quite extensive. Most of the discontinuities were opened behind the holes without any effect on the half barrels. Nevertheless, it is still a reliable and very rapid technique for assessment of blast results.

6.3 EXPERIMENTAL TESTS AT SITES 1 AND 2

At Site 1, five different patterns were designed for the experimental investigation of wall-control blasting methods. Figure 6.2 shows the relationship between spacing, burden and hole diameter for these patterns.

At Site 2, both single and rows of holes were drilled in bedded limestone. The spacing varied between 1.5 and 2 m for the 100 diameter, and 2.5 and 3 m for 150 mm borehole diameter holes. The explosion and borehole pressures for different diameter of charge are given in Table 6.3. The respective burdens were 1.0 m and 1.5 m. The details are shown in figure 6.3. At Site 1, each borehole were loaded to 30 cm collar at the top, and the length of collar remained the same as before for 100 mm diameter holes and increased to 60 cm for 150 mm diameter holes at Site 2.

6.3.1 Fracture Formation vs. Decoupling

6.3.1.1 Single Hole (Site One)

Two single holes, 50 mm in diameter and four single holes, 100 mm in diameter, were blasted to analyze fracture propagation around the holes in the presence of the discontinuities. The two types of explosives used in this series of tests were SUPERFRAC 4000 and PRIMAFLEX, (see Table 6.1). In the first (P25) and the third

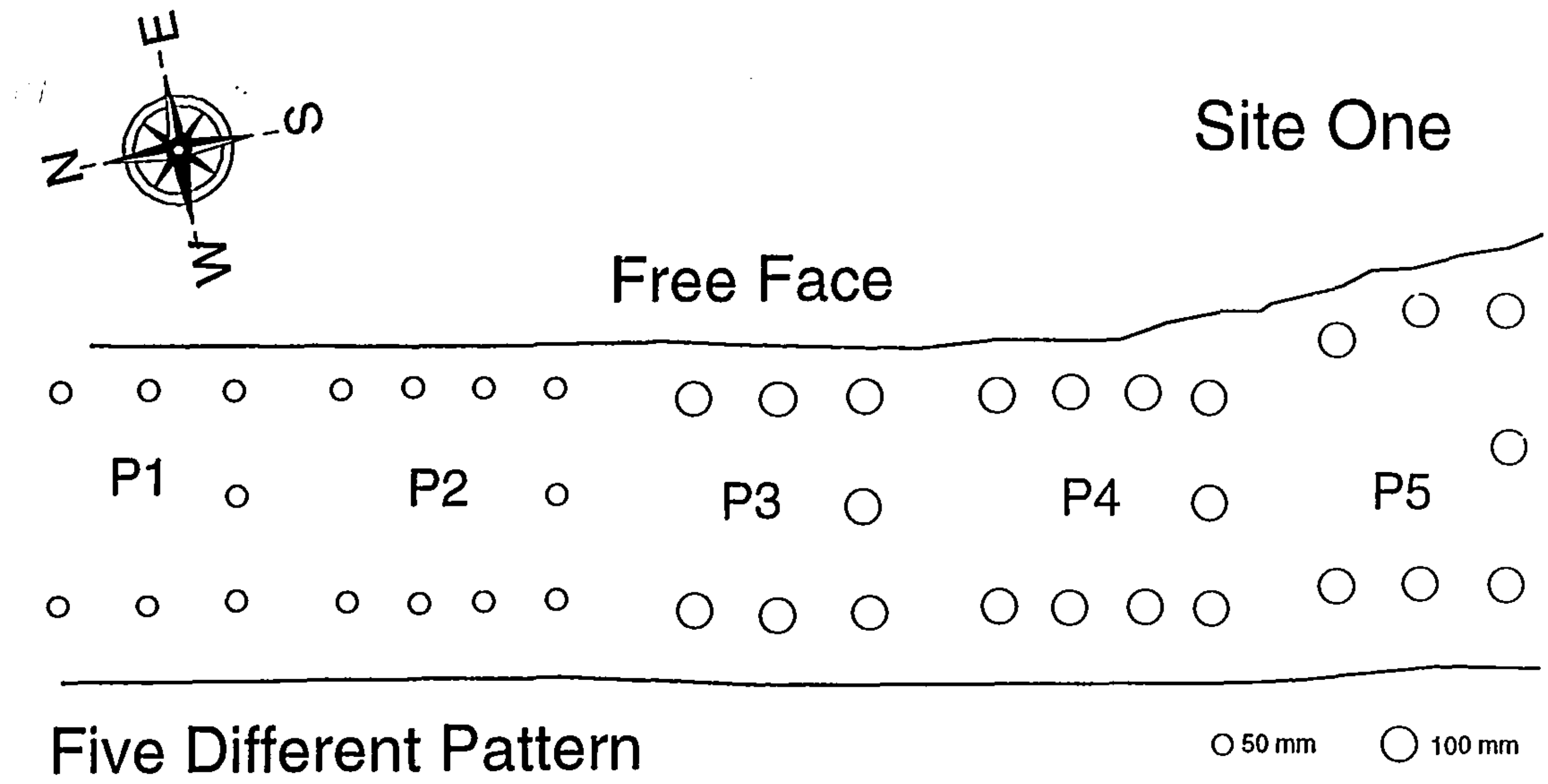

Figure 6.2 : Blast designs (pattern 1 to 5) at Site 1.

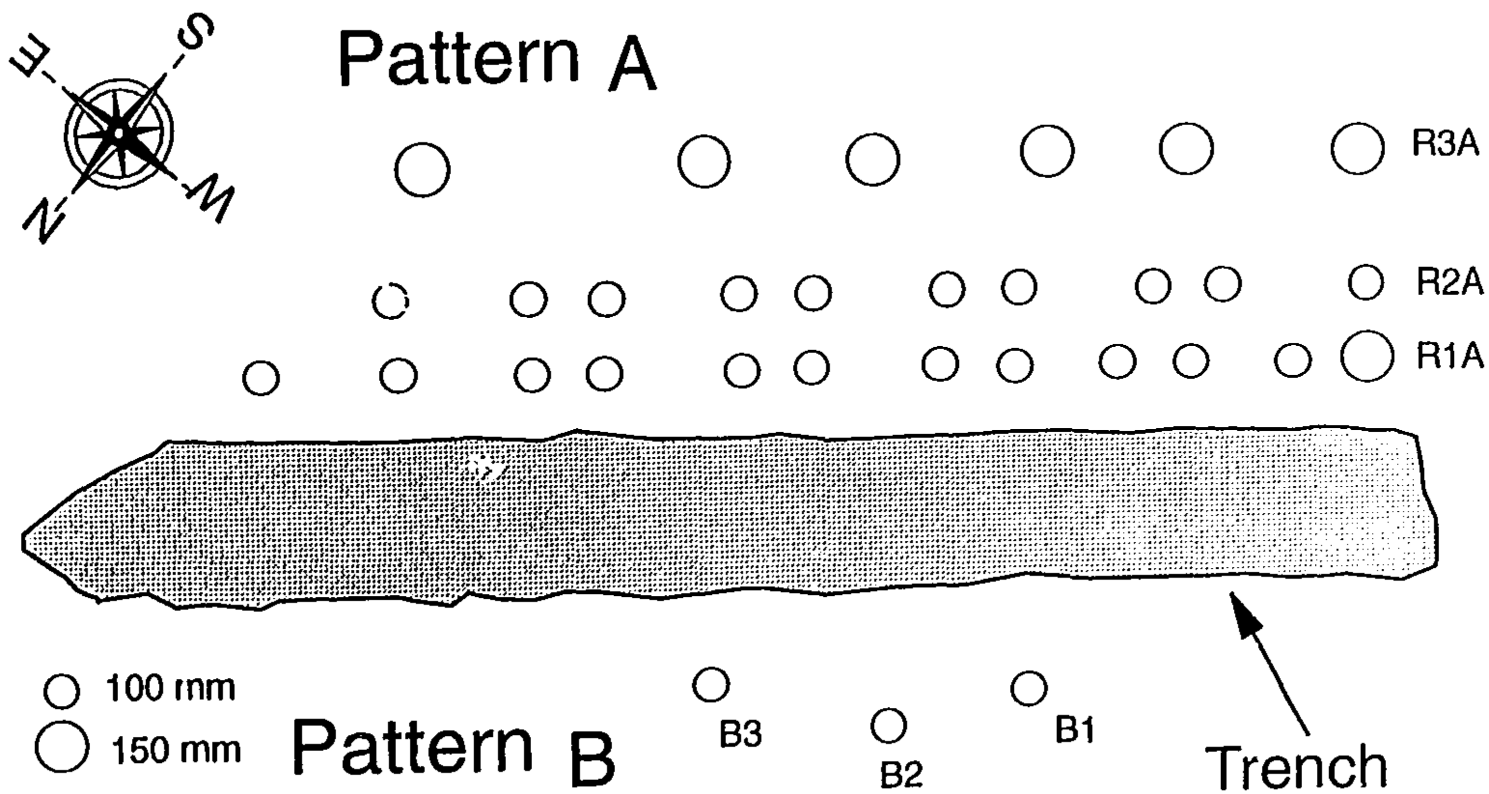

Figure 6.3 : Blast designs at Site 2.

Table 6.3 : Calculated borehole pressure for different decoupling ratio employed at both Sites.

Type of Explosives	Borehole Diameter (mm)	Charge Diameter (mm)	Detonation pressure (MPa)	Explosion Pressure (g/cc)	Decoupling Ratio	Borehole Pressure (MPa)
PRIMAFLEX (Detonating Cord)	50	10	14000	7000	0.2	147.0
	100	10	14000	7000	0.1	28.0
SUPERFRAC 4000 (Emulsion with AN prills)	50	25	5120	2560	0.5	485.0
	100	25	5120	2560	0.25	90.0
	150	25	5120	2560	0.25	35.0
	100	32	5720	2880	0.32	190.0
MAGNAFRAC 3000 (Aluminized Emulsion)	100	25	5780	2890	0.25	104.0
	100	32	6180	3090	0.32	200.0
	100	40	6560	3280	0.40	360.0
	150	40	6560	3280	0.27	140.0
	150	50	7260	3630	0.33	260.0

(P41) blast one 50 diameter mm hole and one 100 mm diameter hole were detonated by PRIMAFLEX. The same was repeated with 25 mm diameter cartridge of SUPERFRAC 4000 in shots number two and five. In the two last blasts, two 100 mm diameter holes were detonated by 25 mm and 32 mm cartridges of Superfrac 4000, respectively. Hole number P25 was located between rock foliations. It was crossed by one of them and the other two foliations were located at the sides of the holes (Fig. 6.4(a)).

In the second shot, the hole (P29) was located between two inclined discontinuities, with the distances equal to 4 and 6 borehole diameters from them. A discontinuity with a distance of 3 times the borehole diameter from the hole centre was located at the back of the hole # P41, and hole # P45 was drilled far from the discontinuities (distances are greater than 7 times borehole diameter), (Fig. 6.6(a)).

The nature of placement of holes # P31 and # P49 is illustrated in figure 6.8. As the figure shows, three discontinuities are located around the first hole (P31), whereas,

Table 6.4 : Characteristics of single-hole blast at Site 1.

Shot NO.	Burden	Spacing	Borehole Diameter	Charge Diameter	Decoupling Ratio	Type of explosive
	(m)	(m)	(mm)	(mm)		
1	1.5	-	50	10	0.2	PRIMAFLEX
2	1.5	-	50	25	0.5	SUPERFRAC
3	1.5	-	100	10	0.1	PRIMAFLEX
4	1.5	-	100	25	0.25	SUPERFRAC
5	1.5	-	100	25	0.25	SUPERFRAC
6	1.5	-	100	32	0.32	SUPERFRAC
* All holes were 2 m in depth, and had a collar of 0.3 m.						

the second hole (P49) was located in front of a single discontinuity at a distance of about 2.5 borehole diameters. The distances between hole P31 and the parallel discontinuities are about one and two times borehole diameter and from the third one is about 0.5 borehole diameter. The characteristics of the blasts are shown in Table 6.4.

6.3.1.2 Results and Discussion of Single-Hole Blast at Site 1

In shots # 2 (25 mm diameter cartridge in 50 mm diameter hole) and # 6 (32 mm cartridge in 100 mm diameter hole) the rock was completely fragmented, and the holes were not visible after blast. In shot number 3 (11 mm diameter detonating cord in 100 mm hole), no fractures were visible around the hole (Figs. 6.4(b), 6.6(b) and 6.8(b)). Therefore, the dynamic tensile strength of the rock must be greater than the 28 MPa (see Table 6.3). Based on the results obtained in these tests series, PRIMAFLEX and 25 mm diameter cartridges of SUPERFRAC 4000 were selected for 50 mm and 100 mm diameter holes respectively.

In shot # 1 (P25) three fractures could be seen around the borehole wall, the first one was a pre-existing closed fracture which was opened to about 8 times borehole diameter after blast. Two other fractures also emanated from the hole to the foliations in the rock at each side. In shot # 4 (25 mm cartridge in 100 mm hole) four cracks were visible around the hole (P45), two of them perpendicular to the discontinuities, and the other two opened in the same direction as the foliation. The lengths of the parallel and perpendicular fractures to the foliation were about 6 and 9 times borehole diameters, respectively. In shot # 5, the hole (P31) was located between three discontinuities, two of them were parallel to each other and the other one was perpendicular to the previous ones. The cracks developed from the borehole wall perpendicular to the discontinuities. The length of the cracks were about 5 to 7 times the borehole diameter. A broken area was visible between the borehole wall and the nearest pre-existing fracture which was located at the right side of the hole with a distance equal to 2 times borehole diameter (Figs. 6.5, 6.7 and 6.9).

In each of these three shots (shots # 1, 4 and 5) the holes still remained visible after the blasts. There was however, considerable damage up to 0.5 m below the surface, due to spalling or cratering effect of the explosive charge. A fracture system consisted of a series of cracks of irregular length, radiating from the hole in different directions. These fractures were less uniform and were usually perpendicular or nearly perpendicular to the discontinuities. This system of fractures was caused by the tensile hoop stress represented by the expansion of the explosion gases. The number and the length of the fractures should be a function of the borehole pressure, but the pre-existing discontinuities (especially the opened ones) control these two parameters.

6.3.1.3 Single Hole (Site 2)

The first phase of tests in this experimental investigation was devoted to determining the optimum charge diameter and analysing the effect of the discontinuities upon the fracture patterns around single-hole blasts. A series of 5 single-hole blasts using two different types of explosives with several charge diameters, were used to determine

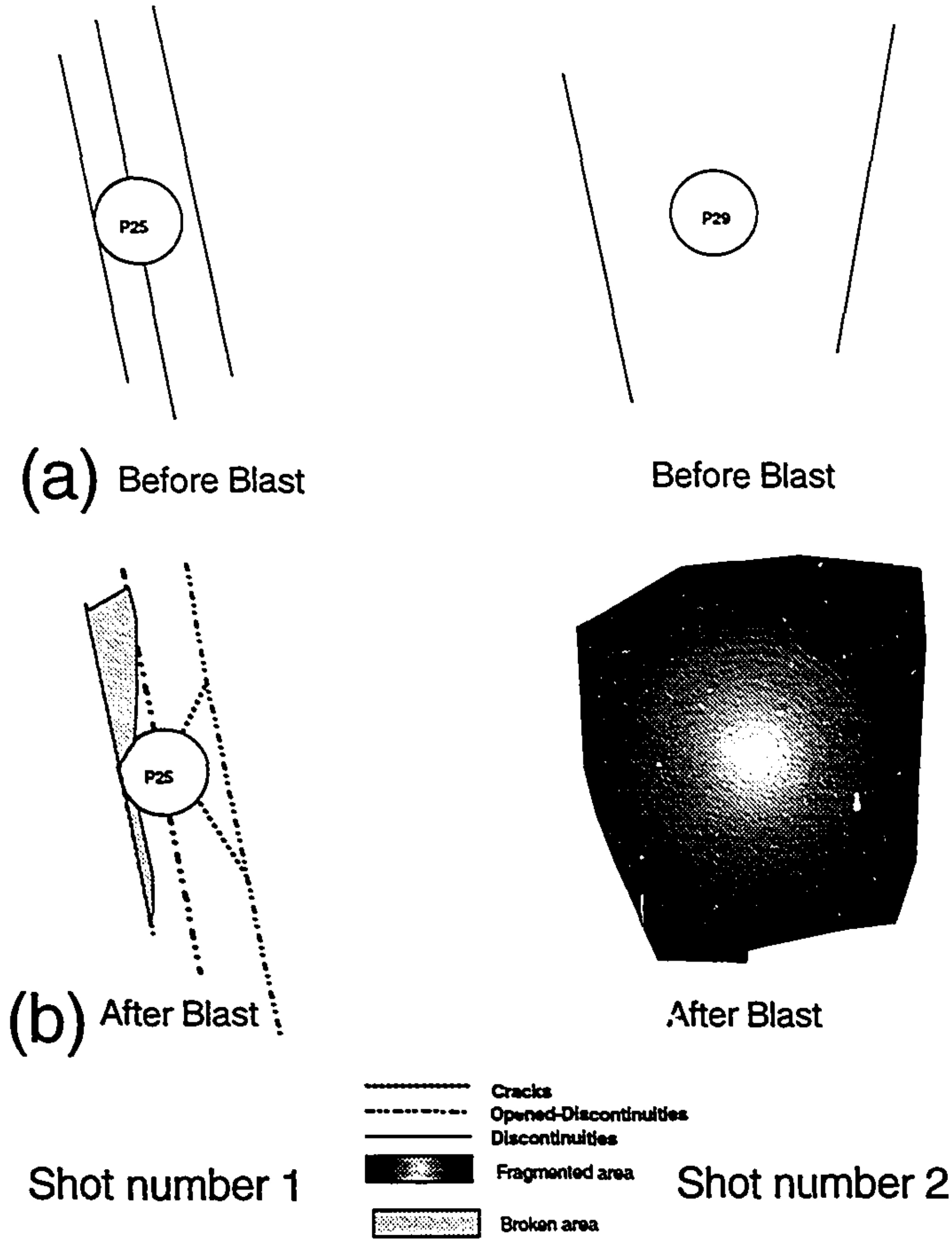

Figure 6.4 : Schematic layouts and results of shots number 1 and 2 at Sit 1. (PRIMAFLEX in 50 mm dia. hole, shot #1, and 25 mm dia. SUPERFRAC in 50 mm dia. hole, shot # 2)

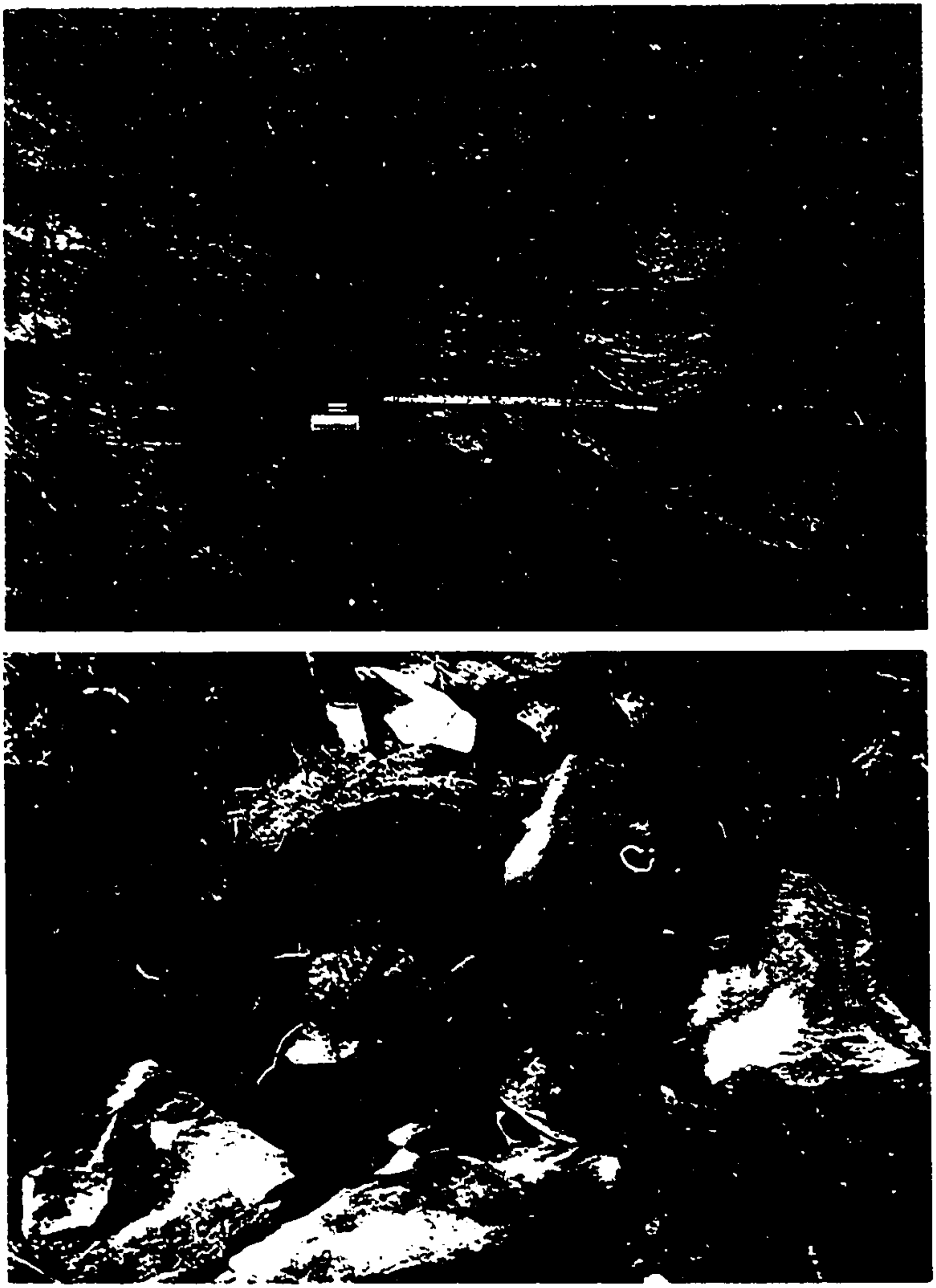

Figure 6.5 : Photographic results of shots number 1 and 2 at Site 1.

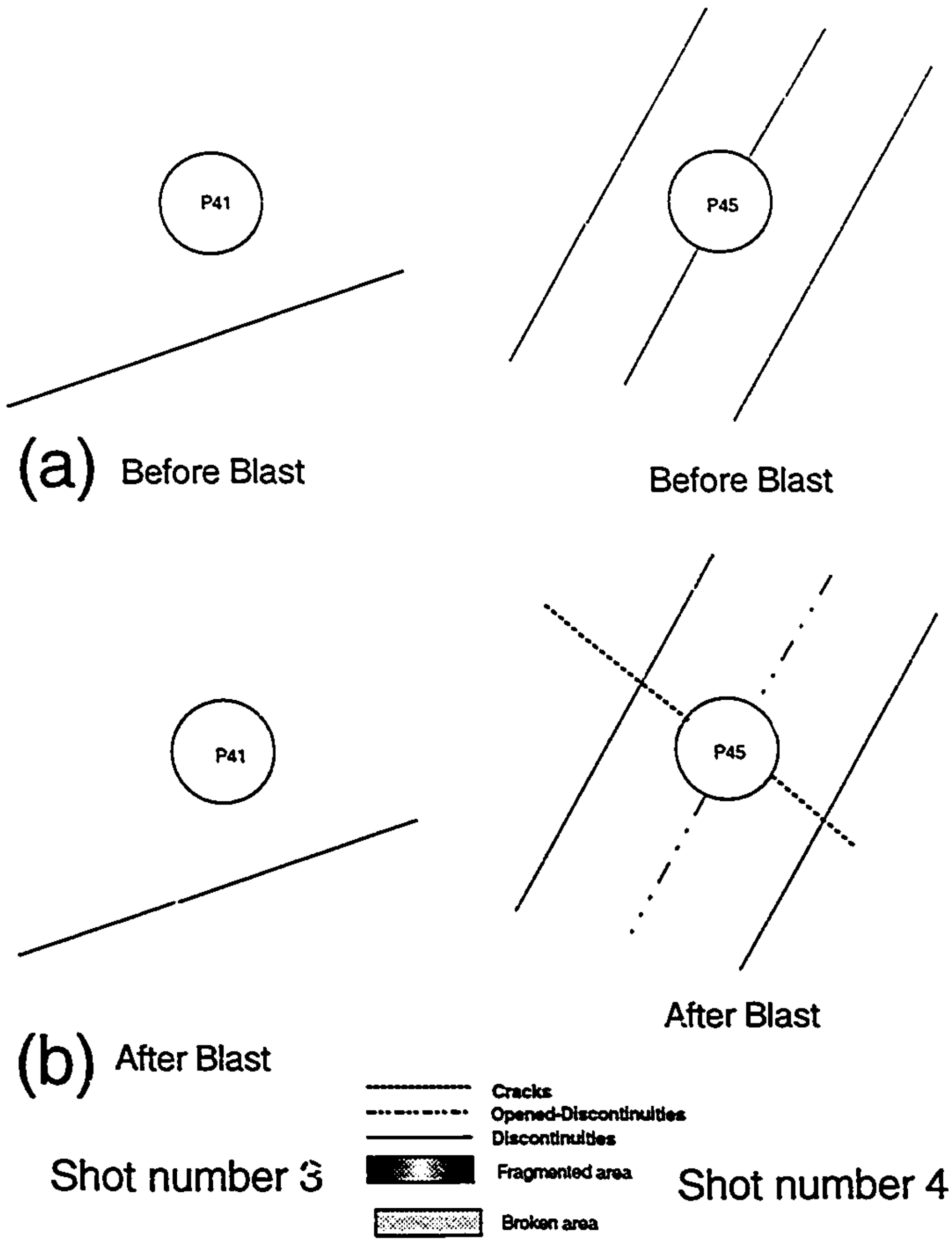

Figure 6.6 : Schematic layouts and results of shots number 3 and 4 at Site 1. (PRIMAFLEX, shot #3, and 25 mm dia. SUPERFRAC in 100 mm dia. holes, shot # 4)

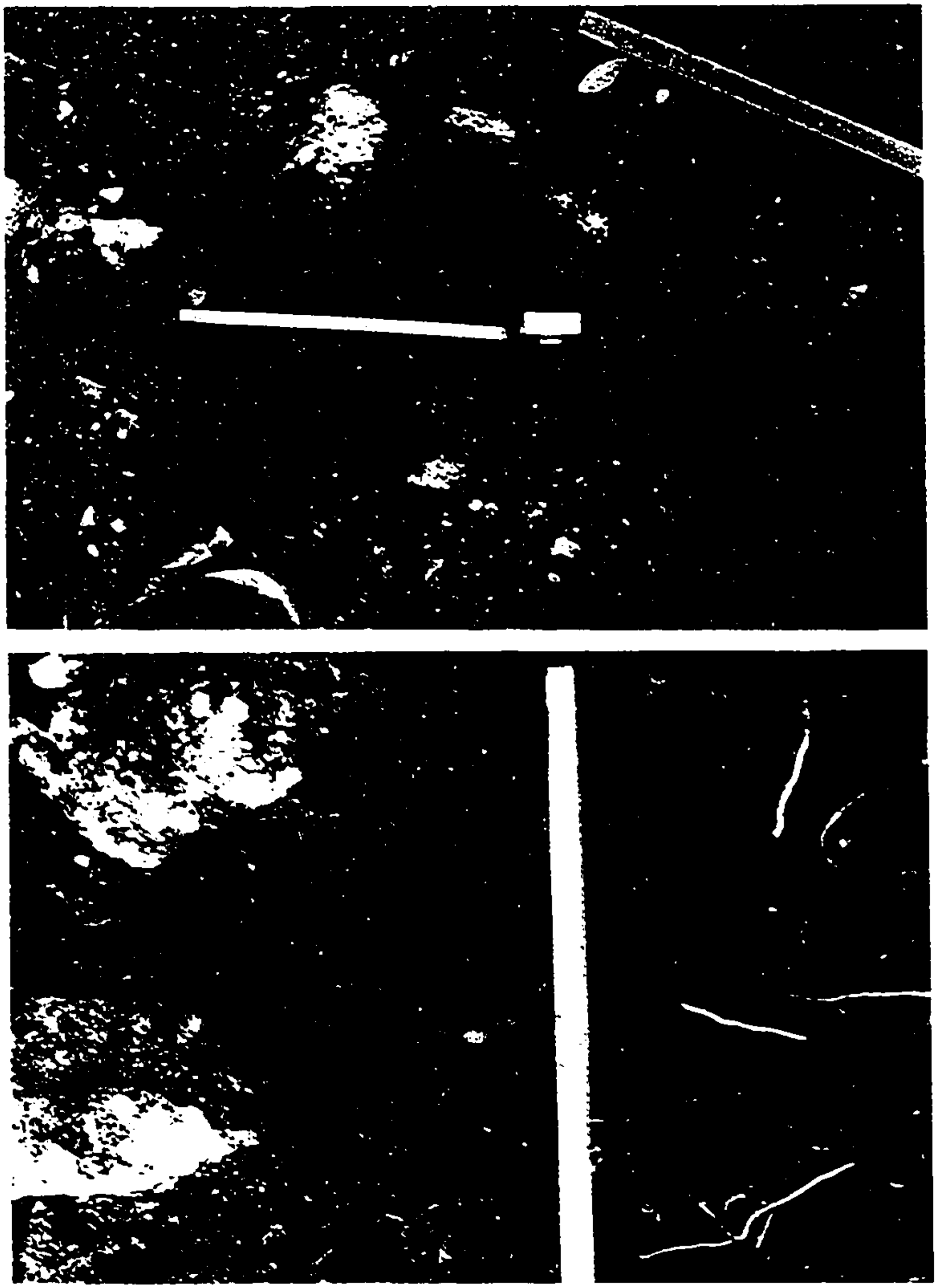

Figure 6.7 : Photographic results of shots number 3 and 4 at Site 1.

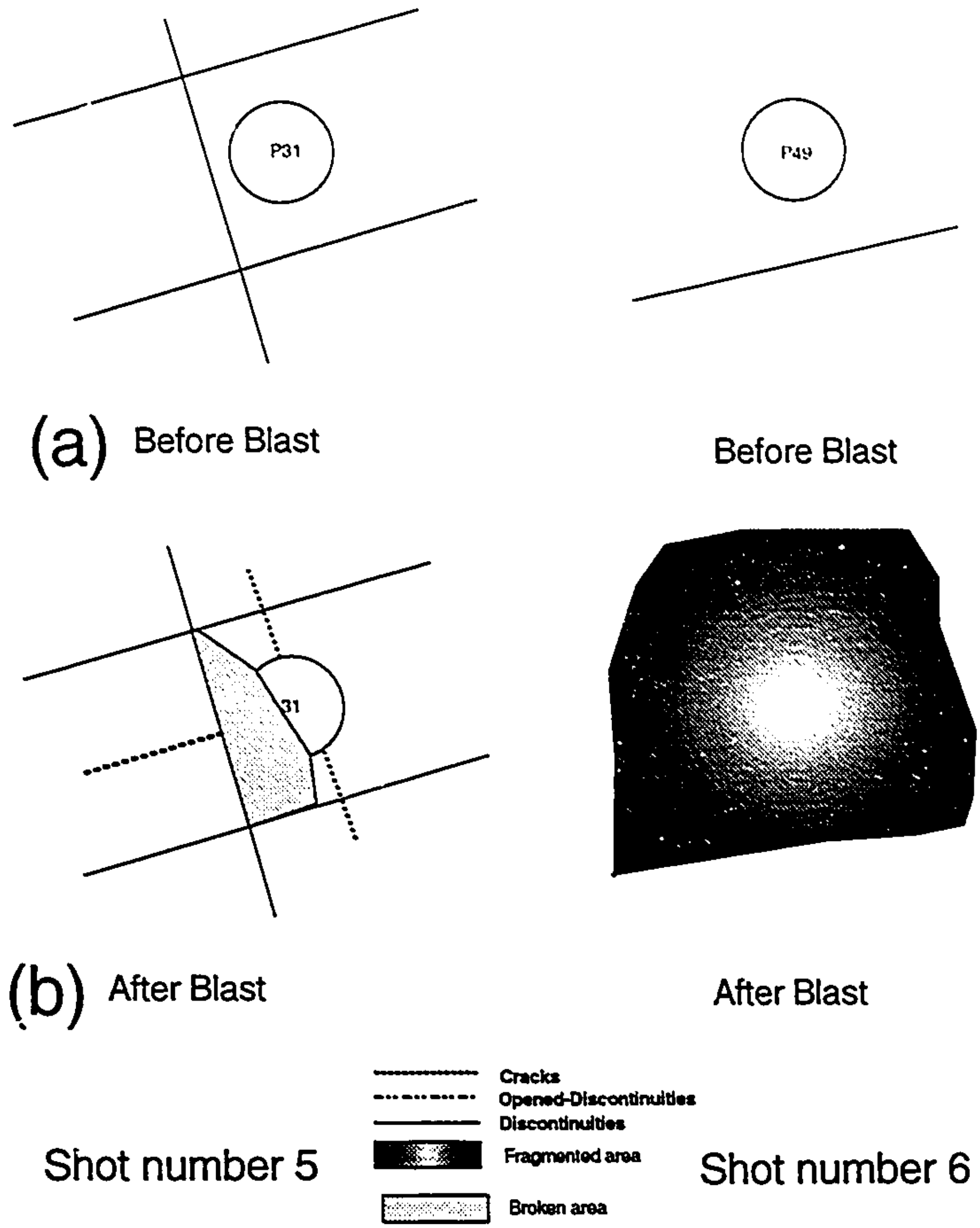

Figure 6.8 : Schematic layouts and results of shots number 5 and 6 at Site 1. (25 mm dia. SUPERFRAC in 100 mm dia. holes)

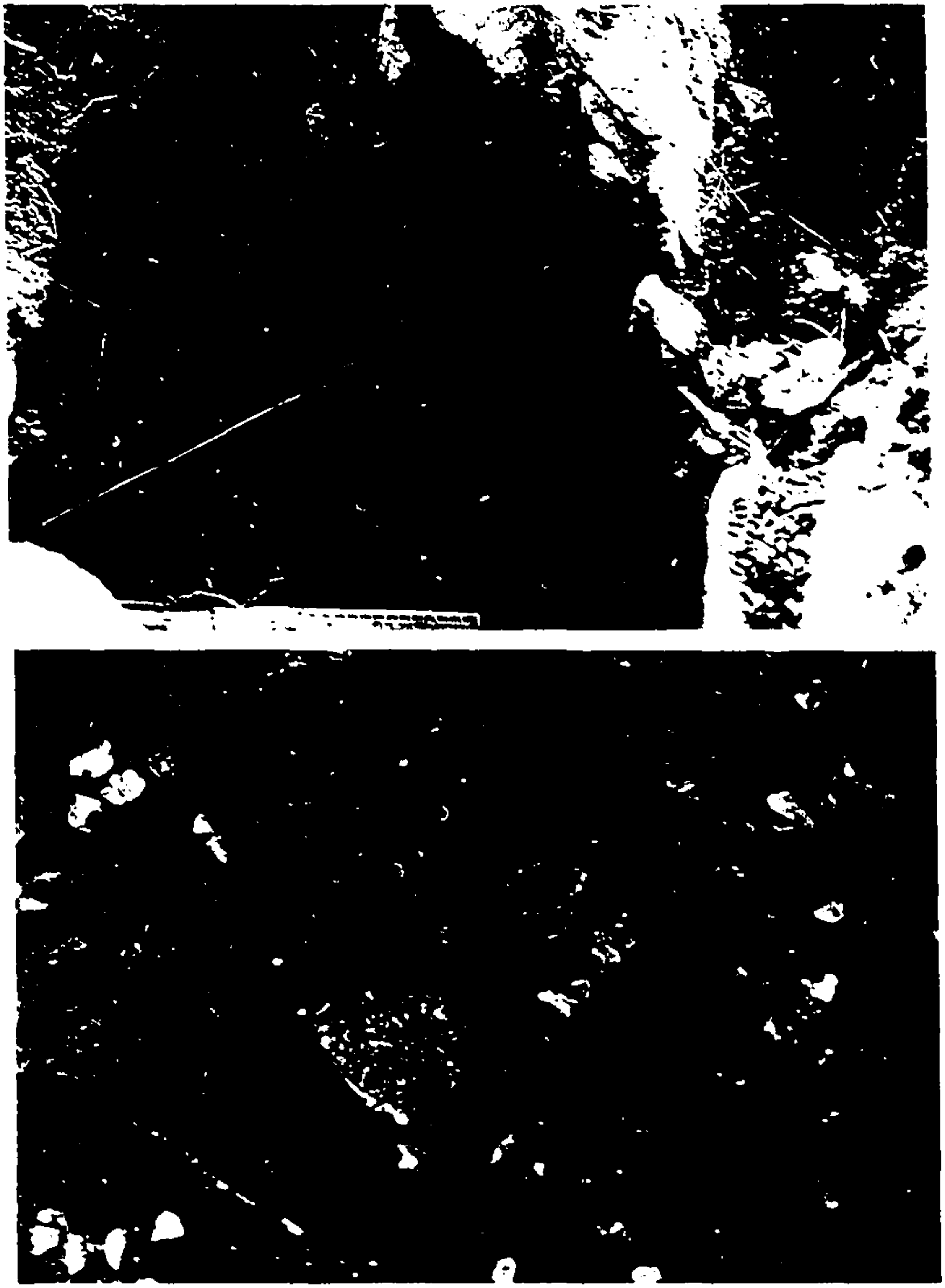

Figure 6.9 : Photographic results of shots number 5 and 6 at Site 1.

Table 6.5 : Characteristics of 5 single-hole Shots at Site 2.

Shot No.	Burden	Spacing	Borehole Diameter	Charge Diameter	Decoupling Ratio	Type of explosive
	(m)	(m)	(mm)	(mm)		
1	1.8	-	100	25	0.25	MAGNAFRAC
2	2.1	-	100	32	0.32	MAGNAFRAC
3	1.0	-	100	40	0.40	MAGNAFRAC
4	1.0	-	150	25	0.17	SUPERFRAC
5	1.0	-	150	25	0.17	SUPERFRAC
* All holes were 3 m in depth, and had a collar of 0.3 m in 100 mm holes and 0.6 m in 150 mm holes.						

the relationship between formation of cracks and decoupling ratio, in the presence of pre-existing discontinuities.

Cartridged emulsion explosives (MAGNAFRAC 3000 and SUPERFRAC 4000) were used in 100 mm and 150 mm diameter boreholes, respectively (see Table 6.1). In shot # 1, the hole was loaded with 25 mm diameter MAGNAFRAC. In shots # 2 and # 3 the conditions were similar to shot # 1, except for the decoupling ratio. The diameter of the charge was increased from 25 mm to 32 mm and 40 mm for the second and the third shot respectively. The first hole (B1) was located between two discontinuities, one of them was at the right side of the hole at a distance of about one borehole diameter, and the other one was located at the left side of the hole at a distance of about 4 times borehole diameter (Fig. 6.10 (a)).

The second hole (B2) was located between a weak plane and a closed joint with the distances equal to 5 and 1.5 times borehole diameter from them, respectively. The characteristics of the shots are given in Table 6.5. A weak plane with 5 mm width was located at the back of the third hole (B3) and continued to the front of the second hole. The distance between the centres of the holes and the weak plane was about 10 times borehole diameter. A closed joint with a distance equal to 2 times borehole diameter was also located at the right side of the third hole (B3) (Fig. 6.10(a)). In the second phase two 150 mm diameter holes were loaded by 25 mm cartridges of Superfrac 4000 with a collar length of about 0.15 m. In the first shot the hole (R3A1) was located at a greater distance from the discontinuities, whereas, in the second shot, the hole (R1A1) was drilled between two parallel joints. These joints formed an angle of about 45° to the free face, and the distances between the centre of the hole and the discontinuities were about 1 and 3 times borehole diameter (Fig. 6.13(a)).

6.3.1.4 Results and Discussion of Single-Blasts at Site 2

The results from the 100 mm diameter hole tests (holes # B1, B2 and B3) strikingly display the correlation between fracture formation, borehole pressure, and the pre-existing discontinuities of the rock mass. As the diameter of the charge increases (i.e. increasing of borehole pressure), the cracks from the borehole wall become larger and wider, as would be expected (Figs. 6.10-12).

Four radial fractures can be seen around hole B1. The first one is nearly perpendicular to the nearest discontinuity at the right side of the hole with a distance about 1.5 times borehole diameter. The fracture crossed the discontinuity and continued to a distance of about 4 times the borehole diameter. The second fracture is perpendicular to the pre-existing open fractures at a distance of about 5 times borehole diameter from the left side of the hole. It propagated from the borehole wall to the pre-existing fracture, merged with the latter for some distance, and then emerged at right angles and terminated of the second open fracture. The third and the fourth fractures were created at the front of the holes to the discontinuities located at the right and the left side of the hole, forming an angle of about 45° to the free face.

In the second shot, the borehole pressure was increased by using a bigger diameter charge in comparison to the previous shot. A 10 mm wide fracture developed from the borehole wall to the nearest weak plane located at the right side of the hole at a distance of about 4 times the borehole diameter. Two other fractures were formed at the opposite side of the dominant fracture to a closed joint at left side of the hole B2. One of them was perpendicular to the joint and the other one was nearly perpendicular to it, and in the process, opened the formerly closed joint to a weak plane at the front of hole. The distance of the weak plane from the centre of the hole is about 10 times the borehole diameter. A fourth fracture was formed from the borehole wall to the pre-existing fracture at the left side of the hole. Figures 6.10(b) and 6.12(b) show that the dominant fracture did not cross the weak plane at the right side of the hole, and the plane was completely opened by the explosion gases.

In the third shot, the hole was located between a weak plane at the back of the hole and a free face, and loaded with 40 mm diameter SUPERFRAC. The distances of the centre of the hole from the face and the weak plane were equal to 10 and 8 times borehole diameter respectively. As figure 6.12(b) shows, the hole disappeared and the rock was extensively fractured from the weak plane to the free face. Again, the role of the open discontinuity is clearly demonstrated in this blast. In terms of blast results, the effect of a weak plane located behind the hole is very similar to the free face.

In the fourth and the fifth blasts, the 150 mm diameter boreholes were loaded with 25 mm diameter MAGNAFRAC and SUPERFRAC respectively. In shot # 4, two fractures formed and terminated at the two pre-existing parallel discontinuities (spaced 0.5 m apart) located on the opposite sides of the hole. The hole was located between these two joints at distances 2 and 4 times borehole diameter from the left and the right side respectively. In blast # 5, the hole was shot with SUPERFRAC with approximately the same as in shot # 4. No cracks were formed around the hole. This was because the distance of the nearest discontinuity from the hole centre was greater than 10 times borehole diameter (Figs. 6.13(b) and 6.14).

The results obtained from these series of tests show that the effective dynamic tensile strength of rock should be greater than 35 MPa (the calculated borehole pressure for this geometry), as no fractures were formed with these blasts. Decoupling ratio plays a critical role in the formation of fractures, but their characteristics (number, length and width) are dictated by the discontinuities in the rock mass. In the presence of any pre-existing fractures, all cracks propagate from the borehole wall perpendicular or nearly so to the discontinuities. The width of any open discontinuities has a key influence on the distribution of the fractures.

As shown in chapter 5 (Fig. 5.17) a wide weak plane behaves more like a free face than a closed joint which may be much closer to the borehole. This promotes the formation of the dominant crack in the direction of the former than the latter. Figures 6.10(b) and 6.12 (a) clearly confirm these theoretical predictions. In this case, the dominant crack is formed in the direction of the wide weak plane rather than the closed joint located at only 2.5 borehole diameters compared to 4 times the borehole diameter for the former.

In blast # 3, as figures 6.10(b) and 6.12(b) show, the rock completely fractured between the hole, the free face and the weak plane located at the back of the hole. The critical distance between the weak plane and the centre of hole is about 12 times the borehole diameter. As this distance decreases the extent of the damaged part increases. This result is approximately similar to the result predicted by the numerical analysis (Figs. 5.14 and 5.15).

As a result of the fracture patterns produced by different borehole pressure in single-hole blast, a 32 mm charge diameter was finally selected for 100 mm diameter boreholes, and 40 mm and 50 mm diameter for the 150 mm holes. In other words, for this type of rock and for an optimum spacing, about 200 MPa borehole pressure would be necessary to generate a single fracture between the holes. A series of multi-hole blast

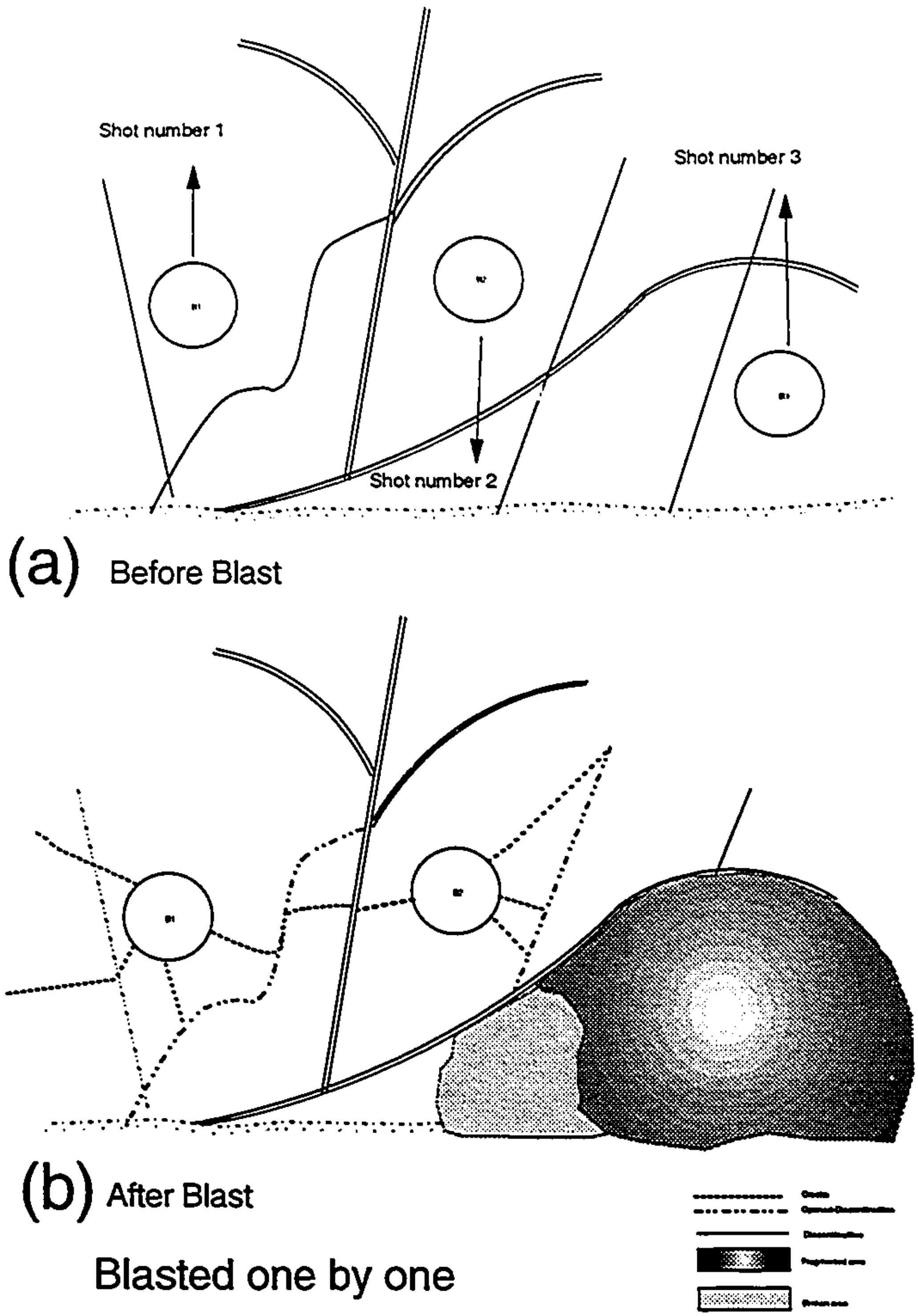

Figure 6.10 : Schematic layouts and results of shots number 1, 2 and 3 at Site 2. (25, 32, and 40 mm dia. MAGNAFRAC in 100 mm dia. holes)

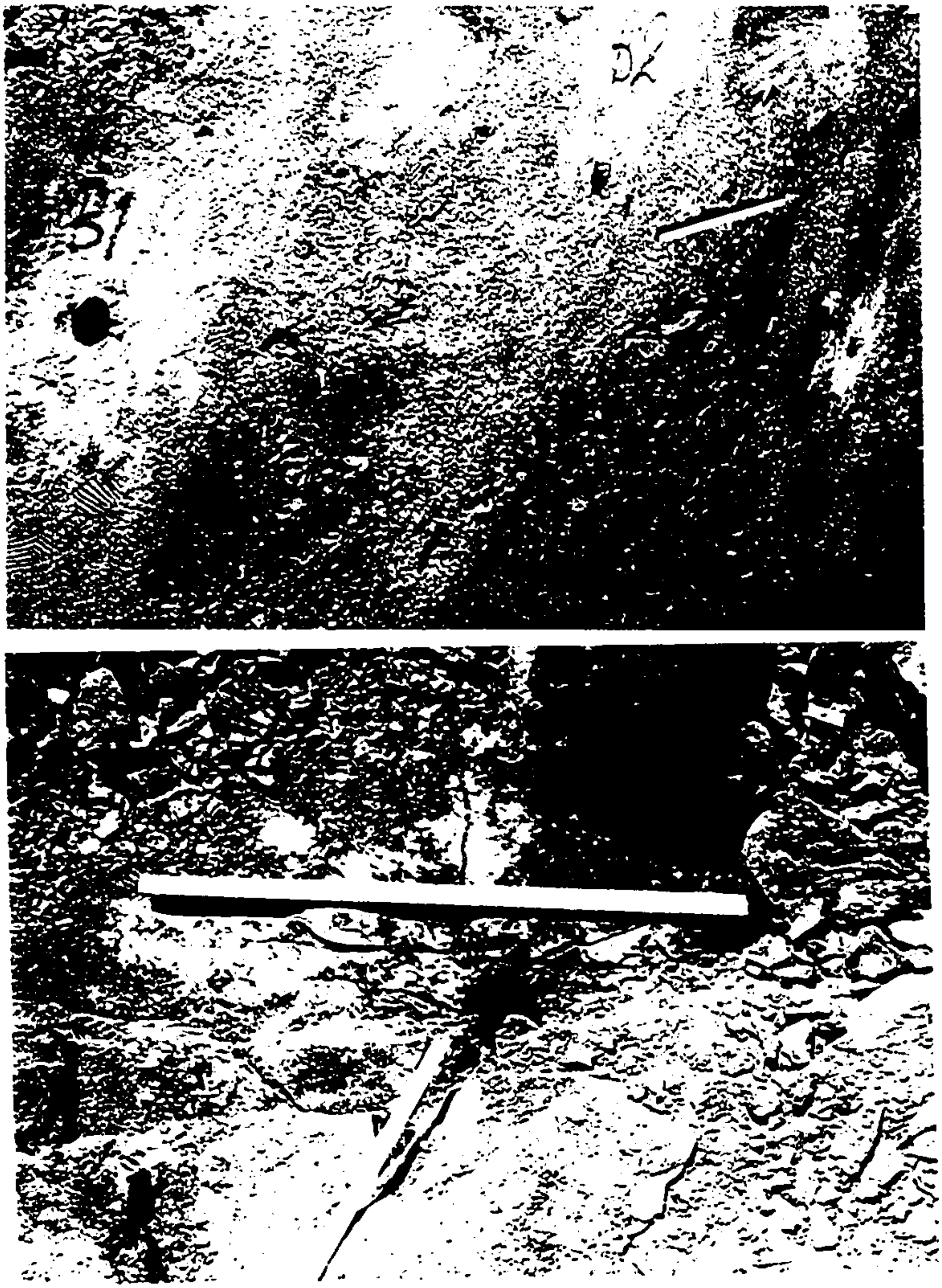

Figure 6.11 : Photographic layouts of shots number 1, 2 and 3, and the result of shot number 1.

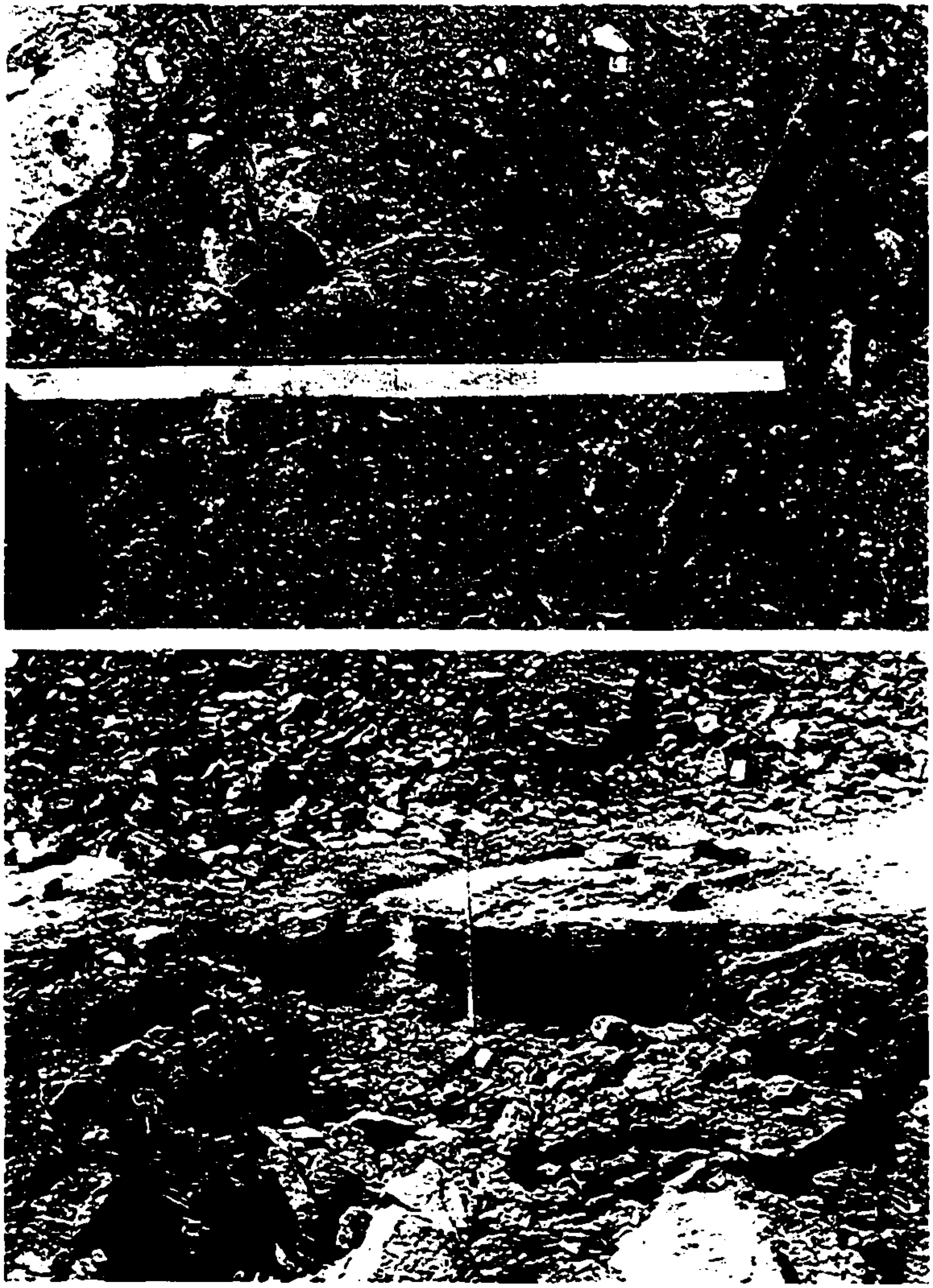

Figure 6.12 : Photographic results of shots number 2 and 3 at Site 2.

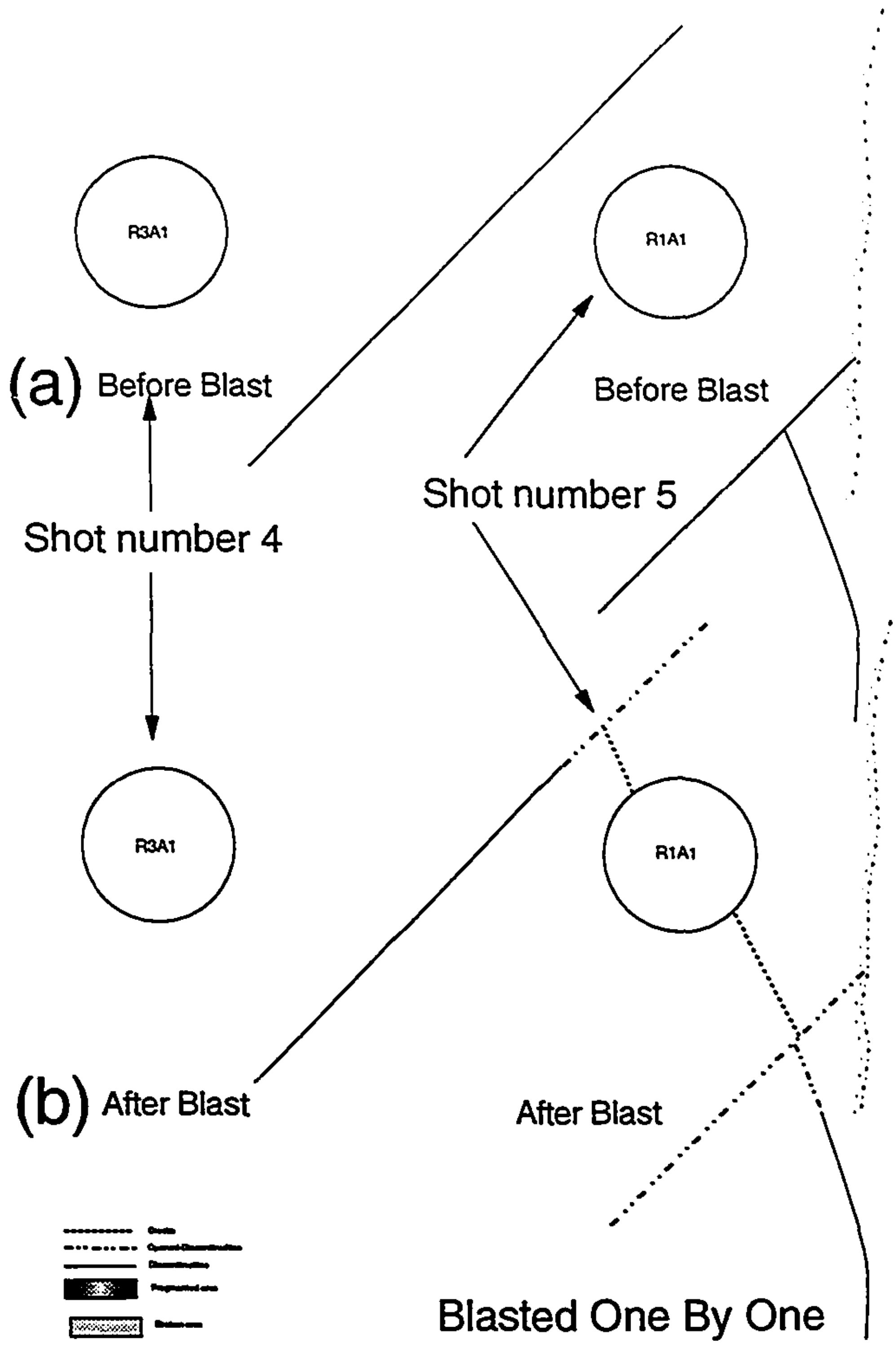

Figure 6.13 : Schematic layouts and results of shots number 4 and 5 at Site 2. (25 mm dia. SUPERFRAC in 150 mm dia. holes)

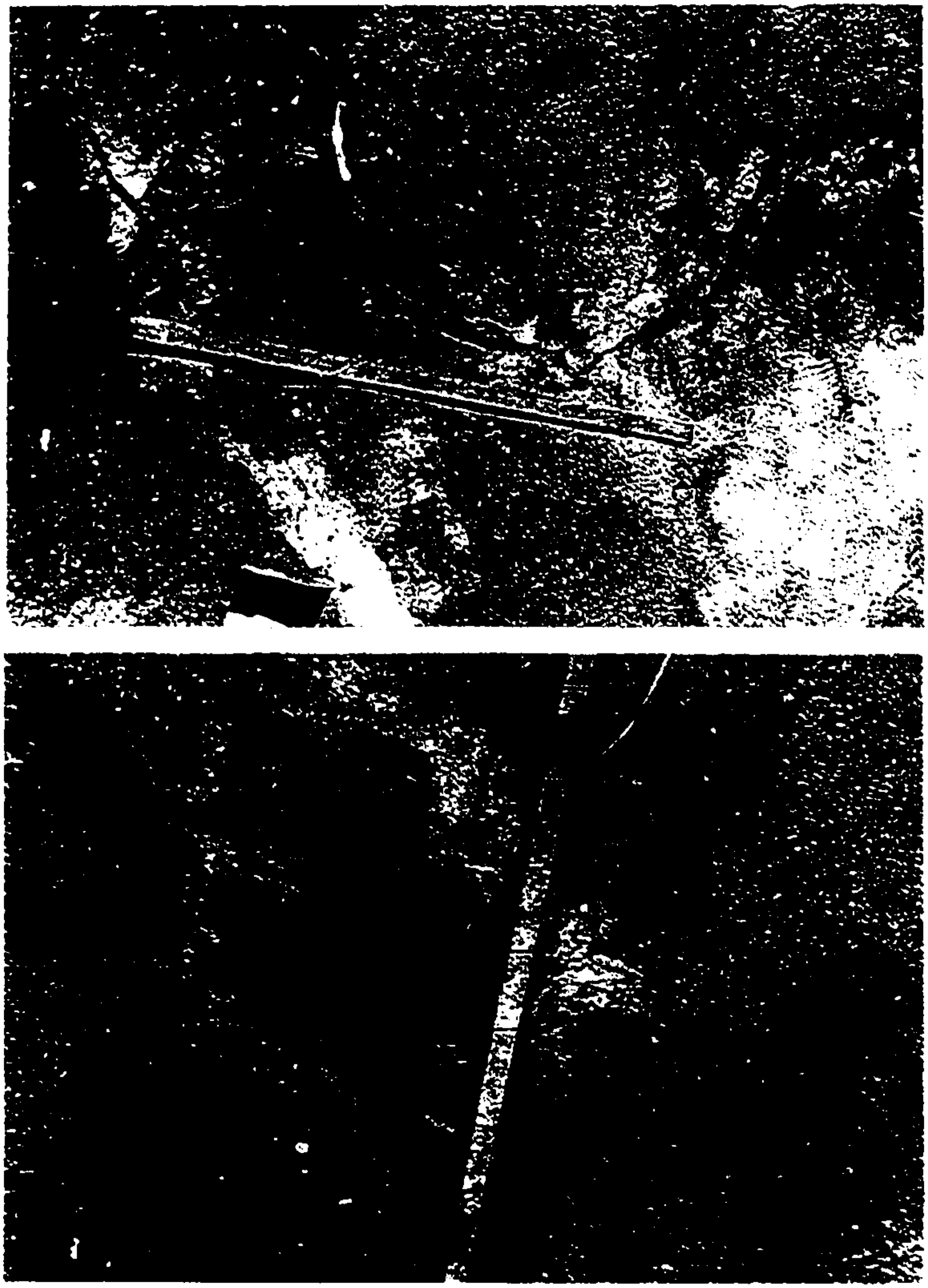

Figure 6.14 : Photographic results of shots numbers 4 and 5 at Site 2.

Table 6.6 : Characteristics of Shots number 6 and 7 at Site 2.

Shot No.	Burden	Spacing	Borehole Diameter	Charge Diameter	Decoupling Ratio	Type of Explosive
	(m)	(m)	(mm)	(mm)		
6	1.5	2.5	150	40	0.27	MAGNAFRAC
7	1.5	2.5	150	40	0.27	MAGNAFRAC
* All holes were 3 m in depth, and had a collar of 0.3 m in 100 mm holes and 0.6 m in 150 mm holes.						

were carried out at Site 2 to investigate the role of borehole pressure. In these blasts, two holes were detonated nearly simultaneously (< 500 μm).

6.3.1.5 Multiple Holes at Site 2 (Finite Burden)

In this blast, (shot #6), two 150 mm diameter holes were loaded with 40 mm diameter of MAGNAFRAC. The first hole was located between two parallel discontinuities, which were located at the left and the right side of the hole, at distances of 0.9 m and 1.0 m respectively. The hole was also crossed by another joint. A 1 mm wide weak plane was located at the front of the second hole (R3A3) and continued to the first hole (R3A2). The second hole was 1.5 m away from the discontinuity, which was located between the holes (Fig. 6.15(a)).

In the next blast (shot # 7), the first hole (R3A4) was surrounded by three parallel joints. The first one was located at the right side of the hole, the second one crossed the hole, and the last one located at the left side of the hole. The angles they formed with the face were about 40°to the centre line connecting the two holes, and the distance of the first and the third of the discontinuities from the centre of the hole were 0.9 m and 0.6 m respectively. The second hole (R3A5) was 1.5 m away from the nearest fracture (Fig. 6.17(a)). The characteristics of the blasts are shown in Table 6.6.

6.3.1.6 Results and Discussions of Multi-Hole Blasts at Site 2

In shot # 6, the first hole (R3A2) was located between two parallel discontinuities, and the hole was crossed by the third one. A narrow weak plane approximately parallel to the face crossed the first hole and continued to the front of the second hole (R3A3). After the blast, two new fractures were formed around R3A2, in addition to the three pre-existing discontinuities (Fig. 6.15(b). Three new fractures were formed around the second hole (R3A3) as a result of simultaneous blast. No inter-connecting fracture developed between two holes with this blast geometry.

Identical blast geometry and explosive was used in the next blast (shot # 7). The first hole was located between three parallel discontinuities, two of them located at the sides of the hole and the other one crossed the hole. The second hole was located at a distance from the discontinuities (distances greater than 6 times borehole diameter). As figures 6.17(b) and 6.18 show, no cracks developed around the second hole (R3A5), and the hole still remained intact on the surface. However, three cracks were formed from the first hole and propagate to the pre-existing fractures. Also, the discontinuity crossing the hole was opened to the free face at the front of the hole, and to a distance between 6 times borehole diameter at the back of the hole.

The only difference between these two blasts (# 6 and # 7) was that the first hole (R3A2) in blast # 6 was half-filled with water, whereas the rest of the holes were dry. As figures 6.15(b) and 6.17(b) show, the width of the crack and the opened discontinuity in the first blast (blast # 6) are much greater than in the second blast (blast # 7). This illustrates the lack of decoupling (and hance the higher borehole pressure) due to presence of water in hole (R3A2).

In these two blasts (# 6 and # 7) the pressure was not enough to create a fracture between the holes, although some fractures were developed and propagated towards the

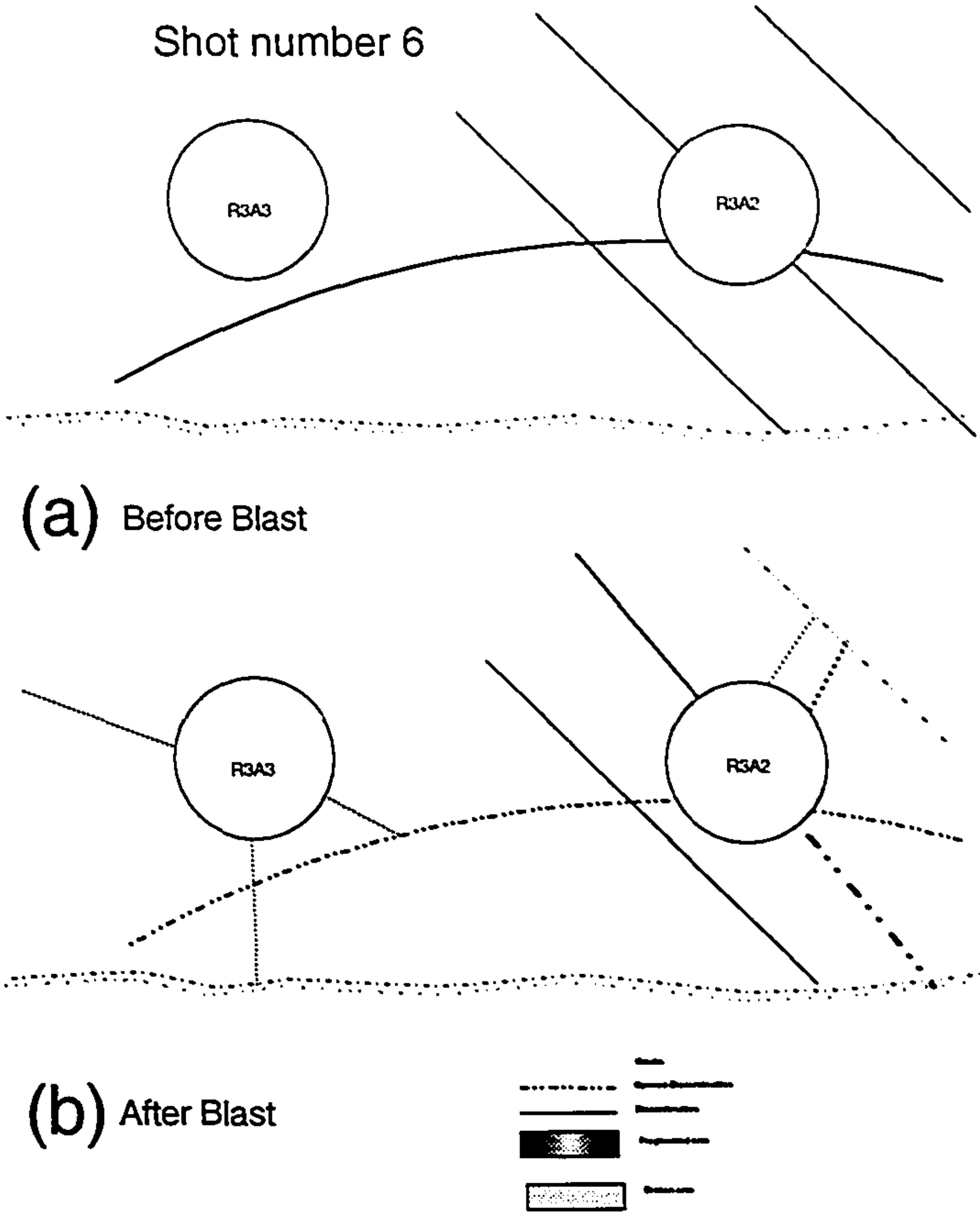

Figure 6.15 : Schematic layout and result of shot number 6 at Site 2. (40 mm dia. MAGNAFRAC in 150 mm dia. holes)

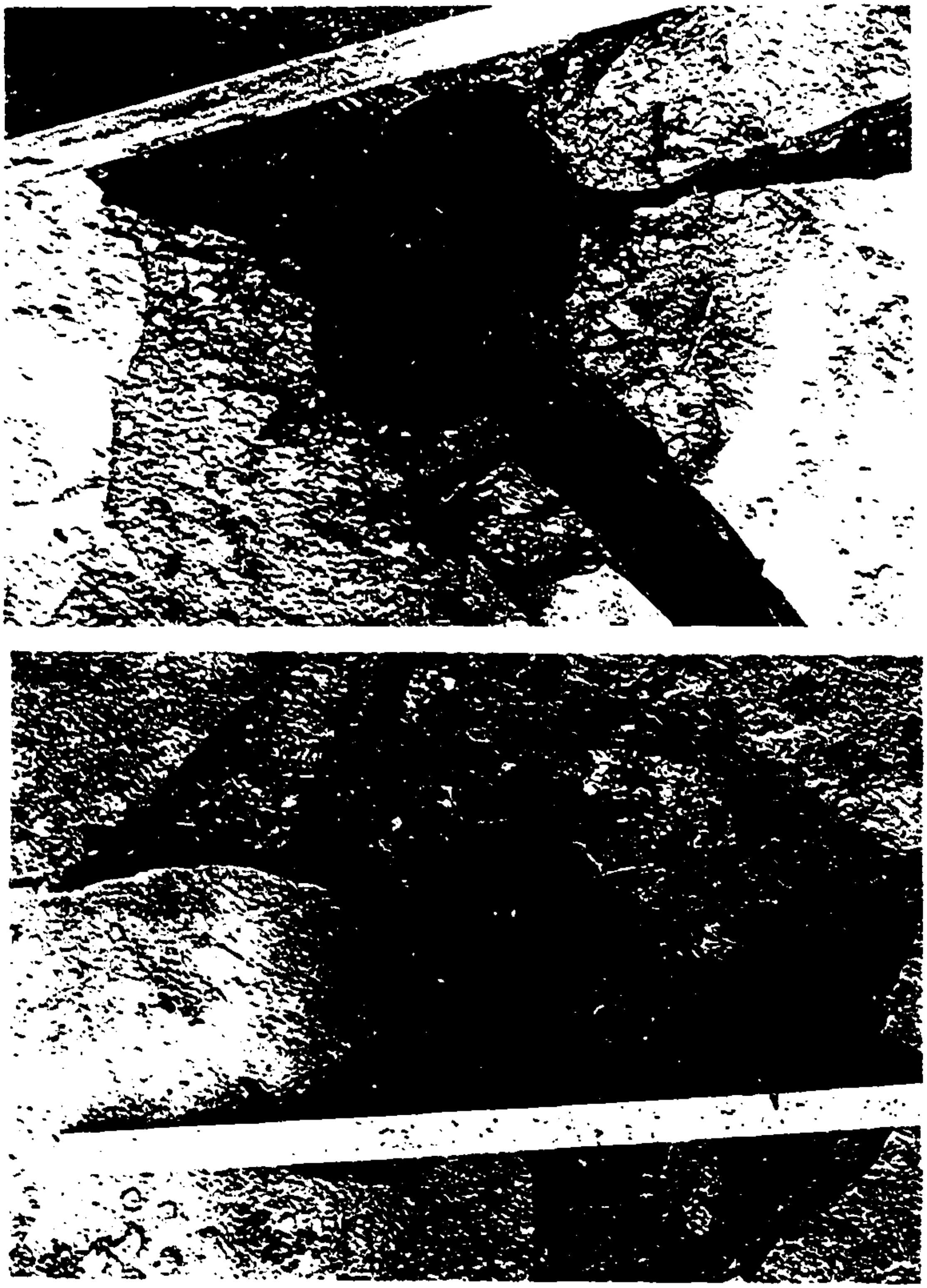

Figure 6.16 : Photographic result of shot number 6 at Site 2.

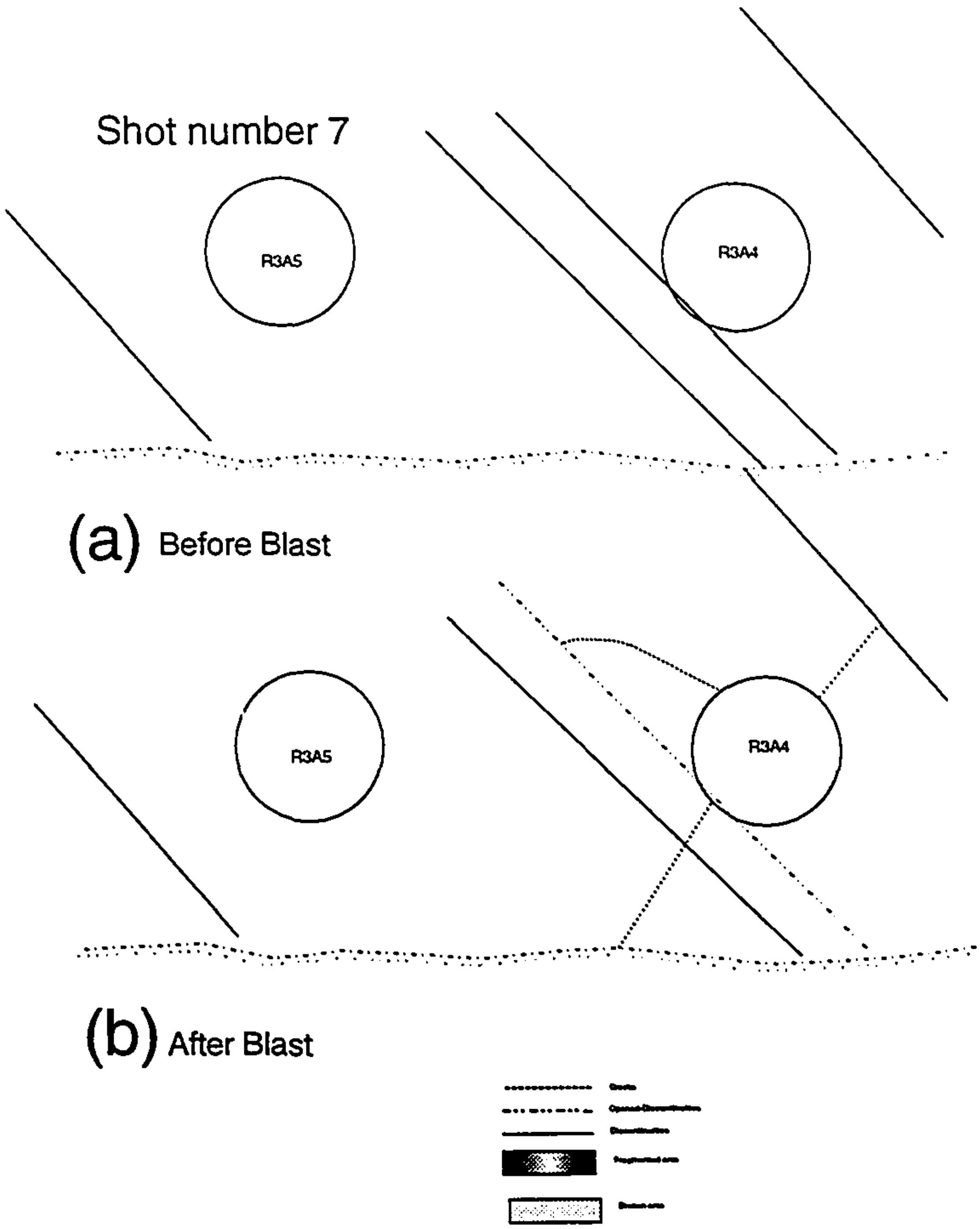

Figure 6.17 : Schematic layout and result of shot number 7 at Site 2. (40 mm dia. MAGNAFRAC in 150 mm dia. holes)

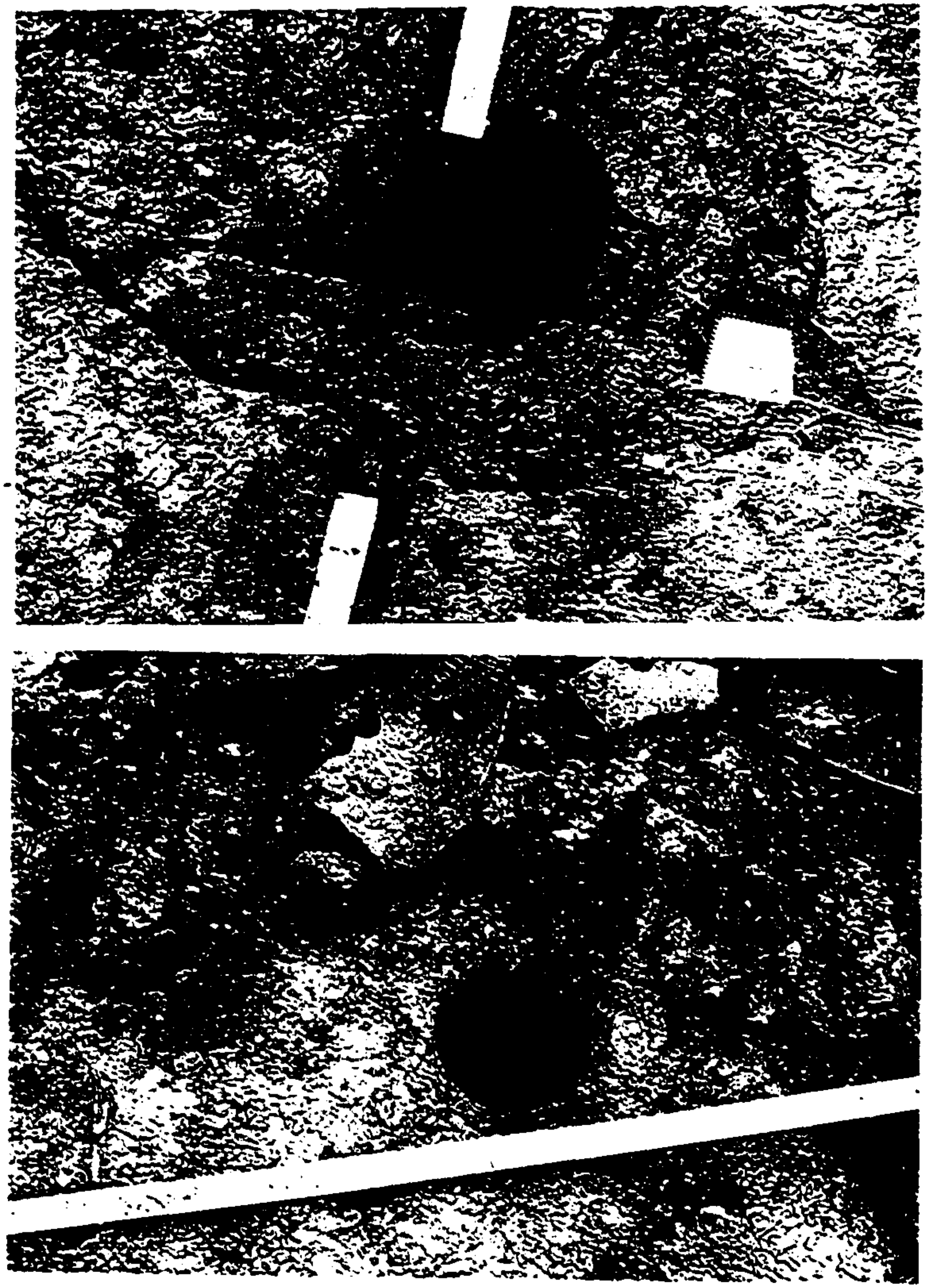

Figure 6.18 : Photographic result of shot number 7 at Site 2.

discontinuities. This illustrates the role of discontinuity on fracture formation, especially where the borehole pressure at each hole was not adequate to reinforce each other in developing a new single fracture between the holes.

6.3.2 Fracture Formation as a Function of Spacing

6.3.2.1 Site One (Infinite Burden)

In the first blast (shot # 7), the holes were drilled with spacing equal to 18 times borehole diameter for very large burden (30 times borehole diameter). The holes were loaded with PRIMAFLEX and detonated simultaneously (Fig. 6.19(a)). In the next test (shot # 8), all other conditions remaining same, spacing was increased from 18 to 24 times borehole diameter. A discontinuity was located at the back of the holes with distances of 1 and 4 times borehole diameter from the first hole (P11) and the second hole (P12) respectively. The second discontinuity, parallel to the first one, crossed hole P12. A closed joint, which was nearly perpendicular to the centreline, was located at the left side of the second hoie (P12), at a distance equal to 10 times borehole diameter. Figure 6.21(a) shows the layout of the blast geometry and the discontinuities.

In this blast (shot # 9), the separation between the holes was increased to 30 times borehole diameter, all other conditions remaining same. An inclined discontinuity was located at the front of hole P13 and formed an angle of about 20° with the face. The distance between the discontinuity and the borehole wall was equal to 6 times borehole diameter. A foliation plane touched the borehole wall at the left side of the first hole (P13) and intersected the face at an angle of 65°. A closed joint was located very close to the second hole (P14), and it was crossed by another discontinuity at the back of the hole. The centre line was crossed by the two parallel discontinuities, which were located at the right side of the first hole and at the left side of the second hole at distances of about 8 and 3 times borehole diameter from the centre of the holes respectively (Fig. 6.23(a)). The blast geometry is shown in Table 6.7.

Table 6.7 : Characteristics of Shots number 7, 8 and 9 at Site 1.

Shot NO.	Burden	Spacing	Borehole Diameter	Charge Diameter	Decoupling Ratio	Type of Explosive
	(m)	(m)	(mm)	(mm)		
7	1.5	0.9	50	10	0.2	PRIMAFLEX
8	1.5	1.2	50	10	0.2	PRIMAFLEX
9	1.5	1.5	50	10	0.2	PRIMAFLEX
* All holes were 2 m in depth, and had a collar of 0.3 m.						

6.3.2.2 Results and Discussion of Blasts number 7, 8 and 9 at Site 1

Whit shot # 7, a single fracture developed between the holes, but the foliations were also opened up to a distance of about 7 times borehole diameter. As figures 6.19(b) and 6.20 show, a new crack also appeared to have developed unconnected to the two holes. This was presumably due to expansion of explosion gases into a closed fracture not visible prior to lasting.

When the spacing was increased from 18 to 24 times borehole diameter (shot # 8), the role of the pre-existing fractures in the crack propagation was more noticeable than in the previous shots (smaller spacing). No clean fracture developed between the holes, and the holes were joined to the discontinuities by perpendicular or nearly perpendicular cracks (Fig. 6.21).

For spacing greater than 24 times hole diameter, no fracture was visible between the holes. As figures 6.23(b) and 6.24 show, a foliation plane parted open, in the first hole (P13), by the detonation products, which led to subsequent opening other foliation planes. No additional fractures resulted from the borehole pressure. In the second hole (P14) a small radial fracture was created which crossed the nearest parallel foliation which itself was parted open.

Based on these results, it is concluded that the maximum spacing between the holes can be as high as 18 times borehole diameter in the absence of any type of open discontinuities. At Site 1, the spacing should be reduced to less than 15 times borehole diameter and in some cases to about 10 times borehole diameter, due to fractured nature of rock mass prior to blasting. The tests also shown that the influence of discontinuities located at a distance greater than half spacing, is negligible on the blast result. Consequently, the spacing was reduced to 15 times borehole diameter or lower in the subsequent series of tests.

6.3.2.3 Site Two (Finite Burden)

In these tests, the holes were loaded with MAGNAFRAC, and detonated simultaneously. Simultaneity, in this case implies two holes firing within 500 μs of each other. The spacing between holes was 1.5 m and the burden 1.0 m. A discontinuity was located at the left side of the first hole (R1A2), and the other one was crossed by the second hole (R1A3). The distance between the discontinuity and the hole centre was about 15 times borehole diameter. The joint was very tight, the width being about 1 mm (Fig. 6.25(a)).

In shot # 9, the spacing was increased from 1.5 m to 2.0 m , with all other conditions remaining same. A joint plane was located between two holes with a distance of about 1.5 m and 0.5 m from the first (R1A6) and the second (R1A7) holes respectively. The hole R1A7 was crossed by a second discontinuity. A 10 mm wide weak plane filled with clay was located at the right side of this joint and crossed it 1.5 m away from the face (Fig. 6.27(a)). The characteristics of the blast is given in Table 6.8.

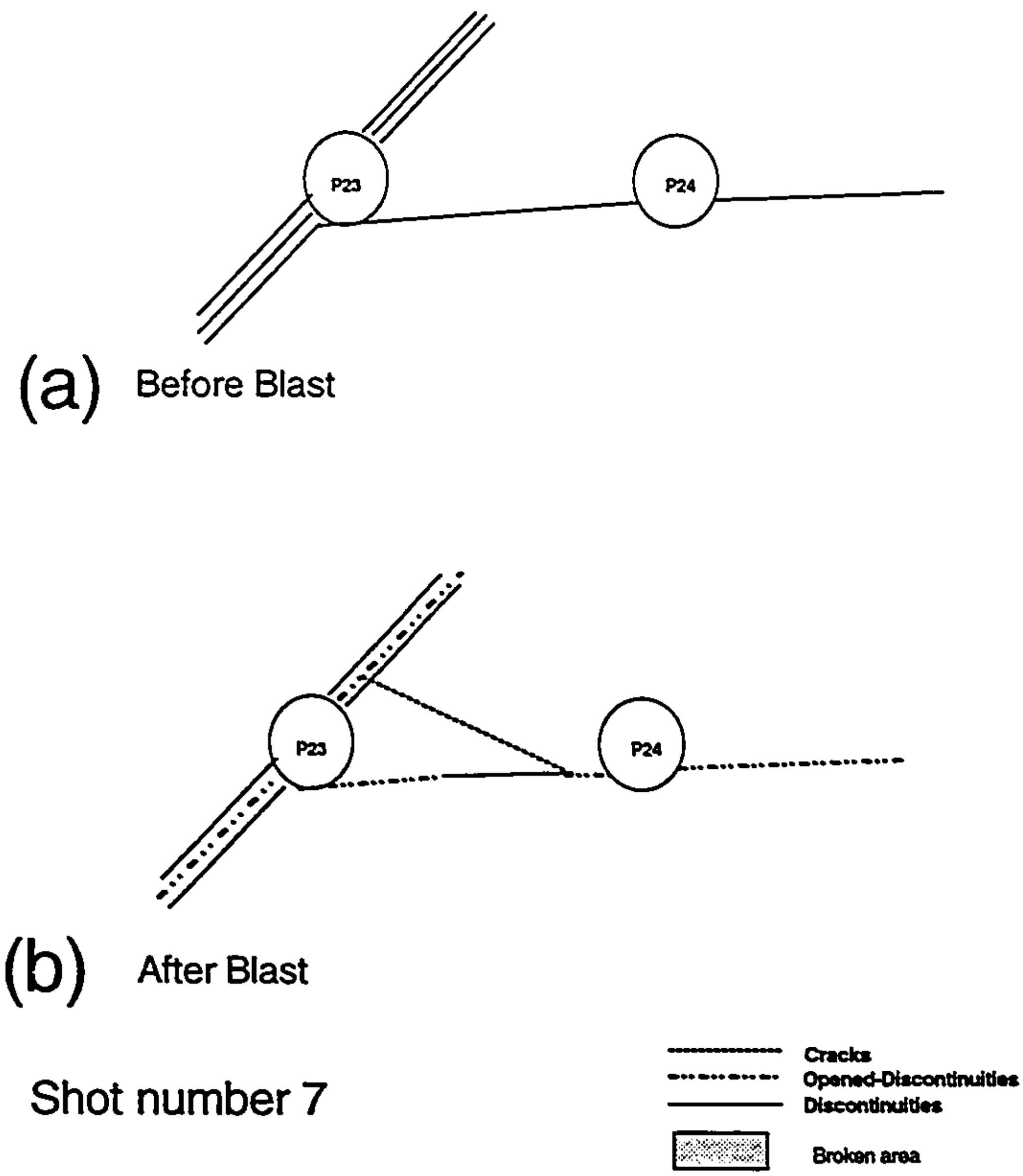

Figure 6.19 : Schematic layout and result of shot number 7 at Site 1. (PRIMAFLEX in 50 mm dia. holes)

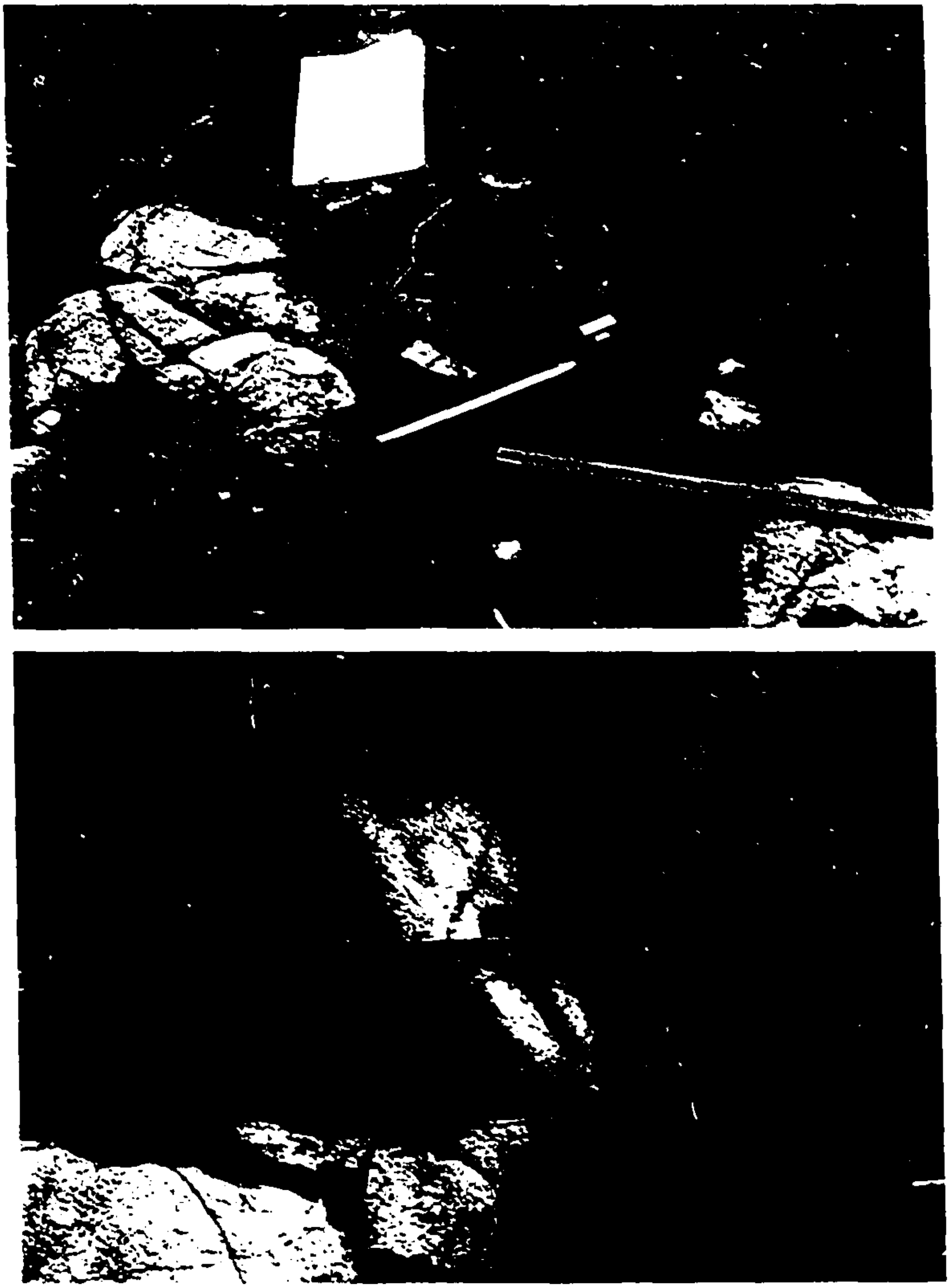

Figure 6.20 : Photographic result of shot number 7 at Site 1.

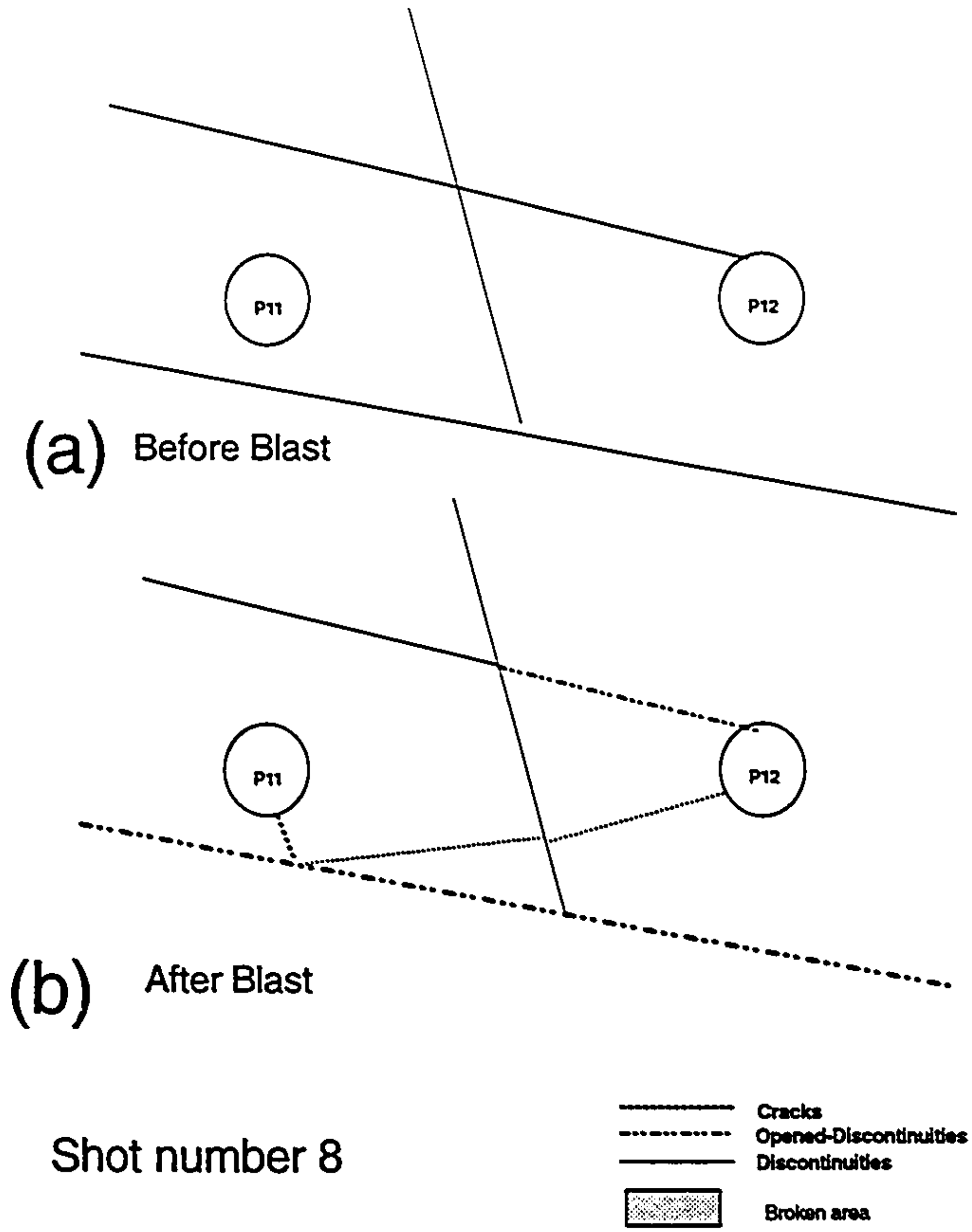

Figure 6.21 : Schematic layout and result of shot number 8 at Site 1. (PRIMAFLEX in 50 mm dia. holes)

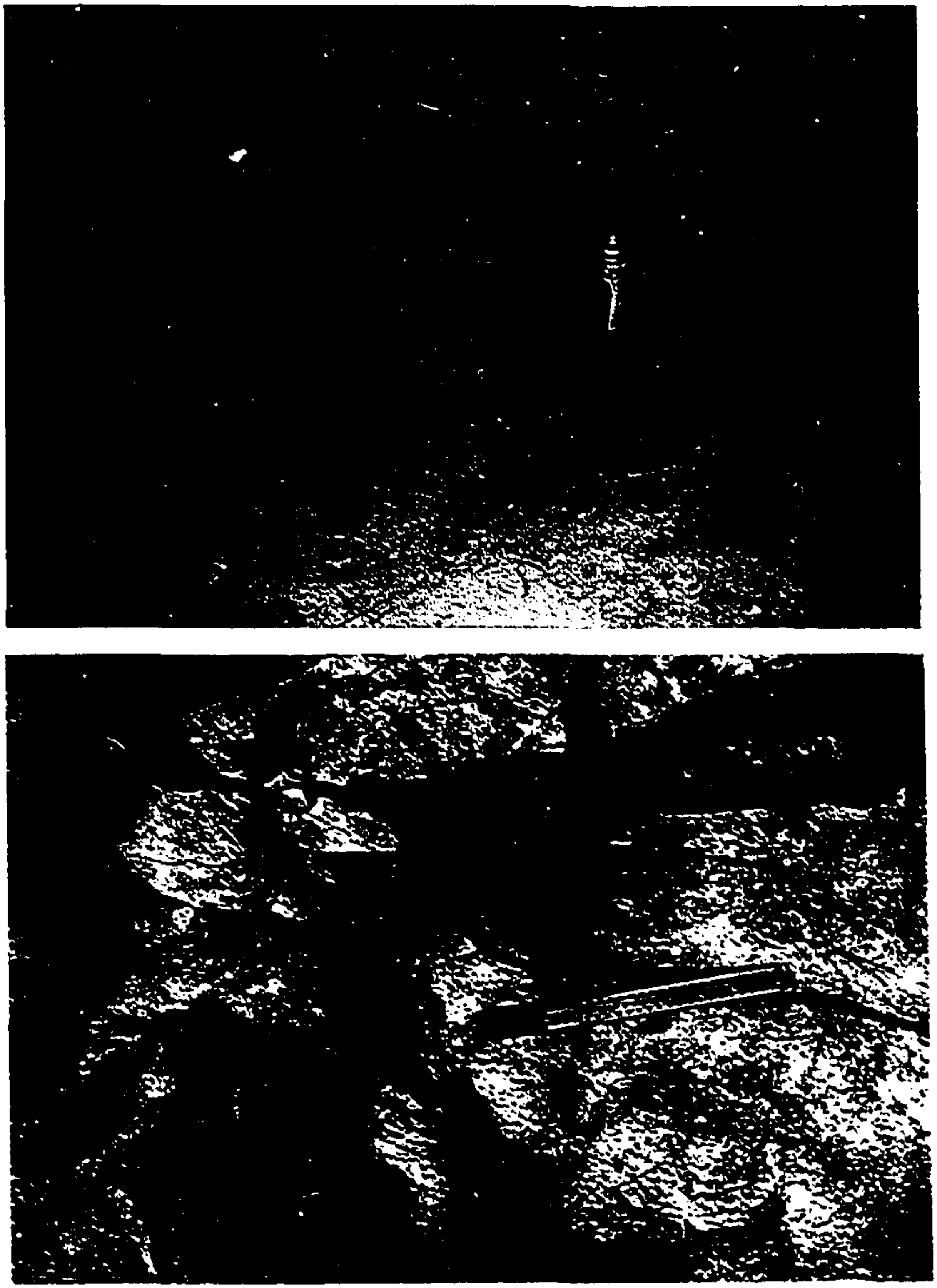

Figure 6.22 : Photographic result of the shot number 8 at Site 1.

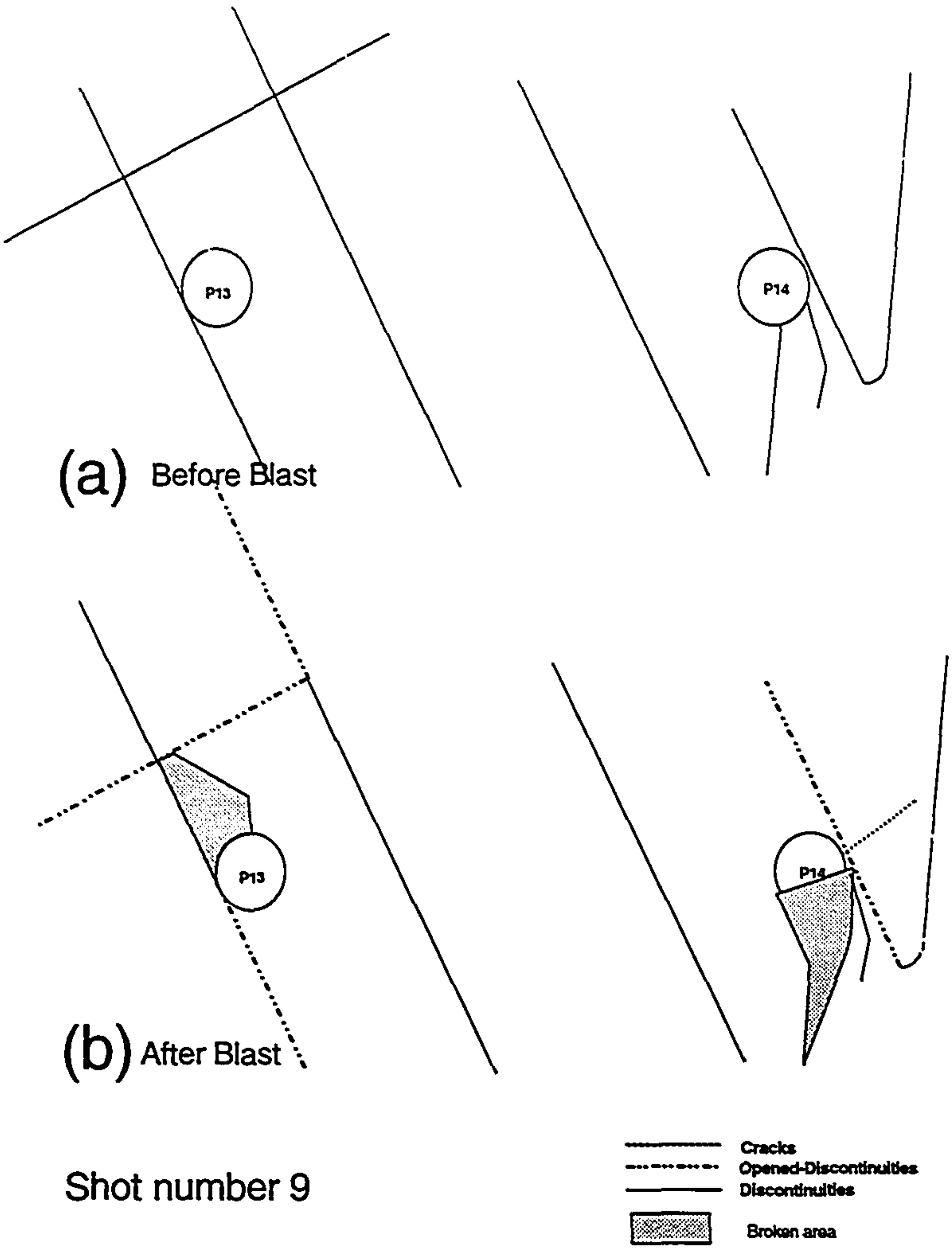

Figure 6.23 : Schematic layout and result of shot number 9 at Site 1. (PRIMAFLEX in 50 mm dia. holes)

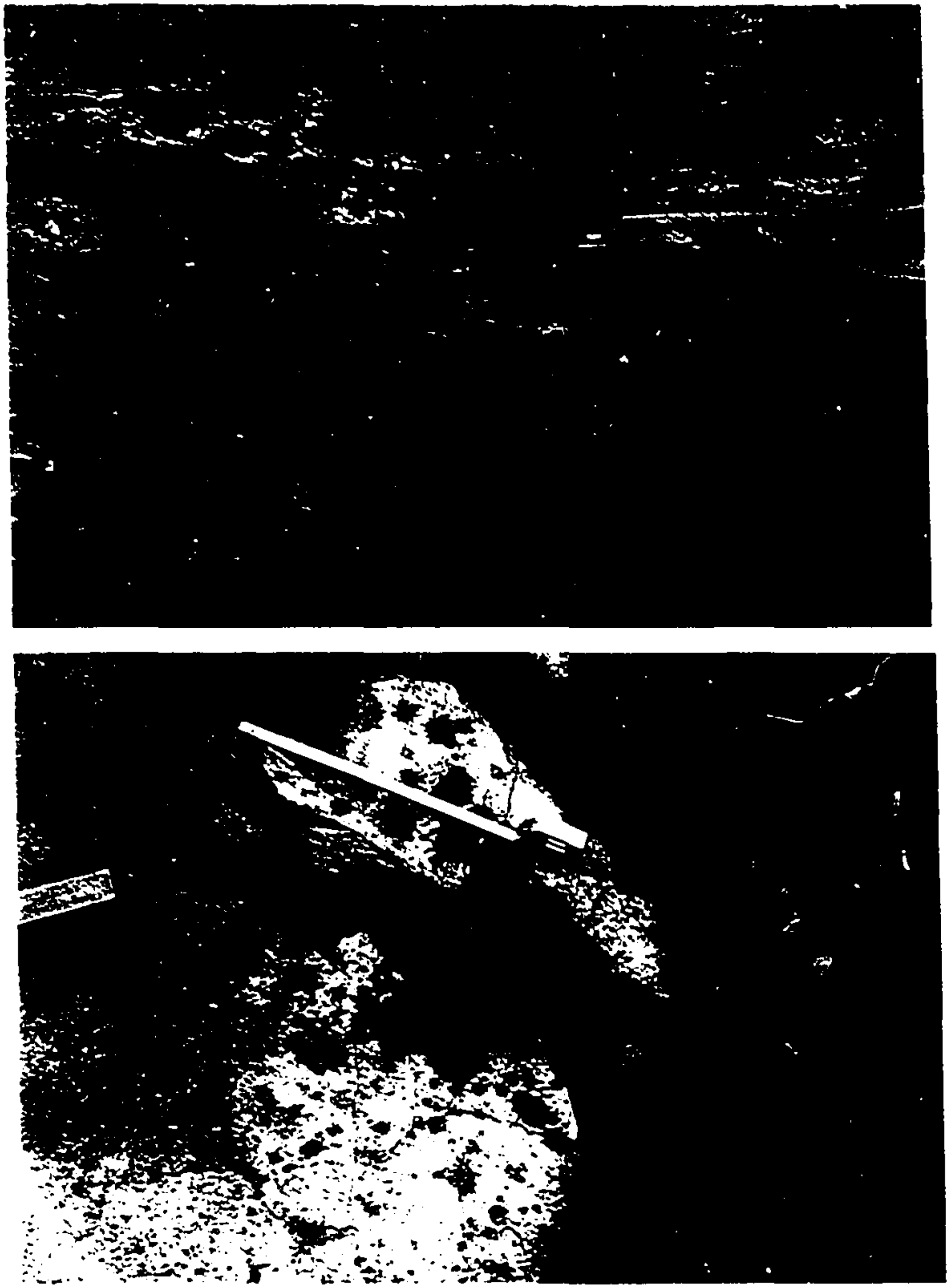

Figure 6.24 : Photographic result of shot number 9 at Site 1.

Table 6.8 : Characteristics of Shots number 8 and 9 at Site 2.

Shot No.	Burden	Spacing	Borehole Diameter	Charge Diameter	Decoupling Ratio	Type of Explosive
	(m)	(m)	(mm)	(mm)		
8	1.0	1.5	100	32	0.32	MAGNAFRAC
9	1.0	2.0	100	32	0.32	MAGNAFRAC

* All holes were 3 m in depth, and had a collar of 0.3 m in 100 mm holes and 0.6 m in 150 mm holes.

6.3.2.4 Results and Discussions of Blasts number 8 and 9 at Site 2

The results show an open discontinuity, located at 12 times borehole diameter has no effect on the blast results. This is illustrated in figures 6.25 and 6.26. In this blast (shot# 8), the half hole was clearly visible on the face. For the second hole (R1A3), which was crossed by the other discontinuity, one quarter of the hole remained on the face to a depth of 0.5 m below the surface. This joint was opened at the back of the hole to a distance of about 6 times borehole diameter. As the depth increased, the 'quarter hole' was changed to a 'half hole'. A hump remained between the two holes, especially close to the second hole, and up to a depth of 0.5 m below the surface. As mentioned earlier, the joints and the weak planes at this site were usually open to about 0.7 m below the surface. This could be the reason for the excessive loss in top region of hole R1A3, and of the hump between the holes below the surface.

Based on this analysis, it is concluded that the spacing of the hole should be reduced to 10 times borehole diameter in order to develop a very clean smooth face. This reduction in spacing would also place the hole R1A3 farther away from the discontinuity. This would result in significant improvement in the quality of the wall-control blast.

In the next blast (shot # 9), two crack developed from the first hole and the second holes up to the nearest discontinuities. These cracks essentially formed the outline of the new blast face, which was Z-shaped, instead of being a smooth face in the place of the two holes (Figs. 6.27 and 6.28). Although both holes exhibited excellent half holes after the blast, the blast result would be considered unsatisfactory due to this Z-shaped outline. However, this latter shape is exactly according to the theoretical predictions outline in chapter 5. The pre-existing discontinuity between the two holes critically controlled this fracture formation. Also, the rock fragment originally between hole R1A7 and open weak plane on the right side was blasted out to a distance about 4 borehole diameters.

As the distance of the pre-existing fractures from the borehole wall was decreased, the number and the width of the fractures were also increased. For distances less than 2.5 times the hole diameter, the rocks were completely shattered between the borehole wall and the discontinuities. This is in accord with prediction from the numerical analysis (Chapter 5, section 5.5.1). When pre-existing fractures crossed the holes, both the number and the length of new cracks decreased or were altogether absent. This is due to the rapid decrease in the borehole pressure resulting from penetration of explosion gases into the discontinuities.

6.3.3 Effect of Discontinuity Parallel to Free Face on Crack Formation

6.3.3.1 Site One (Infinite Burden)

In the first blast (shot # 10), the holes were located between two parallel discontinuities with a spacing of 0.4 m. The distances between the centre of the first hole (P43) from the front and the back discontinuities were about 1 and 3 times borehole diameter respectively. As figure 6.29(a) shows, the condition of the second hole (P44) with respect to the discontinuities in a mirror image of P43.

In shot # 11, a discontinuity roughly co-linear with the three holes (P51, P52 and

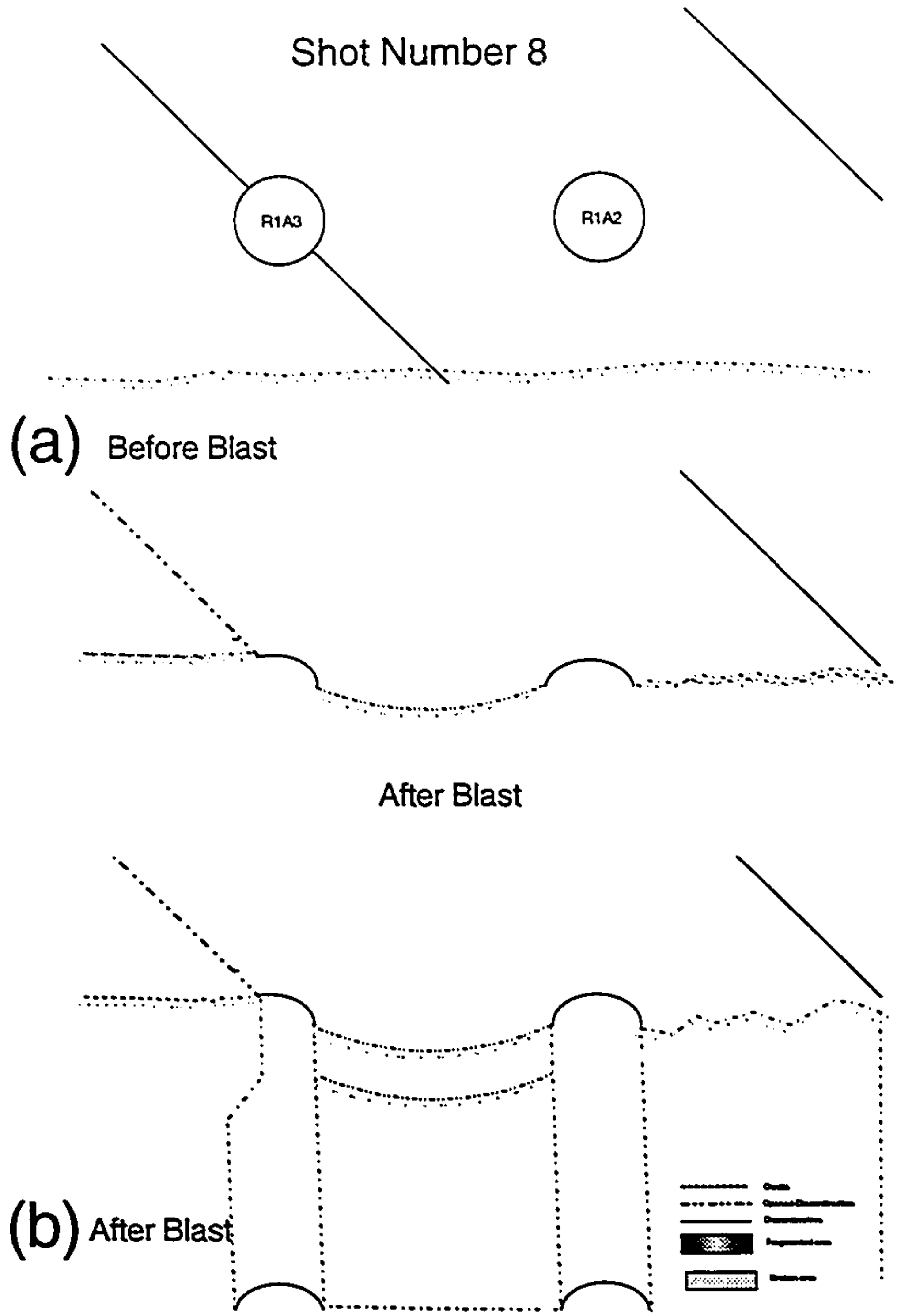

Figure 6.25 : Schematic layout and result of shot number 8 at Site 2. (32 mm dia. MAGNAFRAC in 100 mm dia. holes, HCF = 85%)

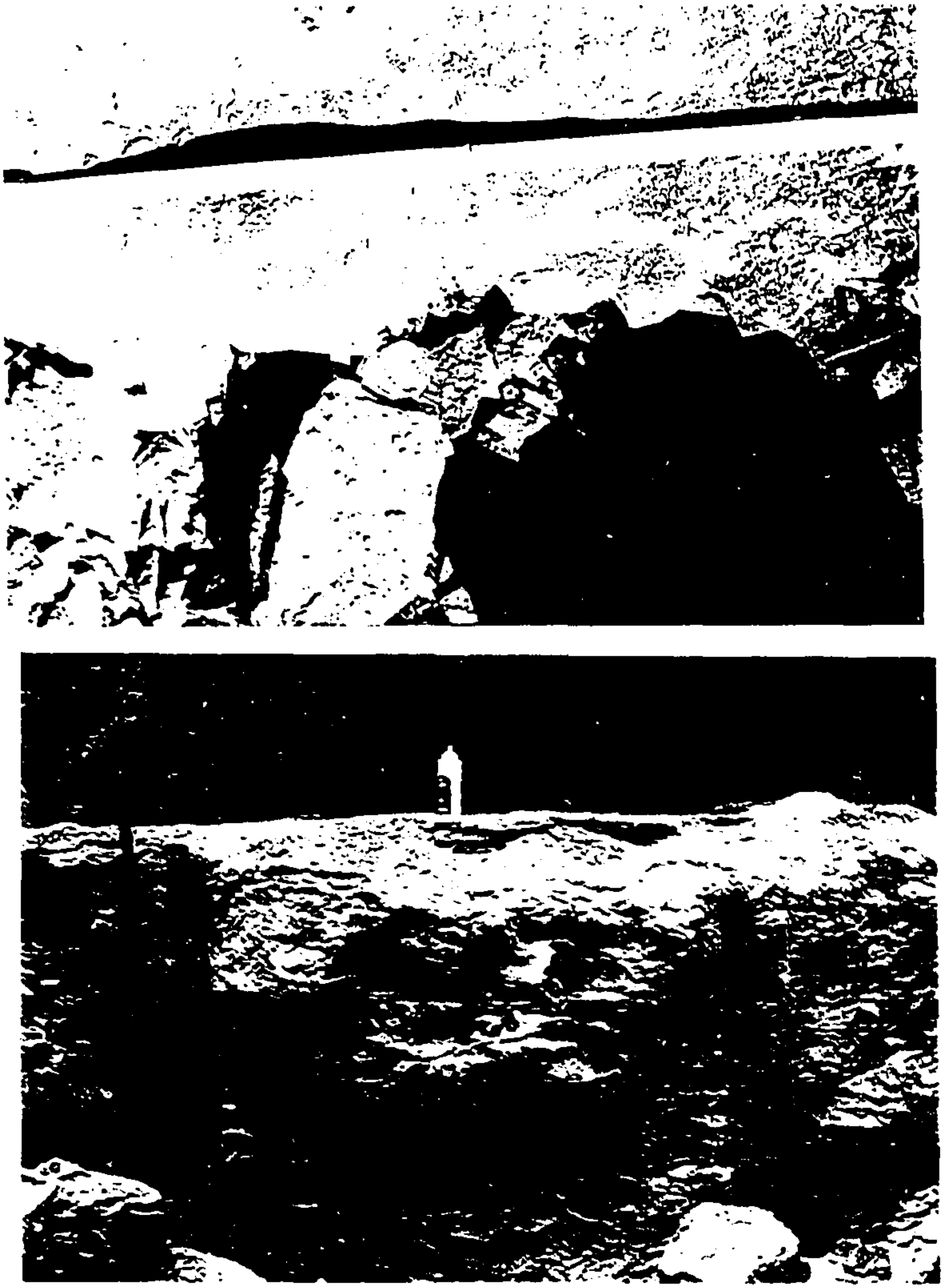

Figure 6.26 : Photographic result of shot number 8 at Site 2.

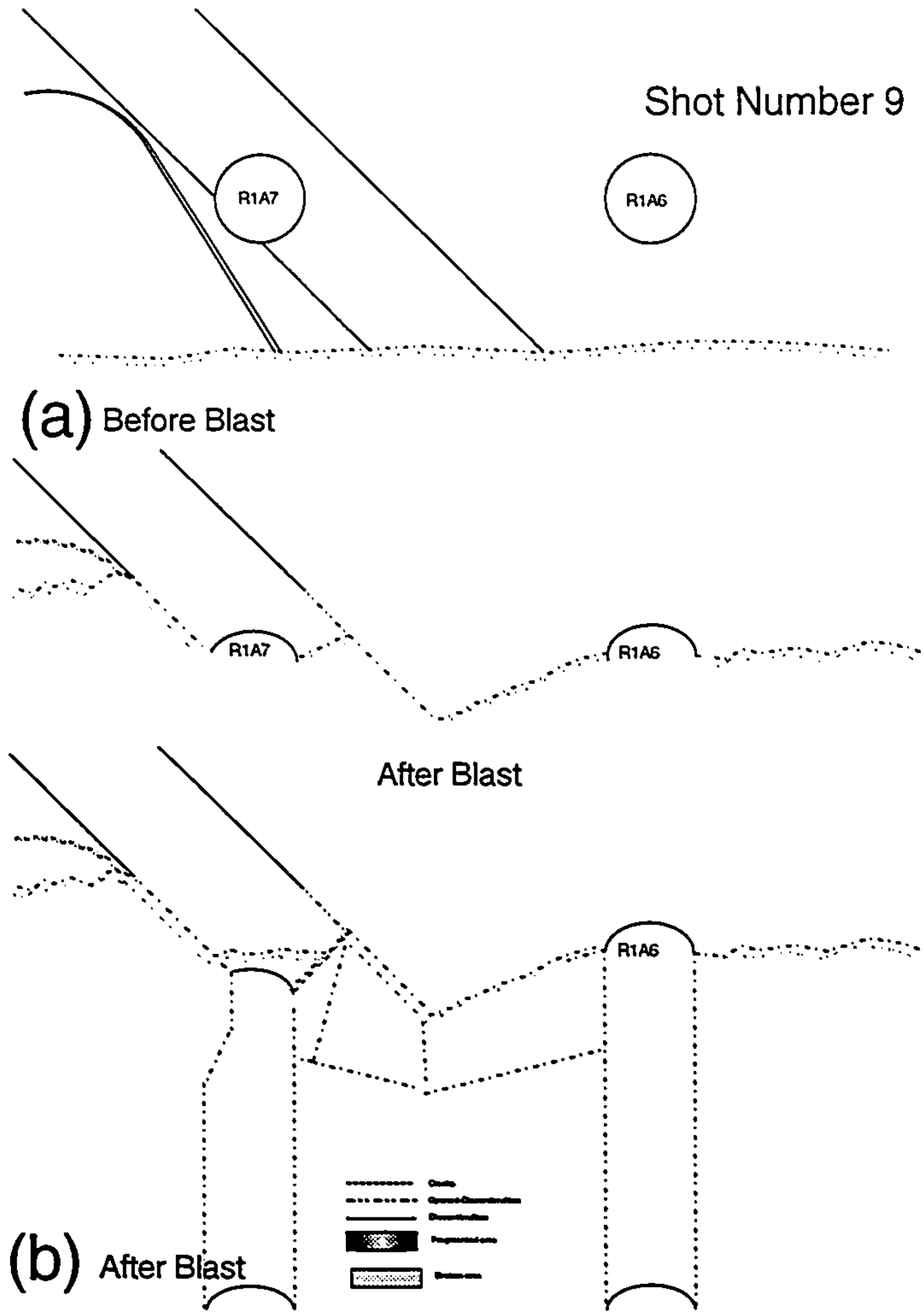

Figure 6.27 : Schematic layout and result of shot number 9 at Site 2. (32 mm dia. MAGNAFRAC in 100 mm dia. holes, HCF = 94%)

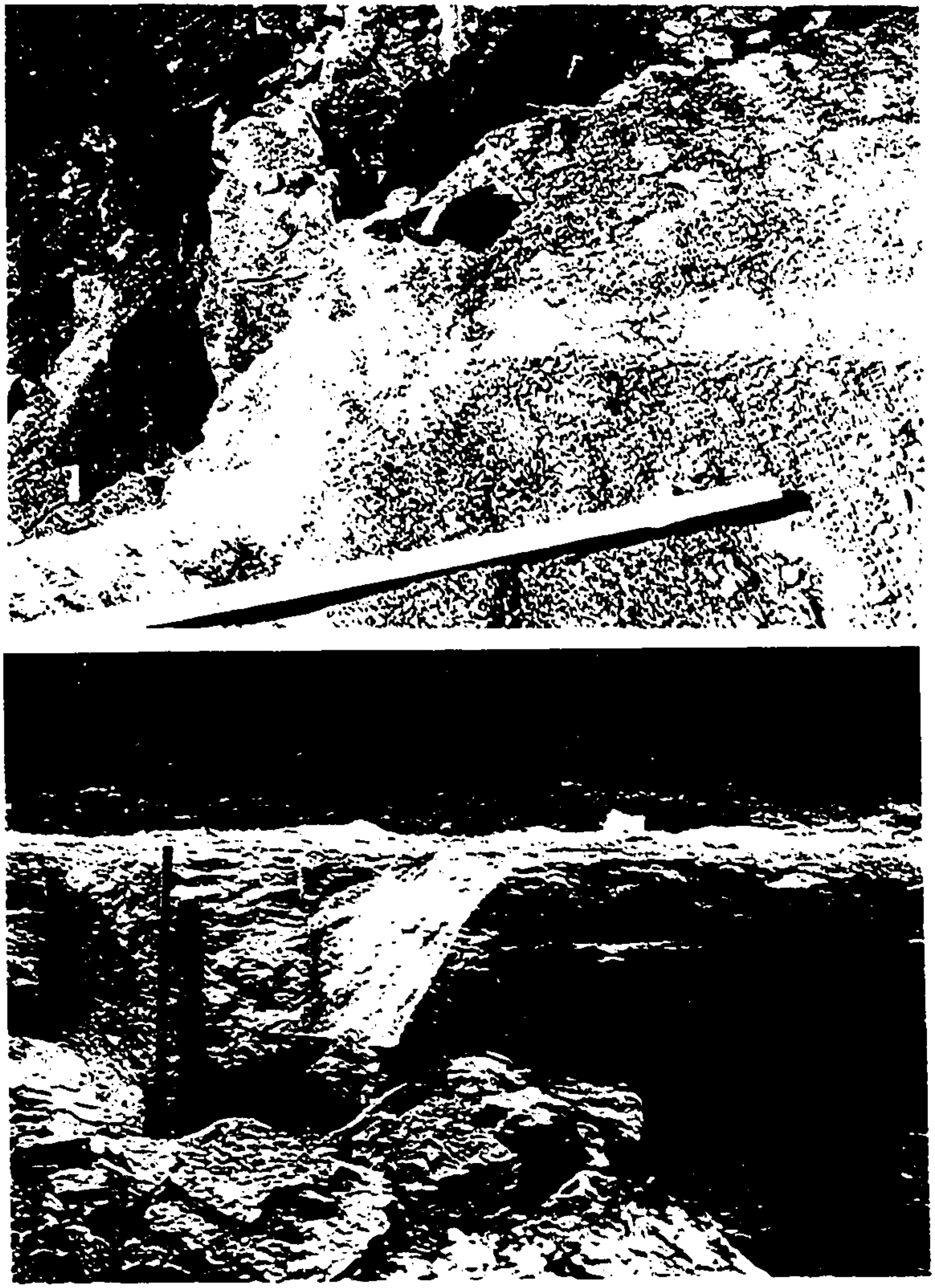

Figure 6.28 : Photographic result of shot number 9 at Site 2.

Table 6.9 : Characteristics of Shots number 10 and 11 at Site 1.

Shot No.	Burden	Spacing	Borehole Diameter	Charge Diameter	Decoupling Ratio	Type of Explosive
	(m)	(m)	(mm)	(mm)	-	
10	1.5	1.2	100	25	0.25	SUPERFRAC
11	1.5	1.2	100	25	0.25	SUPERFRAC
* All holes were 3 m in depth, and had a collar of 0.3 m in 100 mm holes and 0.6 m in 150 mm holes.						

P53) was located at distances of about 0.1 m, 0.15 m and 0.5 m respectively. Another discontinuity was located at the left side of hole P51 and was 0.02 m from it. It was roughly parallel to the two other discontinuities. The latter were located equi-distant ($\sim$0.5 m) from two neighbouring holes as shown in figure 6.31(a). Table 6.9 shows characteristics of the blasts.

6.3.3.2 Results and Discussion of Blasts number 10 and 11 at Site 1

As the result of the blast # 10, the fractures from the first hole (P43) developed perpendicular or nearly perpendicular to the discontinuities. The length c the cracks were about 5 times borehole diameter and continued behind the pre-existing fracture. The reason could be that the discontinuity was completely closed. In contrast since the second hole was drilled very close (less than 2 times borehole diameter) to the open discontinuity, the rock was extensively fractured between hole and the discontinuity due to the blast. A radial fracture also developed to the other discontinuity at the opposite direction. A single fracture was formed between the boreholes. However, in actual blasting, the new free face would be followed either of pre-existing discontinuities rather the new crack between the holes (Figs. 6.29(b) and 6.30). In shot # 11, no crack formed between holes # P52 and # P53. This was due to the presence of pre-existing discontinuities as shown in figure 6.31. The rock was shattered between the wall of these

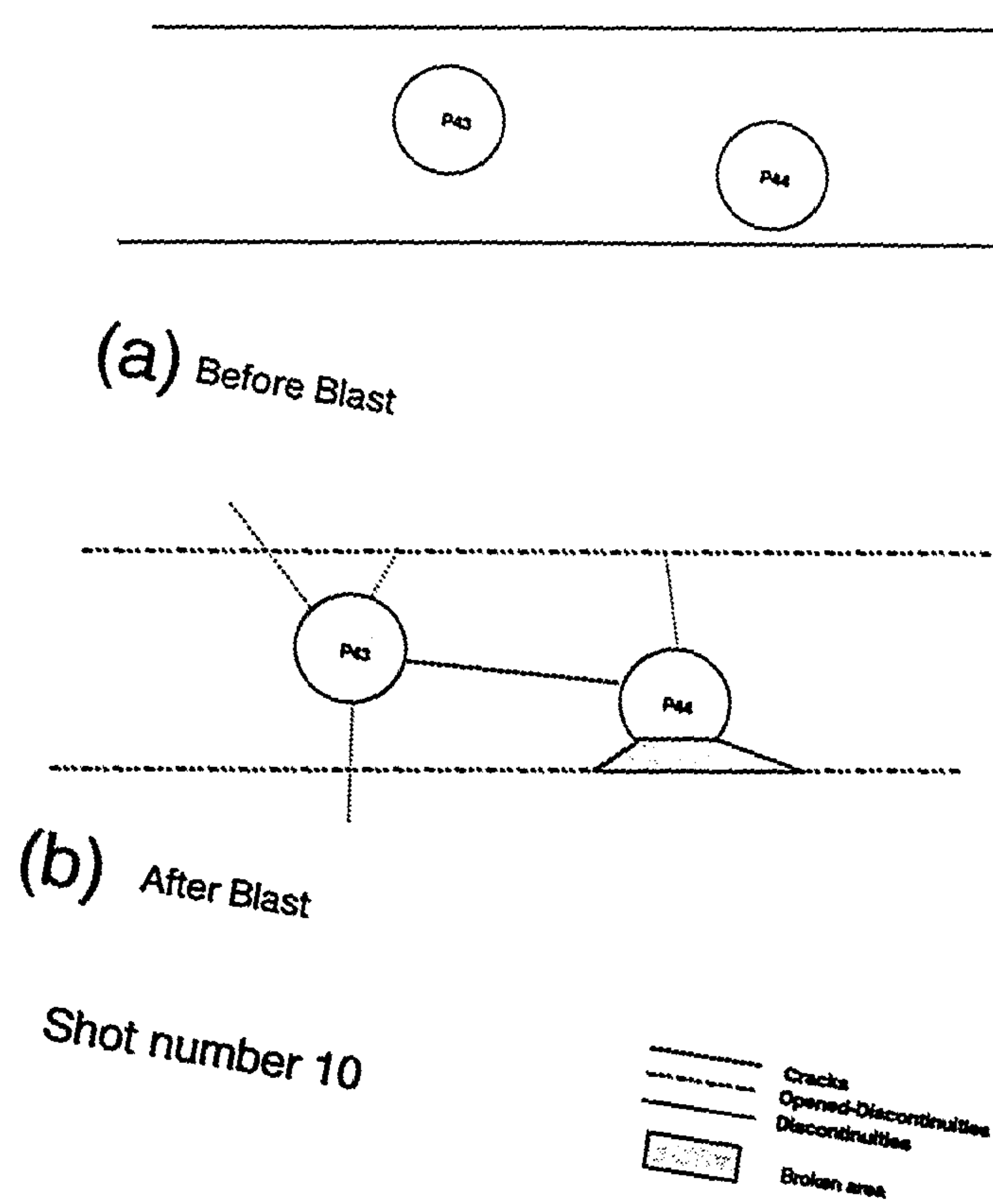

Figure 6.29 : Schematic layout and result of shot number 10 at Site 1. (25 mm dia. SUPERFRAC in 100 mm dia. holes)

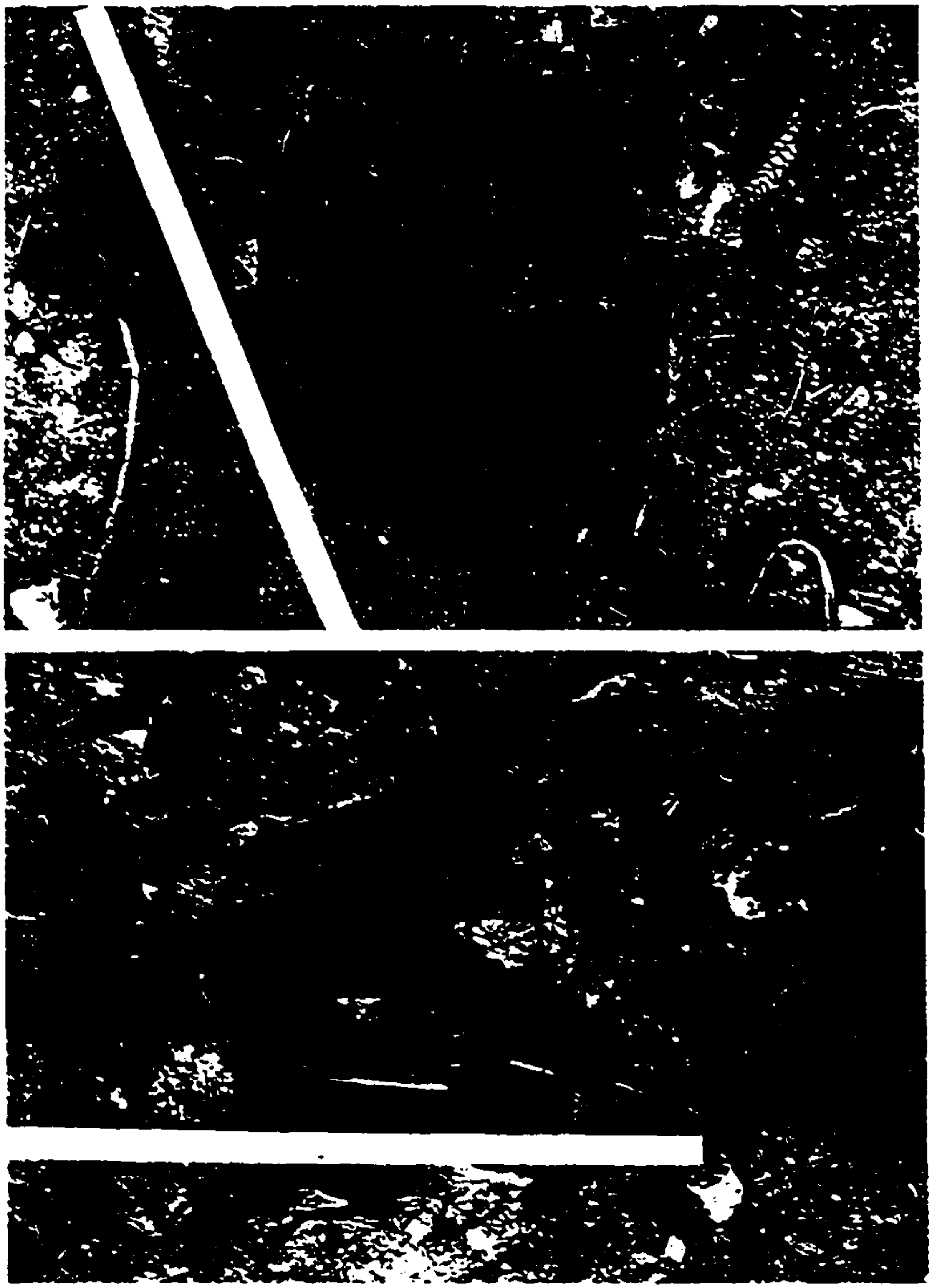

Figure 6.30 : Photographic result of the shot number 10 at Site 1.

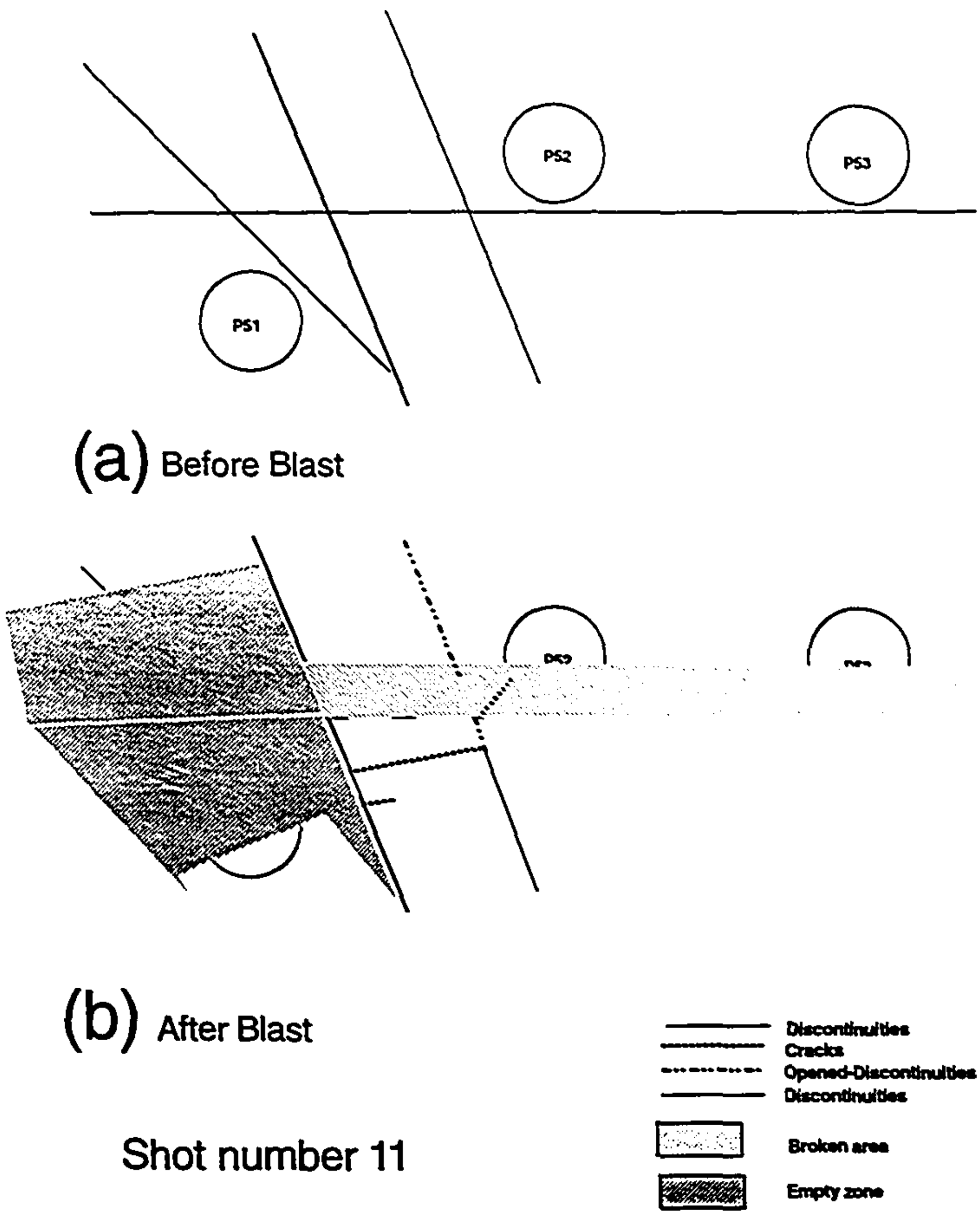

Figure 6.31 : Schematic layout and result of shot number 11 at Site 1. (25 mm dia. SUPERFRAC in 100 mm dia. holes)

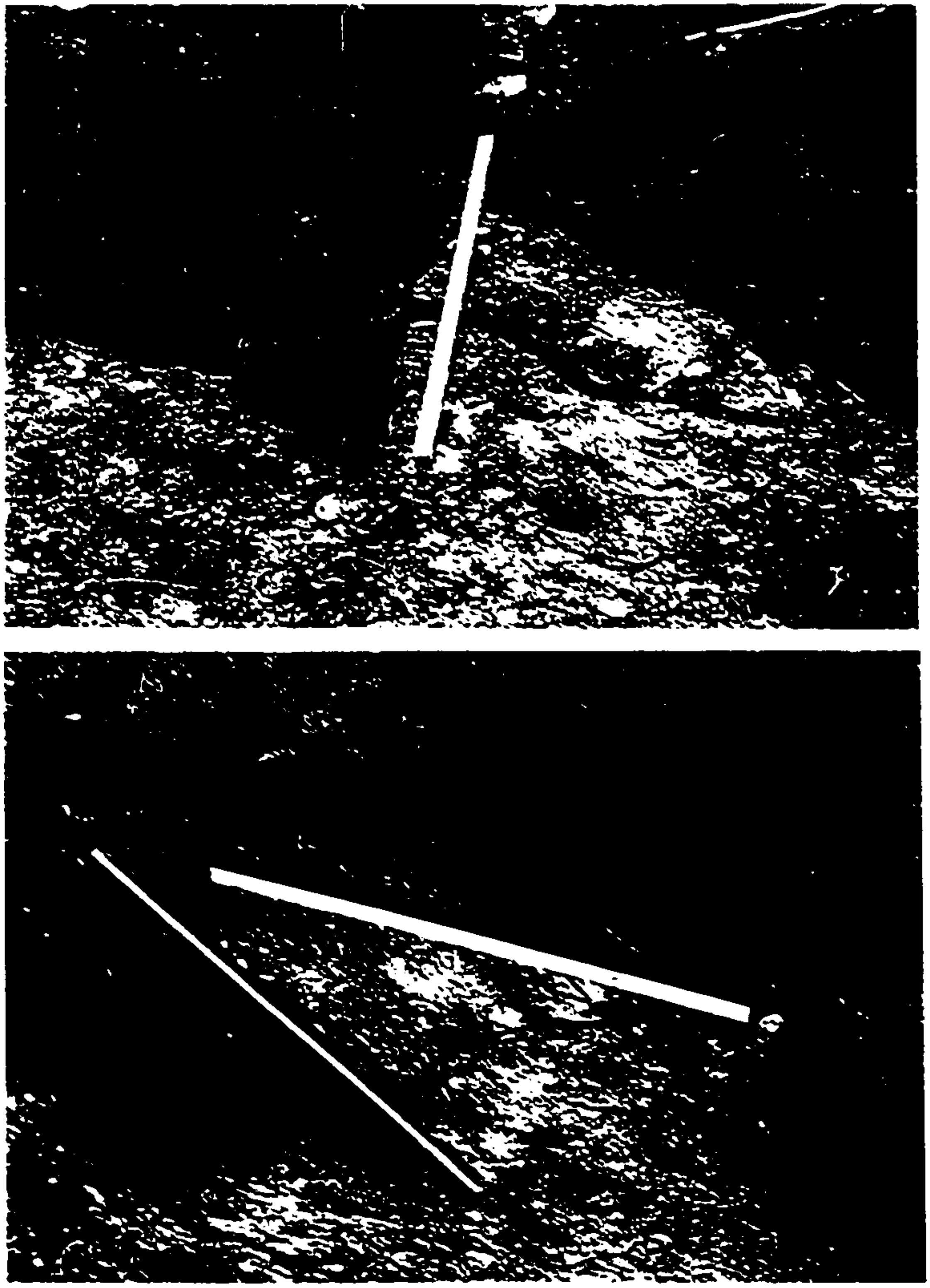

Figure 6.32 : Photographic result of shot number 11 at Site 1.

boreholes and nearly parallel foliation. The shattering continued along this discontinuity until hole P51. This essentially implies that with very large burdens, the pre-split line would coincide with a the parallel discontinuity near the holes (Figs. 6.31(b) and 6.32).

6.3.3.3 Site 2 (Finite Burden)

In this blast (Shot # 10), a 5 mm wide weak plane was located at the back of the holes, with the distances equal to 7 and 3 times borehole diameter from the first hole (R1A4) and the second hole (R1A5) respectively. It had an elliptical shape which started from the face and crossed the joint at the back of the holes. These types of discontinuities were usually filled with clay to a depth ranges of 0.5 to 1.5 m (Fig. 6.33(a)). Two other discontinuities were oriented about 45° to the centre line. The respective distances between the middle discontinuity and holes R1A4 And R1A5 were 5 and 10 times borehole diameter respectively. Two parallel joints with 0.2 m spacing were also located at the left side of the first hole, and the distance between the centre of the hole and the nearest joint was 1.5 times borehole diameter (Fig. 6.33(a)).

In Shot # 11, the 2 mm wide shallow open joint was located at the back of the holes at distances of about 0.6 m and 1.0 m from holes R2A5 and R2A6, respectively. The opening was filled with clay. The closed joint near hole R2A5 was at a distance equal to 0.8 m. Hole R2A6 was crossed by a similar joint of the two open, one was at the midpoint between the holes, and the other was about 0.5 m from hole R2A6 (Fig. 6.35(a)).

In blast # 12, the first hole (R2A9) was located between two parallel opened joints with a spacing equal to 0.5 m. These two joints were connected to each other by a weak plane which was located at the back of the hole at a distance of 0.2 m from the centre of the hole (Fig. 6.37(a)). The fourth discontinuity was an open joint, which was located between the holes at distances equal to 1.2 m and 0.8 m from the first and the second

Table 6.10 : Characteristics of Shots number 10, 11 and 12 at Site 2.

Shot No.	Burden	Spacing	Borehole Diameter	Charge Diameter	Decoupling Ratio	Type of Explosive
	(m)	(m)	(mm)	(mm)	-	
10	1.0	1.5	100	32	0.32	SUPERFRAC
11	1.0	2.0	100	32	0.32	SUPERFRAC
12	1.0	2.0	100	32	0.32	SUPERFRAC
* All holes were 3 m in depth, and had a collar of 0.3 m in 100 mm holes and 0.6 m in 150 mm holes.						

holes, respectively. The fifth discontinuity was located at the right side of hole R2A10 at a distance of about 0.2 m from the centre of the hole. The blast geometry and explosive used in these experiments are given in Table 6.10.

In shot # 18, a 5 mm wide weak plane was located in front of the holes (R2A7 and R2A8). It was 0.9 m and 0.15 m away from the borehole walls of R2A7 and R2A8 respectively. The plane with a half elliptical shape, started from the face at the left side of the holes and crossed the face at the right side of them. The blast geometry remained similar to the previous shot (See Figs. 6.55(a) and Table 6.18).

6.3.3.4 Results and Discussion of Blast numbers 10, 11 and 12 at Site 2

The role of a weak plane on the blast result is clearly illustrated at the left side of the picture in figures 6.33(b) and 6.34. Hole R1A4 shattered completely to a depth of 1 m below the surface. The rock fragmented between borehole wall and weak plane. An extensively shattered zone between hole R1A4, the discontinuity at the right side of the hole and the weak plane at the back of the hole was also visible. The weak plane was opened to the free face. Consequently, the wall of the weak plane will be the new face after removing the rock.

In shot # 11, a shallow weak plane with an approximately half elliptical shape was located at the back of the holes and crossed by several opened and closed-discontinuities behind the boreholes. The area between the holes and the weak plane was completely shattered after the blast (Figs. 6.35(b) and 6.36). The result is comparable to the results obtained by numerical analysis for a weak plane parallel to the face at the back of the holes.

In the last blast of this test series (shot # 12), the first hole (R2A9) was completely shattered, because it was located between three discontinuities (two weak plane and one joint) which crossed each other at the back of the hole (Figs 6.37(b) and 6.37). One weak plane was located at the back of the hole and started from the second weak plane at the left side of the hole and continued to the joint at the right side of the hole. The distance of the rear weak plane from the hole was about 4 times borehole diameter. The shattered zone, at the back of the hole, was placed between the borehole wall and the intersection point of these three continuities (Figs 6.37(b) and 6.38).

In the presence of discontinuity at the front of holes, the rock was remained between the holes, and overbreak could be easily seen in the front of the face. A single fracture developed from the first hole to the second hole, but not along the direction of the centreline (see Figs 6.55(b) and 6.56). As shown in the previous chapter at section 5.5.2.2, a weak plane parallel to the face at the front of the holes causes the stresses to increase between the borehole wall and the plane, and reduces the stresses at the middle of spacing between the holes. Therefore, a hump between the holes, and the large size of the rock in this blast can be also explained by the numerical analysis.

6.3.4 Effect of Perpendicular Discontinuity on Crack Formation

6.3.4.1 Site One (Infinite Burden)

In this blast (shot # 12), a nearly perpendicular discontinuity was located at the

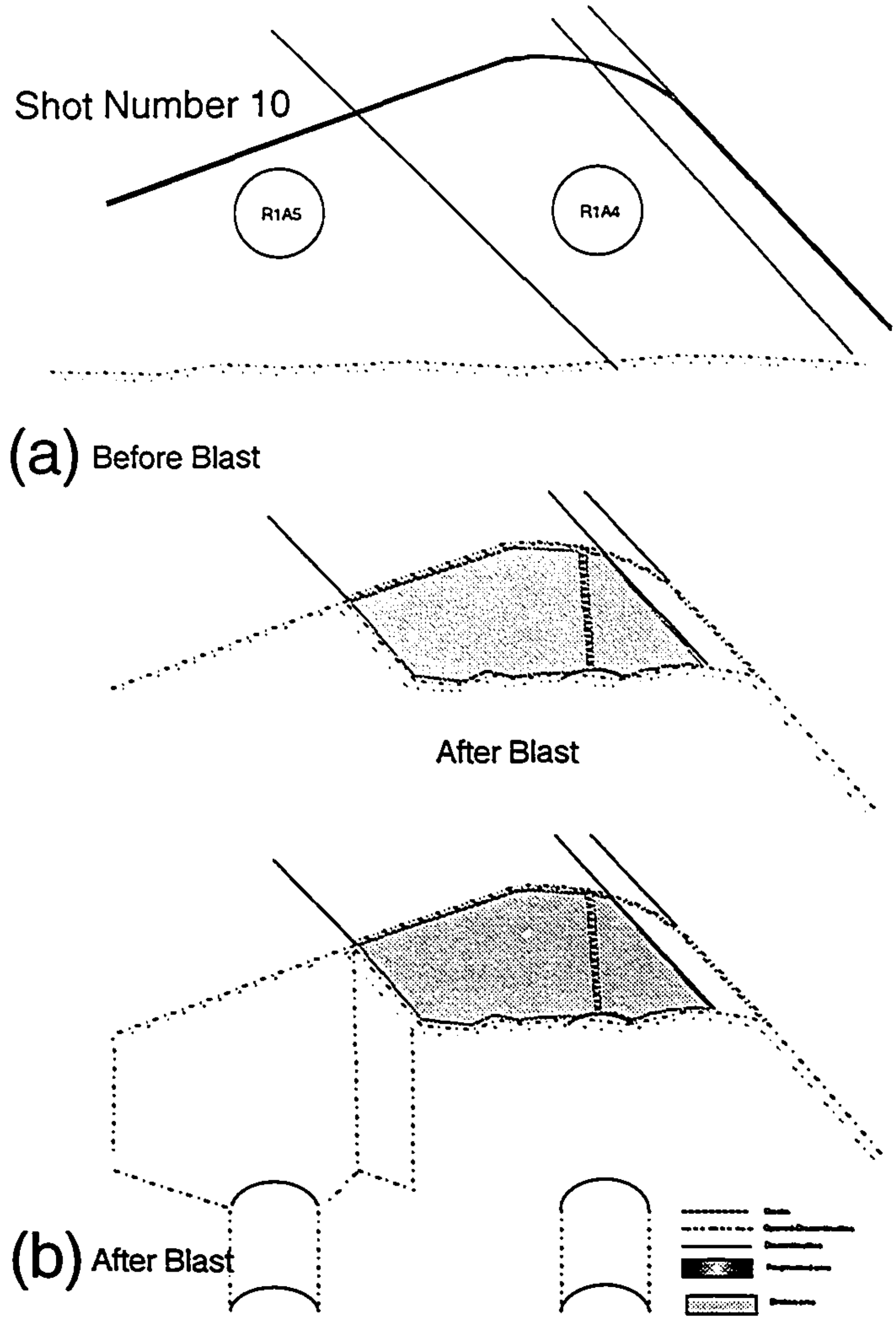

Figure 6.33 : Schematic layout and result of shot number 10 at Site 2. (32 mm dia. SUPERFRAC in 100 mm dia. holes, HCF = 46%)

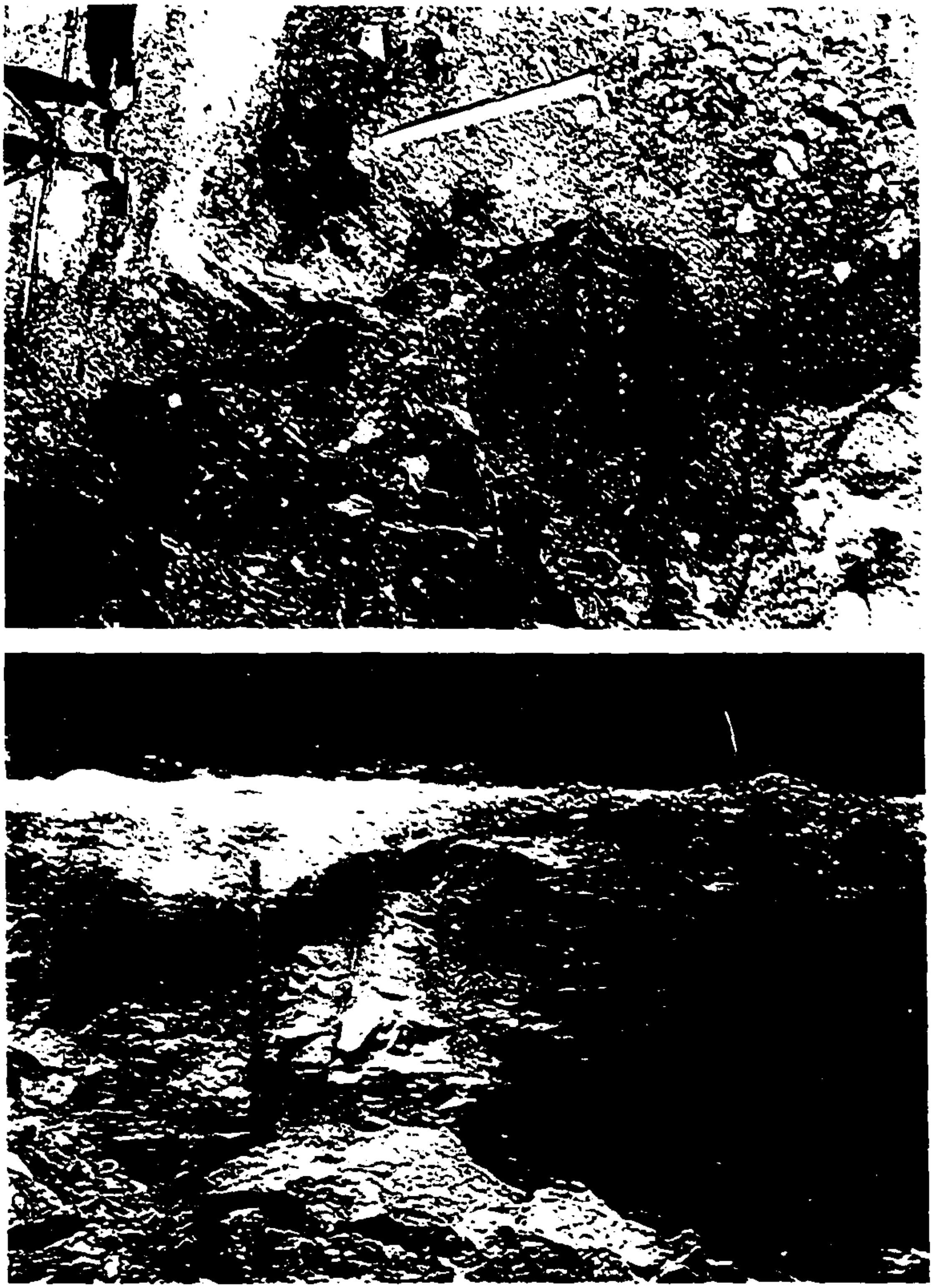

Figure 6.34 : Photographic result of shot number 10 at Site 2.

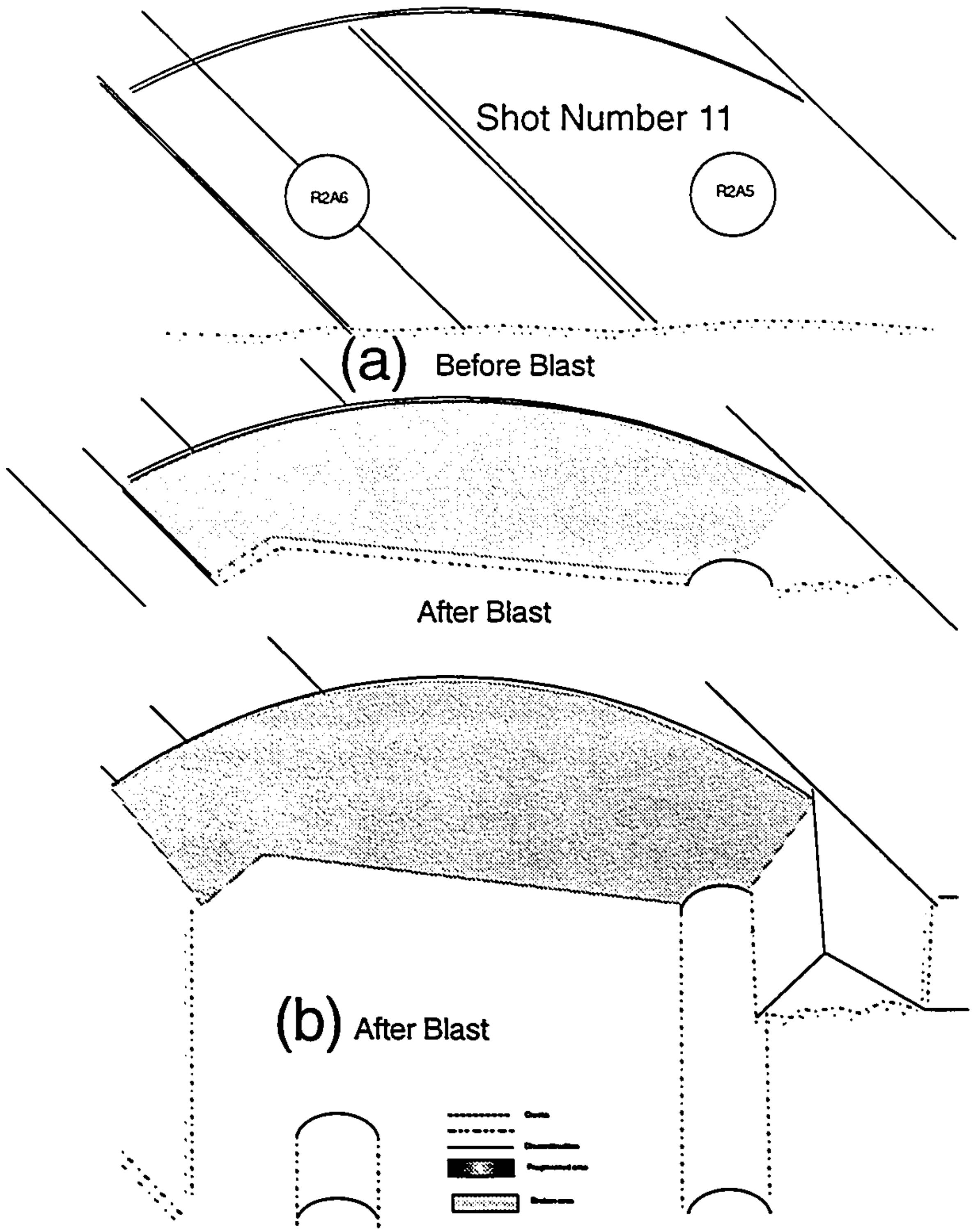

Figure 6.35 : Schematic layout and result of shot number 11 at Site 2. (32 mm dia. SUPERFRAC in 100 mm dia. holes, HCF = 56%)

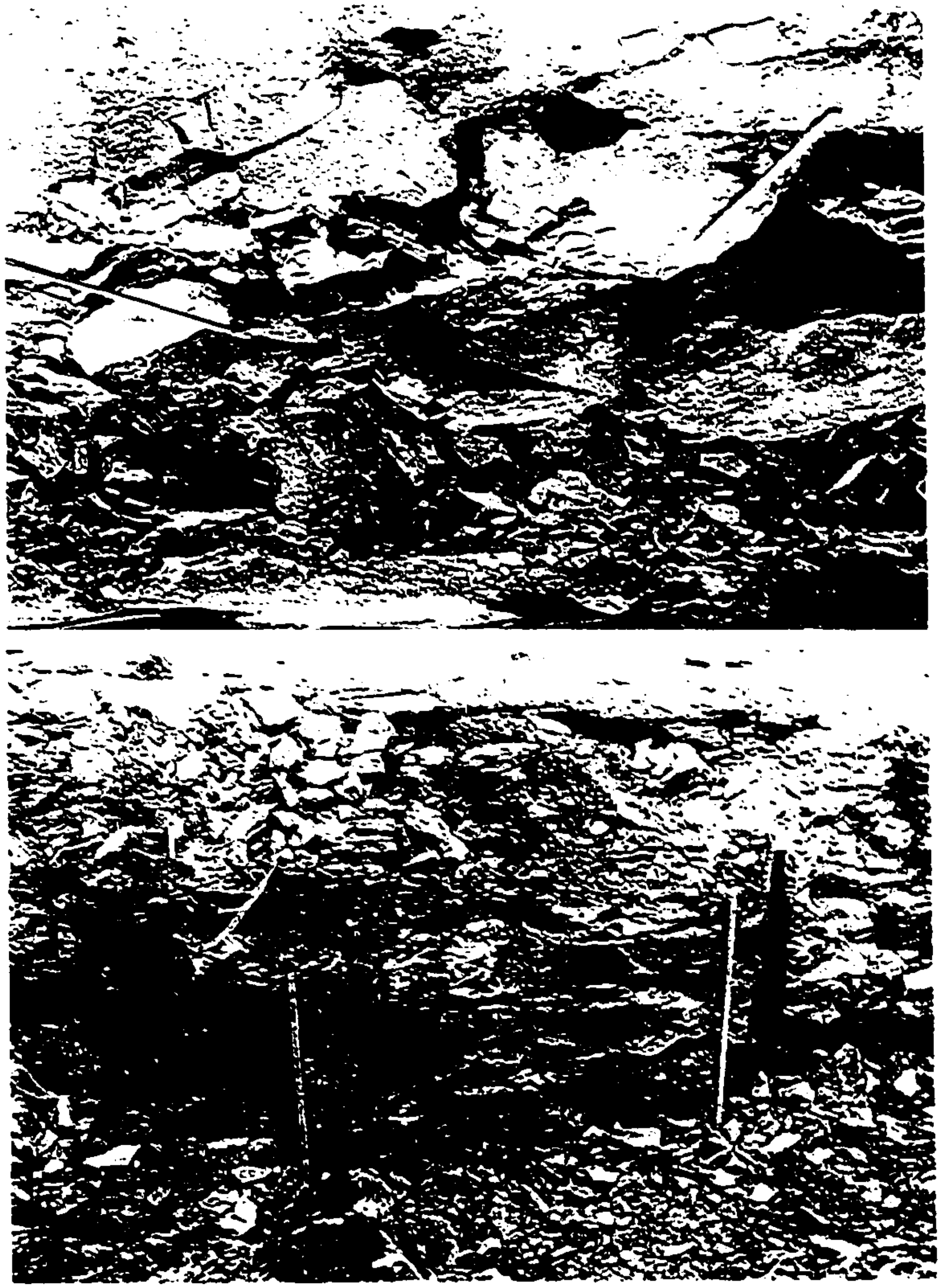

Figure 6.36 : Photographic result of the shot number 11 at Site 2.

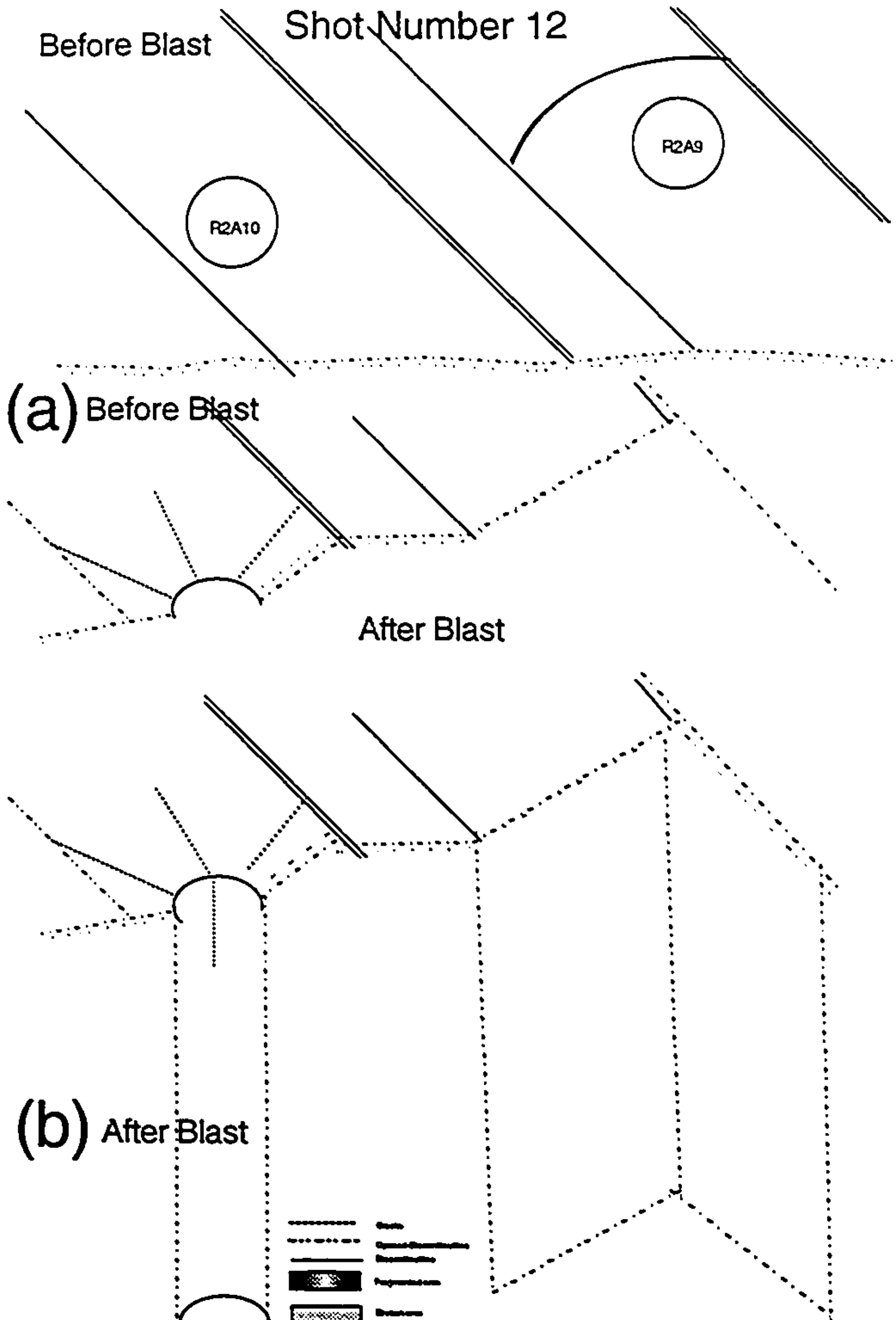

Figure 6.37 : Schematic layout and result of shot number 12 at Site 2. (32 mm dia. SUPERFRAC in 100 mm dia. holes, HCF = 40%)

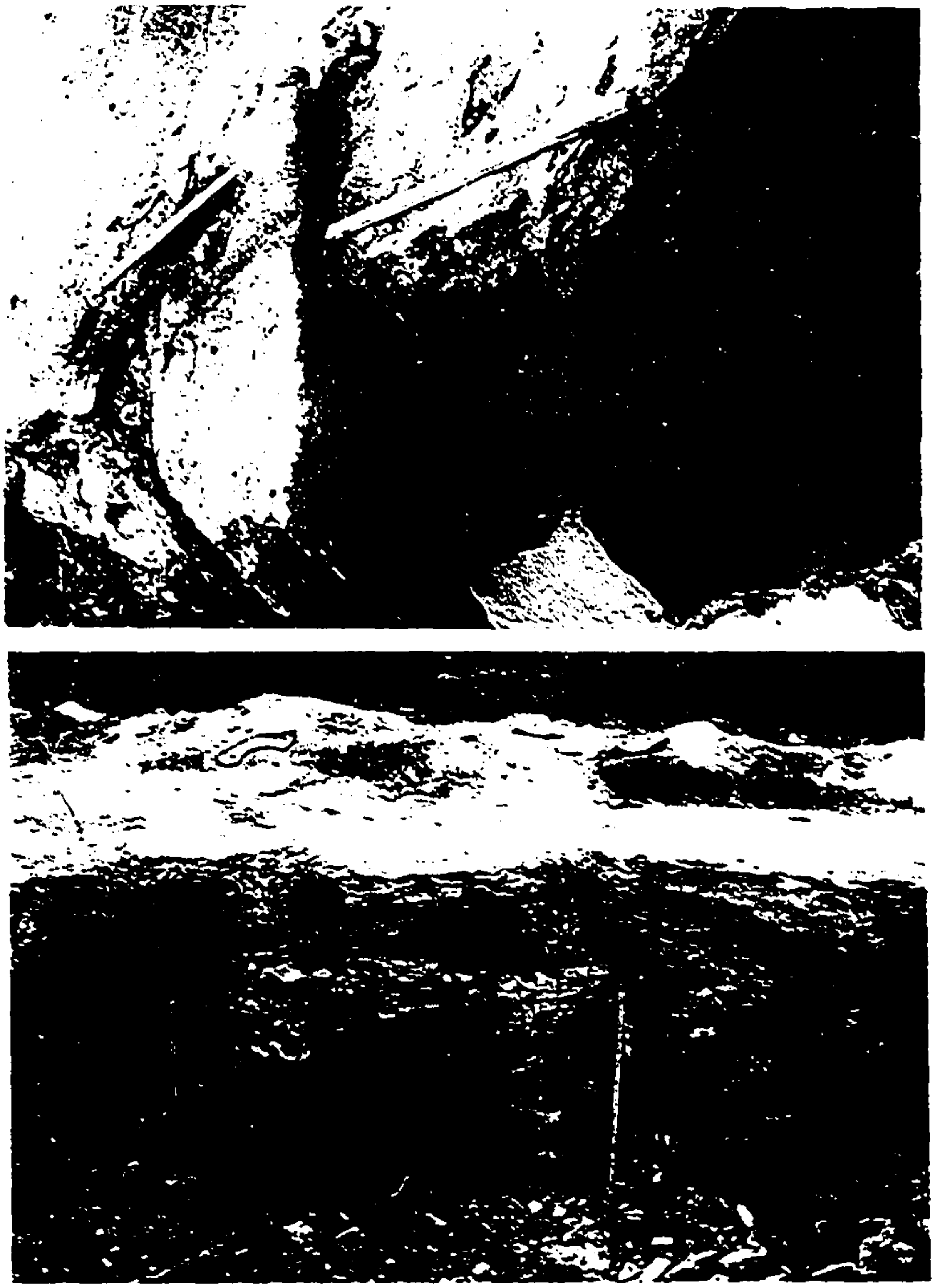

Figure 6.38 : Photographic result of shot number 12 at Site 2.

Table 6.11 : Characteristics of Shot number 12 at Site 1.

Shot No.	Burden	Spacing	Borehole Diameter	Charge Diameter	Decoupling Ratio	Type of Explosive
	(m)	(m)	(mm)	(mm)	-	
12	1.5	0.9	50	10	0.2	PRIMAFLEX
* All holes were 2 m in depth, and had a collar of 0.3 m.						

middle of the centreline. Two other discontinuities parallel to the centreline were located at the front and the back of the holes at distances equal to 7 and 2 times borehole diameter from the hole centre respectively (Fig. 6.39(a)). An inclined-discontinuity was located at the left side of the second hole and at 2 times borehole diameter. A fifth discontinuity which formed an angle of 35° with it, and was 4 times borehole diameter away from the centre of hole number P27 (Fig. 6.39(a)). The characteristics of the blasts are shown in Table 6.11.

6.3.4.2 Results and Discussion of the Blast number 12 at Site 1

The results are shown in figures 6.39(b) and 6.40. A fracture developed along the centre line between the holes. This could be due to the perpendicular discontinuity which was located approximately at the middle of spacing. However, the area between the boreholes wall and the nearest parallel discontinuity was badly fractured. In addition, an area between the hole P27 and the inclined-discontinuity on the left was also fractured. This region had a triangular shape.

It should be noted that all the distances between the discontinuities and the corresponding boreholes were smaller than the half-spacing. The exception to this was the parallel discontinuity much farther away, and as expected, was not affected by the blast. The rock was badly fractured between the holes and the nearest discontinuities

Table 6.12 : Characteristics of Shot number 13 at Site 2.

Shot No.	Burden	Spacing	Borehole Diameter	Charge Diameter	Decoupling Ratio	Type of explosive
	(m)	(m)	(mm)	(mm)	-	
13	1.0	2.0	100	32	0.32	SUPERFRAC
* All holes were 3 m in depth, and had a collar of 0.3 m in 100 mm holes and 0.6 m in 150 mm holes.						

(Figs. 6.39(b) and 6.40). In this blast, although a fracture developed along the centreline, the effective free face would not coincide with this fracture plane, but with the pre-existing parallel discontinuity.

6.3.4.3 Site Two (Finite Burden)

In this blast (shot # 13), a 4 mm wide weak plane was located between the second (R1A11) and the third holes (R1A12) (Fig. 6.41(a)). An open joint (2 mm wide), perpendicular to this weak plane was located at the middle of spacing between the second and the third holes, as shown. The hole R1A12 was also crossed by another weak plane, which started from the face and continued to the back of hole R1A12. The discontinuities and the blast geometry are shown in Fig. 6.41(a). The characteristics of the blast are shown in Table 6.12.

6.3.4.4 Results and Discussion of Blast number 13 at Site 2

The results of this blast are shown in figures 6.41(b) and 6.42. The fracture normal to the free face between holes R1A11 and R1A12 was largely unaffected in the back direction after the blast. A smooth wall was created between these two holes, which indicates that the discontinuity normal to the face and located at mid-point does not have any effect on the final results. The results obtained by numerical analysis confirm these

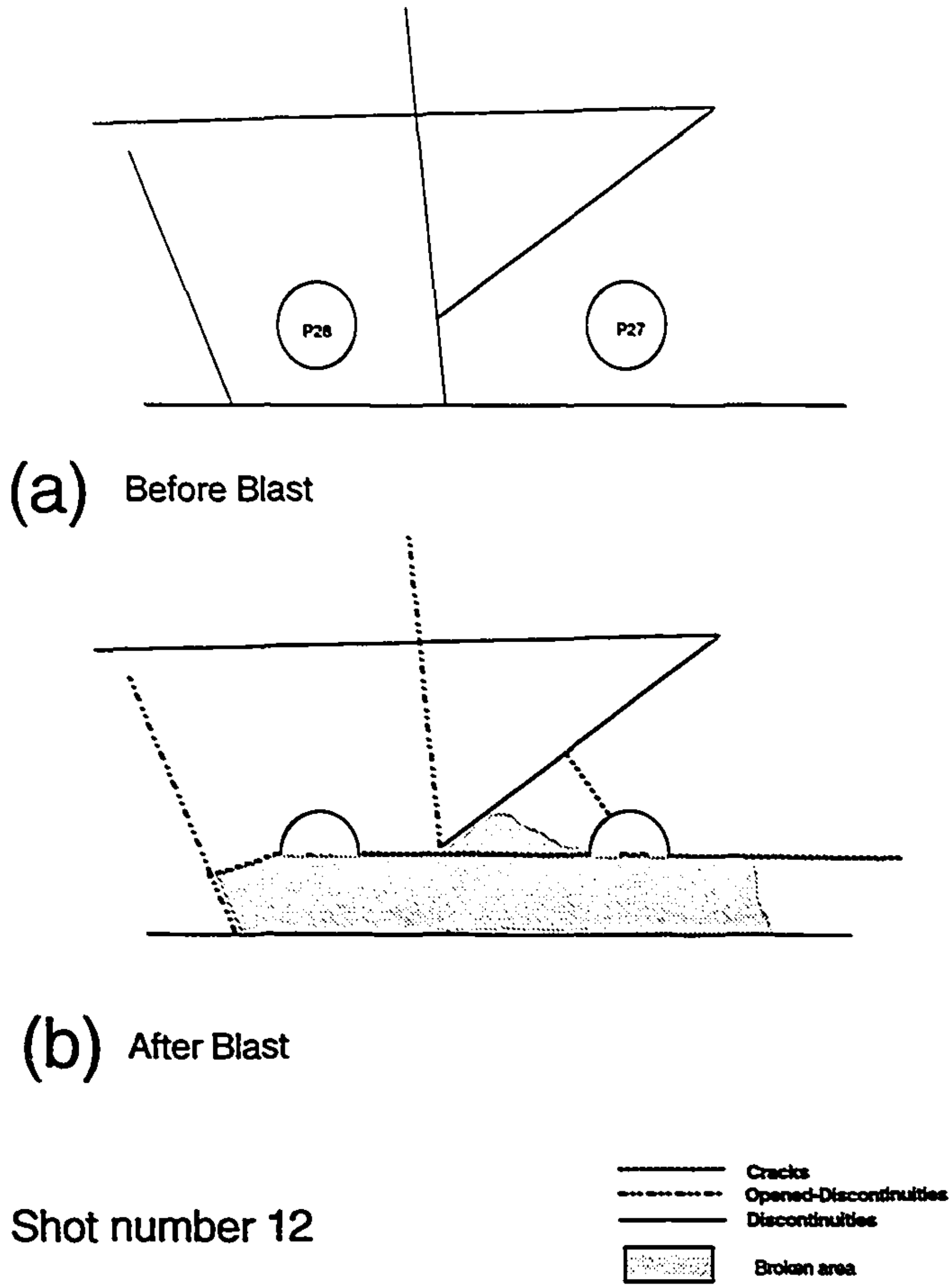

Figure 6.39 : Schematic layout and result of shot number 12 at Site 1. (PRIMAFLEX in 50 mm dia. holes)

Figure 6.40 : Photographic results of shot number 12 at Site 1.

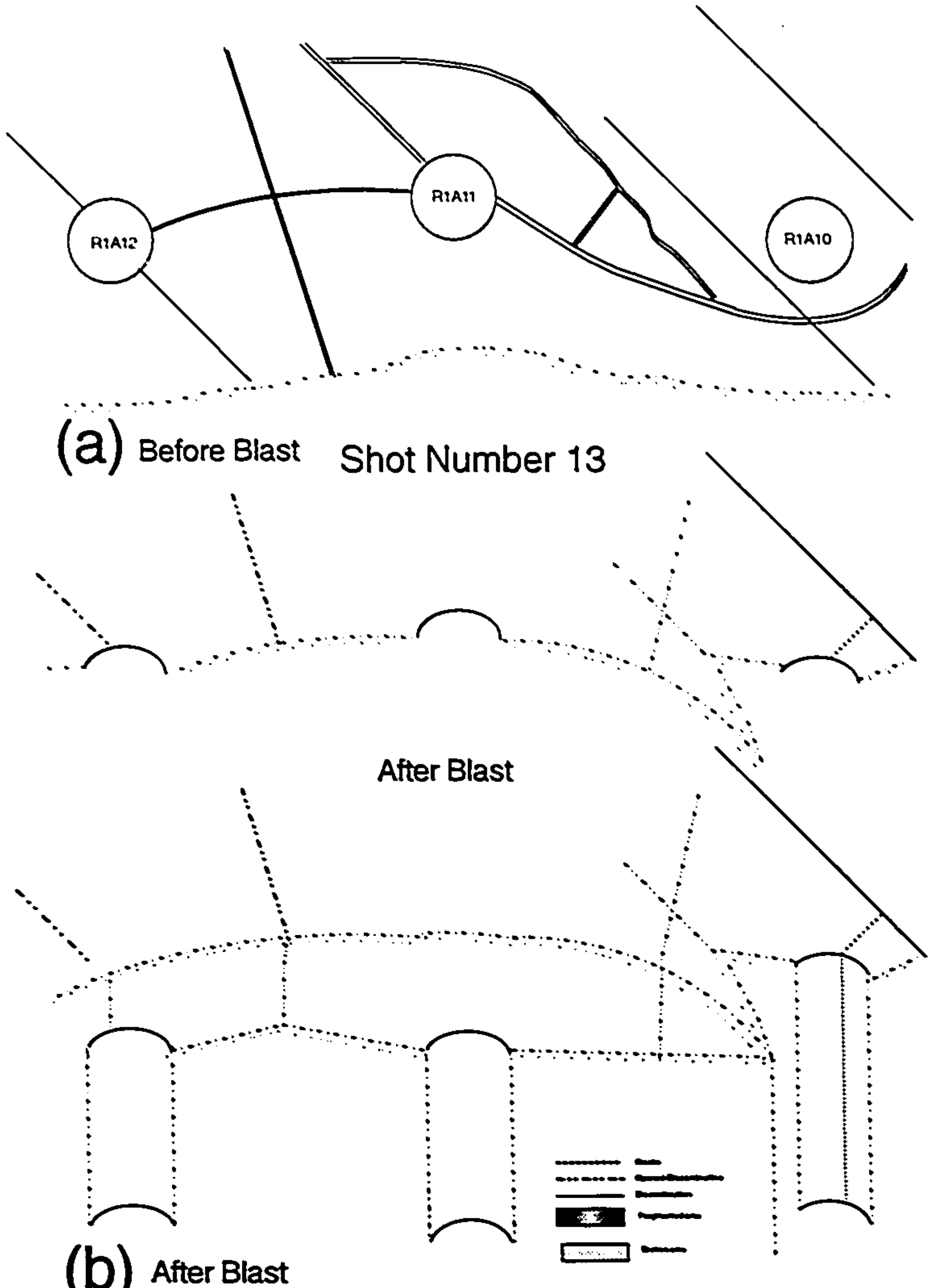

Figure 6.41 : Schematic layout and result of shot number 13 at Site 2. (32 mm dia. SUPERFRAC in 100 mm dia. holes, HCF = 68%)

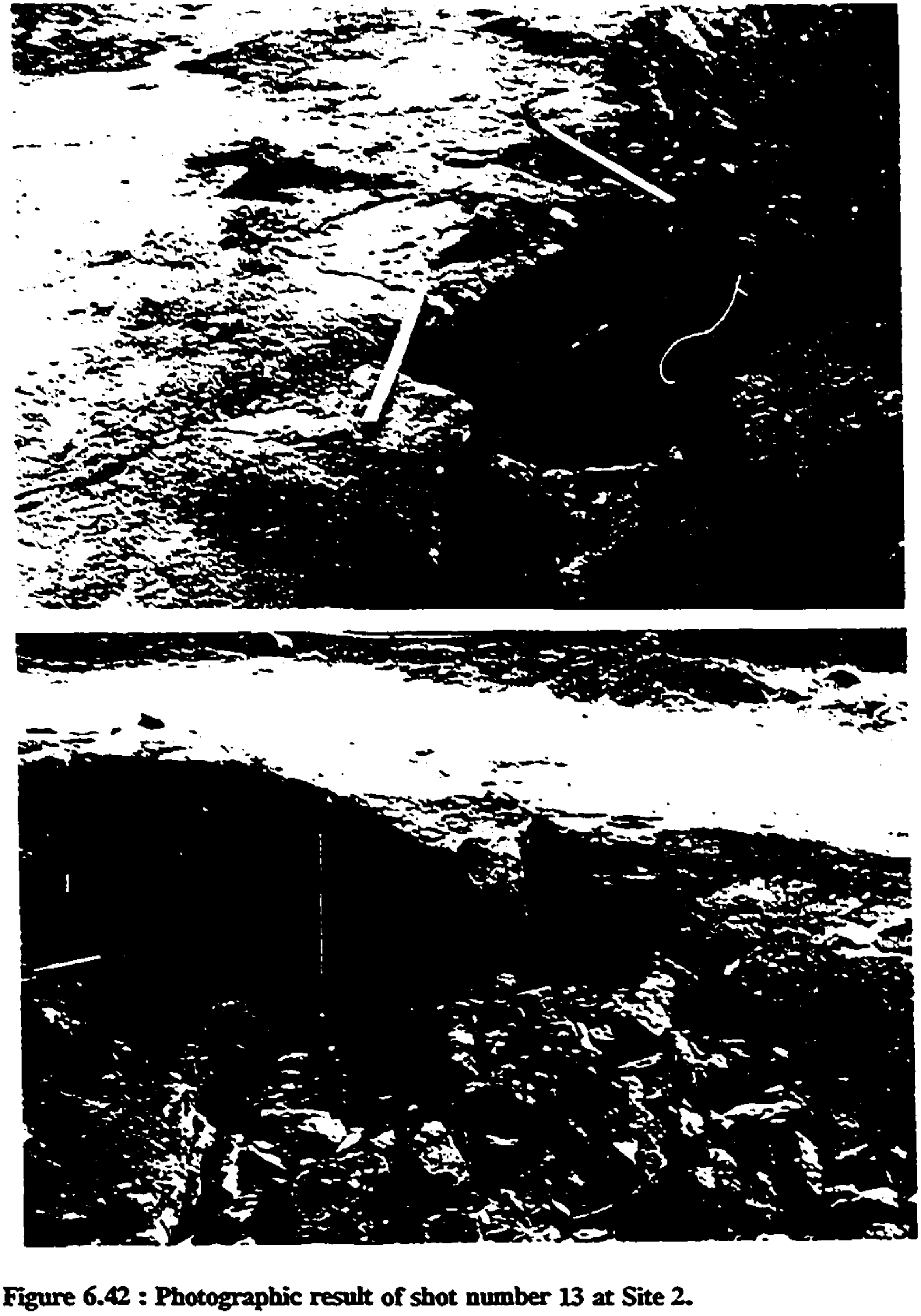

Figure 6.42 : Photographic result of shot number 13 at Site 2.

findings (see figure 5.29). The nature of fracture formation between R1A10 and R1A11 will be discussed in the following section with more complex alignment of pre-existing discontinuities.

6.3.5 Effect of Complex Discontinuity on the Fracture Formation

6.3.5.1 Site One (Infinite Burden)

The centreline between the hole P21 and hole P22, was crossed by two intersecting discontinuities as shown in figures 6.43, 6.44. These two met each other close to the hole P21 and formed angles of about 45° and 25° to the centreline. The holes P21 and P22 were located at distances of 1.5 and 2.5 times borehole diameter from the first discontinuity and 5 and 10 times borehole diameter from the second one respectively. Three additional inclined-discontinuities were also located around the holes. The nearest discontinuities to these were, 0.5 time borehole diameter from hole P21 and 1 and 3 times borehole diameter from hole P22 (Fig. 6.43(a)).

In blast # 14, the first hole P32 was drilled between the two foliations of rock. Their respective distances were about 1 and 3 times borehole diameter (Fig. 6.45(a). Another discontinuity crossed the hole and was approximately perpendicular to the foliations. The second hole (P33) was located between four parallel discontinuities with distances of 0.07 m, 0.15 m, and 0.25 m respectively. The hole was crossed by on of the discontinuities. The characteristics of the blasts are given in Table 6.13.

6.3.5.2 Results and Discussion of Blasts number 13 and 14 at Site 1

In shot # 13, the foliation located close to the borehole wall was opened by the products of the detonation. Three orthogonal cracks developed from hole P21 and the two discontinuities. The area between the boreholes and the nearest discontinuity was shattered, and the two intersecting discontinuities between the holes were opened to about

Table 6.13 : Charr :teristics of Shots number 13 and 14 at Site 1.

Shot No.	Burden	Spacing	Borehole Diameter	Charge Diameter	Decoupling Ratio	Type of Explosive
	(m)	(m)	(mm)	(mm)	-	
13	1.5	0.9	50	11	4.55	PRIMAFLEX
14	1.5	1.4	100	25	4.0	SUPERFRAC
* All holes were 2 m in depth, and had a collar of 0.3 m.						

6 times borehole diameter. The results show that the intensively fractured zone is found by two nearest discontinuities (Figs. 6.43(b) and 6.44).

The role of the multiple discontinuities around the holes was further investigated with shot # 14. In this case, fracture formation was controlled totally by the pre-existing fractures (Fig 6.45(a) and 6.46). Some shattered zone were however evident around each hole, but these were limited extent. As figures 6.45(b) and 6.46 show, no fracture along the centreline was formed in this case. The half holes were visible in the direction of the pre-exiting fractures.

6.3.5.3 Site Two (Finite Burden)

In this blast (shot # 14), an open fracture was located at the back of hole R1A9, and extended to the free face. At the centreline it was 1.2 m from hole R1A9 (Figs. 6.47(a) and 6.47). Another open fracture originated about 0.8 m from R1A8 near the centreline, and extended behind the hole. A third open fracture extended from the free face to the back of hole R1A8. It was also intersected by a closed joint to the left side of hole R1A8 at a distance of about 0.3 m (Fig. 6.47(a)). The characteristics of the blast are given in Table 6.14.

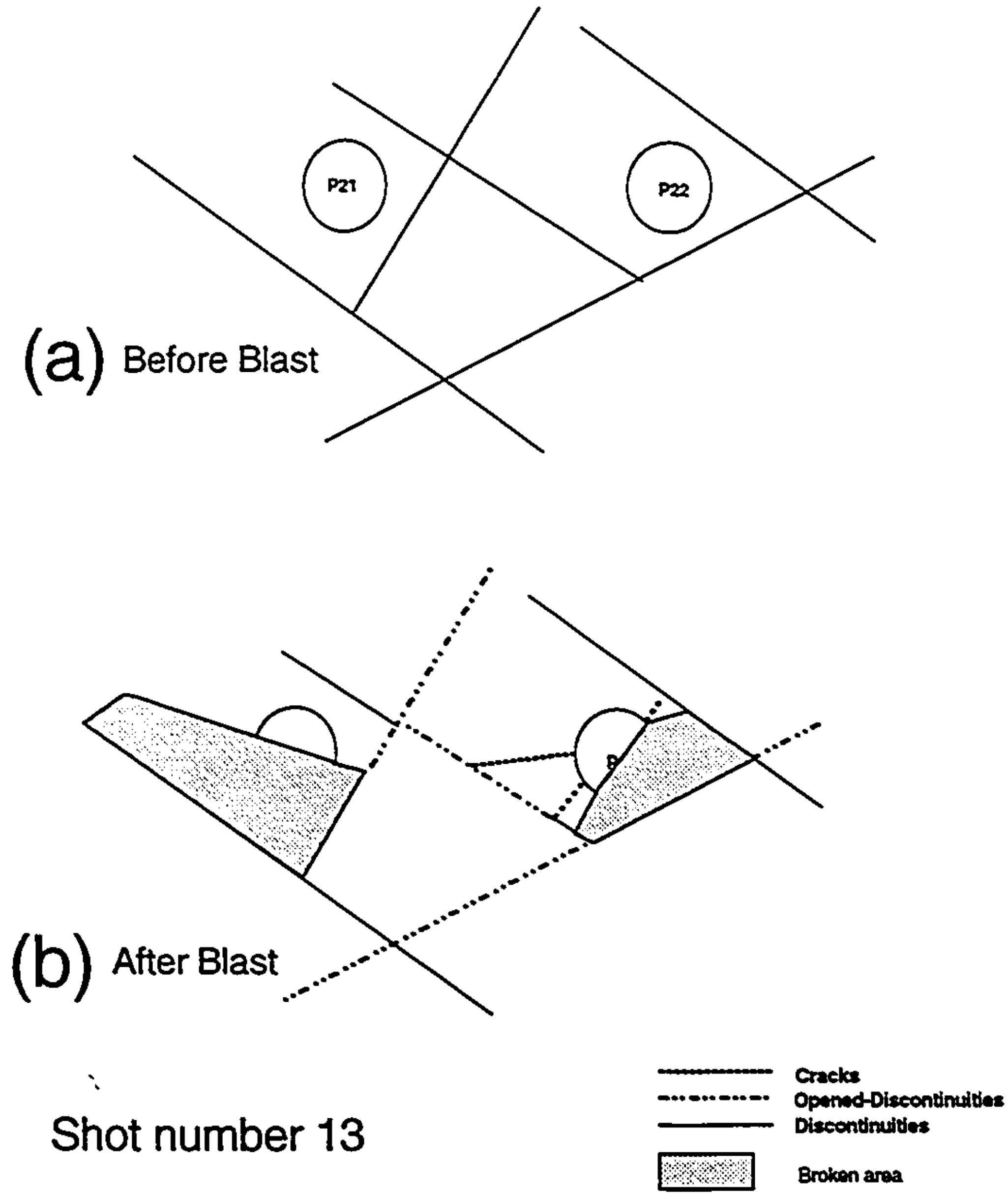

Figure 6.43 : Schematic layout and result of shot number 13 at Site 1. (PRIMAFLEX in 50 mm dia. holes)

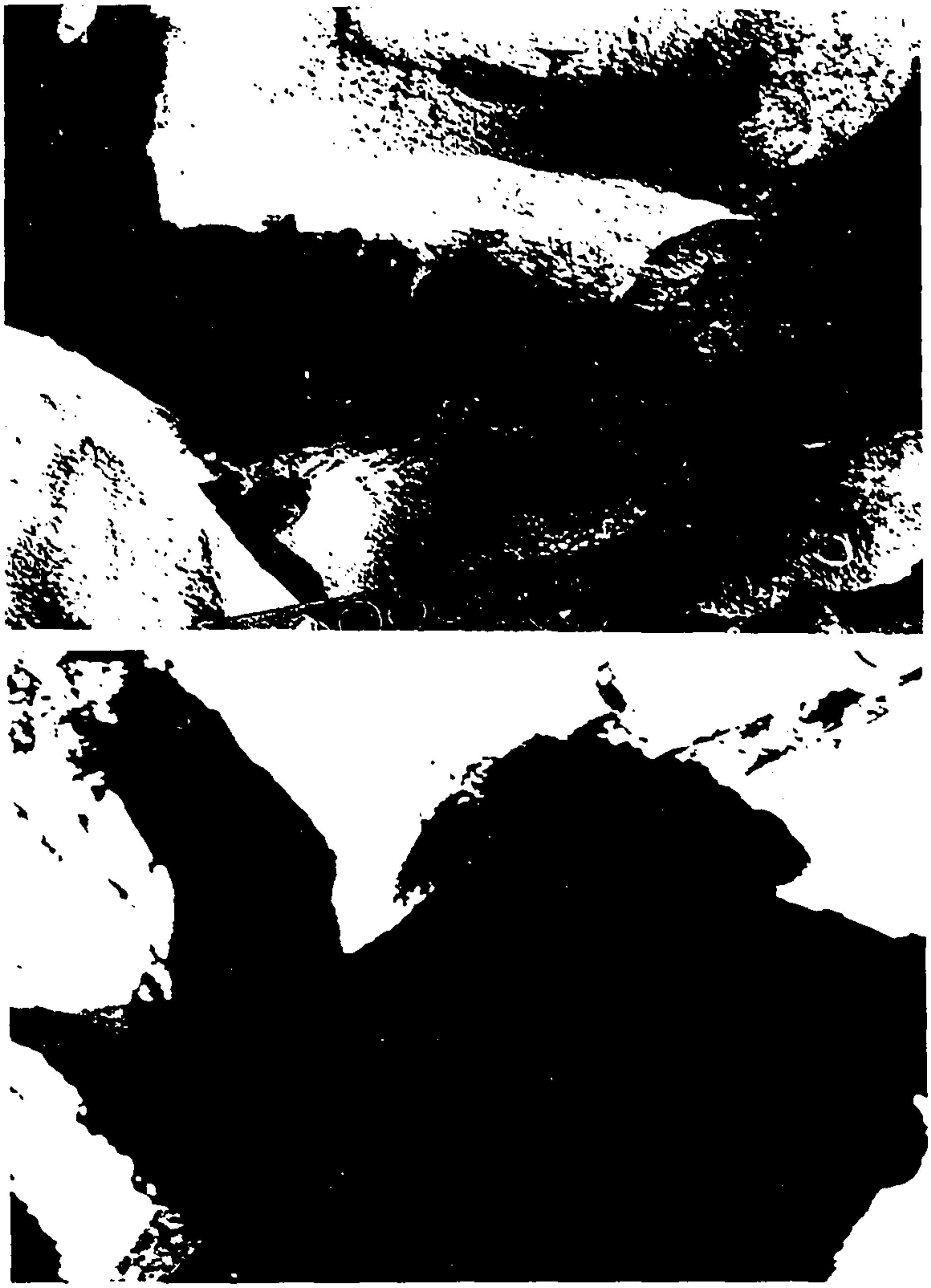

Figure 6.44 : Photographic result of shot number 13 at Site 1.

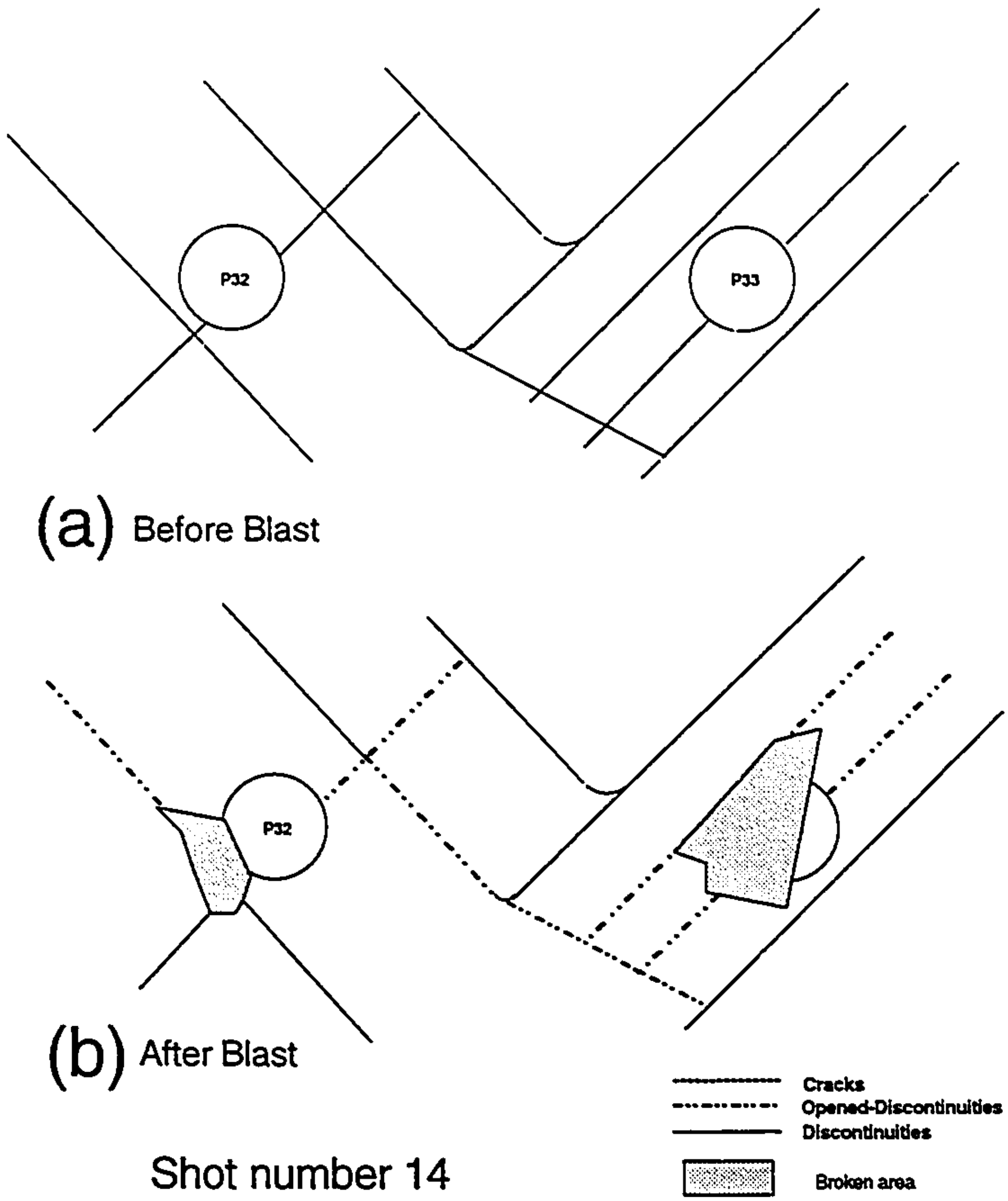

Figure 6.45 : Schematic layout and result of the shot number 14 at Site 1. (25 mm dia. SUPERFRAC in 100 mm dia. holes)

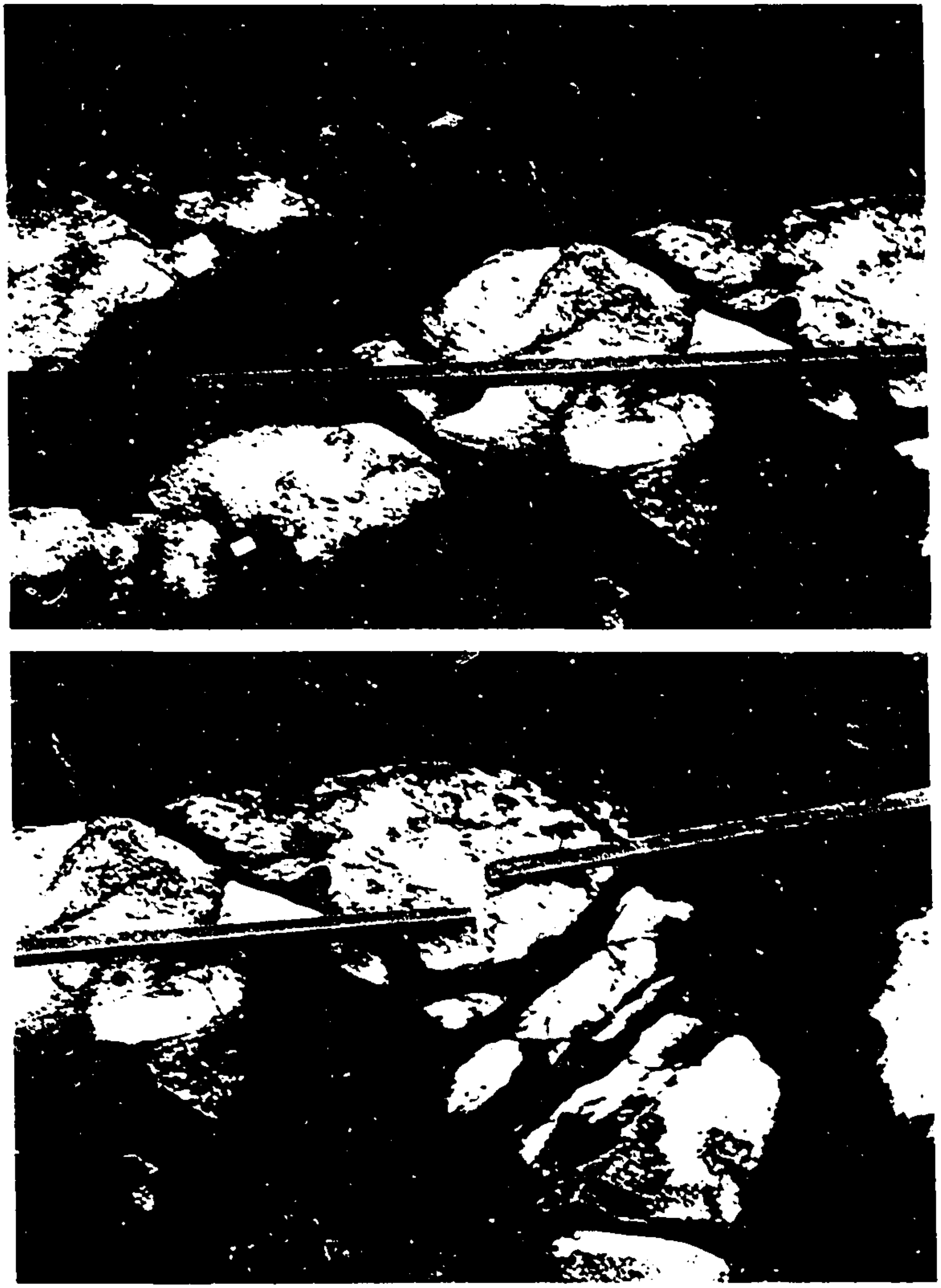

Figure 6.46 : Photographic result of shot number 14 at Site 1.

Table 6.14 : Characteristics of Shot number 14 at Site 2.

Shot No.	Burden	Spacing	Borehole Diameter	Charge Diameter	Decoupling Ratio	Type of Explosive
	(m)	(m)	(mm)	(mm)	-	
14	1.0	2.0	100	32	0.32	MAGNAFRAC
* All holes were 2 m in depth, and had a collar of 0.3 m.						

6.3.5.4 Results and Discussion of Blast Results at Site 2

In blast # 14, a zone bounded by the three open fractures around hole R1A8 was shattered and blasted out. The same applied to region around hole R1A8. No smooth face however, was formed along the centreline (Figs. 6.47(b) and 6.48).

It is instructive to analyze here the results of previous blast (shot # 13) with similar complex discontinuities (Fig 6.41(a). In this case, hole R1A10 was located between two parallel joints. The perpendicular distances between the left and right side of discontinuities with the centre of hole R1A10 were 3.5 and 2 the times borehole diameter, respectively. An open joint (7 mm wide) was located at the front of the hole; crossed two other joints before meeting hole R1A11. The characteristics of the blast are shown in Table 6.11.

The results obtained in blast # 13 (between R1A10 and A1R11) are essentially similar to that of shot # 14. All pre-existing fractures were opened at the back of the hole to a length of about 5 times borehole diameter, except the one which was normal to the face. However just as in blast # 14 the segment of rock in front of R1A10 was shattered and blasted out.

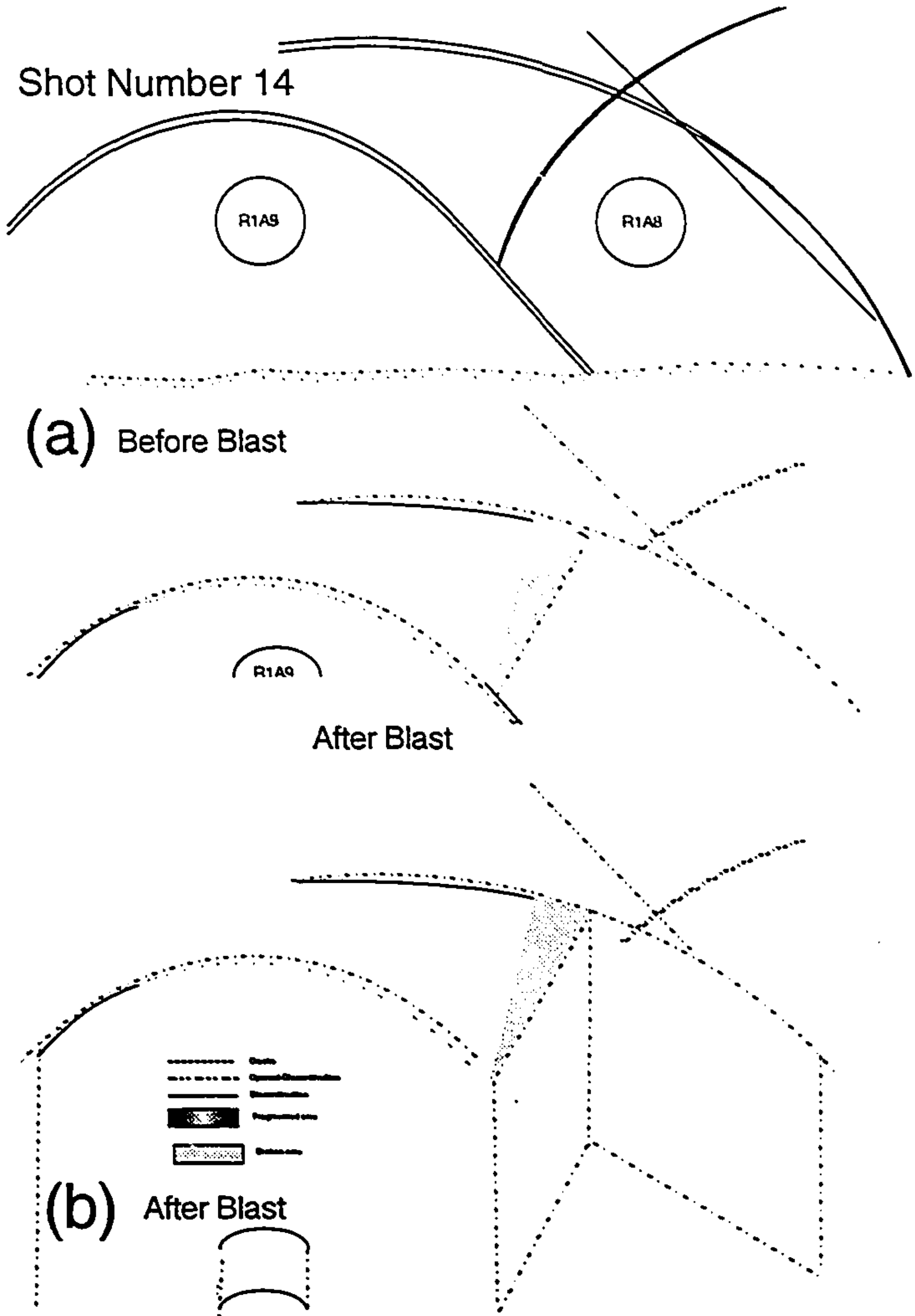

Figure 6.47 : Schematic layout and result of shot number 14 at Site 2. (32 mm dia. MAGNAFRAC in 100 mm dia. holes, HCF = 20%)

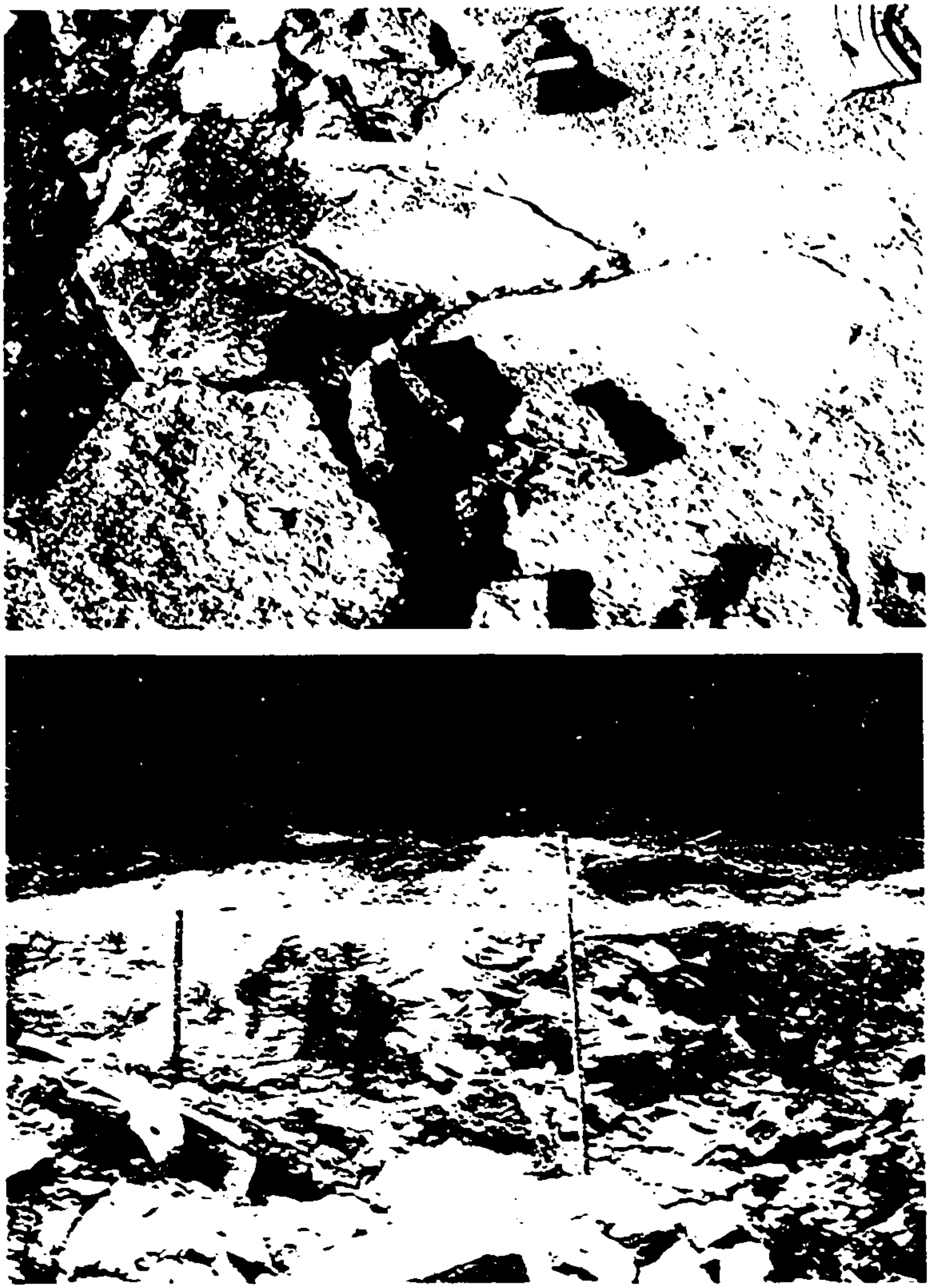

Figure 6.48 : Photographic result of shot number 14 at Site 2.

6.3.6 Effect of Inclined Discontinuity on Fracture Formation

6.3.6.1 Inclined Discontinuity Between Holes at Site Two (Finite Burden)

In this blast (shot # 15), All four joints were oriented at an angle of 45° to the face. Two of these crossed holes R2A3 and R2A4 (Fig 6.49(a). The other joints were 0.7 m and 0.3 m from holes R2A3 and R2A4 respectively.

In the next blast (shot # 16), there were similar parallel joints, except two of them were open, and only one crossed a hole (Fig. 6.51(a)). The joints flanking hole R3A6 were 0.2 m and 1.3 m away respectively. The corresponding distances for the two joints from hole R3A7 were 1.7 m and 0.5 m. The details of the blast are given in Table 6.15.

Table 6.15 : Characteristics of Shots number 15 and 16 at Site 2.

Shot No.	Burden	Spacing	Borehole Diameter	Charge Diameter	Decoupling Ratio	Type of Explosive
	(m)	(m)	(mm)	(mm)	-	
15	1.0	2.0	100	32	0.32	SUPERFRAC
16	1.5	3.0	150	50	0.33	MAGNAFRAC
* All holes were 3 m in depth, and had a collar of 0.3 m in 100 mm holes and 0.6 m in 150 mm holes.						

6.3.6.2 Results and Discussion of Blasts Number 15 and 16 at Site 2

In shot # 15, the cracks developed from the boreholes perpendicular to the discontinuity. The latter was opened up further and the rock mass around both R2A3 and R2A4 was shattered and blasted out. This resulted in an irregular face, with Z-shape fracture outlines, visible to a depth 0.5 m from surface. This coincided with the depth, to which joints were opened by the weathering (Figs. 6.49(b) and 6.50).

In the next blast (shot # 16), two cracks which were nearly perpendicular to the

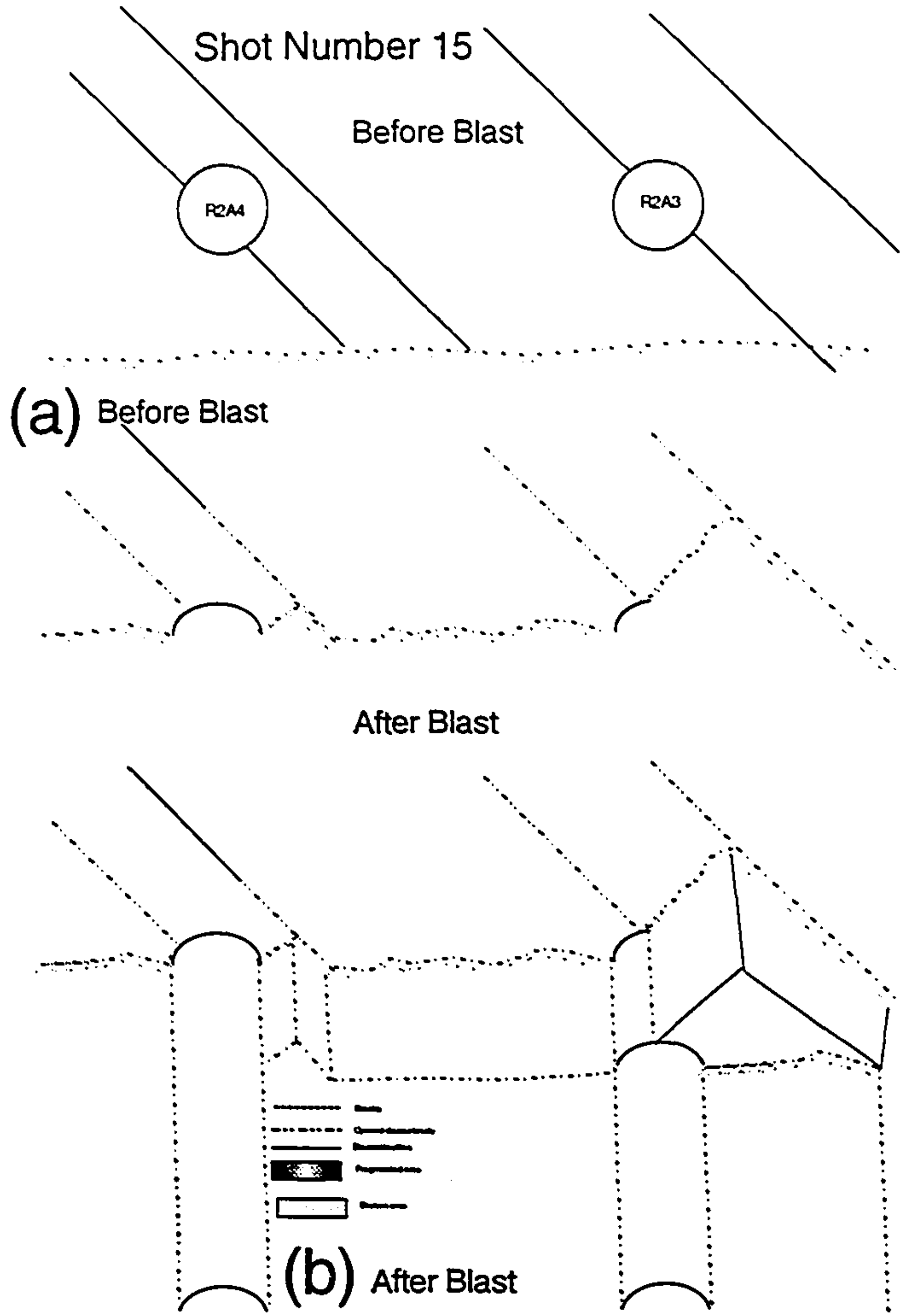

**Figure 6.49 : Schematic layout and result of shot number 15 at Site 2.
(32 mm dia. SUPERFRAC in 100 mm dia. holes, HCF = 90%)**

Figure 6.50 : Photographic result of shot number 15 at Site 2.

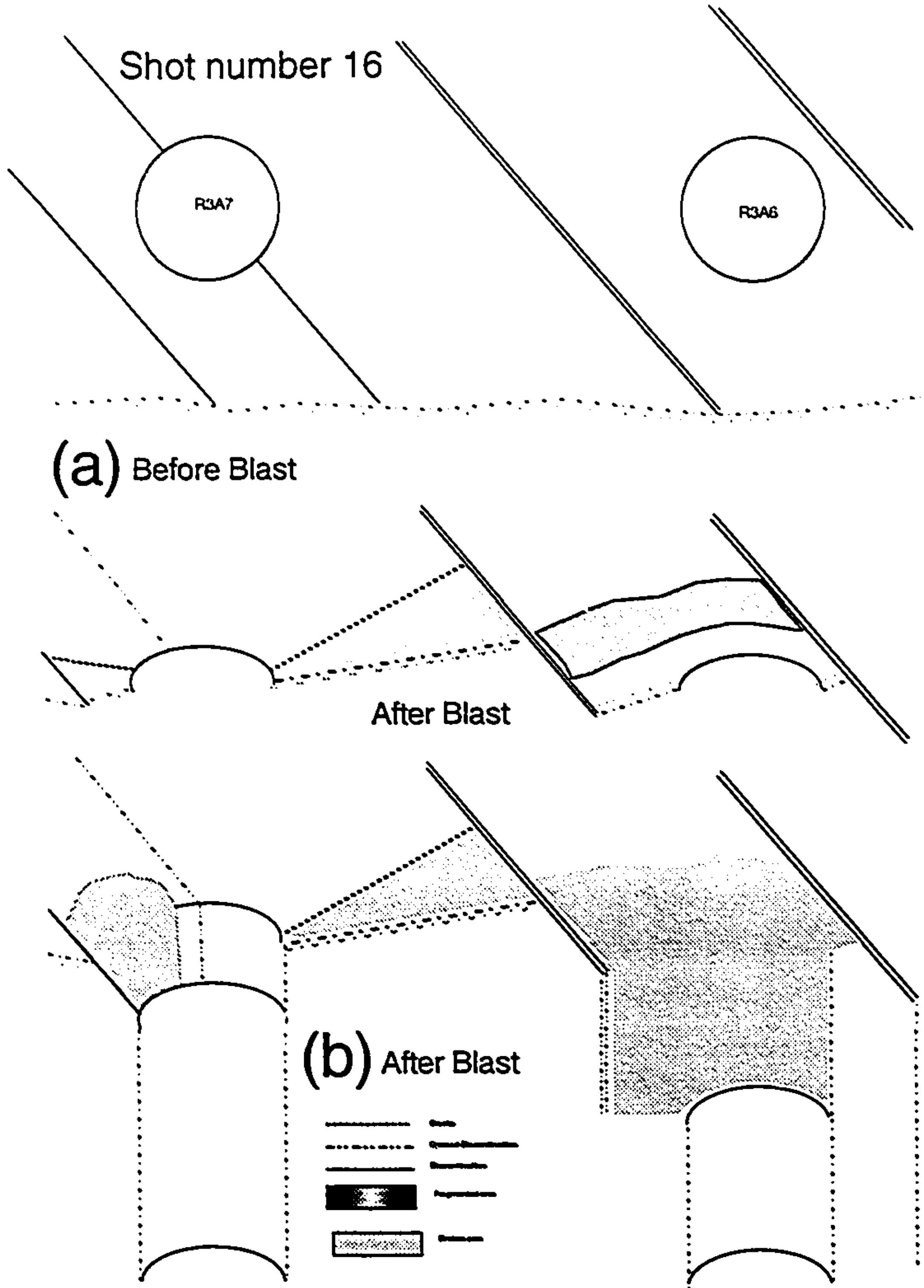

Figure 6.51 : Schematic layout and result of shot number 16 at Site 2. (32 mm dia. MAGNAFRAC in 100 mm dia. holes, HCF = 64%)

Figure 6.52 : Photographic result of shot number 16 at Site 2.

joint between the holes were formed. This also resulted is the same Z-shaped outline, extending up to 1 m below the surface. Shattering of rock was confined to the area between hole R3A7 and the discontinuity, as expected. A small area between the discontinuity which crossed hole R3A7 and the pre-existing fracture, was also shattered. Only a quarter of the hole was visible to 0.5 m depth below the surface (Figs. 6.51(b) and 6.52).

6.3.6.3 Inclined Discontinuity Outside of Two Holes at Site 2 (Finite Burden)

In this test (shot # 17), the first discontinuity was located at the left side of hole number R2A1 at a distance of about 0.8 meters. This joint was opened by weathering or previous shots to about 0.5 m below the surface. The other discontinuity was located at the right side of the second hole (R2A2) and was approximately 0.5 m away (Fig. 6.53(a)). The spacing between the two holes was 2 m and was clear of discontinuities between them. The characteristics of the blast are shown in Table 6.16.

6.3.6.4 Results and Discussion of Blast Results at Site 2

In shot # 17, two parallel discontinuities were located at the left and the right sides of the first and second holes, respectively. No pre-existing fracture was visible between the holes. After blast, a fracture developed normal to the discontinuity from the first hole. The distance of this joint from the hole centre was about 7 times borehole diameter (less than the half spacing), (Figs. 6.53(b) and 6.54). The distance of the other discontinuity from the second hole (R2A2) was about 12 times borehole diameter (larger than the half spacing). As the figures show, it had little effect on the blast result. A hump remained between the holes up to a depth of 0.7 m below the surface, similar to shot # 6. This could be due to the presence of a shallow open-discontinuity close to the borehole wall which resulted is lower pressure at the other side of the holes. Below this depth

Table 6.16 : Characteristics of Shot number 17 at Site 2.

Shot No.	Burden	Spacing	Borehole Diameter	Charge Diameter	Decoupling Ratio	Type of Explosive
	(m)	(m)	(mm)	(mm)	-	
17	1.0	2.0	100	32	0.32	MAGNAFRAC
* All holes were 3 m in depth, and had a collar of 0.3 m in 100 holes mm and 0.6 m in 150 mm holes.						

there was no hump visible between the holes, and the half hole was clearly visible on the face.

In shot # 11, an extensively fractured zone also developed between the second hole (R2A6) and the nearest (2 times borehole diameter from the centre of the hole) discontinuity at the right side of the hole. This joint was opened up to a depth of 3 m below the surface, and the half cast of the second hole was absent throughout this depth (Figs. 6.35(b) and 6.36). As the figures show, a fractured zone is also visible between the first hole and the discontinuity which is located at left side of the hole.

6.3.7 Effect of Intersecting Discontinuity with Holes on Fracture Formation

6.3.7.1 Site Two (Finite Burden)

In this blast (shot number 18), in addition to the presence of a weak plane at the front of the holes, four parallel joints inclined at an angle of about 45° to the face were located at the side of the holes. The first and the fourth one with distances equal to 1.0 m and 0.5 m were located at the left side of the first hole (R2A7) and at the right side of the second hole (R2A8), respectively. The first hole was crossed by one of the discontinuities and the other one was tangential to the wall of the second borehole. The relationship between the blast geometry and the discontinuities is illustrated in figure 6.55(a). Table 6.17 presents the characteristic of the blast.

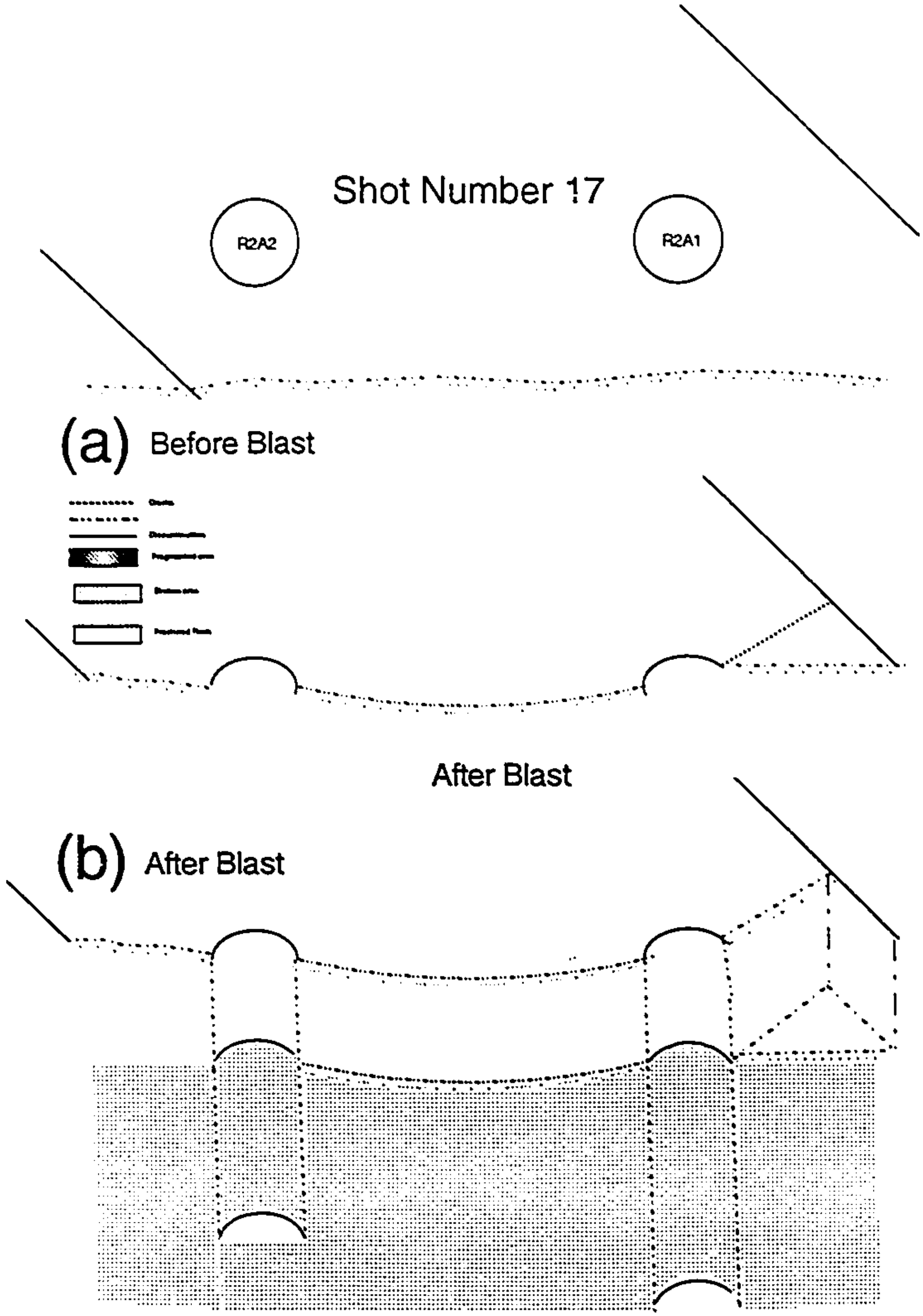

Figure 6.53 : Schematic layout and result of shot number 17 at Site 2. (32 mm dia. MAGNAFRAC in 100 mm dia. holes, HCF = 80%)

Figure 6.54 : Photographic result of shot number 17 at Site 2.

Table 6.17 : Characteristics of Shot number 18 at Site 2.

Shot No.	Burden	Spacing	Borehole Diameter	Charge Diameter	Decoupling Ratio	Type of Explosive
	(m)	(m)	(mm)	(mm)	-	
18	1.0	2.0	100	32	0.32	MAGNAFRAC
* All holes were 3 m in depth, and had a collar of 0.3 m in 100 mm holes and 0.6 m in 150 mm holes.						

6.3.7.2 Results and Discussion of Blast Results at Site 2

The intersecting joint at hole R2A7 in shot # 16, was opened up further after the blast to a distance of about 10 times borehole diameter. The rock was broken at the front of the first hole (R2A7), and at the left side of the hole to the discontinuity which was located at 6 times borehole diameter. As figure 6.56 shows, the resulting fracture was normal to the discontinuity at the left side of the hole. A crack also developed from the wall of discontinuity behind that to the other discontinuity which was crossed by the second hole. A fractured zone resulted at the back of the holes to a distance of about 5 times borehole diameter, due to this fracture. Despite this backbreak, the half barrels of the holes were completely visible after the blast (Figs. 6.55(b) and 6.56).

6.4 COMPARISON BETWEEN EXPERIMENTAL RESULTS AND THEORETICAL PREDICTION

In normal blasting fragmentation of rock by explosives proceeds in three stages. In the first, fracturing occurs at and near the borehole wall, due to compressive (radial) stresses associated with the detonation pressure in the borehole. This is followed by fracturation around the borehole due to propagating shock waves in rock. In the last stage, the initial fractures are further opened up and extended by the borehole pressure. Penetration of the high pressure explosion gases into the cracks plays a major role in

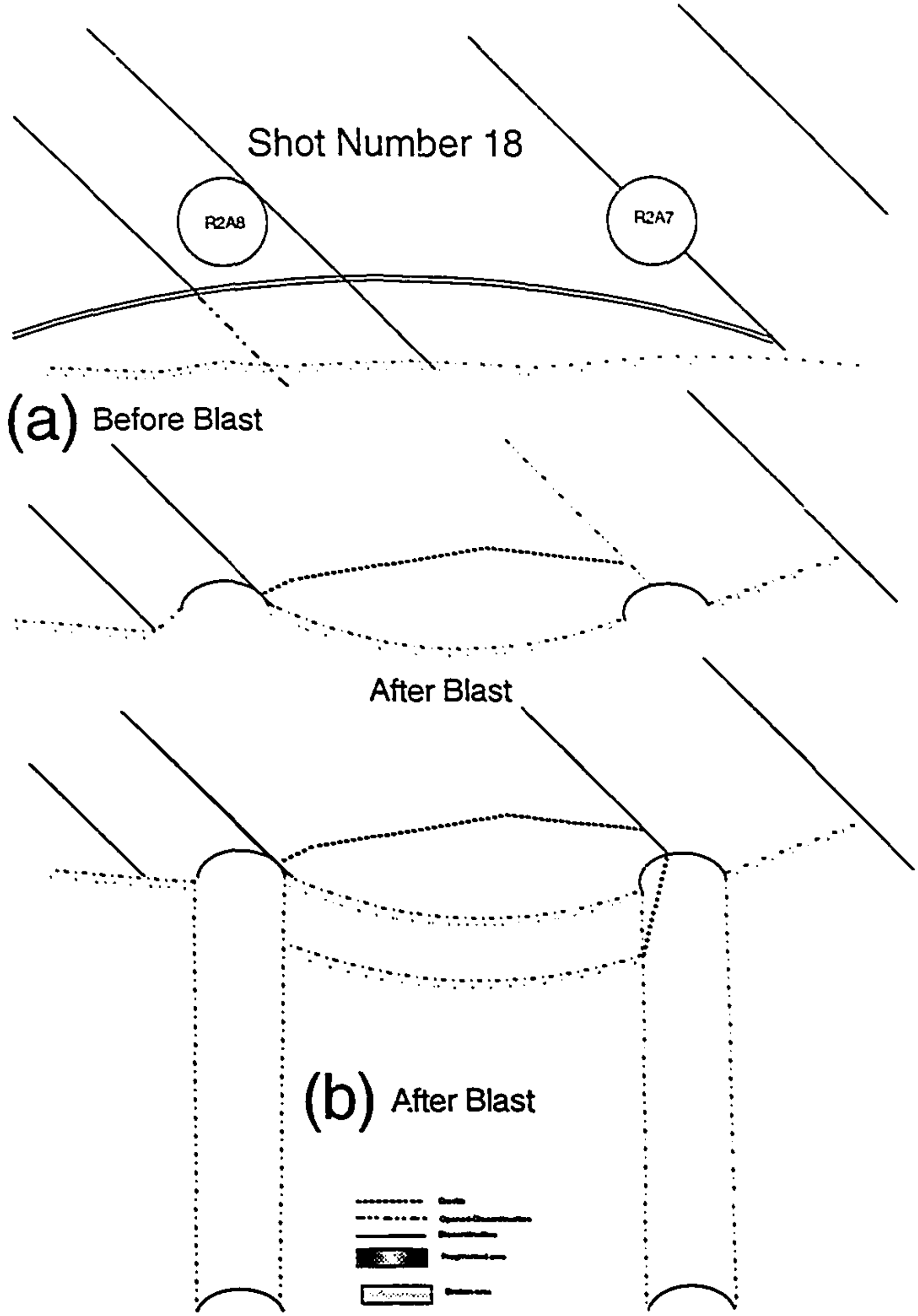

Figure 6.55 : Schematic layout and result of shot number 18 at Site 2. (32 mm dia. MAGNAFRAC in 100 mm dia. holes, HCF = 90%)

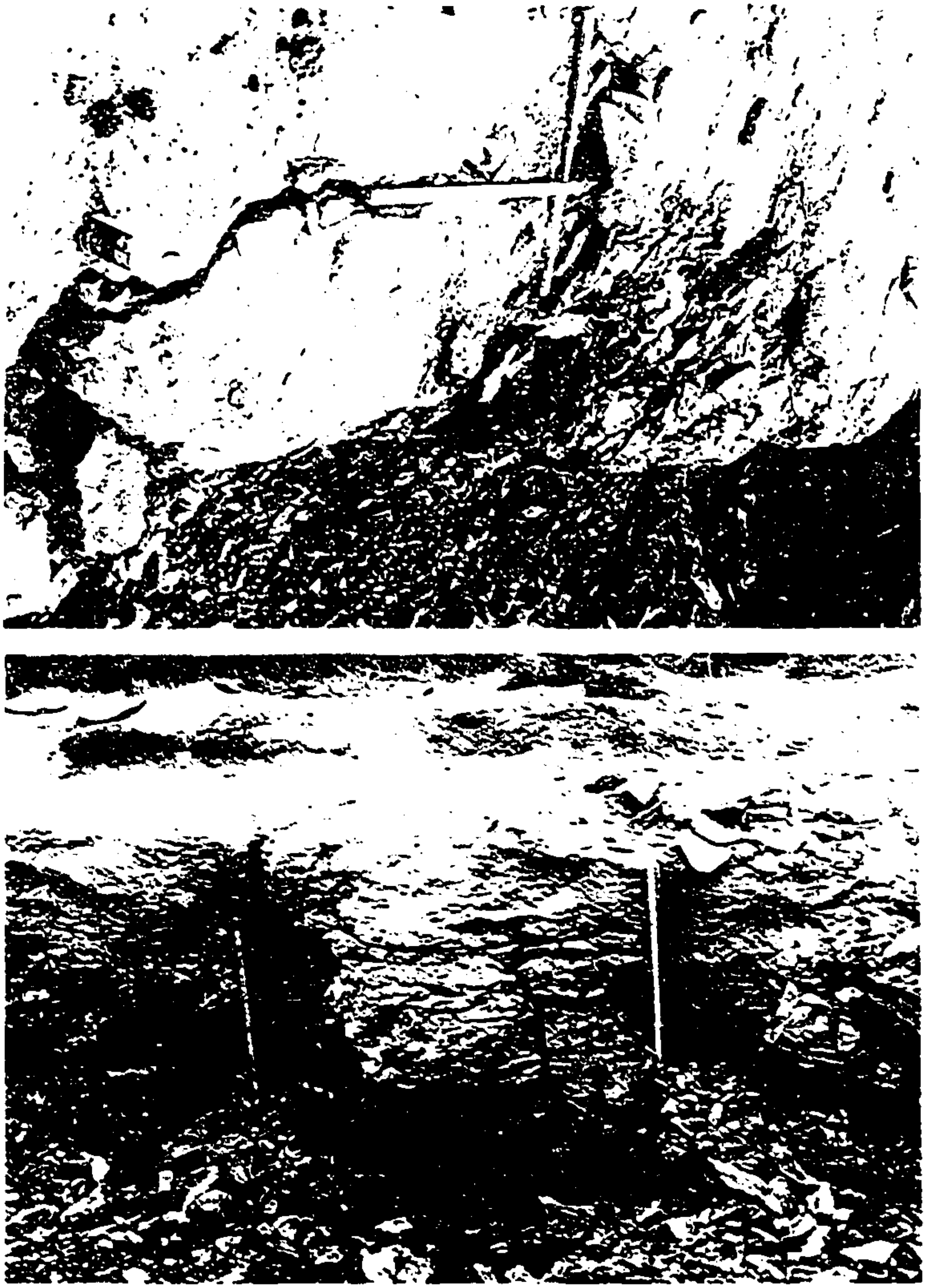

Figure 6.56 : Photographic result of shot number 18 at Site 2.

multiplication and extension of fracture in this later stage of the blasting process.

In wall control blasting technique, the aim is to eliminate or minimize the first two stages of fragmentation. This is accomplished by suitable choice of low-detonation pressure explosives or by appropriate decoupling of explosive column in the borehole. Therefore, the quasi-static pressure (borehole pressure) will be mainly responsible for creating a smooth and clean fracture plane between the holes. The charge diameter should be reduced to that the effective borehole pressure is not much higher than the compressive strength of the rock. This would prevent crushing of rock in the borehole wall. It requires a much lower level of pressure to extend an existing crack than creating a new one and explosion gases penetrating into crack tips provide the best means to achieve it. However, it is still prudent to generate sufficient borehole pressure to enable tensile crack onset at the midpoint between holes. The numerical models employed in this study can not be used to predict the effect of gas penetration into the crack tips.

As the results of the first test series at Site 1 show, a burden larger than 1.4 times spacing could be considered infinite. The results of the numerical analysis for two different spacings (10 and 15 times borehole diameter) also predicted that the difference in stress distribution in the burden region at these distances for the same spacing is negligible (Figs. 5.17, a and b). In the absence of a free face, the optimum spacing for a suitable charge diameter could be between 12 to 18 times borehole diameter (depending on the tensile strength of rock) in an intact and homogenous rock. This range would have change in an inhomogeneous rock mass, depending on the characteristics of discontinuities and the properties of the rock mass.

The presence of any type of nearby discontinuity either parallel or inclined to the face, causes a shattered area between the wall of the boreholes and the discontinuities. The effective blast face would then coincide with the discontinuity. The degree of fracturation would greatly depends on the distance of the discontinuity from the borehole as well as its width.

The theoretical analysis predicts that a weak plane perpendicular to the centreline at the middle of spacing does not have any effect on the blast result. As shown in the experimental part, the influence of such discontinuities to the final face on the blast result is negligible.

In the experimental investigation it was shown that, as the width of the discontinuities increased the number of cracks which developed from the hole to the discontinuity aiso increased. A weak plane wider than 60 mm, which is filled with the gouge material, plays a role similar to a free face. Figure 6.34 clearly shows the influence of the width of pre-existing fracture on crack formation. The rock is fragmented below the surface to the depth of that the discontinuity had been opened before blasting. This is accordance with the theoretical predictions (Fig. 5.16).

The presence of an discontinuity which is oriented at an angle to the centreline between the holes results in the formation of triangular fracture zone between it and the borehole, the final face assumes roughly a Z-shape. The results obtained by numerical analysis predict the same results as the field investigation (Fig. 5.25).

New fractures seldom cross a pre-existing open fracture or weak plane. The latter normal acts as a fracture terminator. Further lengthening of pre-existing fractures depends on the distance of the plane from the borehole wall and the properties of the filled material. In a few cases, where the width of the discontinuity is less than 5 mm, the penetration of the gases inside the discontinuity causes a wedging action on the wall of the fracture and creates a tensile stress zone behind the wall of discontinuity. If this stress is strong enough (i.e. greater than the tensile stress of rock), a second fracture could be developed at the other side of the discontinuity.

6.5 CONCLUSION

A compressive study was made to analyze formation of the cracks around single holes and between two or three simultaneously detonated holes. The effect of pre-existing fractures and the influence of blast geometry upon resulting fracture zone and on the final face were studied experimentally. Three types of explosives with several cartridge diameters were used. The experiments involved three different borehole diameters at two different sites, with characteristically different rock types. Several single-, double-and triple-hole system, were detonated to analyze the effects of conditions of discontinuity on the blast results. The tests were conducted under both infinite and finite burdens.

To minimize borehole crushing and significant overbreak, the magnitude of the pressure on the borehole wall should be reduced. It should be lower than the compressive strength but substantially higher than the tensile strength of the rock. For a given rock mass and a borehole diameter, charge decoupling, spacing and burden should be chosen based on the properties of the rock mass and the nature of existing structural discontinuities.

For a successful blast in an intact rock, the spacing between the holes could be greater than twice the length of the longest crack which is obtained for a single hole. In the presence of discontinuities around single or multiple holes, resulting fracture characteristics would depend strongly on the characteristics of the former, including its orientation with respect of blast geometry.

Fracture propagation depends largely on the type of explosive employed, decoupling ratio, and the blast geometry, in addition to the properties of the rock mass. In all wall-control blasting methods this ratio should be smaller than 0.5, because the detonation velocity of most explosives ranges from 4000 m/s to 5500 m/s, and a charge diameter equal to even half borehole diameter results in extremely high level of stress on the borehole wall. A suitable decoupling ratio for wall-control blasting would generally be between 0.2 and 0.3 for pre-splitting (infinite burden) and between 0.3 and 0.4 in the case of a blast with a free face.

In the absence of a free face, (i.e. pre-split blasting: infinite burden) the best result would be obtained by a small borehole diameter (about 75 mm) and hole spacing of about 10 to 15 times the borehole diameter, and preferably the former. In the presence of a free face, the pressure inside the hole must be greater than in the earlier case, because in addition to developing a fracture zone between the holes, the rock must be broken in the burden region. The burden can be equal to 10 times the borehole diameter with a spacing ranging between 15 to 20 times the borehole diameter.

The fractures are initiated at the borehole wall by the shock wave and extended around or between the holes by the pressure exerted by the expanding explosion gasses in the borehole wall. For typical decoupling conditions, the pressure at the midpoint between the holes does not have sufficient amplitude to cause onset of a new crack at this location. It has been clearly shown that the pressure on the borehole wall is much greater than those at any other points, especially at the midpoint between the holes.

Any discontinuities lying parallel to the final face at the back of the holes leads to development of very high stresses between it and the boreholes, and produces a shattered area in this region. The degree of fracturation depends on the distance of the discontinuity from the borehole, but the final face most likely coincide with discontinuity itself, rather than intended free face. Pre-existing fractures located at the front of the holes, on the other hand, lead to generate overbreak and create a hump between the holes. The minimum distance between the parallel discontinuity at the back direction and the boreholes should be at least half spacing, for the former to have negligible effect on the blast results. This of course applies only to a 'closed' discontinuity. Any 'open' discontinuity with a wide larger than 50 mm effectively behaves like a free face. Conversely, no damage zone was visible for a discontinuity perpendicular to the centreline at the midpoint.

As the angle of the discontinuity with the design face decreases from 90°, the area of the damage zone between the holes and the discontinuity increases, and the shape of the final wall changes from a smooth face to a zagged or nearly Z-shape. The area of the damage zone is greater than that predicted by numerical analysis, as expected. This is due to explosive gas action on pre-existing fractures.

A closed-discontinuity or an opened-discontinuity cemented by filling materials has a little effect on the results of the blast. In contrast, an open discontinuity filled with gauge or low strength materials has significant effect on the blast results. It normally leads to increased damaged area. An open discontinuity 50 mm wide or more plays a role similar to a free face.

The length and the width of the opening depends on the distance of the discontinuity from the blasthole as well as the width of the discontinuity before the blast. In some cases, a pre-existing fracture is opened up to a distance of about 15 times the borehole diameter.

Penetration of the explosive gases into pre-existing fractures can create secondary fractures behind the wall of the discontinuity. This phenomenon depends on the width of the discontinuity and the pressure amount of the explosive gases. This is the reason that the extent of damage zone is greater than that of predicted by numerical analysis.

The results of the field investigation are in good agreement with theoretical predictions. However, the pressure levels applied in the borehole in the blasting experiments were significantly different than those in the numerical analysis. The pressure applied on the borehole walls in the experiment was about one sixth of that used for the numerical analysis. Except for the discontinuities, the medium in the numerical model is assumed to be continuous, homogenous and isotropic. More importantly, the penetration effects of the high pressure explosion gases in generating new cracks and extending existing ones is not accounted for in the model. The magnitude amount of pressure required to create a fracture is much higher than that required to extend or branch a fracture. In the same, the prediction of numerical models in this investigation are to be viewed as being on the conservation side.

The experimental investigation detailed here does have some limitations. Only small to medium diameter boreholes (50 mm to 150 mm) were employed. The bench height was limited to 3 m, and no stemming used in the holes. Future work should include larger borehole diameters and higher bench heights, and more accurate damage assessment techniques than the HCF technique alone. The role of stemming on the results should be also investigated in detail.

CHAPTER 7

INVESTIGATION OF WALL-CONTROL BLASTS ALONG ROADCUTS

7.1 INTRODUCTION

During a trip along a route several outcrops can be usually seen at the sides of a road. The faces of these roadcuts, the colour, the height and the width differ from one location to another. Some of them are stable, clean and smooth with consistently visible half barrel holes perpendicular or nearly perpendicular to the surface, whereas others are irregular and rough with fractures and small or large blocks of rock which could fall at any moment. At a glance, it would be appeared that the smooth face has been cut by a saw, and the irregular face had been blasted badly. However, the characteristics of each roadcut are different from place to place along the route.

All these cuts at the sides of the road are carried out by blasting, and generally the type of explosive used, the diameter of charge and the geometry of the blast are kept constant along the route. Therefore, the most important parameters which are variable from one site to another are the properties of the rock mass. The dynamic strength and elastic properties and nature of structural discontinuities control the results of the blasts. These parameters significantly contribute to the degree of smoothness and the stability of the face in a perimeter blast.

Because of the many variations in rock structures, the properties of a rock mass can be different from one site to another and also in the different parts of a site. It might appear a through field investigation of all these conditions would be nearly impossible. However, a statistical conclusion from direct observation over a wide area in different rock types with several structures can be used as an alternative to the tests, as well as providing verification of analytical techniques, and field guidelines for practical blasting.

In this chapter an attempt has been made to discuss and explain the results obtained by perimeter blasting in the presence of the various discontinuities in several rock types along two highways in the United States of America. These two routes cover a wide range of geological conditions. The total of 17 roadcuts in Highway 89 and 91 were selected for this study. The boreholes are generally 75 mm diameter and about 1.0 spacing with lengths ranging between 5 to 15 m. The structural discontinuities of these roadcuts were mapped and recorded by the photographs. The dynamic and static properties of the rocks are measured in the laboratory for each cut. The relationship between the discontinuities and the final face as well as the role of hole deviation, are also discussed.

7.2 LOCATION

Highways 89 and 91 are located in the state of Vermont and run in a north-south direction. Out of the seventeen roadcuts selected along these two Highways, nine of them are located between the Canadian border and the town of Montpelier on Highway 89 and the others are along Highway 91, from the Canadian border to the town of St. Johnsbury. Figure 7.1 shows the location of these two sites.

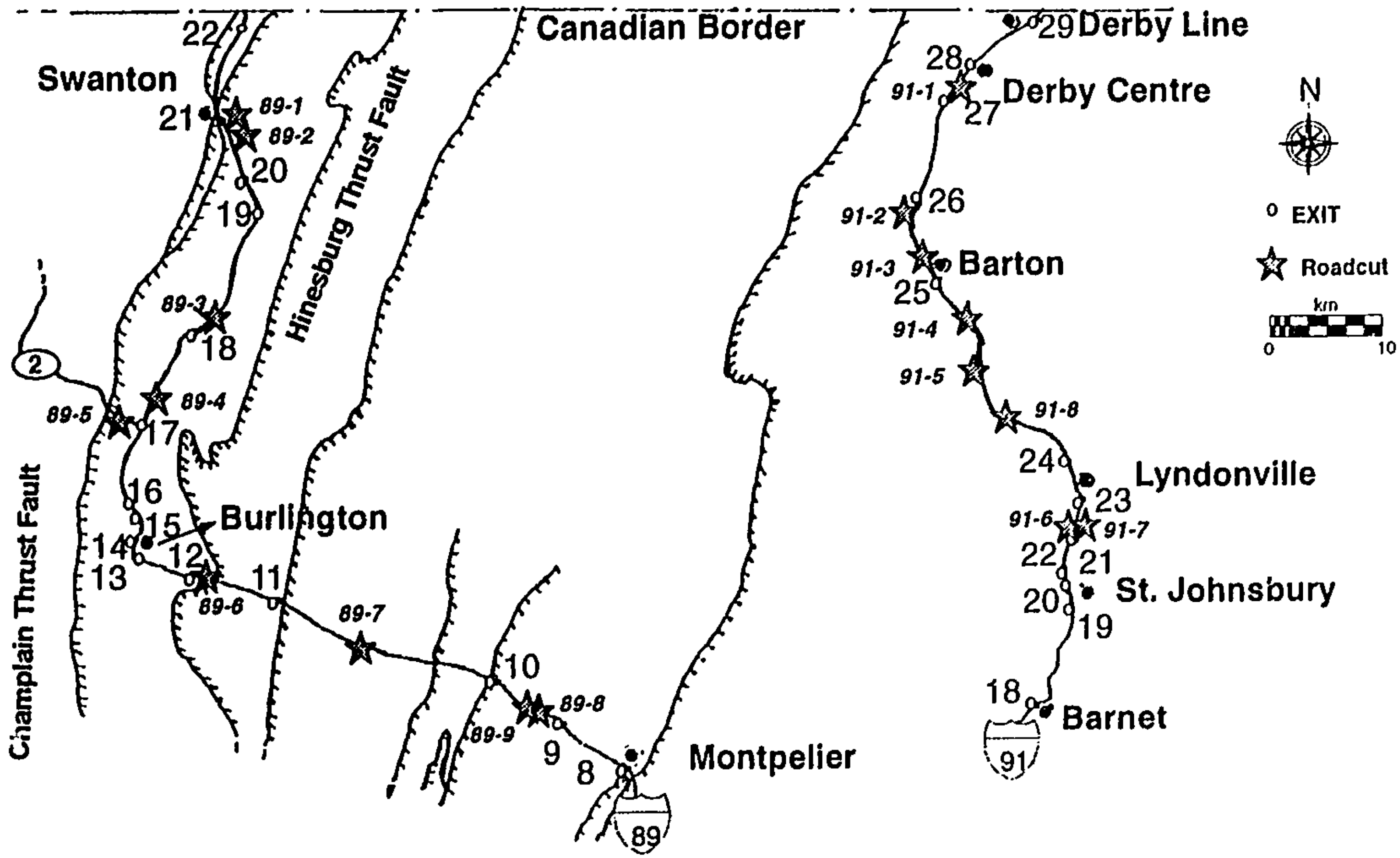

Figure 7.1 : Location of selected roadcuts on Highway 89 and 91 in U.S. A.

7.3 GENERAL GEOLOGY OF THE AREA

The study of the Appalachian geology area, Taconic and Green mountains and Champlain and Hinesbury thrusts have attracted the attention of geologists for a long time. Therefore, the geology of the state of Vermont has received a great deal of intensive field study. A detailed discussion on the geology of this region is beyond the scope of the present research program; only the relevant section are presented briefly. This is based on the following sources: Roadside Geology of Vermont by Van Diver (1987); Environmental Geology of Vermont numbers 1, 2 and 3 by Stewart (1974, 1973 and 1971); Guide book for field trips in Vermont by Doolan and Stanly (1972); Studies of Appalachian geology by Zen, et al. (1968); and The Geology of the Lyndonville area, Vermont by Eric and Dennis (1956).

The New England Upland consists of Vermont and New Hampshire and presents a plateau-like landscape. The White mountains in New Hampshire, and Taconic and Green mountains in Vermont are the principal mountains of this landscape. The green mountains are the dominant topographic features in central Vermont. They are one part of the Appalachian Mountains system. The area mostly consists of metamorphosed sedimentary and volcanic rocks, which have been interrupted by numerous igneous bodies (Ratte and Ogden, 1989). The metamorphic history of these rocks is complex, as the rocks were subjected to frequent periods of deformation. The rocks comprise mostly of slate, phyllite, low-grade schist, quartzite and marble.

The layered rocks are buckled into large scale upfolds and downfolds with a general north-northeast trend. Thrust faults are the dominant structures of western Vermont, however, they are not visible in the outcrops and roadcuts studied. Champlain thrust extends approximately 120 km from Cornwall, Ontario to Rosenburg, Vermont, and places lower Cambrian delestone with some quartzite on highly deformed middle Ordovician shale and thinner beds of carbonates.

The selected roadcuts on Highway 89 are located in the quadrangles of Milton-St. Albans, Burlington-Middlebury and Barre-Montpelier regions in Vermont. The first two regions are divided into subdivisions with different bedrocks, structures and topography. These are the Green Mountains to the east and the Champlain lowland to the west, boundary marked by the Hinesburg-Oak Hill fault. As mentioned before, the Green Mountains have been subjected to more deformation and greater intensity than the Champlain Lowland. The secondary structures such as schistosity, drag folds, fracture cleavage and jointing are common to all areas of the mountains. The thrust faults are very common structural features in the western part of these regions. The Champlain thrust that runs northward to the Canadian border, the Hiensburg thrust that forms the boundary between Champlain Lowland and Green Mountains, the Hogback thrust, Monkton thrust and Vergennes thrust are located in these areas. In addition to the thrust faults, the region has been cut into a series of blocks by high angle faults that trend northeast and high angle faults trending east-west.

The selected roadcuts on Highway 91 are mostly located in the Lyndonville quadrangle in northeastern Vermont, between the Green Mountains and New Hampshire plutonic belt. The Waits River formation and Gile Mountain are the two sedimentary formations that crop out within the Lyndonville quadrangle. The rock consists of an alteration of graywakes, quartzites, siliceous limestones and volcanics, in which are emplaced a number of cross-cutting "granite" plutons. Two phases of deformation are recorded in the rocks: an early one marked by a sericite schistosity essentially parallel to the bedding and isoclinal drag fold; and a later one, marked by slip cleavage in some rocks and schistosity in others.

7.4 RESULTS OF THE FIELD OBSERVATIONS

7.4.1 Geology of the Highways Roadcuts

Highway 89 crosses from the west to the east side of the Champlain thrust fault at exit 21 (10 km from the Canadian border), just before passing over Rock River (Fig 7.1). The road is approximately parallel to the Champlain Thrust from exit 19 to the town of Burlington. Five roadcuts were chosen in this part of the road, four of them (89-1, 89-2, 89-3 and 89-4) are located between the border and Burlington and the fifth one located at route 2 at a distance about 3 km from the intersection of Highway 89 at the west of exit 17 (89-5). In this part of the route, the rock were metamorphosed at low temperature, with limestone and dolomite into marble and sedimentary rocks of slate. Several large roadcuts with complex folding are located near exit 18 to Georgia centre. The route crosses Malletts Creek fault near the Mallets Bay south of exit 17, and follows about 9 km in early Cambrian Monkton quartzite. This quartzite is a distinctively red- to buff-coloured, thin-bedded rock that also contains relatively thick layers of marble.

Between Burlington and Montpelier the route crosses the layers, folds and faults of the bedrock. This is a shelf sequence between exits 13 and 12, mainly consisting of marbles and quartzites formed by the metamorphism of shallow water, continental shelf sediments. Exit 12 lies almost astride the Hinesburg thrust fault, a profound structural boundary that places Cambrian Camels Hump schists over the marbles. The schists are dark brown in roadcuts east of exit 12, and locally striped with thin white quartz lenses. They are mostly metamorphosed greywacke, a kind of muddy sandstone from the deeper water environment that was east of the shelf sequence. Several large roadcuts are located between exit 11 and 12 in the schists. Most are attractive greenish biotite schists in which the colour comes from the soft micaceous mineral chlorite. Many also contain metamorphic garnet, and nearly all reveal abundant quartz lenses between the layers. Roadcut number 89-6 is located closed to exit 12 near the Hiensburg thrust fault, and the seventh one located between exits 11 and 10.

At south Duxbury, the road crosses yet another major thrust fault. Nearly 9 km from exit 9 the roadcuts expose brownish, more biotite-rich schists of the Hazens Notch thrust fault slices. Between exits 10 and 8, the serpentine belt of the Row-Hawely slices is crossed by the route. Most of the rocks are thinly-leaved phyllite with lustrous cleavage surface. Roadcuts number 8-89 and 9-89 are located in this region (Fig 7.1).

On Highway 91, between the Canadian border and the town of Barnet, many roadcuts expose phyllite, schists and micaceous quartzites of metamorphosed Devonian Gile mountain formation, and marbles phyllite, and schists of metamorphosed Devonian Waits River formation (Fig. 7.1). Several large bodies of granite are located at the north part of the route, part of the Devonian New Hampshire plutonic series.

Between exit 27 and 28 to Newport, the rock contacts between the granite and abundant blocks of schist engulfed in it. Whitish granitic dikes that cut through both schist and granite formed from residual melt that worked its way into fractures, in the already crystallized granite near the margins of the pluton (Roadcut 91-1).

Between Braten and Lyndonville, roadcuts show thick marble layers, originally limestone. The marble is inter-bedded and inter-graded with phyllites and schists, locally folded into rather fluid layers and streaky forms. The darker inter layers commonly contain innumerable thin lenses and layers of white quartz (Roadcuts 91-2 to 91-5 and 91-8). Between Lyndonville and St. Johnsbury roadcuts contain phyllites with inter-layers of dark green amphibolite, metamorphosed basalt (Roadcuts 91-6 and 91-7).

7.4.2 Criteria of Assessment

The current practice for rapid evaluation of blast results is the half cast factor (HCF), appearing on the blast face which applied for the face. The term HCF is expressed as a percentage of the blasthole half barrels visible on the final face. As mentioned in the previous chapter, in many cases in spite of the presence of half barrels on the face, the damage zone was visible behind the face. Most of the discontinuities were opened behind the holes without any effect on the half barrels. Nevertheless, it is still a very reliable and rapid technique for assessment of blast results.

7.4.3 Properties of Rock at the Roadcut Sties

To assess the condition of the rock, both static and dynamic properties of the rock at each site were measured. Static properties were measured from the core samples, which were prepared from a block of rock, selected from each roadcut. Uniaxial compressive strength and modulus of elasticity, were obtained from the stress-strain curve; the tensile strength was measured Brazilian Test.

The dynamic modulus of elasticity and Poisson's ratio were determined by ultrasonic velocity (P-wave and S-wave) measurements. The modulus of elasticity and Poisson's ratio were measured in the laboratory from the block samples selected from each roadcut, by measuring the propagation velocity of the longitudinal and transverse waves in the target sample (Tables 7.1 and 7.2). A mechanical pulse of short duration is applied to the rock samples, and the velocity of the P-wave and S-wave were calculated by measuring the time required for compressive and shear waves to travel between the source and the receiver. The elastic modulus are calculated from these two velocities and the density of the rock sample.

It should be noted that rocks have different behaviour under dynamic loading as compared to static loading, the former being normally higher. The seismic properties were measured on blocks ($\sim$ 30 cm sides) whereas, static properties were measured on small core samples. This would explain the sometimes higher modulus obtained under static measurements.

7.4.4 Strength of Rock

An optimum charge for a given borehole diameter mainly depends on the strength

Table 7.1 : Properties of rock at 9 roadcuts along Highway 89.

Roadcut No.	Type of Rock	Uniaxial Com. Strength	Tensile Strength	E_s	E_d	ν	Density	P-Wave Velocity	S-Wave Velocity
-	-	(MPa)	(MPa)	(GPa)	(GPa)	-	(g/cc)	(m/s)	(m/s)
89-1	Marble	34.4	3.0	61.2	68.2	0.23	2.76	5260	3110
89-2	Meta-Calcarious Mudstone	255.0	10.3	81.1	92.6	0.22	2.70	6400	3820
89-3	Meta-Calcarious Mudstone	133.5	12.8	74.0	86.0	0.23	2.77	5100	3560
89-4	Sandy Limestone	183	10.5	88.4	89.3	0.21	2.80	5100	3610
89-5	Quartz Sandstone with Calcite Matrix	212	18.0	80.0	85.0	0.27	2.63	6390	3550
89-6	Meta-graywake	42	5.0	65.0	58.0	0.21	2.79	4770	3040
89-7	Chloritic Schist	61	6.0	29.0	32.5	0.26	2.90	2100	3710
89-8	Quartz Schist	41	3.8	60.5	81.0	0.28	2.78	5830	3340
89-9	Chloritic Quartz Schist	130	10.7	43.0	69.0	0.19	2.77	5220	3230

E_s : Static Modulus of Elasticity E_d : Dynamic Modulus of Elasticity ν : Possion's Ratio

Table 7.2 : Properties of rock at 8 roadcuts along Highway 91.

Roadcut No.	Type of Rock	Uniaxial Com. Strength	Tensile Strength	E_s	E_d	ν	Density	P-Wave Velocity	S-Wave Velocity
-	-	(MPa)	(MPa)	(GPa)	(GPa)	-	(g/cc)	(m/s)	(m/s)
91-1	Granite	88.0	5.7	32.7	20.0	0.25	2.62	2980	1730
91-2	Meta-Siltstone	171.0	18.9	51.0	70.0	0.24	2.74	5490	3180
91-3	Mudstone, Pelitic	168.0	10.5	50.0	60.0	0.21	2.72	4950	3000
91-4	Biotite Quartz Schist	117.0	-	53.0	71.0	0.22	2.77	5430	3260
91-5	Fine Meta-sandstone, Biotite Rich	188.0	14.5	80.6	76.0	0.24	2.75	5670	3240
91-6	Meta-Sandstone, Silica Gel Cemented	150.0	22.0	75.0	77.0	0.25	2.73	5790	3330
91-7	Chlorotic Quartz Schist	153.0	12.5	76.0	43.0	0.25	2.75	4320	2500
91-8	Biotite Quartz Schist	124.0	-	14.0	47.8	0.24	2.70	4910	2670

E_s : Static Modulus of Elasticity E_d : Dynamic Modulus of Elasticity ν : Poisson's Ratio of the rock and the nature of the discontinuities. The compressive and tensile strengths of rock are key parameters in blasting. Crushing of rock around the holes occur, when the compressive stress exceeds the compressive strength of rock. Therefore for a successful wall-control blast, the pressure on the wall of borehole must be smaller than the compressive strength of rock.

Blast geometry, borehole diameter and charge diameter usually remained constant along a route, especially at short distances. As figure 7.16 and 7.18 show, the nature of the structural discontinuities, blast geometry and direction of the blast at these two roadcuts are similar to each other. But the results of the blast are completely different. At roadcut 9-89, a smooth and clean wall with half barrels were clearly visible on the face, whereas at the other one (8-89) the rock was badly fractured and no half holes were visible on the face. The only difference between these two sites was the property of the rock mass. As Table 7.1 shows, the compressive and tensile strengths of the rock at roadcut 9-89 are about 3 and 2.5 times greater than these at roadcut 8-89, respectively. Also, comparison between results of the blasts and the properties of rock at each site clearly indicates that a smooth face was usually developed at sites which had compressive and tensile strengths greater than 100 MPa and 10 MPa, respectively.

7.4.5 Effect of Parallel Discontinuity to Face

The discontinuity parallel to the face behind the final row and, its proximity were demonstrated to have a significant effect on the results of the blast. It is clearly displayed at site number 3 on Highway 89 (Roadcut 3-89). In this case, the rock was badly shattered between the boreholes and the discontinuity between the layers. Therefore, the final face was shifted to a new face behind the line of excavation. As figure 7.6 shows, the roadcut is located on the curve of the Highway, and the distance between the borehole wall and the discontinuity behind the holes is different at the beginning, middle and the end of the site. It clearly shows that only when the distance of the borehole wall was greater than the spacing, then the half holes were generated on the face. For distances smaller than that, the final face is moved from the centreline between the holes to the back of the holes. In this and similar cases, the final face should be the face of the discontinuity and the slope of that approached the dip of the discontinuity. Similar results are also predicted by numerical analysis for a weak plane parallel to the face behind the back of holes (See Chapter 5, Section 5.5.2.2)

7.4.6 Effect of Discontinuity Perpendicular to Face

The effect of discontinuities which are perpendicular or nearly perpendicular to the final line of the excavation, on the blast results is shown in figure 7.18. In this roadcut, the closed discontinuities were nearly perpendicular to the centreline between the holes, and the rock was blasted against the strike of the discontinuities (direction of the blast related to the strike of the discontinuities). As figure 7.18 shows, a clean and smooth face is created by this blast. The half barrels were mostly visible on the face, with little backbreak. The effect of perpendicular discontinuity to the centreline (at the midpoint or near to the boreholes) was discussed in a previous chapter. The result of field observation accords with prediction from the numerical analysis (Chapter 5, Section 5.5.2.2).

The phenomenon of hole deviation was also investigated in this site. It is seen to be a key factor in creating damaged areas. Figure 7.18 shows that the damage zones are normally associated with the holes spaced much closer than their design spacing, due to hole deviation. This problem will be elucidated in greater detail in a subsequent section. In some cases, the spacing between the holes at the bottom of the bench was two times greater than the spacing at the top for the same holes, but the conditions of the face at the bottom remained similar to that near the top. Therefore, the blast could have been carried out with greater spacing than the actual one. In general, excellent wall-control blast results were obtained at this site (Roadcut 9-89), except in locations characterized by excessive hole deviations.

Where a discontinuity perpendicular to the final face was located between the holes, but not at the middle of the spacing, a damage zone was visible between the nearest hole and the discontinuity. At roadcut 2-89, in addition to bedding planes, some pre-existing fractures were located perpendicular to the centreline between the holes (Fig. 7.4). As the figure shows, significant backbreak occurred between the holes and the discontinuity when the holes were drilled close to these perpendicular fractures.

In the case of a joint set, considerable backbreak would be expected to occur when the joints spacing is less than the hole spacing. The degree of the fracturation and damage largely depends on the density of the structure between the holes. In this case, the crest damage would be the major problem after the blast. In site 2-91, multiple perpendicular discontinuities (4 joints per m) were visible on some part of the final face. As figure 7.22 shows, the frequency of the joints are responsible for the damage zone on the face. The rock is extensively fractured and the half holes are not visible in these areas.

In addition to a prominent plane bedding plan in roadcut 5-91, the rock was highly fractured in some parts of the face. This was also due to the presence of large number of pre-existing fractures perpendicular to the centre line, with a spacing smaller than the spacing between the holes (Fig. 7.28). As the figure shows, the presence of these discontinuities leads to extensive fracturing of the blast face.

7.4.7 Effect of Inclined Discontinuity to Face

Whenever the face was crossed by a perpendicular discontinuity to the surface, (inclined discontinuity to the face), it resulted in an uneven and jagged face. The extent of the broken area depended on the angle of the discontinuity. At roadcut 1-91 on

Highway 91, significant backbreak was visible behind an inclined discontinuity to the face. The shape of the face was changed from a smooth to a Z-shape between the holes which were crossed by the pre-existing fracture. The half barrels of the next two holes were also not visible in the direction of the discontinuity. This type of damage continued to where the distance between the holes and this discontinuity exceeded the length of the spacing between the holes (Fig 7.20).

This type of damage is most apparent and best displayed at site 6 on the same Highway (Roadcut 6-91). As figure 7.30 shows, a series of holes are seen to be shattered in front of an inclined discontinuity, with the final face is the plane of discontinuity. The damage zone continued up to where the distance between the holes and the pre-existing fracture exceeded the spacing between the holes. The half barrel holes were absent in this region and a Z-shape is created on the final face. This is exactly according to the theoretical predictions outlined in chapter 5 (section 5.5.2.4).

A comparison between figure 7.20 and 7.30 shows the effect of the angle of discontinuity on the results of the blast. The angle between the face and the discontinuity at Roadcut 1-91 is much greater than the same angle at Roadcut 6-91. Consequently, only two holes did not exhibit half barrels at the first site, whereas more than 10 hole did not exhibit half barrels at the second sites. This shows that half cast factor largely depends on the angle of the inclination of the discontinuity with the final face.

7.4.8 Effect of Discontinuity Intersecting Blasthole

In most sites the blastholes were crossed by different types of discontinuities along their length. The horizontal or nearly horizontal discontinuities are seen to have no effect on the blast results. This was clearly apparent at the face of the final wall at roadcuts number 2-89, 1-91 and 8-91. As figures 7.4, 7.20 and 7.34 show, the final face of the roadcuts, except in areas which were close to the vertical joints at the centreline, were very smooth, and the half barrel holes were visible in most parts of the final face.

The discontinuities inclined to the rock face which were crossed by the wall-control blast holes at any angle were seen to have minimal effect on the blast result. The fractured areas were more apparent visible near the crest, where the intersection point of the hole and the discontinuity was near the surface. This was observed at many sites during the field investigation. Figure 7.8, 7.24 and 7.26 show a smooth face with half barrel holes on the final face of roadcuts. As shown, several inclined discontinuities were crossed by the blastholes at different heights. However the only problematic area was restricted to the crest. As figure 7.24 shows, excellent blast results were obtained in this roadcut in the presence of intersecting discontinuities, except at the top of the face, where the rock close to the discontinuity was badly fractured. The same conditions were visible at Roadcuts 1-91, 4-91, 8-91.

7.4.9 Highly Fractured and Folded Rock

The first roadcut (89-1) is located close to the Champlain thrust fault and consists of dolomite which is lightly metamorphosed. The rock is highly fractured and folded in all directions. As figure 7.2 shows, the strike and the dip of the structures, especially at the right side of the photo, have different directions and in some cases are against each other. A small part of the half barrel holes is visible at middle of the roadcuts where a block of rock is seen to have remained intact. The sixth roadcut is located near the Hinesbury thrust fault (Fig 7.12). It consists of dark brown schist stripped with thin white quartz lenses. The rock was highly fractured and foliated in this area due to the Hinesbury thrust fault. It was very weak and very difficult to make a specimen from the block samples in the laboratory. All the blocks were broken under the pressure of the bit of the coring machine during the sample preparation.

In these two roadcuts, in all probability, the borehole diameter and the spacing remained similar to the previous roadcuts (75 mm and about 0.9 m). Consequently, the final walls were extremely uneven and no half barrel holes were visible on the face.

7.4.10 Effect of a Bedding Plane on a Blast Results

Horizontal or nearly horizontal bedding planes appear to have no effect on the blast results. The effect of inclined bedded rocks, perpendicular or nearly perpendicular to the rock face, is similar to the previous case. This is clearly demonstrated at roadcuts number 2 and 5 on Highway 89. As figures 7.6 and 7.10 show there are no damage zones visible due to the bedding planes. Comparison between these two figures shows an important parameter which is the stability of the final face. In the first roadcut (89-2) the slope of layers are against the slope of the face, whereas at roadcut the slope of the layers is in the same direction as the final face. As figure 5.10 shows, some blocks of rock have been gradually pushed to the front.

As the dip of the layers increases then the influence of the bedded rocks on the results obtained by wall-control blast, also increases. At roadcut 5-91 (Fig. 7.28) the rock consisted of thick marble layers, inter-bedded with schist and phyllite. The layers with a dip approximately equal to 22° to the slope of face were crossed by some vertical joints. As shown in figure 7.28, the face is generally rough, with the thinner layers being fractured irregularly. The degree of roughness depends on the dip, thickness and the strength of the layers. The wall of the roadcut displays a stable face, due to the dip of the rock which is against the slope of the final face. All half barrel holes were visible on the face, except in the region which were close to the vertical joints. This is best displayed at roadcut 2-91 on Highway 91. A .his site, the thin limestone layers were inclined to the final face. The slope of the wall and the dip of the layers were approximately equal but against each other (Fig. 7.22). As the figure shows the resulting face is highly uneven, and in places very jagged. The half barrel holes are visible however, in the thicker layers.

7.4.11 Effect of Hole Deviation

Borehole spacing is one of the most important factors in wall-control blasting methods. A successful blast requires constant spacing between the holes along the entire length of two parallel holes. Therefore extra care should be taken during the drilling of holes on the final line of excavation. However, when the holes deviate, the spacing between holes changes from optimum spacing (maximum borehole separation for a successful blast), resulting is overbreak and damage to the face. Hole deviation can occur between the top and the bottom of the holes in a horizontal plane (between the parallel holes) or in a vertical plane (in the burden region).

Hole deviations depend on several parameters such as alignment and collaring, the condition of the drill, rock type and rock structures, depth and diameter of borehole, and operation. Some of these parameters can be controlled within reasonable limits, but some, especially related to in situ rock, can not be controlled. These factors have been studied in details by Sinkala (1985) and Trudinger (1973).

The problem of hole deviation was particularly noticeable at roadcuts 2-89, 9-89, 1-91, 2-91, 5-91 and 7-91. Frequent hole deviation was clearly visible on the final face of roadcuts number 2-89, 9-89 and 3-91. The rock at these sites was bedded and foliated, and the degree of deviation depended largely on the conditions of the layers and foliation planes. The most important factors responsible for hole deviation appear to be thickness and dip of layers and the strength of the rock mass.

As figure 7.4 shows, small deviation is characteristic of the face composed of nearly horizontal bedded rock with thinner layers at the top of the bench than the bottom. A comparison between this figure and figure 7.10 illustrates the role of the thickness of the layers. In the latter (roadcut 5-89) the thickness of layers at the top is greater than at the bottom. In roadcuts 2-91 and 5.91 the final faces consisted of the thinly bedded rock. As figures 7.22 and 7.28 show the hole deviation is much lower than the previous case at roadcut 2-89. The phenomena of hole deviation is most apparent and best displayed at roadcut 9-89 (Fig. 7.18). The rock at this site was highly foliated with dip of 80°. The rock consists of schists with layers of mica between them. All the holes were seen to diverge "up dip". Also a few irregular deviation were visible on the face. Extensive backbreak was evident around these irregular deviations, especially where the boreholes crossed each other.

It was observed that systematic hole deviation (i.e. holes diverging in the same direction) was characteristic of sites which were bedded with layers of soft and hard bands of rock. Also, the thickness of the individual layers and the relative position of the thicker or thinner layers appears to influence the degree of deviation. As figures 7.2-35 show, the joint planes display little effect on the divergence of the holes, irrespective of the former's orientation . Some Random hole deviations were also visible in some of the roadcut (roadcut 1-91 and 4-89). Theses could be due to the factors related to the conditions of the drill or drill operator.

7.5 WALL-CONTROL BLASTING DESIGN RATIONALE

A number of empirical wall-control blasting design formulas have been proposed during the last four decades (e.g. Paine et al., 19961; Gustafsson, 1973; Sanden, 1974; Calder, 1977; Anon, 1987; Berta, 1990). In addition, a number of relations between blast geometry (especially between burden, spacing and borehole diameter) and charge type and diameters for the perimeter holes are in use (see chapters 3 and 4). All these formula and relationships are based on the results obtained in the field or laboratory for special conditions, and essentially based on rules of thumb.

There are many important parameters which can greatly affect the results of the blast and limit the applicability of these empirical formulas and guidelines. Some of these factors are: type of explosive, rock mass properties, geology, structural discontinuity, orientation of the discontinuity with designed face, distance between the holes and the pre-existing fracture, width of discontinuities and types of filling material. Therefore, during the design of any wall-control blast, the engineer must be conversant in the fundamental concepts and parameters of ideal blast design, and then modify these parameters for a specific field conditions.

Generally, the blasting engineer in faced with two types of variables: controllable and uncontrollable. Borehole diameter, spacing, burden, charge diameter, hole inclination, collar length, bench height, type of explosive, loading type, type of initiation are usually controllable, whereas, geology, rock mass properties, structural discontinuities and orientation of pre-existing fractures with the design face are uncontrollable. Therefore, a blast should be designed based on the controllable parameters and then modified by field tests to reduce the undesirable effect of the uncontrollable factors.

In wall-control blasting, the borehole pressure is one of the most important parameters which can be best controlled by decoupling the explosive charge. Decoupling ratio between the explosive charge and the borehole wall should be smaller than 0.5. This ratio would generally be between 0.2 and 0.3 in case of infinite burden, and between 0.3 and 0.4 in the presence of a free face. The diameter of the pre-split holes can vary between 50 mm to 100 mm for construction industry and 150 mm to 300 mm for open-pit mine. For a pre-split blast (infinite burden) the hole separation could range up to 15 times borehole diameter, and up to 20 borehole diameters in the presence of a free face. For normal wall-control blasting a burden can be defined as being infinite when the ratio of it to spacing is greater than unity.

The effect of some uncontrollable parameters, such as geology and discontinuities, on the blast results are predictable. A discontinuity parallel to design face and located behind the holes results in the creating of a shattered zone between the discontinuity and the boreholes. This discontinuity will represent the final wall provided the distance of that from the borehole to be less than the half spacing. The presence of a similar discontinuity at the front of the holes leads to considerable overbreak and development of a "hump" (unbroken area of rock) between the holes.

A discontinuity oriented normal to the centreline at the midpoint between holes has minimal effect on the blast results. As the angle of the discontinuity with the centreline decreases from 90°, the damage zone between the holes and the discontinuity increases. In this case, the shape of the final face changes from a smooth face to a corrugated shape. The frequency of joints strongly influence the blast results, when the spacing between the joints is smaller than the spacing between the holes. A closed-discontinuity or an open discontinuity cemented with strong materials has little effect on the results of the blast. An open discontinuity, 50 mm wide or more, plays a role similar to a free face.

7.6 CONCLUSIONS

Results of field observation confirm the results obtained by numerical analysis and experimental investigation, which dealt with parameters critical to success of blasts. Analysis of the blast results in the 17 roadcuts clearly demonstrated the key role played by the discontinuities, blast parameters, and the inherent strength properties of the rock in question. The latter (tensile strength) has a direct influence on the degree of smoothness of the blast face. The weaker rocks, as expected, yield the most fractured and uneven blast faces.

Backbreak and damage resulting from the blast, are highly dependent on orientation of discontinuities with the final face. Maximum and minimum backbreak result from discontinuities parallel and perpendicular to the face at the midpoint between the holes, respectively. The degree of damage and outline of the face after the blast is dependent on the orientation of discontinuity with the final face. As the angle between the discontinuity and the final face is decreased from 90°, the amount of the damaged area is increased.

From the field observation it is concluded that the frequency of joints strongly influence the blast results. This is particularly true, when spacing between joints is smaller than the spacing between the holes and the joints are aligned perpendicular or nearly perpendicular to the face. In contrast, the joints intersecting with blastholes on the face, appear to have little effect on the blast results. Some crest fractures may occur, when the points of intersection lie close to the surface.

Hole deviation has an important bearing on wall-control blast results. This is to be expected, as it essentially changes the spacing between the boreholes from the optimal design. However, as the field observations show, hole deviation depended largely on the in situ structure of rock. The hole deviations which were systematic, even with inclined bedding or foliations, had minimal effect on the result of the blast. This type of deviation is found to be usually the result of alternate bands of soft and hard rocks. The degree of deviation is closely generated by the orientation, thickness, frequency and the location of these bands. Some random hole deviations were also visible on the faces of the roadcuts. Most of the damaged areas were apparent around this type of deviation, mostly due to varying spacing between the holes. The faces which displayed random hole deviations, showed no correlation between the hoie deviation and rock structures, in term of smoothness of resulting face.

However, these roadcuts represent extensive wall-control blasting operations, carried out on a routine commercial scale. Even though information on explosive types, decoupling ratios, type of initiation and the effect of passage of time (ageing) on the results of the blast at each roadcut are not available in literature, it is considered a natural extension of the present study to investigate some key parameters such as rock properties, drill hole deviation, and in situ structure of rock on blast results.

Figure 7.2 : Roadcut 1-89 located 12 km from the Canadian border along Highway 89, Vermont.

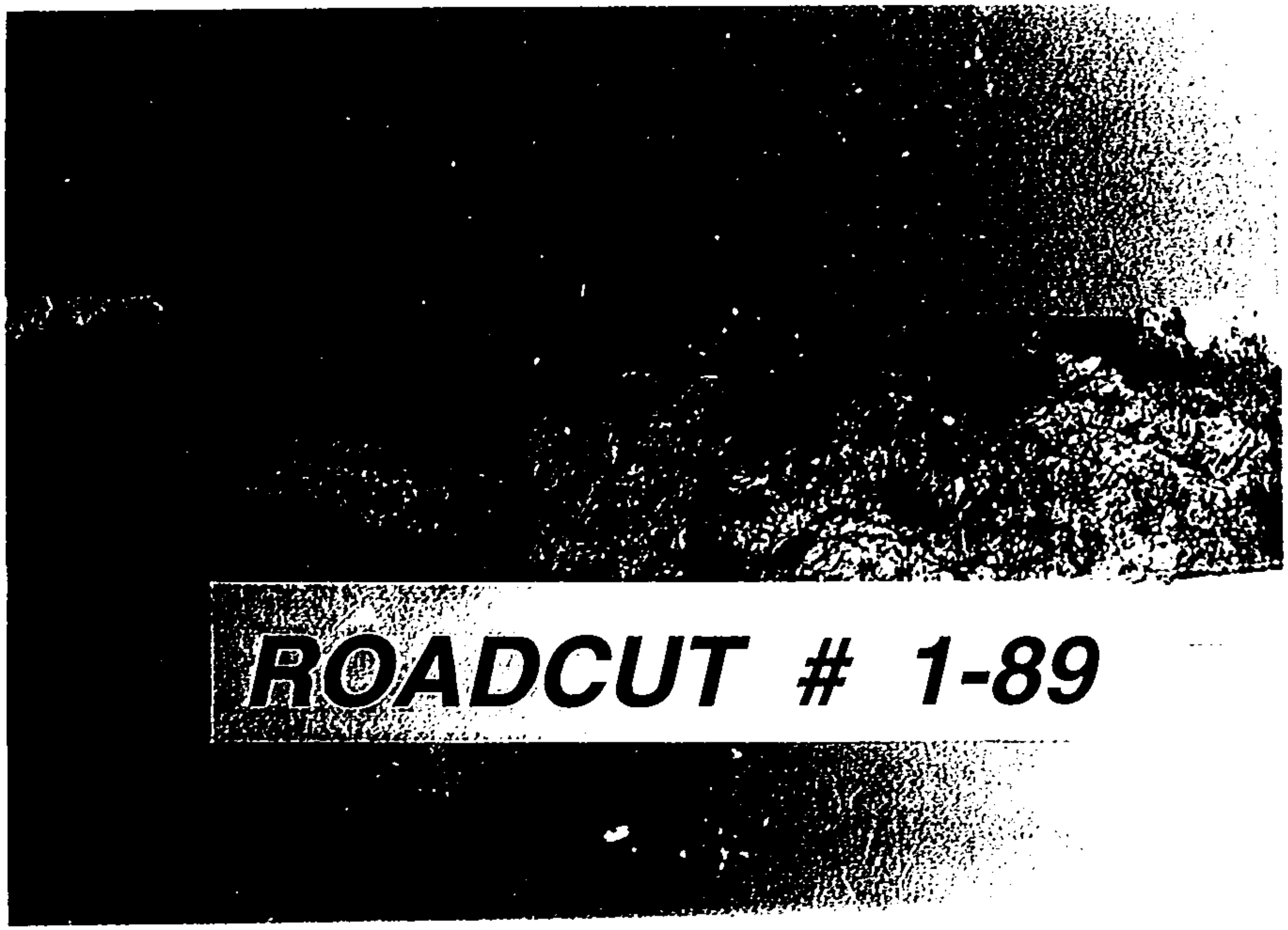

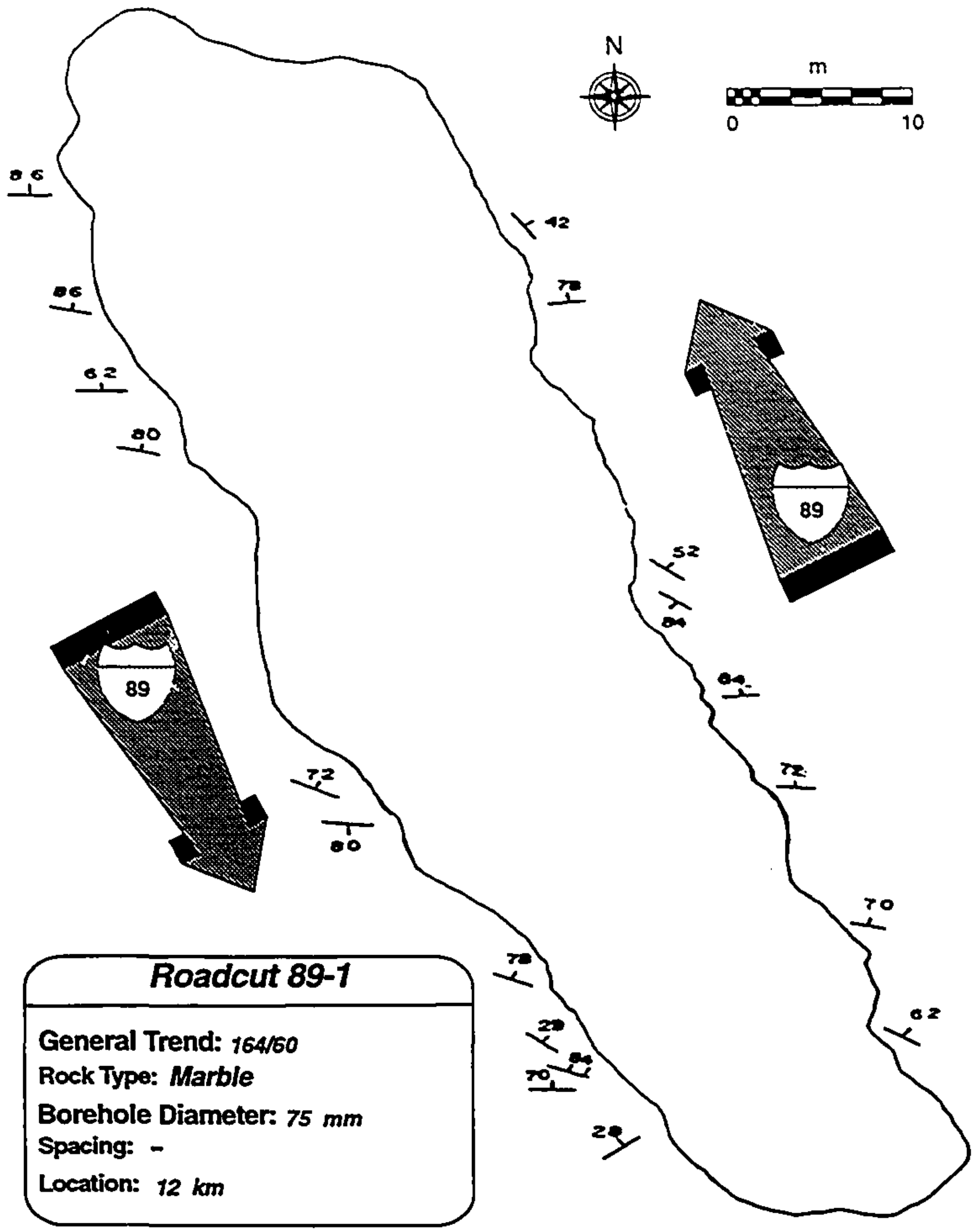

Figure 7.3 : Simplified structural geology of roadcut number 1 along Highway 89.

Figure 7.4 : Roadcut 2-89 located 12.5 km from the Canadian border along Highway 89, Vermont.

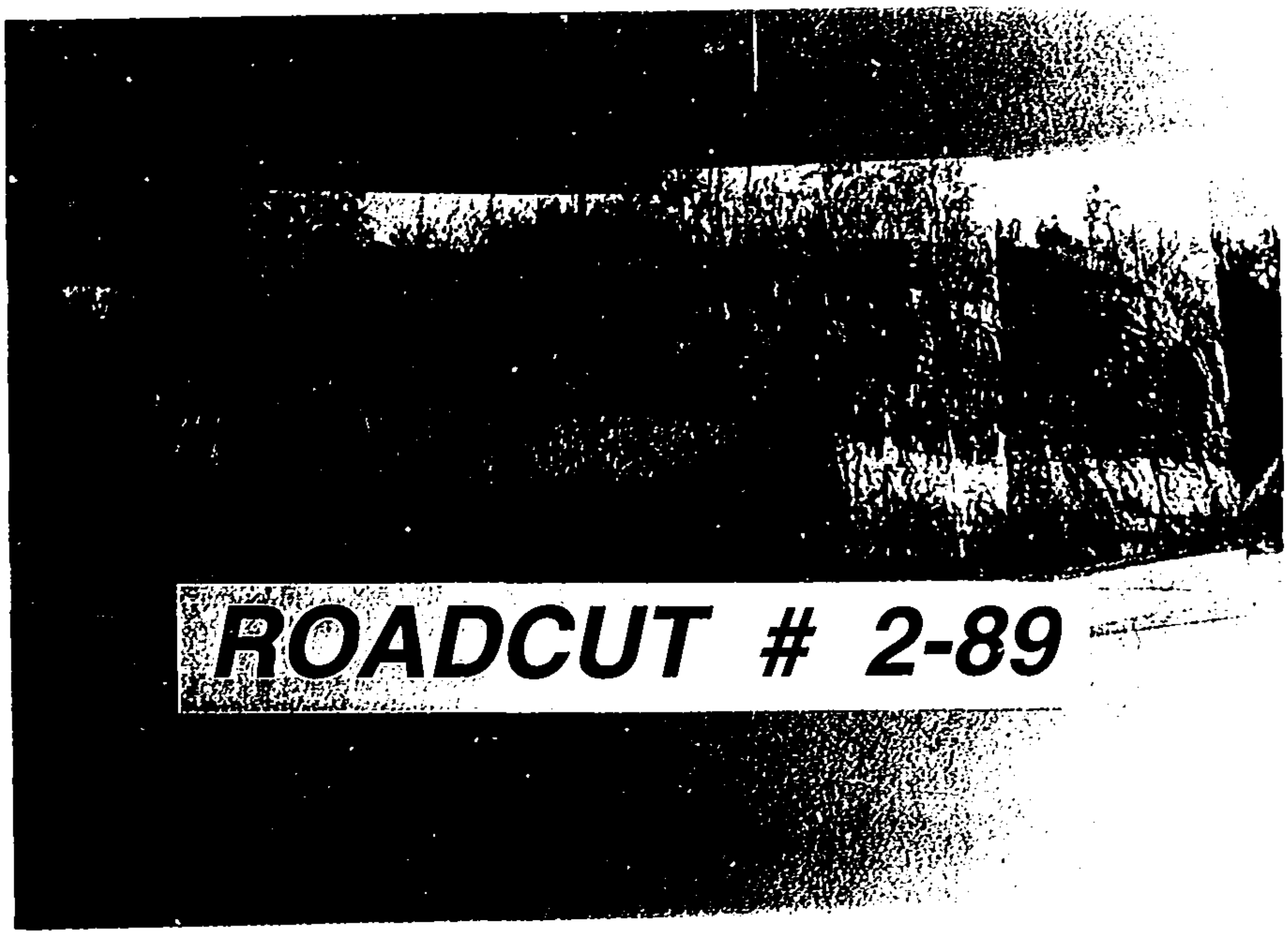

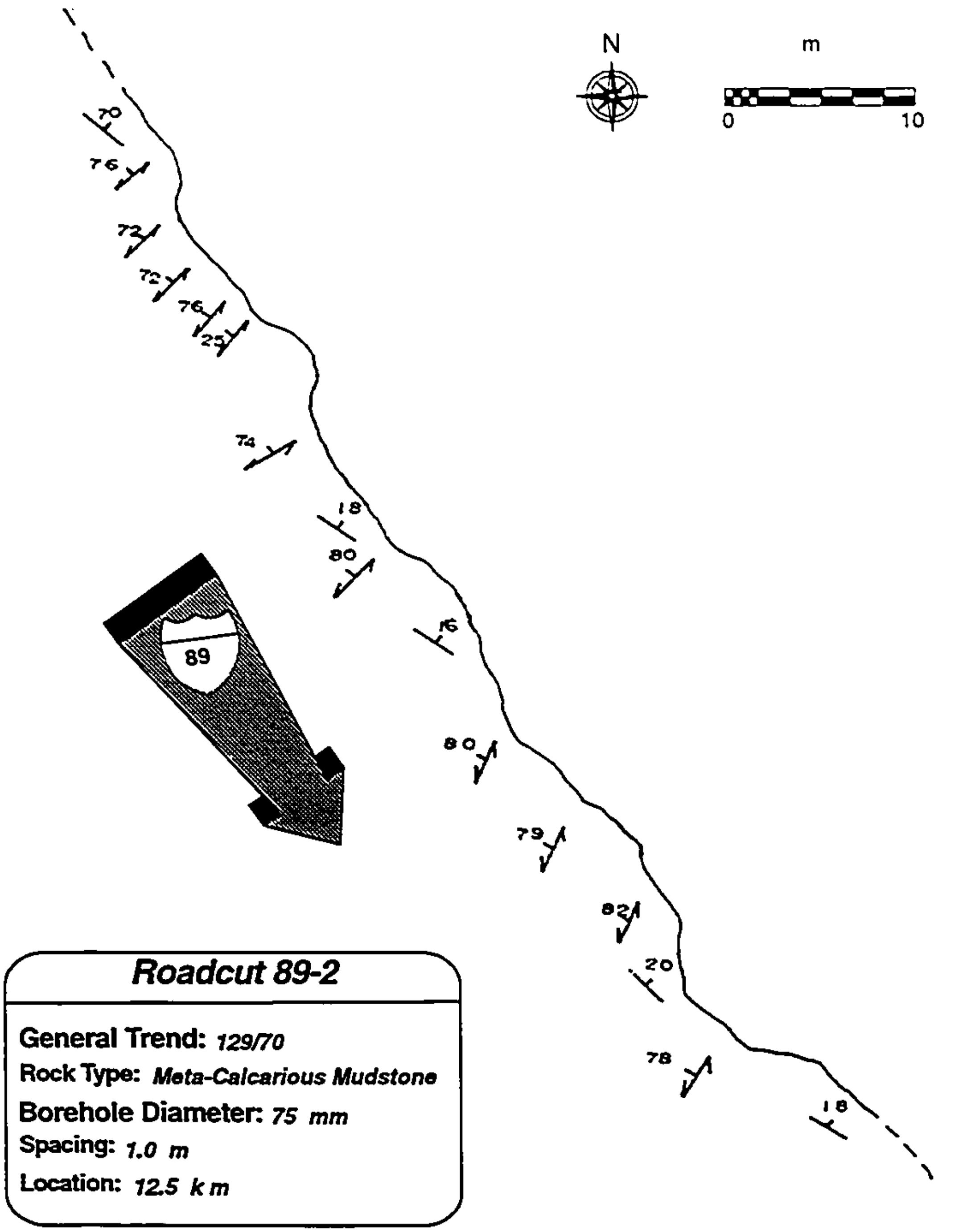

Figure 7.5 : Simplified structural geology of roadcut number 2 along Highway 89.

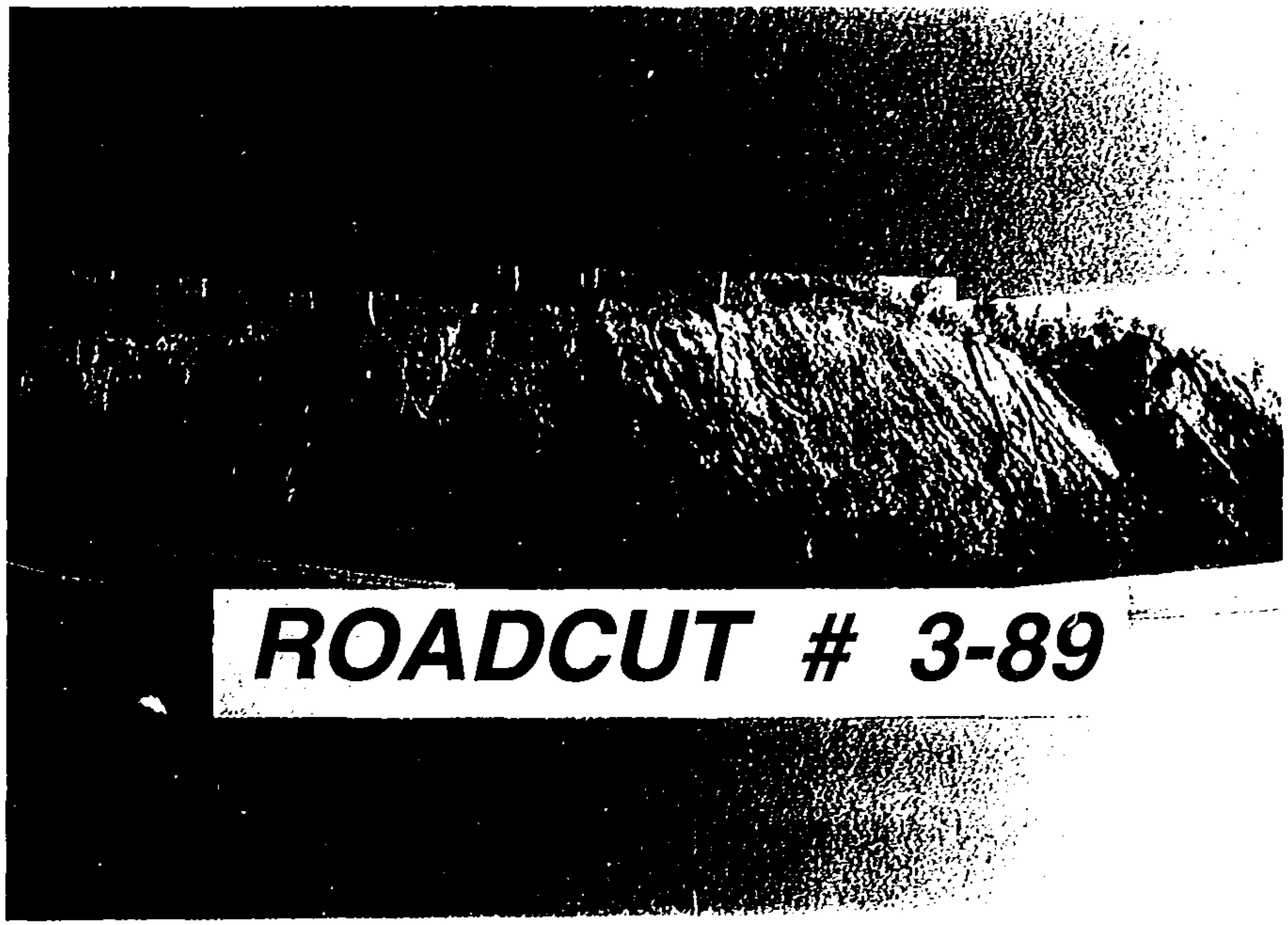

Figure 7.6 : Roadcut 3-89 located 37 km from the Canadian border along Highway 89, Vermont.

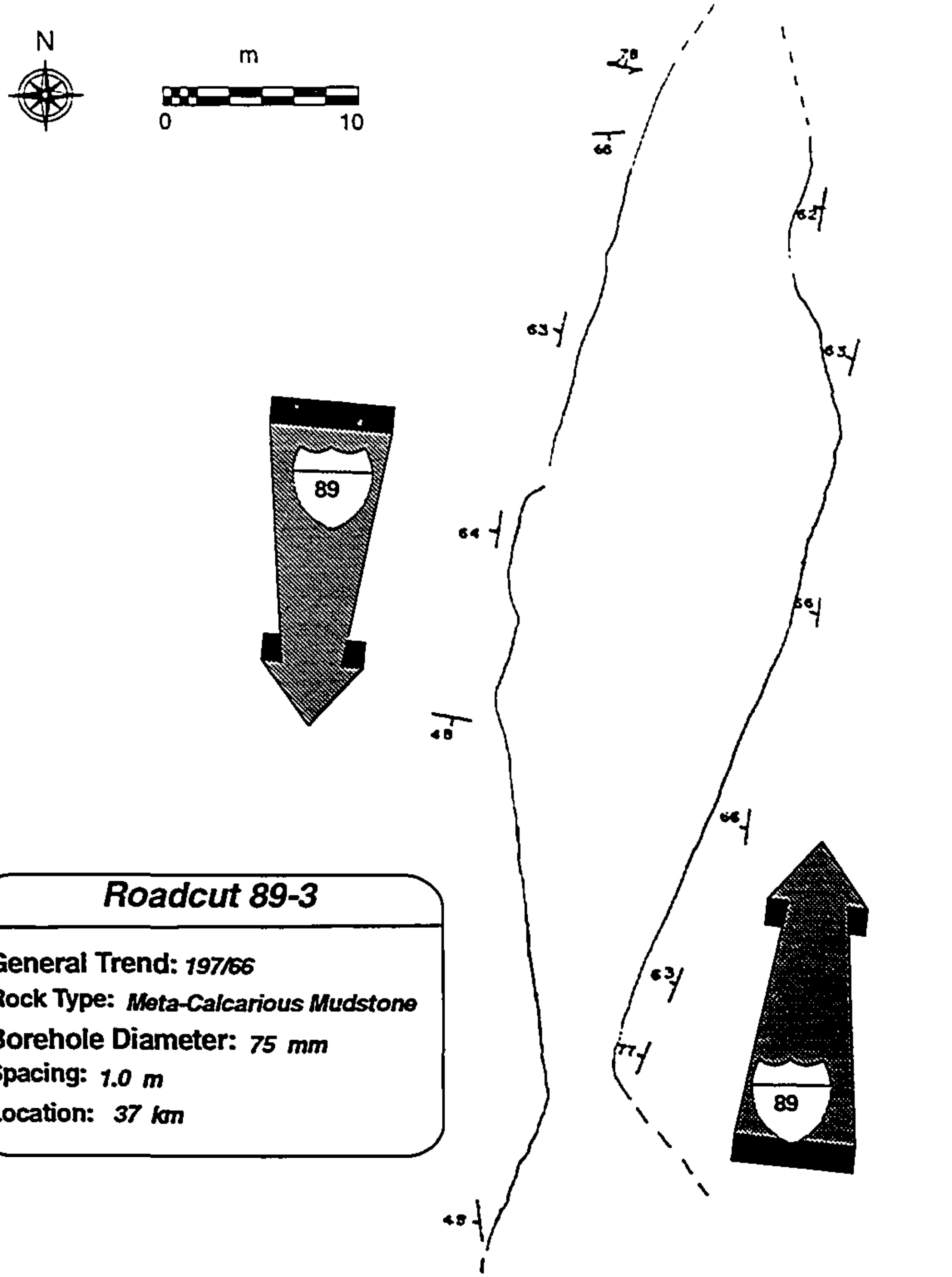

Figure 7.7 : Simplified structural geology of roadcut number 3 along Highway 89.

Figure 7.8 : Roadcut 4-89 located 48 km from the Canadian border along Highway 89, Vermont.

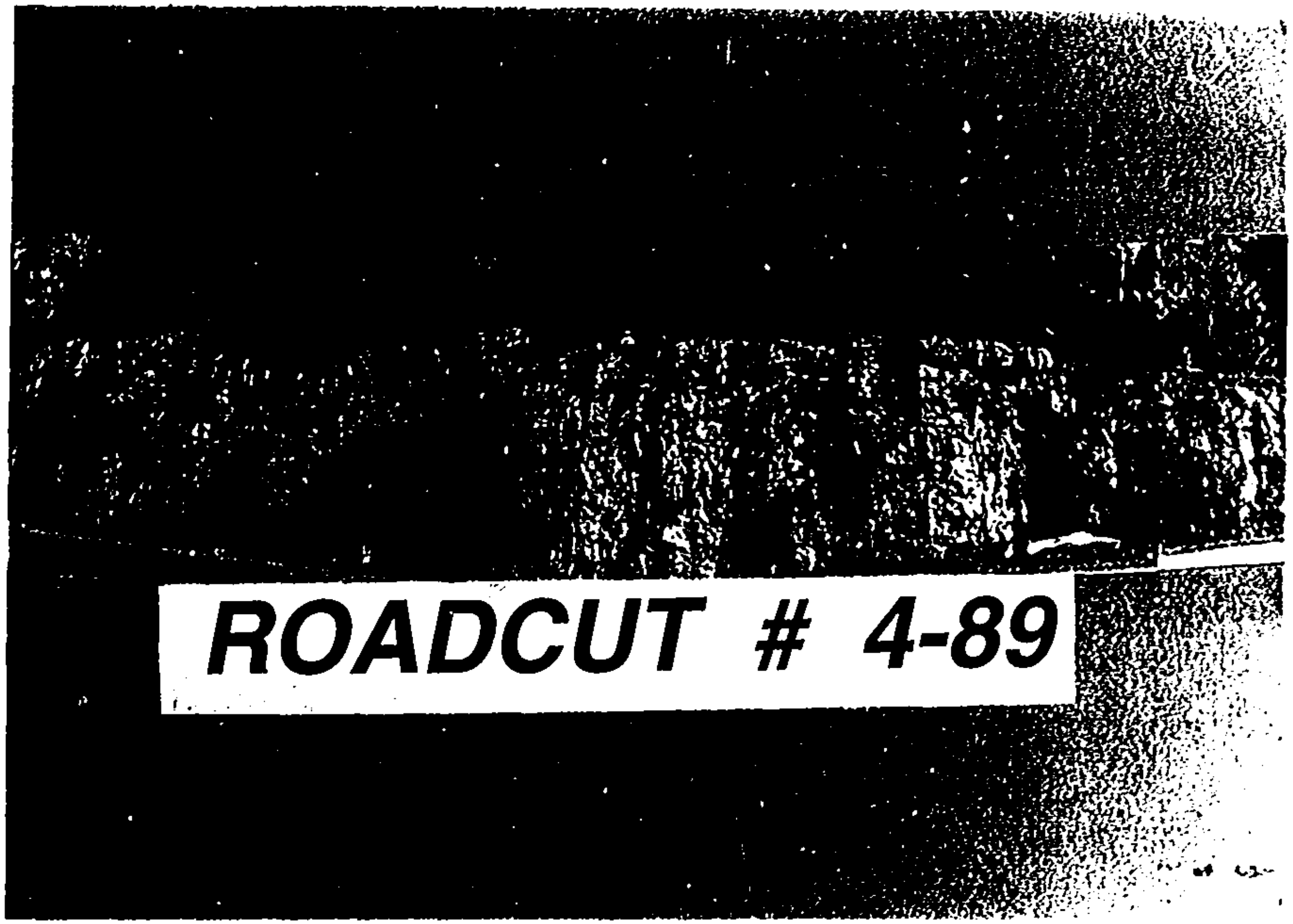

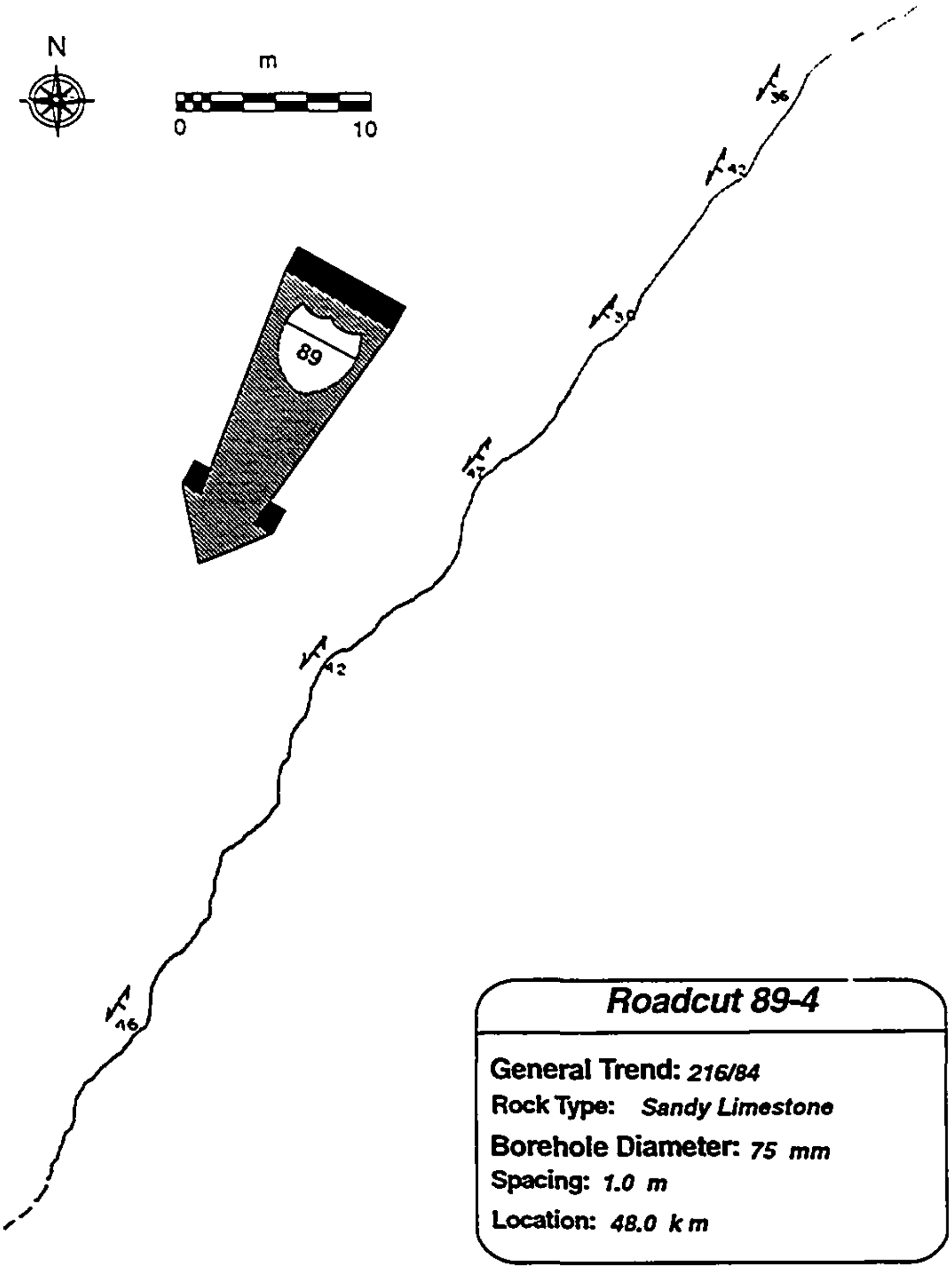

Figure 7.9 : Simplified structural geology of roadcut number 4 along Highway 89.

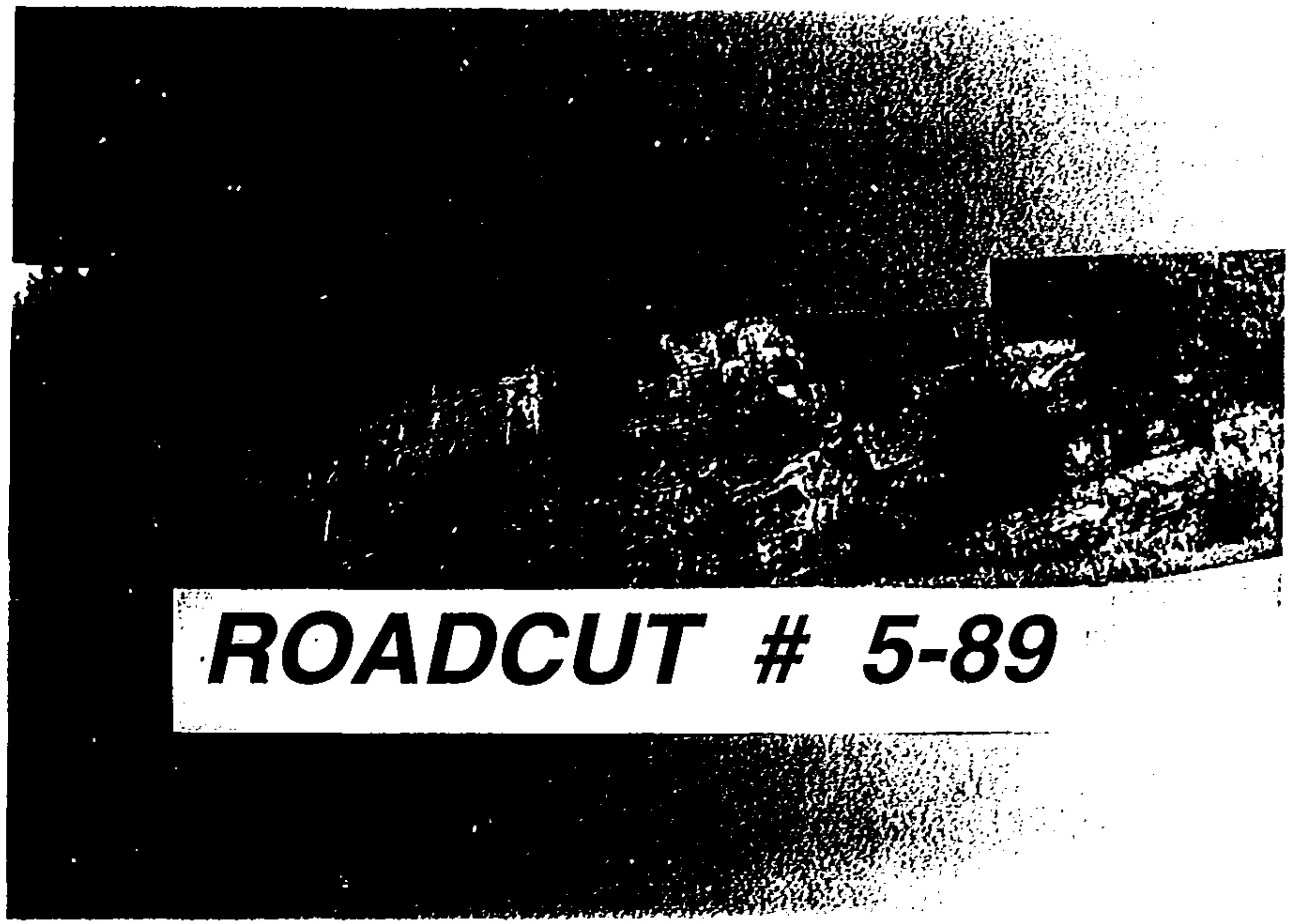

Figure 7.10 : Roadcut 5-89 located 3 km from exit 17 (on Highway 89) along Route 2, Vermont.

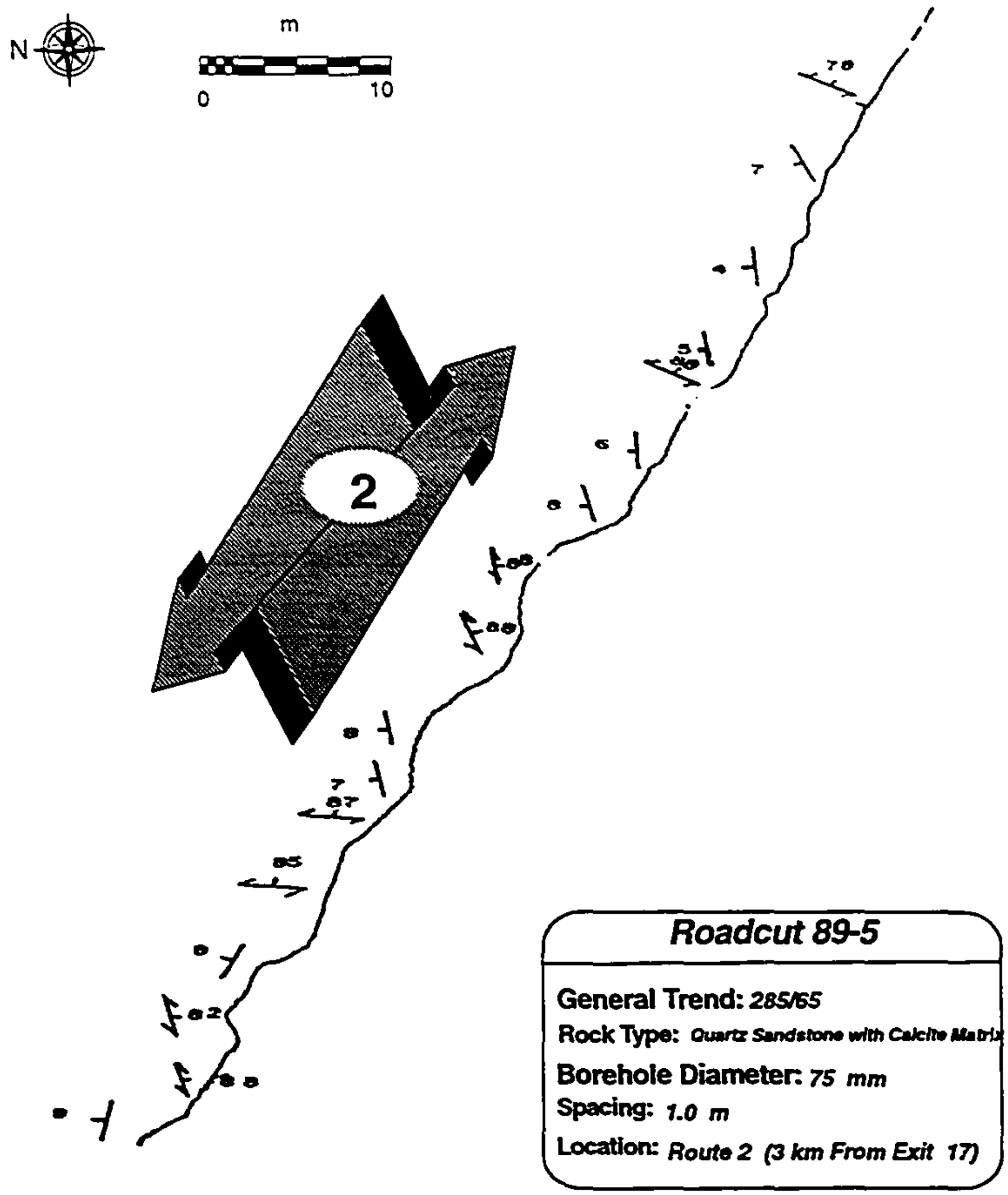

Figure 7.11 : Simplified structural geology of roadcut number 5 along Highway 89.

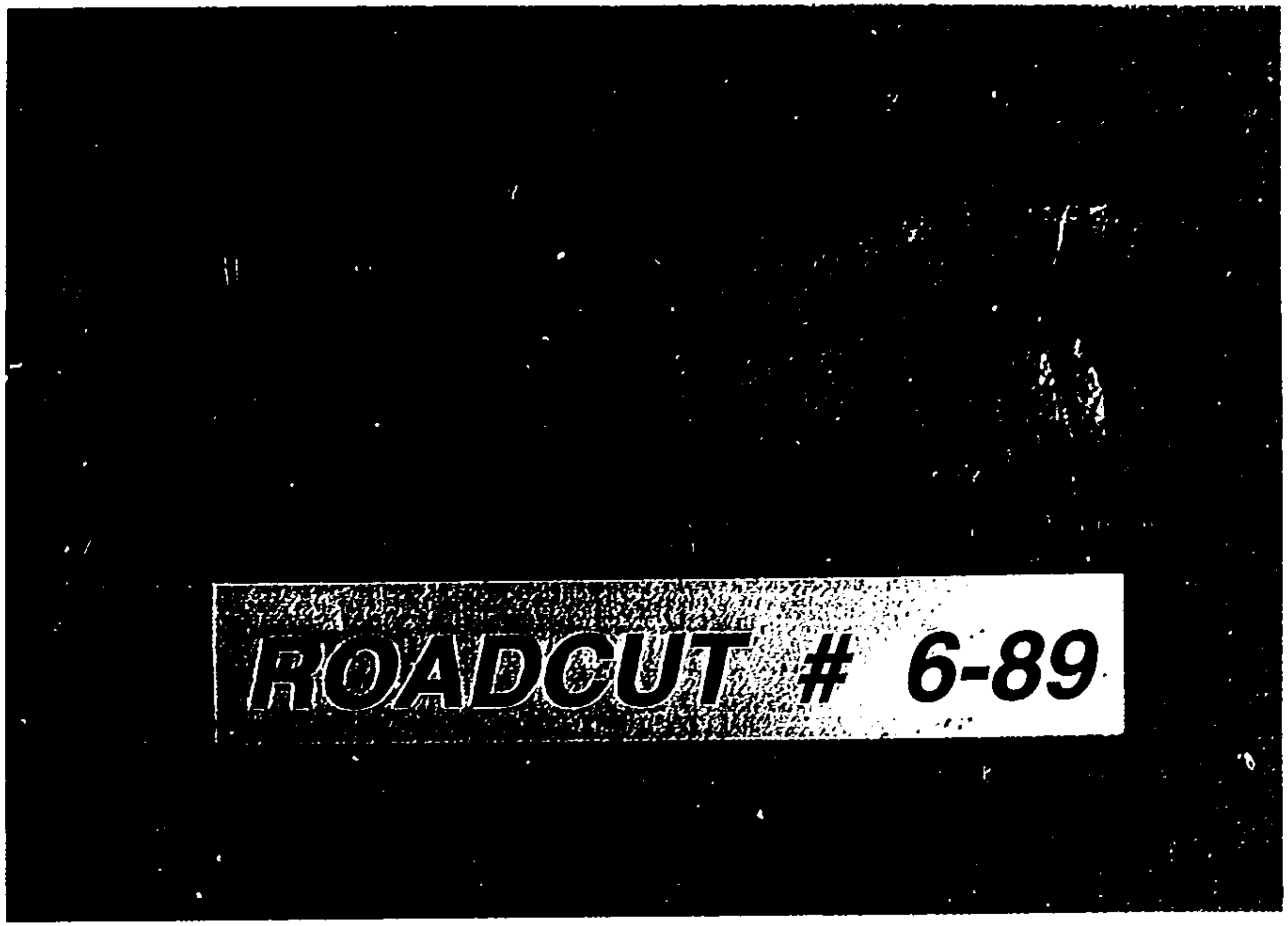

Figure 7.12 : Roadcut 6-89 located 79 km from the Canadian border along Highway 89, Vermont.

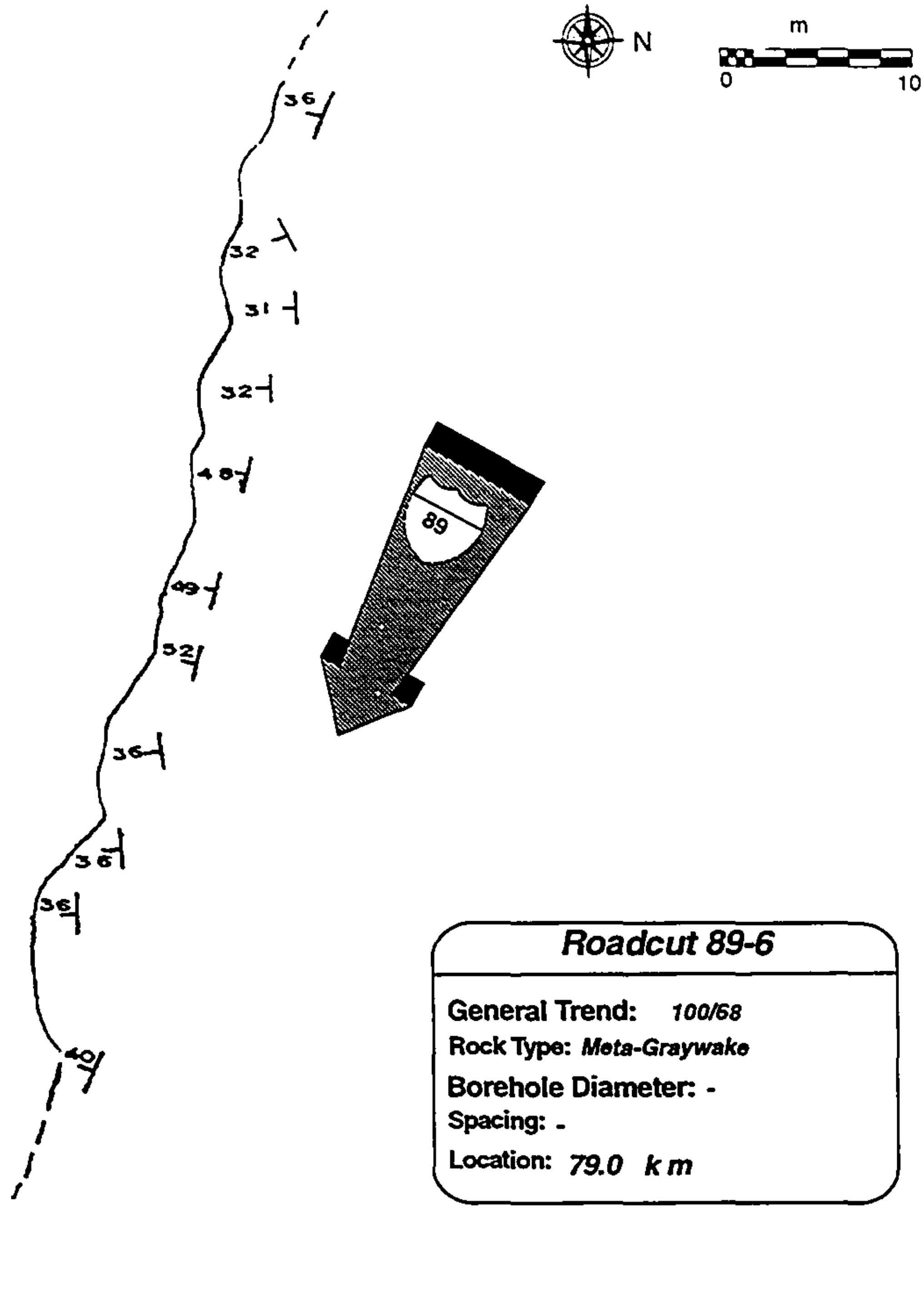

Figure 7.13 : Simplified structural geology of roadcut number 6 along Highway 89.

Figure 7.14 : Roadcut 7-89 located 94 km from the Canadian border along Highway 89, Vermont.

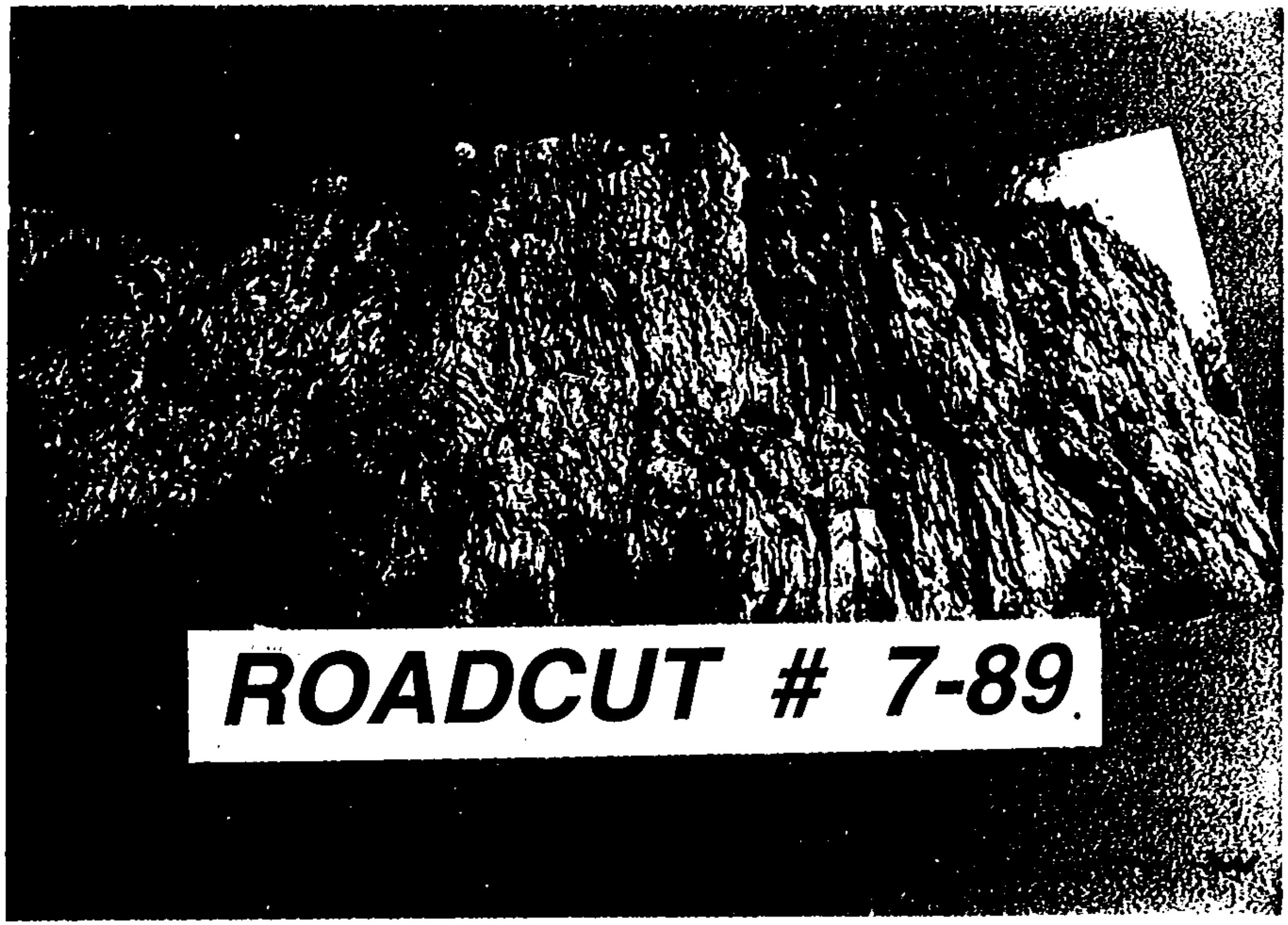

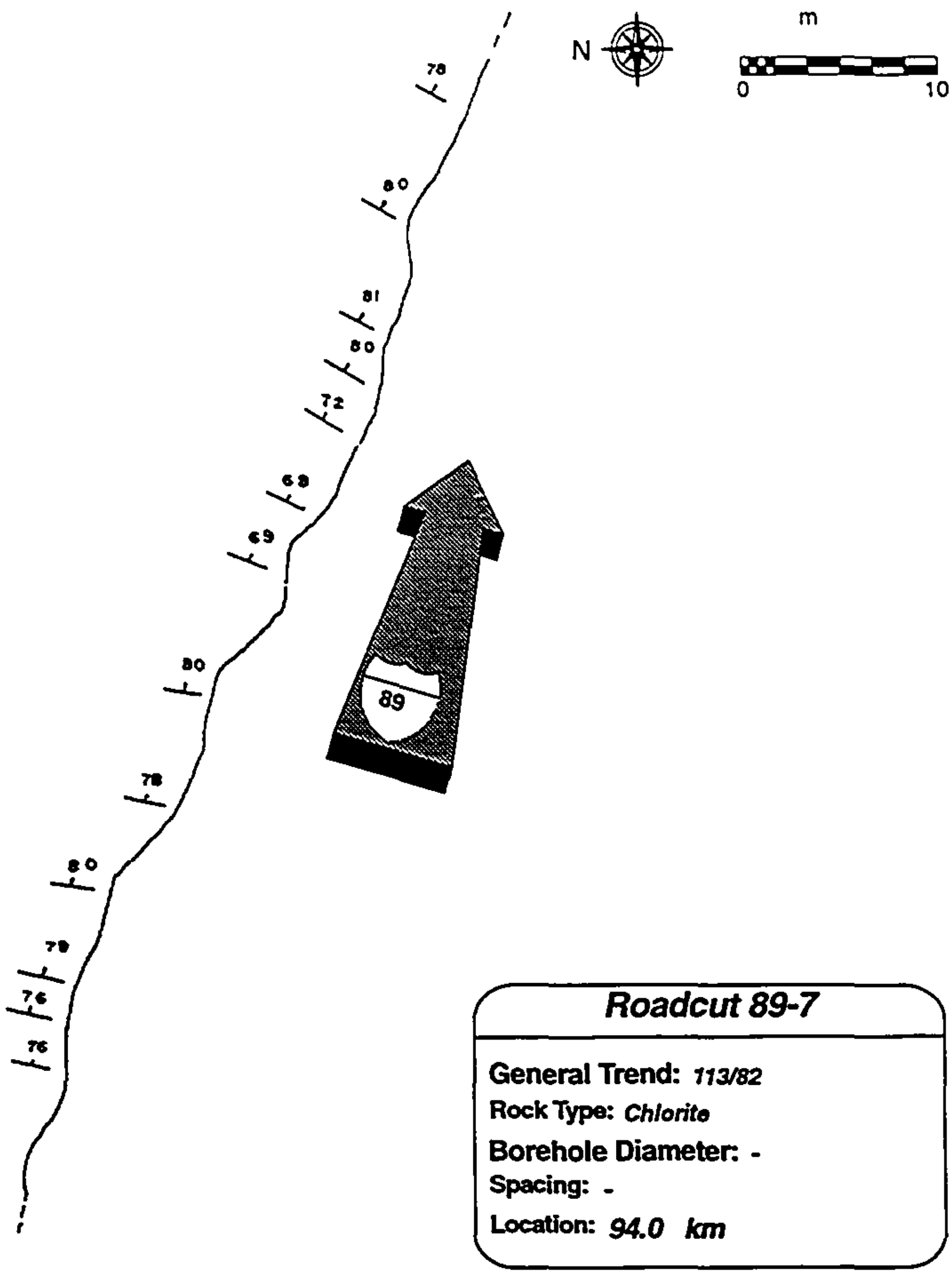

Figure 7.15 : Simplified structural geology of roadcut number 7 along Highway 89.

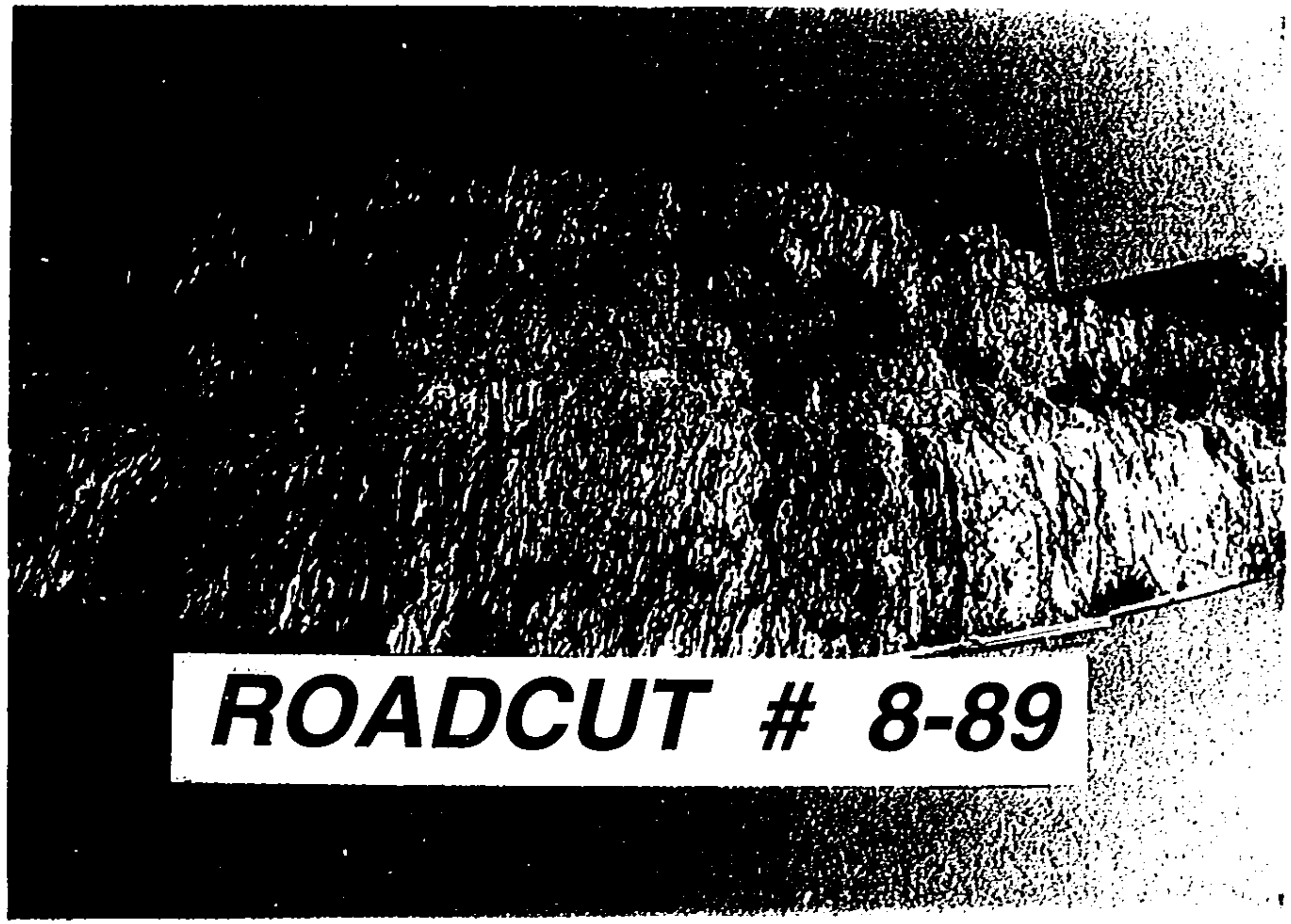

Figure 7.16 : Roadcut 8-89 located 61 km from the Canadian border along Highway 89, Vermont.

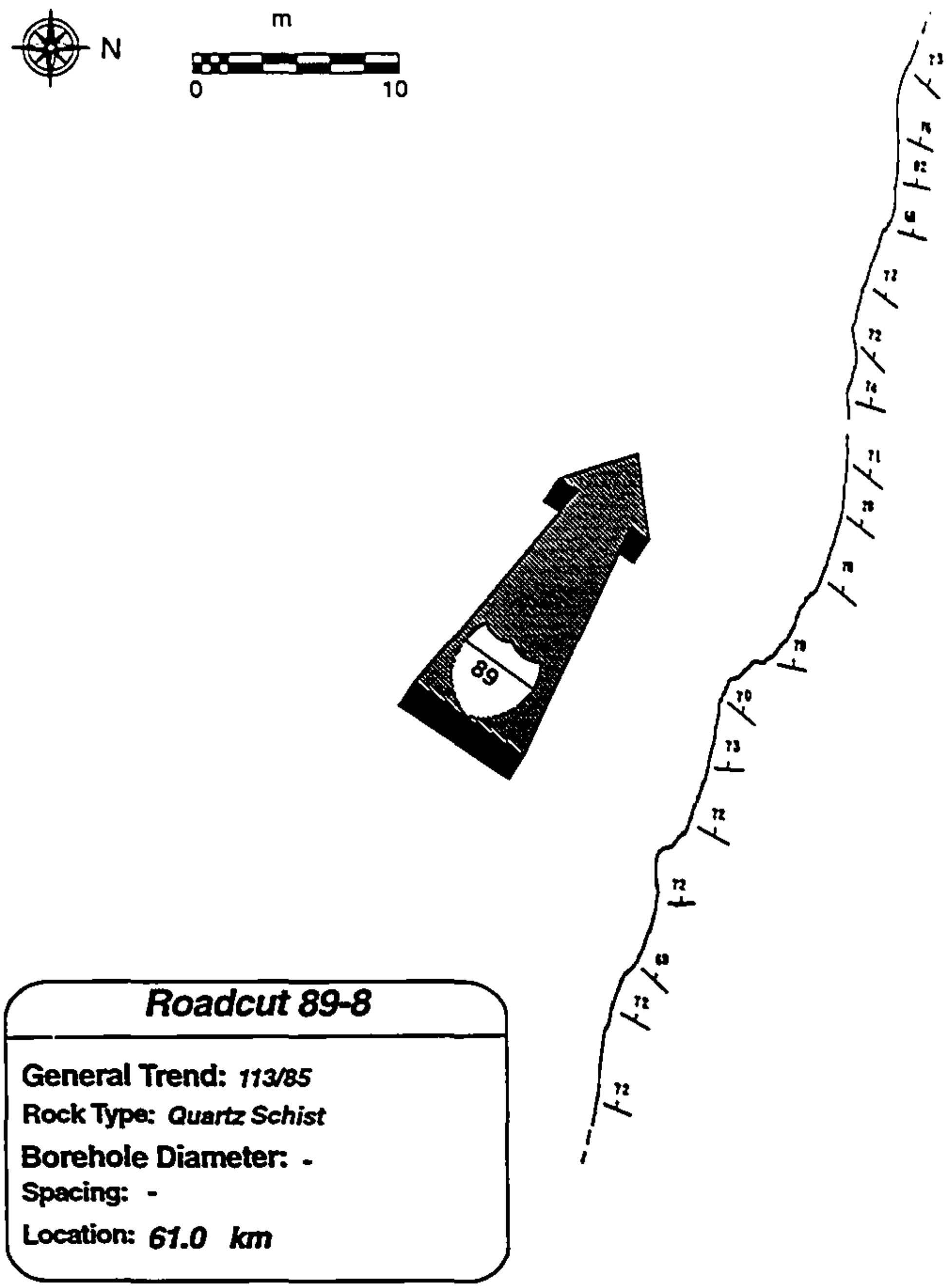

Figure 7.17 : Simplified structural geology of roadcut number 8 along Highway 89.

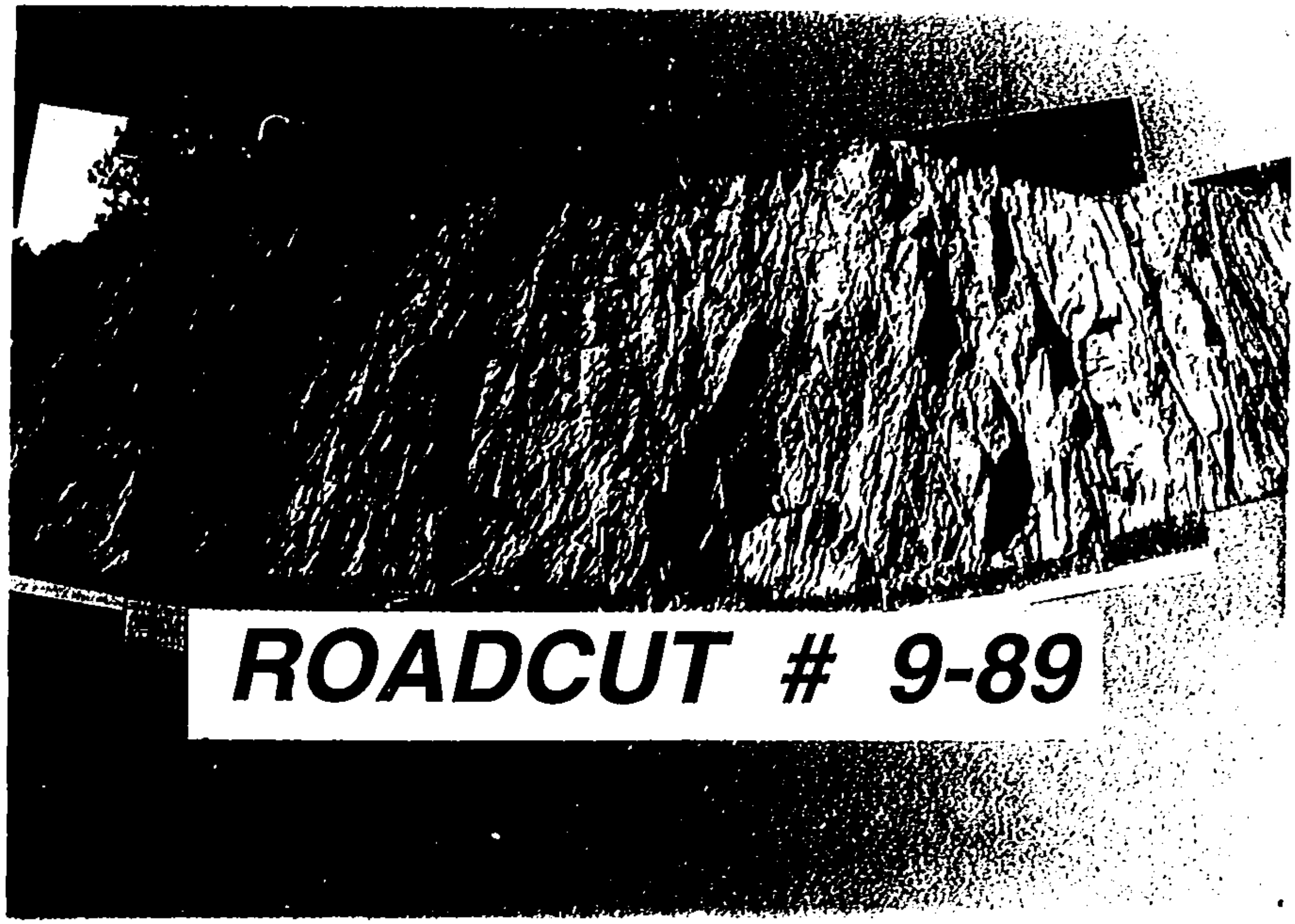

Figure 7.18 : Roadcut 9-89 located 60 km from the Canadian border along Highway 89, Vermont.

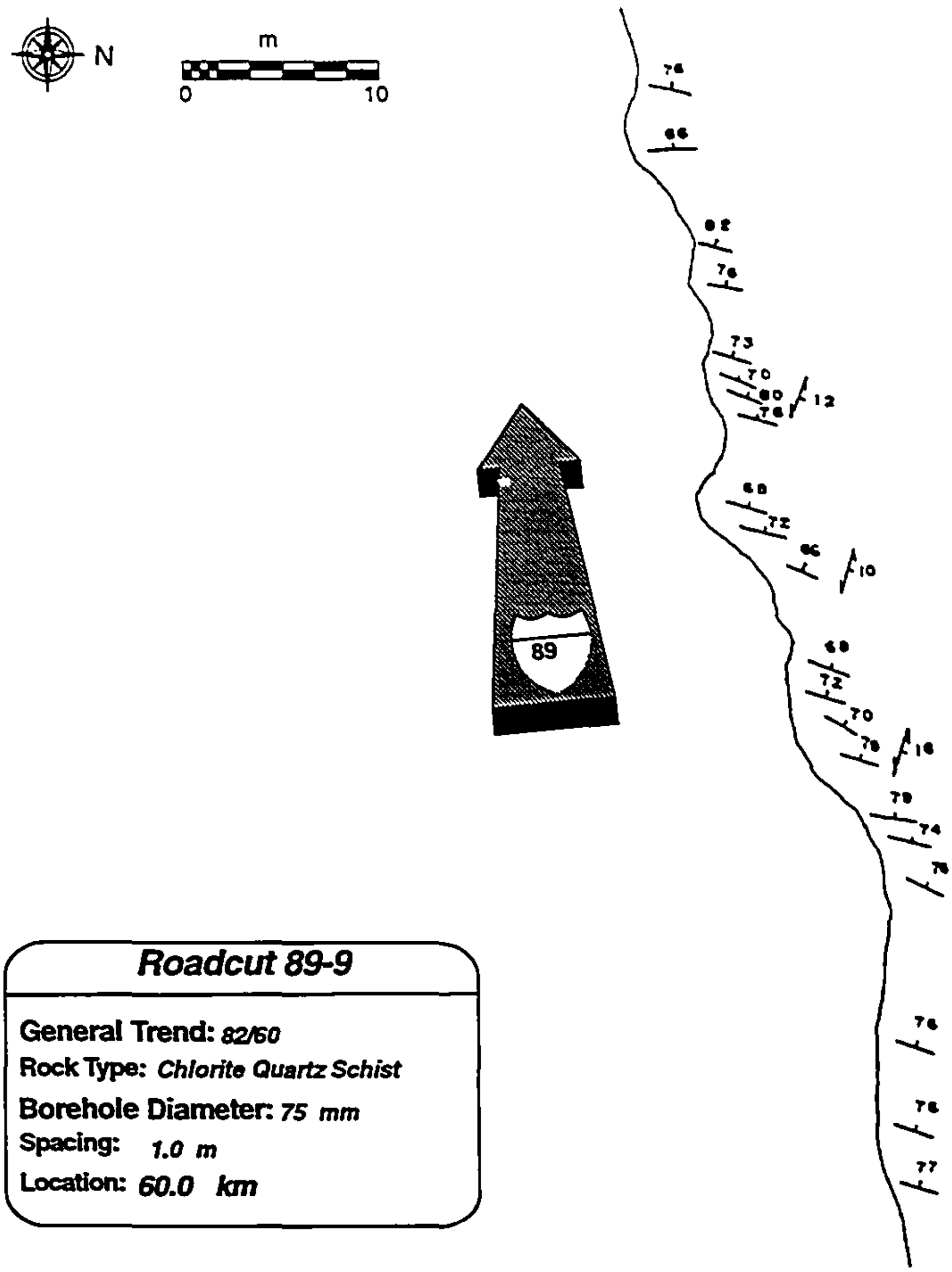

Figure 7.19 : Simplified structural geology of roadcut number 9 along Highway 89.

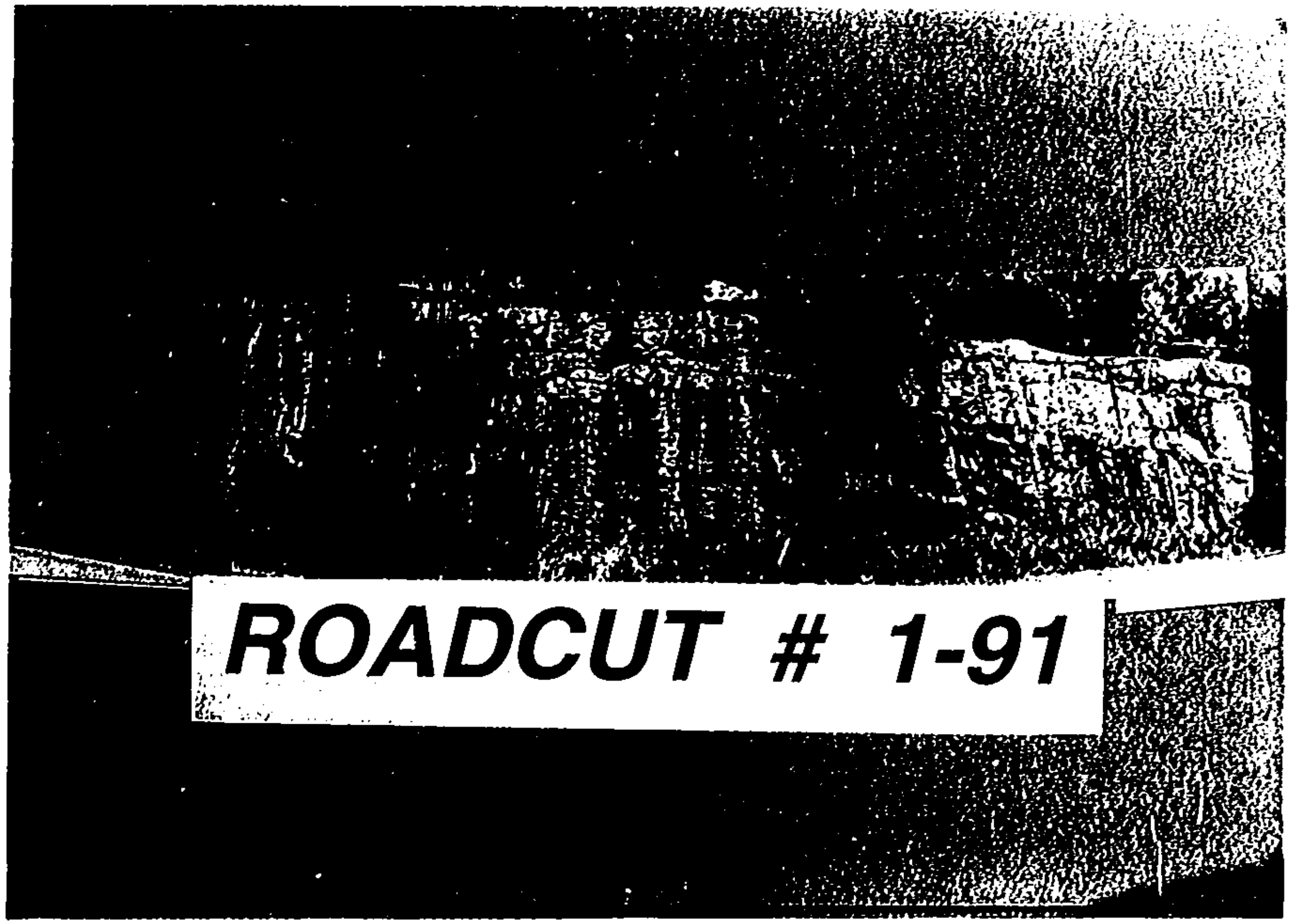

Figure 7.20 : Roadcut 1-91 located 11 km from the Canadian border along Highway 91, Vermont.

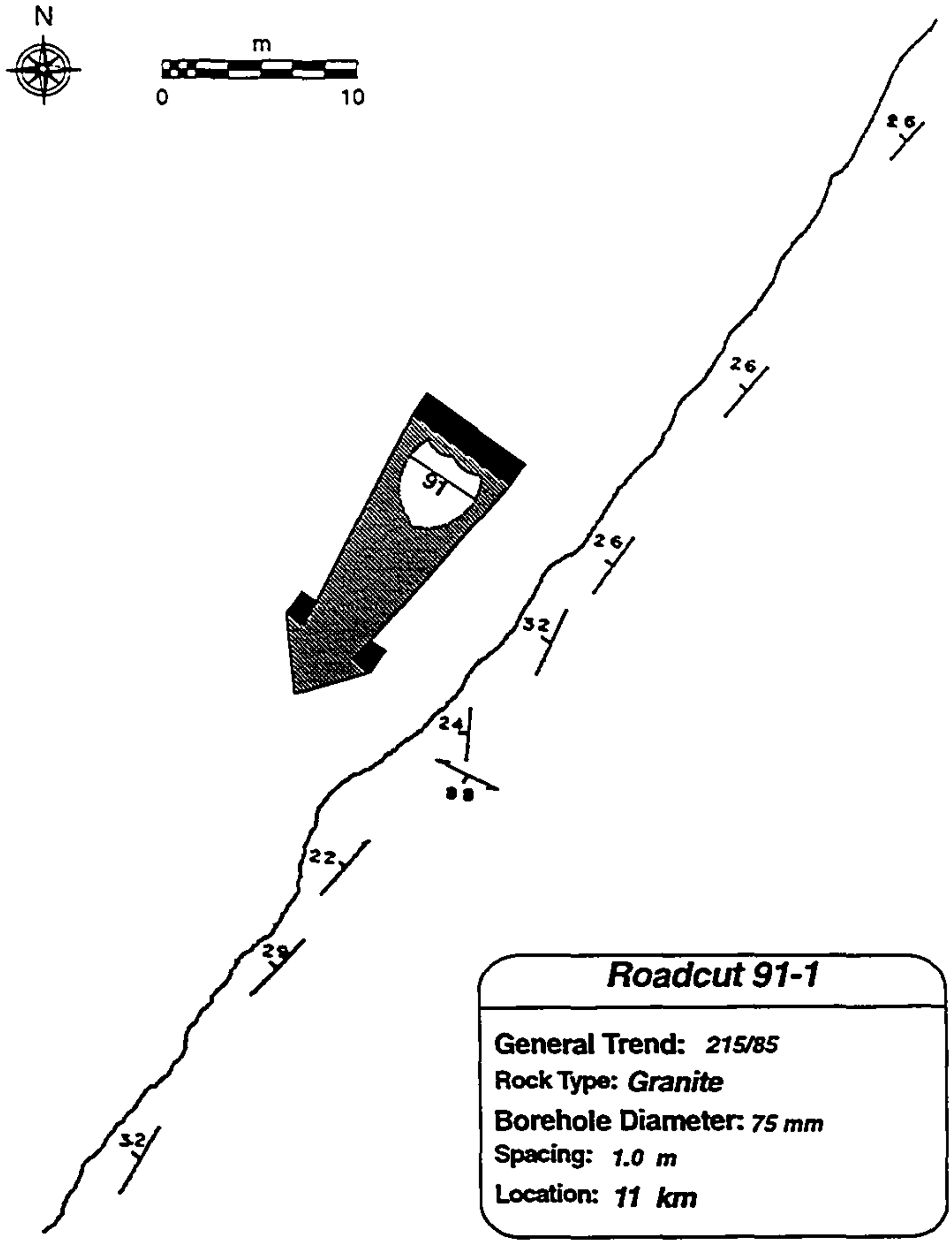

Figure 7.21 : Simplified structural geology of roadcut number 1 along Highway 91.

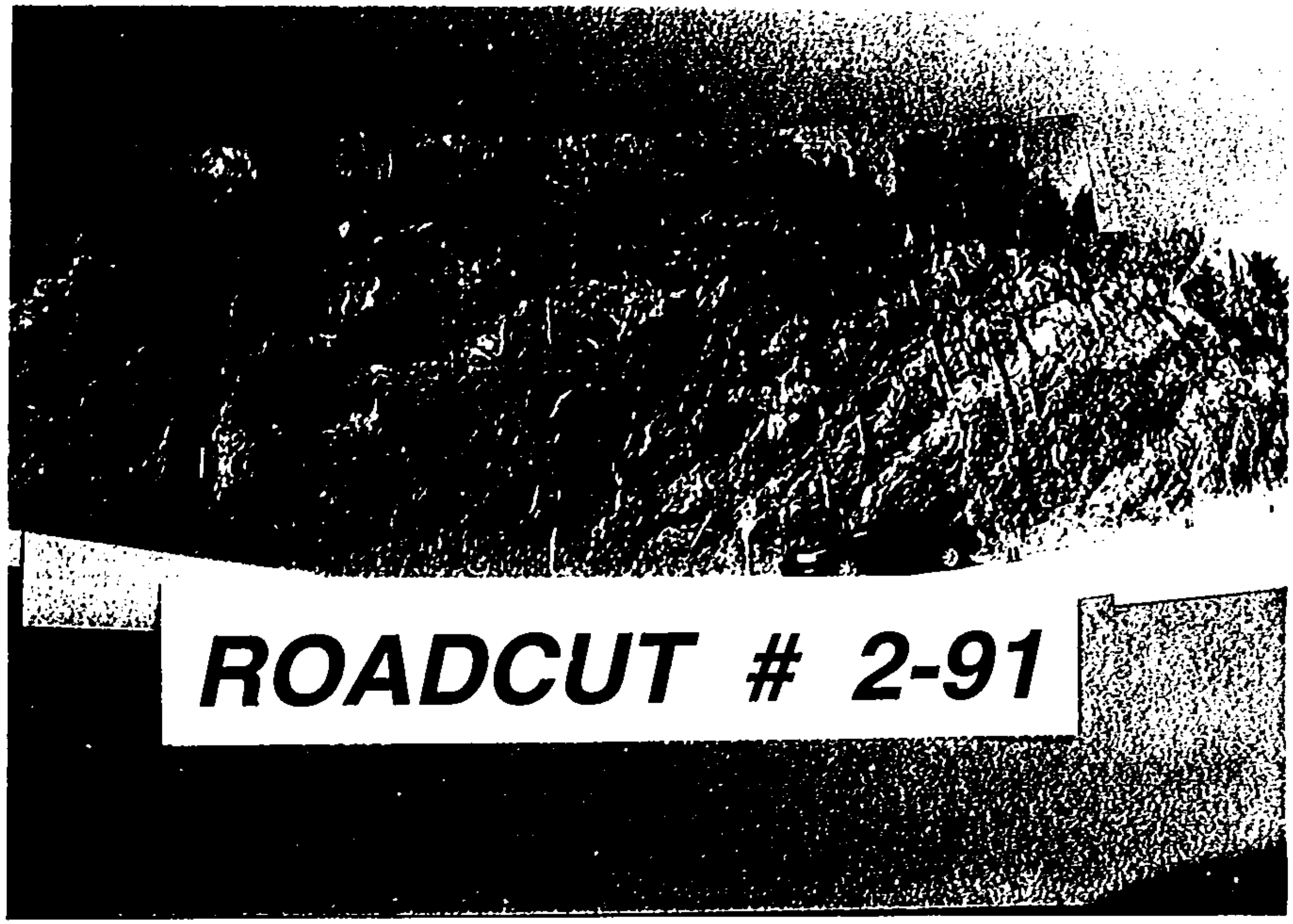

Figure 7.22 : Roadcut 2-91 located 27 km from the Canadian border along Highway 91, Vermont.

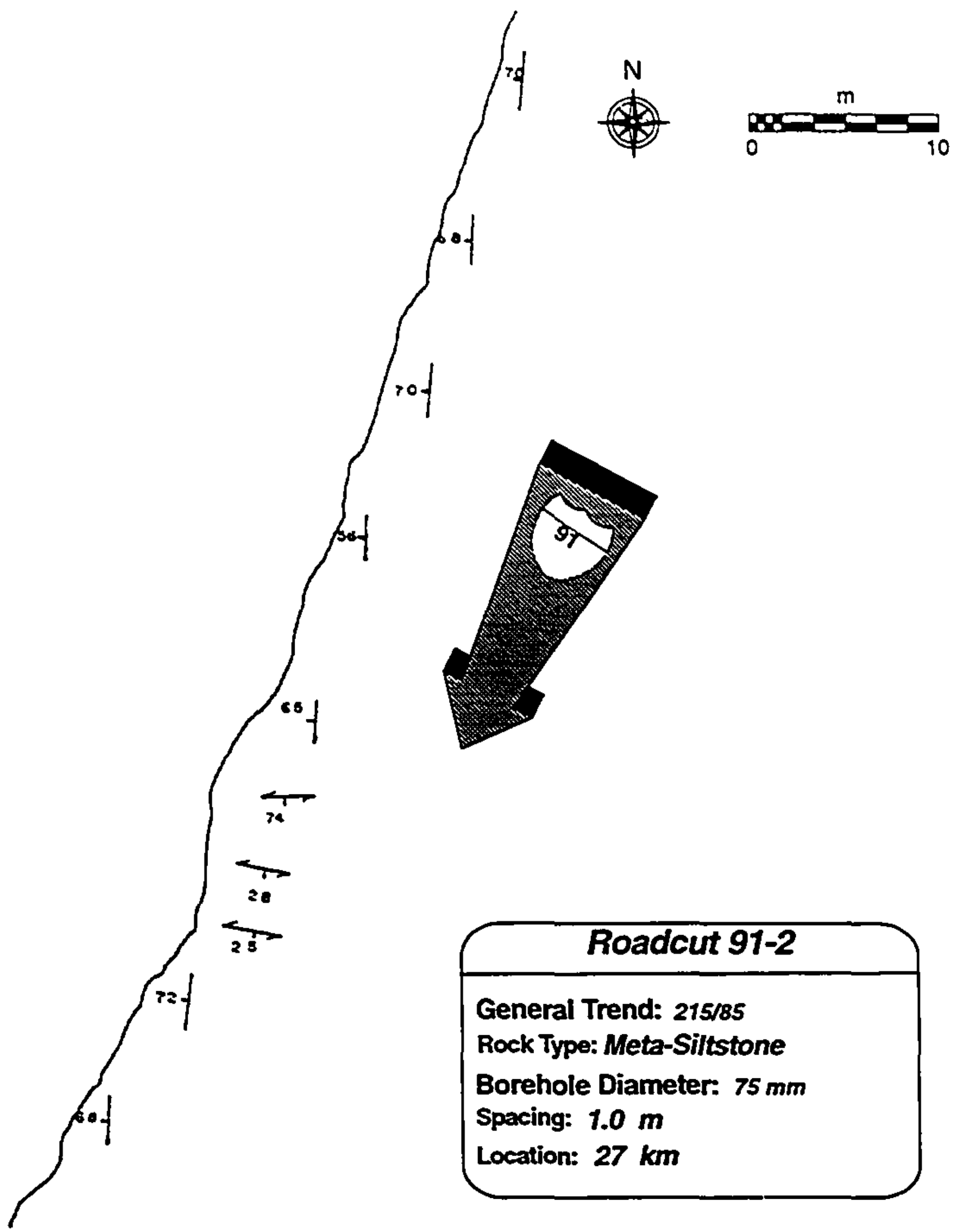

Figure 7.23 : Simplified structural geology of roadcut number 2 along Highway 91.

Figure 7.24 : Roadcut 3-91 located 34 km from the Canadian border along Highway 91, Vermont.

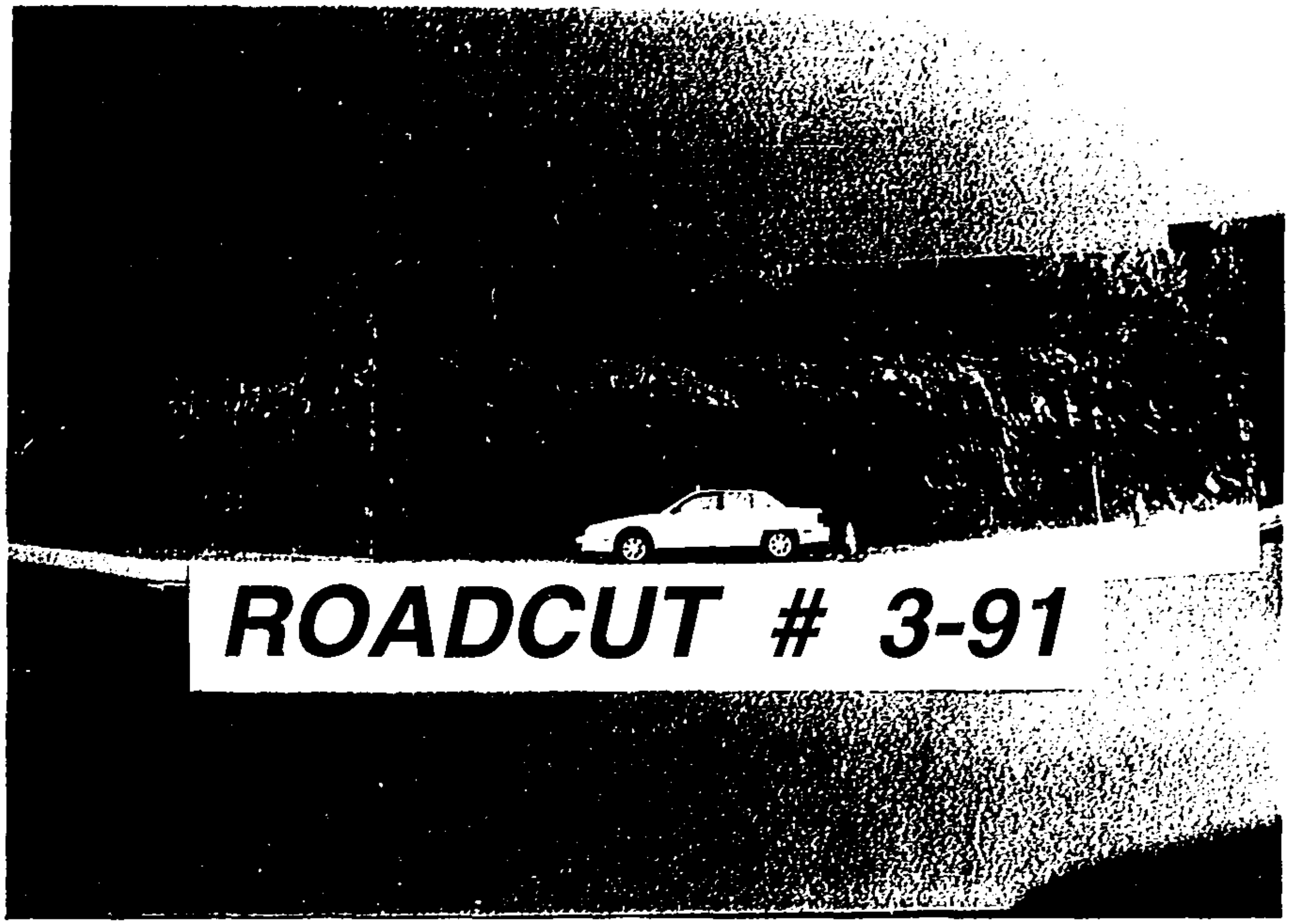

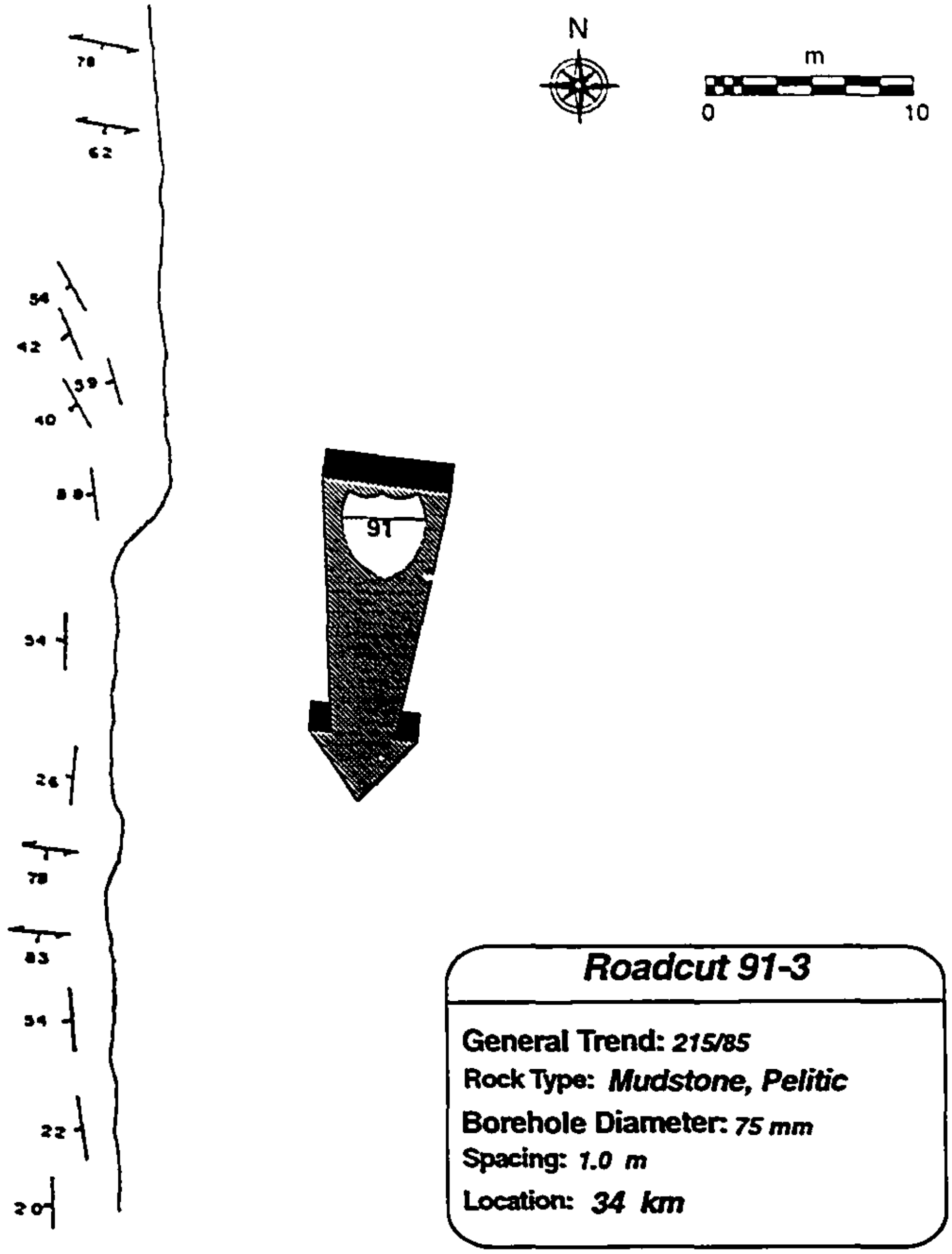

Figure 7.25 : Simplified structural geology of roadcut number 3 along Highway 91.

Figure 7.26 : Roadcut 4-91 located 41 km from the Canadian border along Highway 91, Vermont.

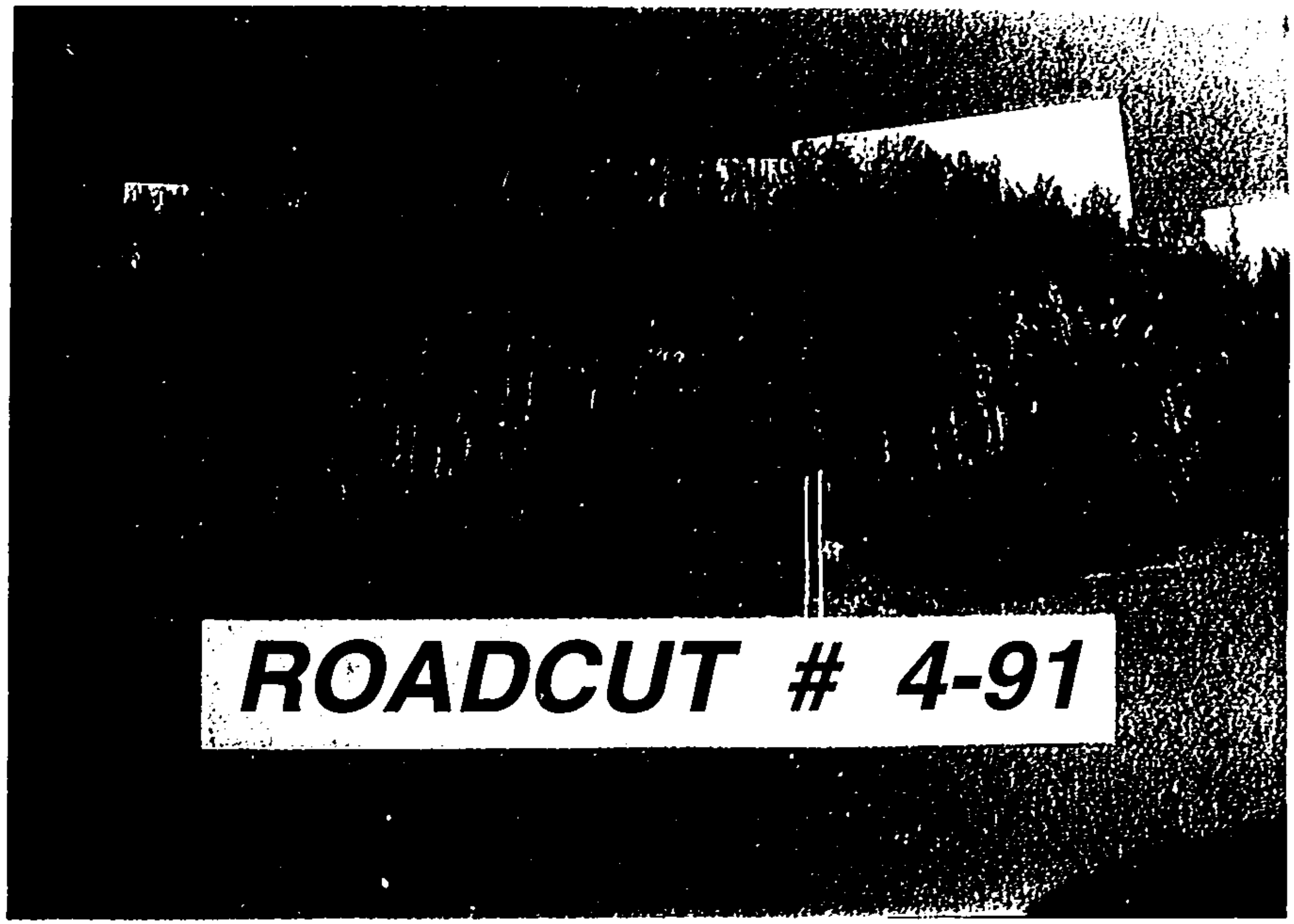

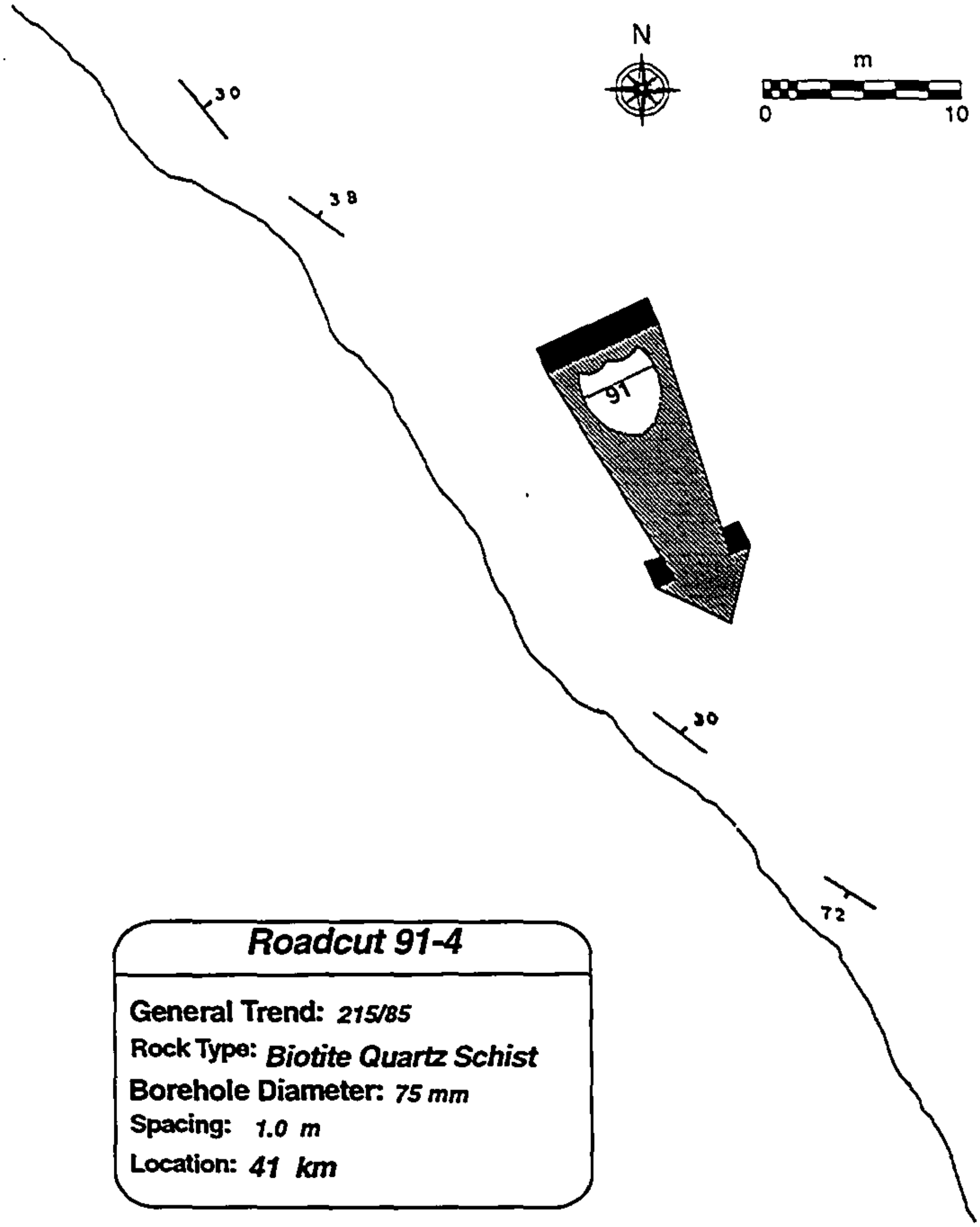

Figure 7.27 : Simplified structural geology of roadcut number 4 along Highway 91.

Figure 7.28 : Roadcut 5-91 located 50 km from the Canadian border along Highway 91, Vermont.

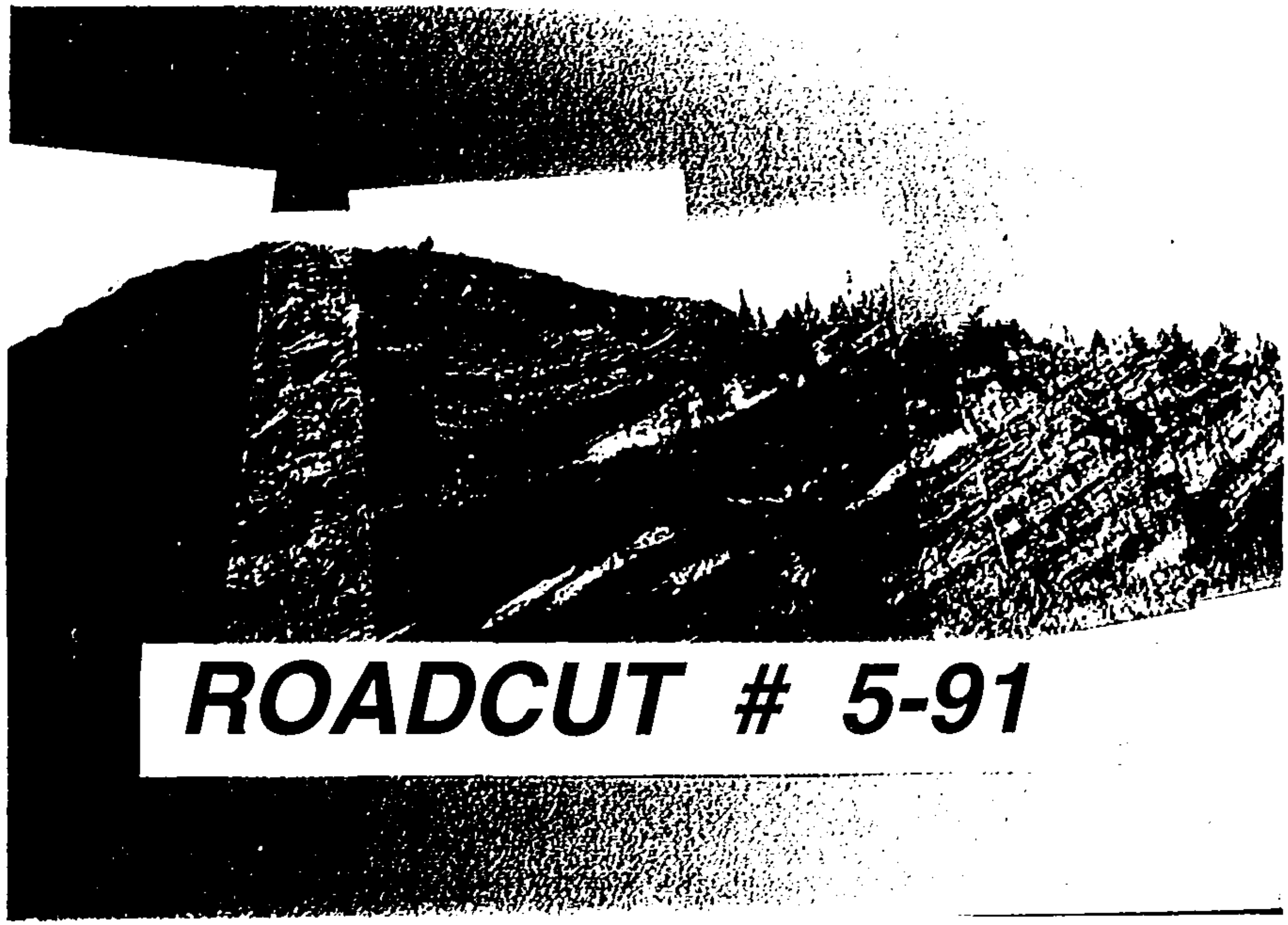

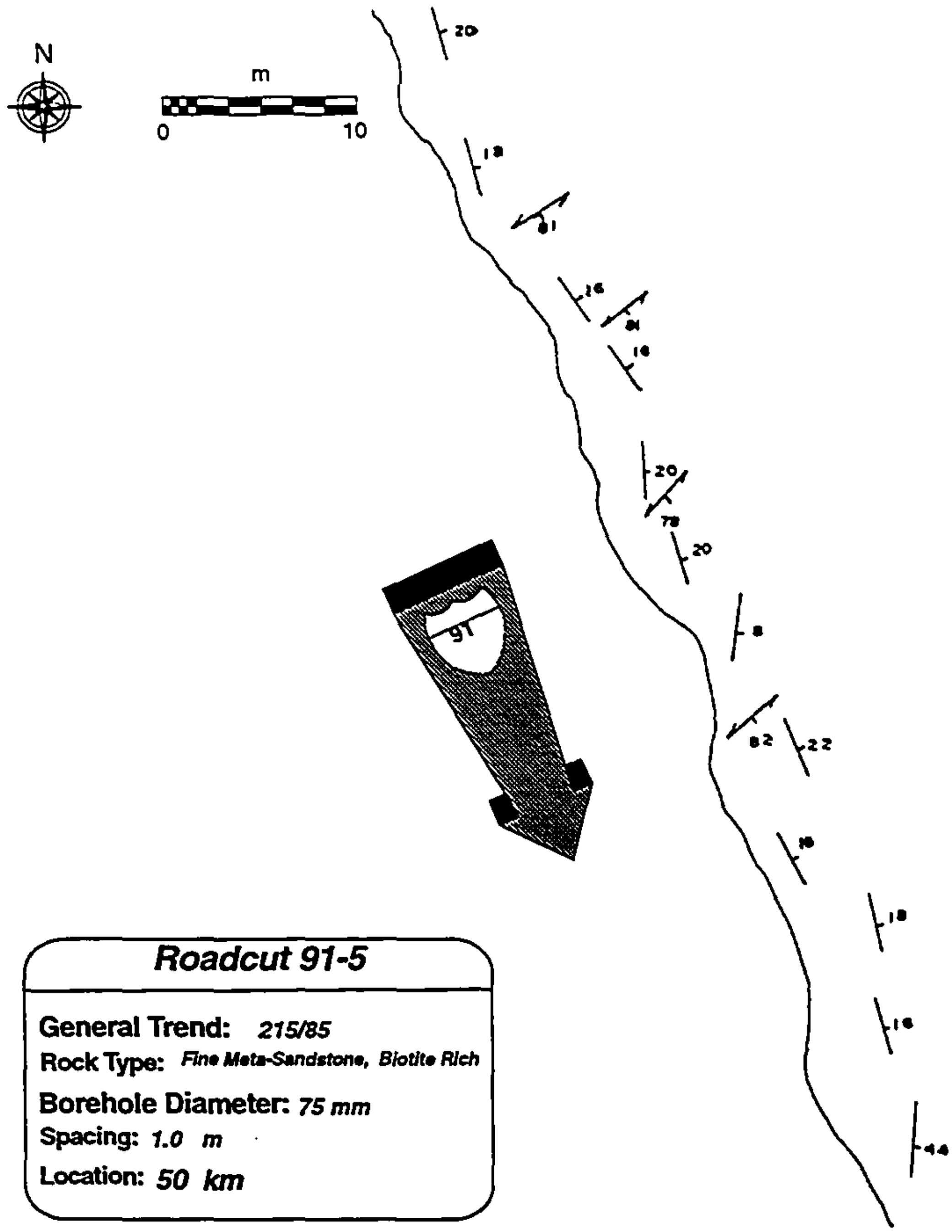

Figure 7.29 : Simplified structural geology of roadcut number 5 along Highway 91.

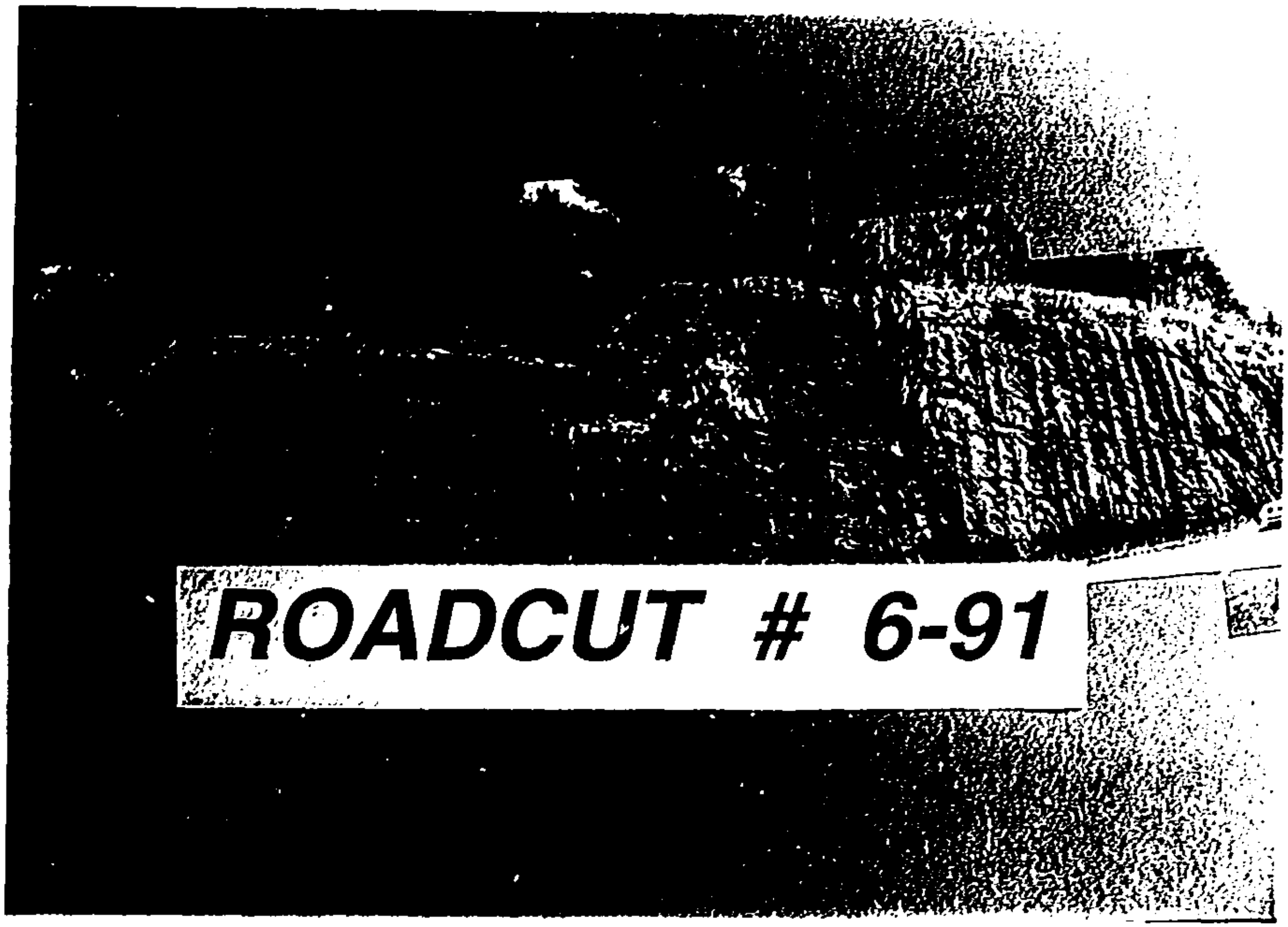

Figure 7.30 : Roadcut 6-91 located 72 km from the Canadian border along Highway 91, Vermont.

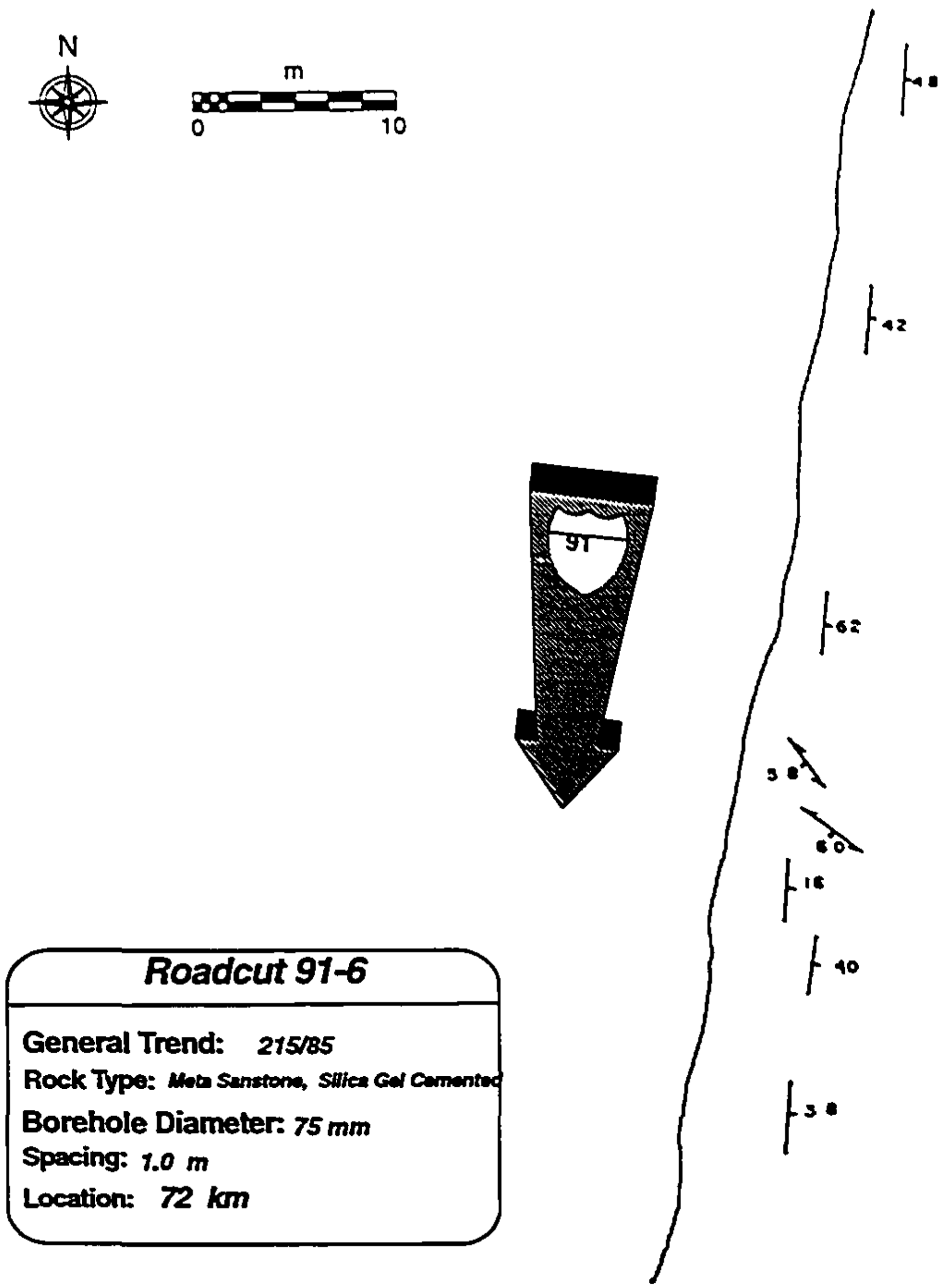

Figure 7.31 : Simplified structural geology of roadcut number 6 along Highway 91.

Figure 7.32 : Roadcut 7-91 located 72 km from the Canadian border along Highway 91, Vermont.

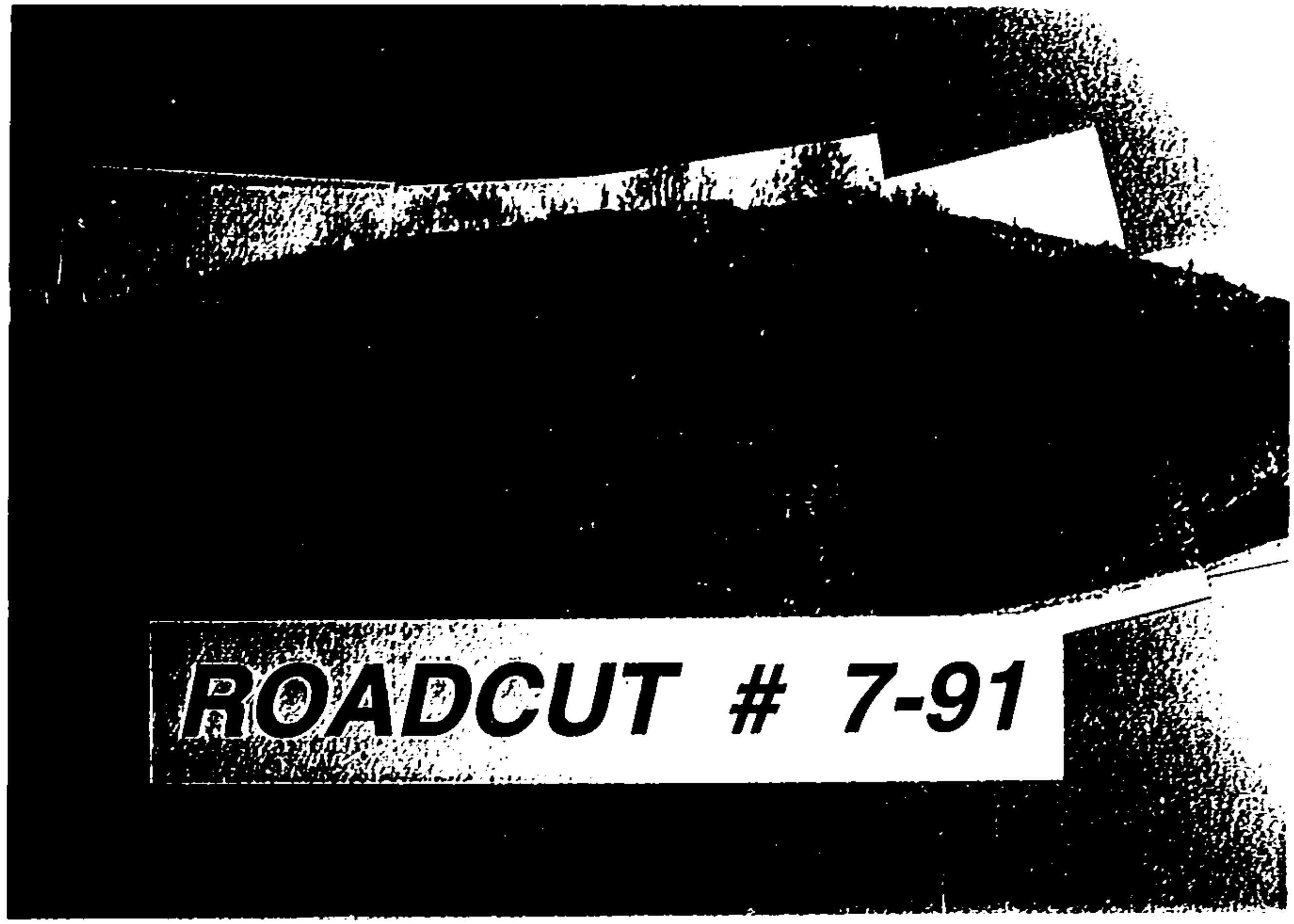

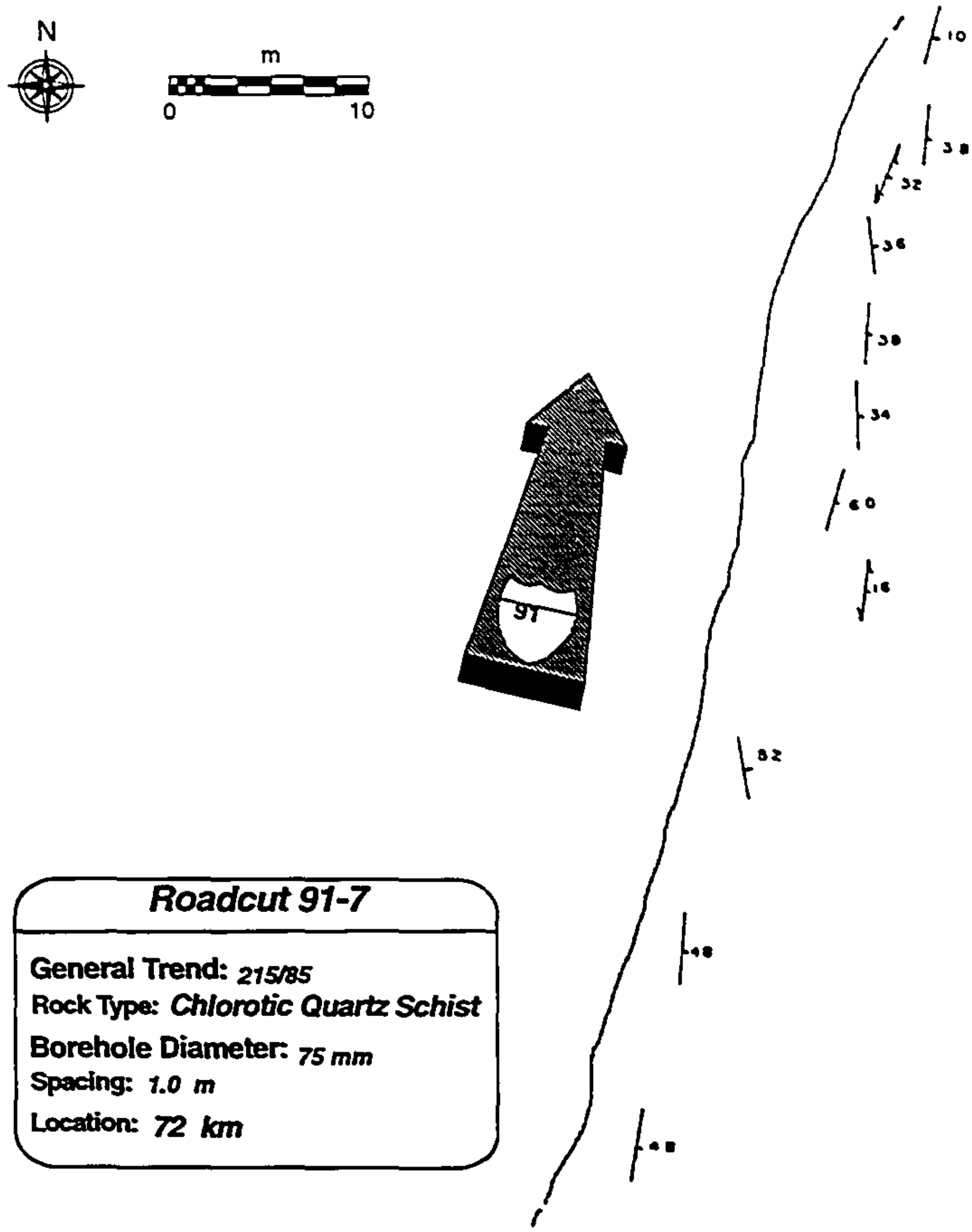

Figure 7.33 : Simplified structural geology of roadcut number 7 along Highway 91.

Figure 7.34 : Roadcut 8-91 located 44 km from the Canadian border along Highway 91, Vermont.

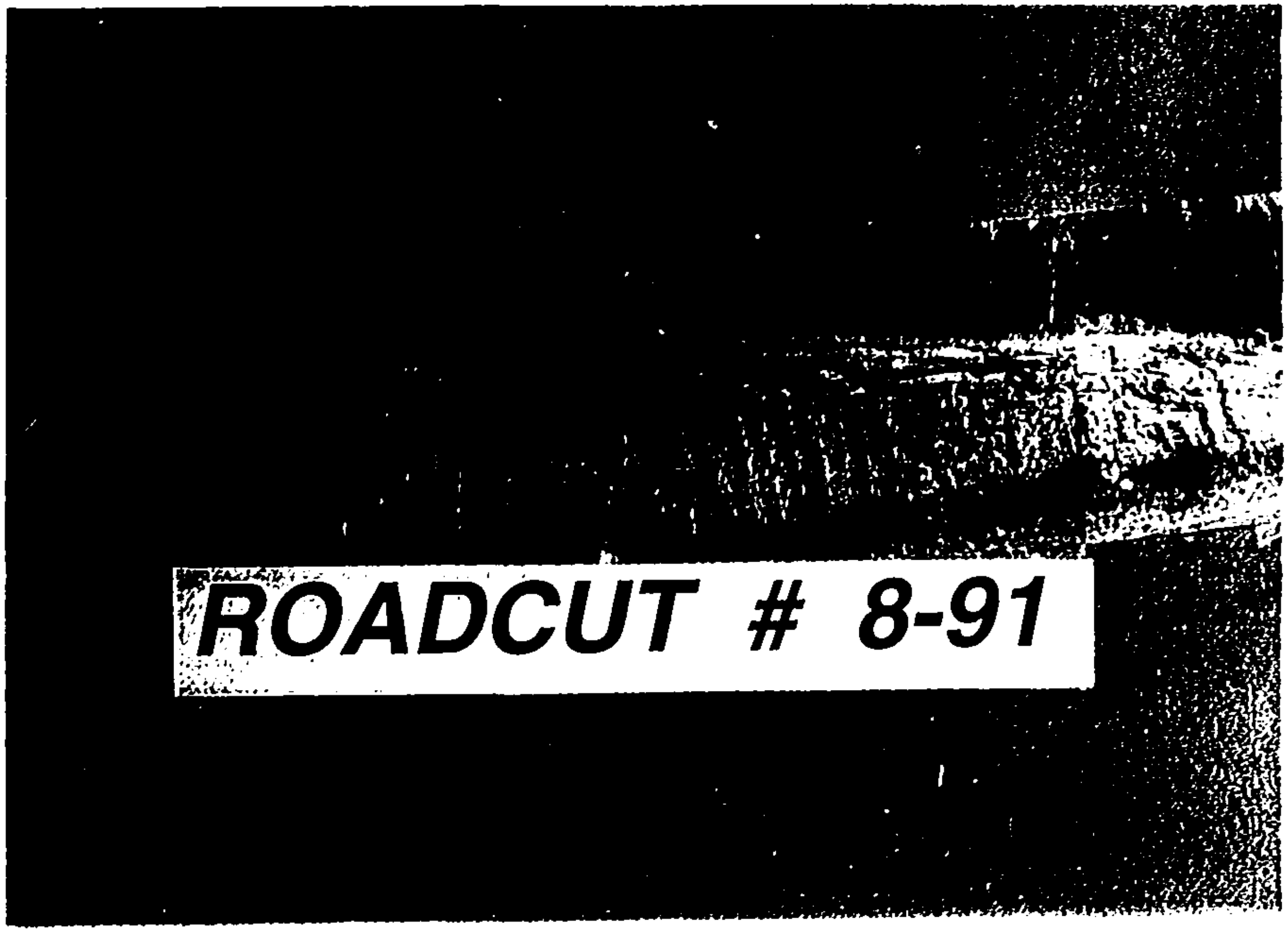

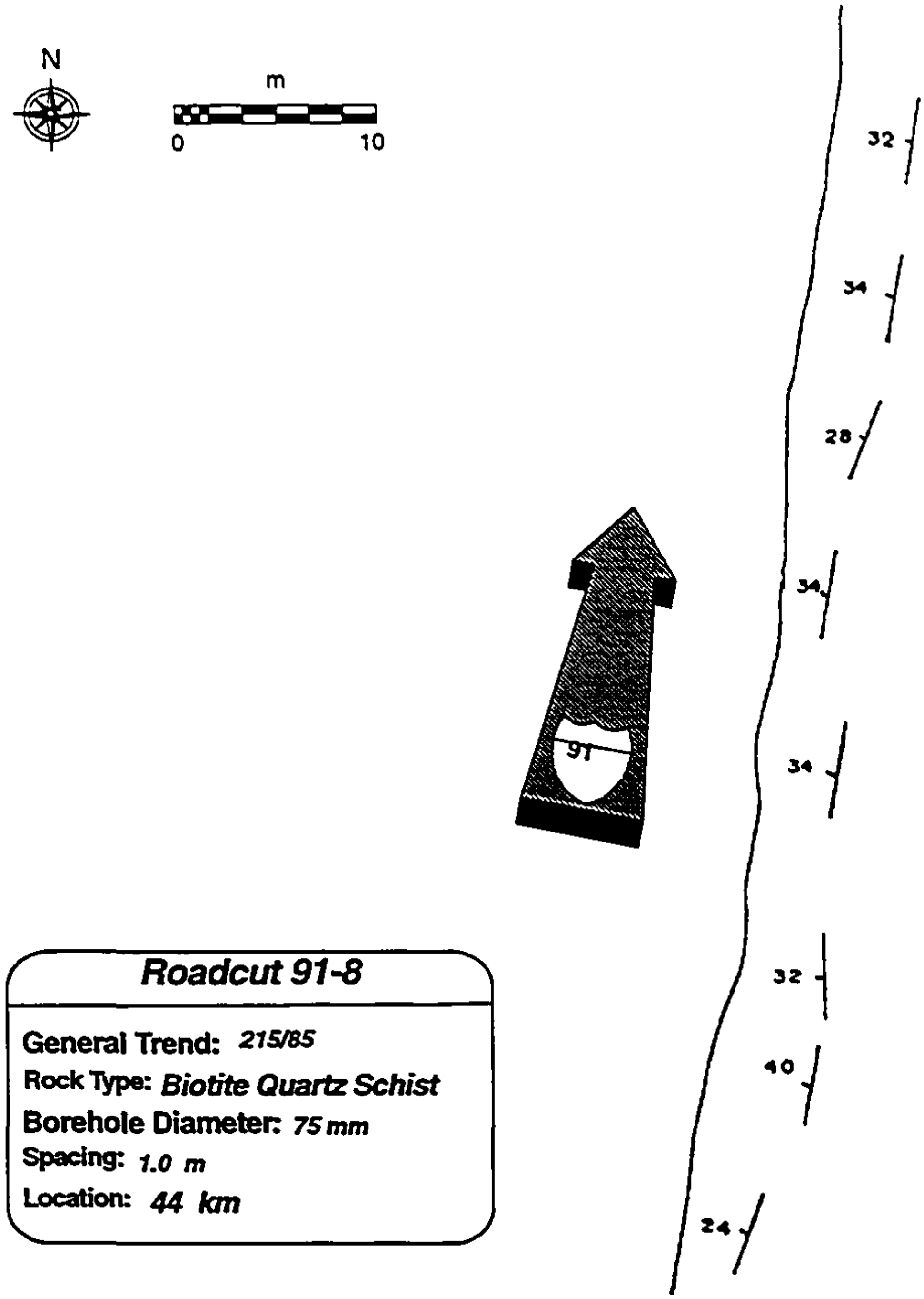

Figure 7.35 : Simplified structural geology of roadcut number 8 along Highway 91.

CHAPTER 8

CONCLUSIONS

8.1 OVERALL CONCLUSIONS

In this study, the mechanism of wall-control blasting methods has been analyzed in detail by the numerical analysis, supported by controlled field experiments, and critical examination of selected roadcuts in a large scale. A key emphasis has been on stress distribution around exploding boreholes and the nature of resulting fractures, especially in the presence of various types of discontinuities.

A total of 32, single and multi-hole blasts were conducted in the experimental program. The boreholes ranged from 50 mm to 150 mm in diameter, and the explosive ranged between 11 mm and 50 mm in diameter. Three different types of explosives with varying detonation properties were employed in the tests. The test sites represented two different rock types, a bedded limestone and a structurally complex peridotite. In addition, 17 roadcuts along selected highways, spanning a total surface area of over 1000 m long × 20 m high, were mapped in detail, to establish correlation between the theoretical prediction and the controlled blasting experiments.

In wall-control blasting process, the fractures are generated around each hole by the explosion pressure immediately behind the detonation front, and then extended or opened by the penetration of explosion gases into them. Numerical analysis shows that the tensile stresses in the region between the holes are much greater than the other regions around the holes. This tension zone between the holes, augmented further by superposition of stresses around the midpoint, in the primary cause of preferential crack growth along the centreline.

The calculated borehole pressure for the experimental tests also show that a crack between the holes is created by this process, and the quasi-static pressure (borehole pressure) plays a principal role in developing this crack, resulting in a smooth blast face between the holes. The full fracture process is due to a combination of the effects of dynamic stress waves and the subsequent quasi-static borehole pressure.

In normal blasting practice, the magnitude of the stresses at the middle of spacing between two holes is insignificant to cause onset of fracture. Numerical analysis shows that the stresses become very small compared to the applied pressure on the borehole wall for distances more than two borehole diameter.

For normal wall-control practices, a burden can be equated to an infinite burden when the ratio of that to spacing becomes greater than unity. Numerical analysis also shows that for a specified blasting condition (e.g. a borehole pressure of 2000 MPa, and a 12 MPa tensile strength of target rock) the spacing between holes can not exceed 15 borehole diameters for onset of tensile crack at the midpoint between the holes. The spacing would of course changes with different borehole pressure or strength of rock.

On the basis of numerical analysis, it is predicted that the shape of fracture zone around each hole would be approximately elliptical. The major axes of these ellipses would coincide with the centreline between the holes. As burden and spacing decrease, this zone would change from the elliptical to a circular shape. Significant backbreak as well as humps between the holes (caused by unbroken rock mass) are also predicted by the shape of these fracture zones.

The ratio between charge and borehole diameters (decoupling ratio) plays a critical role on wall-control blasts. For typical commercial explosives, this ratio should be smaller than 0.5, and preferably between 0.2 and 0.3 for infinite burden, and between 0.3 and 0.4 in the case of finite burden.

The results of numerical analysis, blasting experiments and field observations, show that the nature of discontinuities and the blast geometry (i.e. spacing and burden) play the most important role in generating a smooth blast face.

A discontinuity located parallel to the centreline (final design line) behind the holes has maximum effect on the final result of the wall-control blasts. Numerical analysis shows that presence of weakness plane causes the tensile stress to reach the maximum value at the boundary of the weakness plane; the stresses immediately drop to zero on the wall of plane.

The results obtained by controlled blasting experiments and field observation of several established roadcuts have been shown to be in very good agreement with model predictions. In the case of a discontinuity parallel to the contractive behind the holes, this discontinuity would essentially represent the final wall, provided its distance from the centreline is less than half of the borehole spacing. A similar parallel discontinuity but located at the front of holes, leads to considerable overbreak and undamaged 'humps' between holes.

A discontinuity oriented perpendicular to the face at the midpoint is shown to have minimum effect on the blast results. When the distance between the perpendicular weak plane is changed by moving it closer to one of the holes, the tensile stress field between it and the borehole increases. This leads to creation of an intense fracture zone between the hole and the discontinuity. The results of field observation in the roadcuts show that the joints perpendicular to the free face with spacing smaller than the borehole spacing cause damaged area between the holes and the joints.

Numerical analysis predicts that fractures would be developed along the shorter distance between an inclined weak plane and the nearby borehole. A triangular damage zone occur between each hole and discontinuity, and the degree of the damaged area depends on the angle between the discontinuity and the final face. The results of experimental tests and field observations in the roadcuts also show a Z-shaped outline on the final face, when an inclined discontinuity crossed the final face. The area of the damaged zone is greater than that predicted by the numerical analysis, due to opening of pre-existing fracture by the explosion gases.

The width of a discontinuity as well the nature of material filling it are key parameters effecting the blast results. The results obtained by both numerical analysis and experimental investigation show that as the width of the discontinuity increases the size of the damage zone also increases. This applies to open joints or joints filled with low-strength gouge materials. Joints cemented by strong materials, have no significant effect on stress field. Both experiments and theoretical predictions show that an open discontinuity, 50 mm in width or more, essentially behaves like a free face.

All pre-existing fractures are further opened by penetration of the explosion gases. The length and width of these openings depend on the distance of the discontinuity from the blasthole. An opened discontinuity acts as a fracture terminator, but secondary fractures can be created by the penetration of the explosion gases into narrow joints. It can cause a wedging action on the wall of the fracture and create a tensile stress zone behind the discontinuity. If this stress becomes high enough (i.e. greater than the tensile strength of rock), a second fracture could develop at the other side of the discontinuity.

Investigation of established roadcuts shows that, beside blast design, the three critical parameters affecting the final wall, are structure, strength of rock, and hole deviation. Most of the damage zones are seen to be confined to regions with the irregular hole deviations. In these regions, the holes either cross each other or the spacing of holes along the face is much more random, spacing being much larger or smaller than design guidelines. Systematic hole deviations (i.e. holes diverging in the same direction) are most apparent in regions characterized by pronounced bedding. The degree of deviations depends on the orientation, thickness and the properties of the bedded layers. This type of systematic hole divergence usually have minium effect on the final result of the blasts.

8.2 Claims for Original Research

1. The mechanism of the wall-control blasting methods was studied by numerical analysis and controlled field experiments.

2. The effect of parallel, perpendicular and inclined discontinuities on the stress distribution around a single hole and multiple holes was studied.

3. The results predicted by the numerical analysis were verified by the experimental investigation in two different rock types at two sites.

4. The results of both numerical analysis and field investigation were compared with those at 17 large-scale roadcuts along two highways.

5. The important role of the characteristics on fracture formation and the quality of

the final wall has been demonstrated in details.

8.3 Future Direction of Research

Despite the good agreement between theoretical prediction and experimental findings in this investigation, several important area in wall-control blasting still remain unexplored. This applies to both the explosive source and blast geometry as well to characteristics of rock mass.

All explosive charges are initiated , as in the present investigation, at the bottom of the hole. This given rise to a somewhat conically expanding stress field around the blasthole, due to the finite velocity of detonation in the explosives. The theoretical treatment, on the other hand, dealt with a truly cylindrical stress field. The latter can be only achieved in a borehole where the explosive charge is initiated simultaneously along its entire length. Calculation of detonation parameters in this case, would be much more difficult, but such initiation might lead to lower borehole pressures without the need for decoupling the charge from the borehole wall.

In the present study, two or more holes were detonated within 500 microseconds or less of each other. This was considered "simultaneous", but in terms of superposition of dynamic stresses and stress wave velocity in rock, this time-frame is too long. Blasting experiments should be carried out with higher precision detonators, when these become commercially available.

The information of stress distribution around exploding boreholes generated in this study represents some important findings, especially on the role of discontinuities. However, this is based on the theoretical predictions, not on actual measurements. It would be necessary to validate these estimates through actual measurement of dynamic stresses between boreholes, especially in the presence of discontinuities.

The correlation established between properties of rock (e.g. strength, acoustic impedance, etc.) and blast results is only qualitative. There is a need to design response of rock on a more fundamental basis, such as its fracture toughness, and fracture dynamics in general.

Finally, the relatively lower explosion gas pressure in extension and multiplication of blast-induced fractures around boreholes remains an active field of research. Until such time when this aspect of fracturation has been thoroughly understood and successfully modelled for actual blasting conditions, it will not be possible to establish a truly quantitative predictive model for wall-control blasts.

REFERENCES

Anon, 1987, "Explosives and Rock Blasting," Atlas Powder Company, Field Technical Operation, Dallas, Texas, U.S.A.

Ash, R.L., 1973, "The Influence of Geological discontinuities on Rock Blasting," Ph.D. Thesis, Dept. Min. Eng., University of Minnesota.

Aso, K., 1966, "Phenomena Involved in Pre-splitting by Blasting," Ph.D. thesis, Dept. Min. Eng., Stanford University.

Avey, L., 1990, "Pre-split Economics and Practice at Gold Hield Operating Co.- Chimney Creek Mine," *Proceedings of the Sixteenth Conference on Explosives and Blasting Technique*, International Society of Explosives Engineers, Orlando, Florida, pp. 167-176.

Barker, D.B., Fourney, W.L. and Dally, J.W., 1984, "Influence of Stress Waves on Explosive Induced Fragmentation-Borehole Crack Network," *Proceedings 19th U.S. Symposium on rock mechanics*, Stateline, Nevada, pp. 144-152.

Barnhard, P., 1981, "Direct Measurement of "Borehole" Pressure of Explosives," *Proceedings of the Seventh Conference on Explosives and Blasting Technique*, International Society of Explosives Engineers, Orlando, Florida, pp. 319-326.

Barton, N., 1974, "Classification of Rock Mass to Distinguish Self-Supporting Tunnels From Those Required Support," *Proceeding Symposium Designing Methods in rock Mechanic*, ISRM.

Bauer, A., Glynn, G., Heater, R. and Katsabanis, P., 1984, "A Laboratory Comparative Study of Slurries, Emulsion, and Heavy AN/FO Explosives," *Proceedings of the Tenth Conference on Explosives and Blasting Technique*, International Society of Explosives Engineers, Orlando, Florida, pp. 229-321.

Bauer, A., 1967, "The Status of Rock Mechanics in Blasting," *Proceedings Ninth Symposium on Rock Mechanics*, Colorado School of Mines, Golden, Colorado, pp. 246-261.

Baumgartner, P., 1982, "Rock Breaking and Mechanical Excavation," *14th Canadian Rock Mechanics Symposium*, Vancouver, British Columbia.

Belland, J.M., 1965, "Structure as a Control in Rock Fragmentation," *The Canadian Mining and Metallurgical Bulletin*, pp. 323-328.

Berry, P. and Dantini, F.M., 1981, "Influence of the Geomechanical Characteristics of the Rocks and of the Type of Explosive on the Absorption of the Energy Induced in the Rock by the Explosives," *Proceeding of the Seventh Conference on Explosives and Blasting Technique*, International Society of Explosives Engineers, Phoenix, Arizona, pp. 193-211.

Berta, G., 1990, "Explosives: An Engineering Tool," Italesplosivi, Milano.

Bhandari, S., 1983, "Influence of Joint Directions in Blasting," *Proceeding of the Ninth Conference on Explosives and Blasting Technique*, Dallas, Texas, International Society of Explosives Engineers, Phoenix, pp. 359-369.

Bhandari, S., 1979, "On the Role of Stress Waves and Quasi-static Gas Pressure in Rock Fragmentation by Blasting," *Acta Astronautica*, Vol.6, pp. 365-383.

Bieniawski, Z.T., 1979, "The Geomechanics Classification in Rock Engineering Applications," *Proceeding of the Fourth Conference in Rock Mechanics*, Montreux.

Bieniawski, Z.T., 1978, "Geomechanics Classification of Rock Mass and its Application in Tunnelling," *Proceeding of the Third Conference in Rock Mechanics*, pp. 27-32.

Bieniawski, Z.T., 1976, "The Rock Mass Classification in Rock Engineering," *Proceeding of Symposium on Exploration for Rock Engineering*, Johannesburg, pp. 97-104.

Bjarnholt, G., Holmberg and Finn Ouchterlony, 1983, " A Linear Shape Charge System for Contour Blasting," *Proceeding of the Ninth Conference on Explosives and Blasting Technique*, International Society of Explosives Engineers, Phoenix, Dallas, Texas, pp. 350-358.

Bowie, O.L., 1956, "Analysis of Infinite Plate Containing Radial Cracks Originating at the Boundary of Circular Hole," *Journal of Mathematic and Physics*, Vol. 35.

Brady, B.H.G. and Brown, E.T., 1985, "Rock Mechanics for Underground Mining," George Allen and Vnwin Ltd, London, UK.

Britton, R. and Skidmore, D. 1989, "Time to Breakage Versus Time for Shock Wave Reflectance in Decoupled Explosive Rock Fracturing," *International Journal of Surface Mining and Reclamation*, pp. 111-114.

Burkle, W.C., 1979, "Geology and Its Effect on Blasting," *Proceedings of the Fifth Conference on Explosives and Blasting Technique*, International Society of Explosives Engineers, St. Louis, Missouri. pp. 105-120.

Calder, P.N., Tuomi, J.N., 1980, "Control Blasting at Sherman Mine," *Proceedings of the Sixth Conference on Explosives and Blasting Technique*, International Society of Explosives Engineers, Tampa, Florida. pp. 312-330.

Calder, P.N., 1977, "Perimeter Blasting," Pit Slope Manual, Chapter 7, Canada Centre for Mineral and Energy Technology (CANMET), Ottawa, Ontario, Canada.

Calder, P.N., Morash, B.J. 1971, "Pit Wall Control at Adams Mine," *Mining Congress Journal*, August 1971, pp. 34-42.

Carbonell, R. and Detournay, E., 1995, "Modelling Fracture Initiation and propagation from a Pressurized Hole: A Dislocation-Based Approach," Rock

Mechanics, Daemen and Schultz, Balkema, Rotterdam, pp. 465-470.

Chiappetta, R.F., 1991, "Pre-splitting and Controlled Blasting Techniques, Including Air Decks and Dimension Stone Criteria" *Third High Tech Seminar, Blasting Technology, Instrumentation and Explosives Applications*, San Diego, California.

Clark, B.C., 1987, "Principles of Rock Fragmentation," John Wiley and Sons, Inc., U.S.A.

Chitombo, G. and Scott, A., 1990, "An Approach to the Evaluation and Control of Blast Induced Damage," *The Third International Symposium on Rock Fragmentation by Blasting*, Brisbane, Australia, pp. 239-244.

Coates, D.F., 1965, "Rock Mechanics Principles," Queen's Printer, Ottawa, Canada.

Cole, R.H., 1965, "Underwater Explosions," New York, Dover Publications, Inc., U.S.A.

Cook, M.A., 1974, "The Since of Industrial Explosives," Graphic Service & Supply, Inc., U.S.A.

Cook, M.A., 1971, "The Since of High Explosives," Robert E. Krieger Punlishing Co. Inc., Huntington, N.Y.

Coursen, D.L., 1978, "Cavities and Gas Penetration from Blasts in Stressed Rock with Flooded Joints," *Acta Astronautica*, Vol. 6, pp. 341-363.

Crawford, F.H., 1963, "Heat Thermodynamics and Statistical Physics," Harcourt, Brace & World, Inc, U.S.A.

Day, P.R., 1982, "Controlled Blasting to Minimize Overbreak with Big Boreholes Underground," *Proceedings of the Eighth Conference on Explosives and Blasting Technique*, International Society of Explosives Engineers, New Orleans, Louisiana, pp. 264-274.

Deere, D.U., 1964, "Technical Description of Rock Cores for Engineer-proposes," *Rock Mechanics and Engineering Geology*," Vol. 1, pp. 17-22.

Doolan, B.L.and Stanly, R.S., 1972, "Guidebook for Field Trips in Vermont," *New England Intercollegiate Geological Conference 64th Annual Meeting*, Burlington, Vermont.

Dowding, C.H., 1985, "Blast Vibration Monitoring and Control," Prentic-Hall International, Inc., London.

Du Pont De Memours and Co., Inc., 1969, "Blasters' Handbook," Du Pont, Wilmington, Delaware, Fifteenth Edition.

Eric, J.H. and Dennis, G.D., 1958, "Geology of the Concord-Waterford Area, Vermont," Vermont Development Commission, Vermont.

Farmer, J.W., 1968, "Engineering Properties of Rock," E. and F.N. Spon, Ltd., London.

Fordham, S., 1966, "High Explosives and Propellants," First Edition, Wheaton and Co. Ltd., Great Britain.

Fourney, W.L. Barker, D.B. and Holloway, D.C., 1984, "Fracture Control Blasting," *Proceedings of the Tenth Conference on Explosives and Blasting Technique*, International Society of Explosives Engineers, Lake Buena Vista, Florida, pp. 182-196.

Frantti, G.E., 1977, Near-Field Elastic Ground Response Spectra for Multi-Hole Surface Explosions," *Proceedings of the Third Conference on Explosives and Blasting Techniques*, International Society of Explosives Engineers, Pittsburgh, PA, pp. 149-167.

Free, G.D., 1973, "Evaluation of the relative Performance of Explosives in Rocks," *National Symposium on Rock Fragmentation*," Adelaide, Autralian, pp. 35-40.

Gamble, D.L. and Jow, Y., 1985, "Effect of Basting Vibration on Uncured Concrete Foundations," *Proceedings of the Eleventh Conference on Explosives and Blasting Technique*, International Society of Explosives Engineers, San Diego, California, pp. 124-136.

Ghosh, A., and Daemen, J.J.K., 1995, "Rock Fragmentation in Bench Blasting - A numerical Study," Rock Mechanics, Daemen and Schultz, Balkema, Rotterdam, pp. 553-558.

Ghosh, A., 1990, "Fractal and Numerical Models of Explosive Rock Fragmentation," Ph.D. thesis, Dept. Min. Eng., University of Arizona.

Goodman, R.E., 1989, "Introduction to Rock Mechanics," John Wiley and Sons, New York, U.S.A.

Gregory, C. E., 1984, "Explosives for North American Engineers," 3rd Edition, Gulf Publishing Company, Hoston, Texas.

Gustafsson, R., 1973, "Swedish Blasting Technique," Published by PSI, Gothenburg, Sweden.

Hagan, T.N., 1979, " Rock Breakage by Explosives," *Acta Astronautica*, Vol.6, pp. 329-340.

Haghighi, R.H. and Konya, C.J., 1985, "The Effect of Bench Movement with Changing Blasthole Length," *Proceedings of the First Mini-Symposium on Explosives and Blasting Research*, Atlanta, Georgia, pp. 95-105.

Harries, G., 1973, "A Mathematical Model of Cratering and Blasting," *National Symposium on Rock Fragmentation*," Adelaide, Autralian, pp. 41-54.

Hoek, E. and Bray, J., 1981, "Rock Slope Engineering," Third Edition, The Institution of Mining and Metallurgy, London.

Hoek, E. and Brown, E.T., 1980, "Underground Excavations in Rock," The Institution of Mining and Metallurgy, London, England.

Holmberg, R. and Hustrulid, W., 1981, "Swedish Cautious Blast Excavation at the CSM/ONWI test Site in Colorado," *Proceedings of the Seventh Conference on Explosives and Blasting Technique*, International Society of Explosives Engineers, Phoenix, Arizona, pp. 232-252.

Holmberg, R. and Person, P.A., 1978, "The Swedish Approach to Contour Blasting," *Proceedings of the Fourth Annual Conference on Explosives and Blasting Technique*, International Society of Explosives Engineers, New Orleans, Louisiana, pp.113-127.

Huebner, K.H., 1975, "The Finite Element Method for Engineering," John Wiley and Sons, Inc., U.S.A.

Hunter, C., Fedak, K, and Todoeschuck, J.P., 1993, "Development of Low Density Explosives With Wall Control Applications," *Proceedings of the Nineteenth Annual Conference on Explosives and Blasting Technique*, International Society of Explosives Engineers, San Dieago, California, pp. 549-556.

I.C.I. Blaster's Handbook, 1959, Canadian Industries Limited, Montreal, Canada.

I-DEAS, 1990, " Finite Element Modelling," Structural Dynamics Research Corporation, Milford, Ohaio, U.S.A.

Jaeger, J.C., and Cook, W., 1979, "Fundamentals of Rock Mechanics," Third Edition, Fletcher and Son Ltd, Norwich.

Johansson, C.H. and Persson, P.A., 1970, "Detonics of High Explosives," Academic Press Inc., London.

Jumikis, A.R., 1983, "Rock Mechanics," Second Edition, Trans Tech, Clausthal, Germany.

Kennedy, B.A., 1990, "Surface Mining," Society for Mining, Metallurgy, and Exploration, Inc. Littleton, Colorado.

Khoshrou, S.H., 1993, "A survey of Current Wall-Control Blasting Methods," Department of Mining and Metallurgical Engineering, McGill University, Canada.

Kim, K., and Stout, M.G., 1978, "Determination of Effective Elastic Modulus by Compliance Calibration for Measurement of Fracture Toughness of Rock," *19th Symposium on Rock Mechanics*, Stateline, Nevada, pp. 203-209.

Kleine, T.H., Cocker, A. and Kavetsky, A., 1990, "The development and Implementation of a Three Dimensional Model of Blast Fragmentation and Damage," *The Third International Symposium on Rock Fragmentation by Blasting*, Brisbane, Australia, pp. 181-187.

Kutter, H.K., 1970, "Stress Analysis of a Pressurized Circular Hole with Radial Cracks in Infinite Elastic Plate," *International Journal of Fracture Mechanics*, pp. 233-247.

Kutter, H., 1967, "The Interaction Between Stress Waves and Gas Pressure in the Fracture Process of an Underground Explosion in Rock, With Practical Application to Pre-splitting," Ph.D. Thesis, Dept. Min. Eng., University of Minnesota.

Kutter, H. and Fairhurst, C., 1968, "The Roles of Stress Wave and Gas Pressure in Pre-splitting," *Proceedings Ninth Symposium on Rock Mechanics*, Golden, Colorado, pp. 265-284.

Lande, G. 1983, "Influence of Structure Geology on Controlled Blasting in Secondary Rocks Case History," *First International Symposium on Rock Fragmentation by Blasting*, Lulea, sweden. pp. 555-562.

Lang., L.C., 1979, "Buffer Blasting Techniques in Open Pit Mines," *Proceedings of the Fifth Conference on Explosives and Blasting Technique*, International Society of Explosives Engineers, St. Louis, Missouri, pp. 66-80.

Langefors, U. and Kihlstrom, B., 1978, "The Modern Technique of Rock Blasting," Third Edition, Almquist and Wisksell, Stockholm, Sweden.

Lawry, M.H., 1991, "I-DEAS™ S udent Guide," Structural Dynamics Research Corporation, Milford, Ohaio, U.S.A.

Leinberger, P., Chung, S.H., and Lee, N., 1992, "Blasting Techniques for Pit Wall Control at Inco Limited's Thompson Open Pit," ICI Explosives Canada.

Lizotte, Y.C., 1995, "Study on the Effect of Geology on the Fragmentation of Rock Excavation by Drilling and Blasting," CANMET_MRL, 95-073.

Lizotte, Y.C., 1994 "Controlled Blasting Experiments in Small Drift at the CANMET Experimental Mine," CANMET_MRL, 94-014.

Lizotte, Y.C. and Scoble, M., 1993, "Studies on the Effect of Rock Structure on Fragmentation," *95 Annual General Meeting of CIM*, Calgary.

Marcotte, R., 1980, "Gites et Indices de Chromite au Québec," Ministere de l'Energi et des Ressources, Quebec, Canada.

Marquis, R., 1985, "Géology de la région de Richmond, Cantons de Melbourne et de Durham," Gouverement du Québec, Service de la Géologie, Québec, Cadada.

Mathais, A., 1965, "Pre-Split Blasting," M.Sc. Thesis, Colorado School of Mines, U.S.A.

McHugh, S.L., Curren, D.R. and Seaman, L., 1985, "The NAG-Frag Computational Fracture Model and Its Use for Simulating Fracture and Fragmentation," Society of Experimental Mechanics, Connecticut, pp. 173-185.

McKown, A.F., 1984, "Some Aspects of Design and Evaluation of Perimeter Control Blasting in Fractured and Weathered Rock," *Proceedings of the Tenth Conference on Explosives and Blasting Technique*, International Society of Explosives Engineers, Lake Buena Vista, Florida, pp. 120-151.

Mellor, M., 1976, "Controlled Perimeter Blasting in Cold Regions," *Proceedings of the Second Annual Conference on Explosives and Blasting Technique*, International Society of Explosives Engineers, Louisville, Kentucky. pp. 279-300.

Mitri, H.S., 1993, "Numerical Modelling of Rock Excavation with Cable Bolts," Seminar Notes, McGill University, Montreal, Canada.

Mohanty, B., Yang, R., Leblanc, M., and Kelly, C., 1995, "Dilution Control and vibration Studies at an Underground Mine," *Proceedings of the Twenty-First Annual Conference on Explosives and Blasting Technique*, International Society of Explosives Engineers, Volume II, Nashville, Tennessee, pp. 20-35.

Mohanty, B., 1990, "Explosion Generated Fractures in Rock and Rock-Like Materials," *Engineering Fracture Mechanics*, Vol. 35, No. 4/5, pp. 889-898.

Mohanty, B., 1988, "Parameters Affecting Explosive Energy Release - A Case for Realistic Rating of Commercial Explosives," *Proceedings of the Fourteenth Annual Conference on Explosives and Blasting Technique*, International Society of Explosives Engineers, Anaheim, California, pp. 304-317.

Mohanty, B., 1982, "Characteristic Crack Patterns Close to an Exploding Charge," *14th Canadian Rock Mechanics Symposium*, Vancouver, British Columbia, pp. 32-36.

Mohanty, B., 1981, "Energy, Strength and Performance, and Their Implications in Rating Commercial Explosives," *Proceedings of the Seventh Conference on Explosives and Blasting Technique*, International Society of Explosives Engineers, Phoenix, Arizona, pp. 293-306.

Mojtabai, N. and Beattie, S.G., 1996, "Empirical Approach to Prediction of Damage in Bench Blasting," *Transactions of the Institution of Mining and Metallurgy*, (Section A: Mining Industry), p.p. A75-A80.

Nand, k., 1988, "Damage Criteria for Neraby Stactures During Underground Explosion and Earthquakes," *Fourth Mini-Symposium on Explosives and Blasting Research*, Anaheim, California, pp. 50-95.

Obert, L. and Duvall, W. I., 1966, "Rock Mechanics and the Design of

Structures in Rock," John Wiley and Sons, Inc.

Ouchterlony, F., 1988, "Suggested Methods for Determining the Fracture Toughness of Rock," *International Journal of Rock Mechanic, Science and geomechanics*, Vol. 25, pp. 71-96.

Ouchterlony, F., 1974, "Fracture Mechanics Applied to Rock Blasting", Advances in Rock Mechanics, Volume II, Part B, Washington, Dc.

Owens, W., 1995, "Pre-Splitting Techniques and Applications for the Mining and Construction Industry," *Proceedings of the Twenty-First Annual Conference on Explosives and Blasting Technique*, International Society of Explosives Engineers, Volume II, Nashville, Tennessee, pp. 276-286.

Paine, S., Holmes, D. and Clark, E., 1961, "Controlling Overbreak by Pre-Splitting," *Proceedings of a Symposium Held at the University of Missouri*, Volume 1, February 1961.

Pande, G.N., Beer, G. And Williams, J.R., 1990, " Numerical Methods in Rock Mechanics," Pande, Beer and Williams, .

Paulsen, W.C., 1971, "Finite Element Stress Analysis," Parts 1, 2 and 3, Project Manger Ivan Sorvall Inc. Norwalk, Conn.

Rao, S.S., 1989, "The Finite Element Method in Engineering," Second Edition, Pergamon Press, Oxford, New York.

Ratte, C.A. and Ogden, D.G., 1989, "Marble Granite and Slate Industries of Vermont, Field Trip Guidebook T362," *28th International Geological Congress*, Vermont.

Rinehart, J.S., 1965, "Dynamic Fracture Strengths of Rocks," *VII Symposium on Rock Mechanics*, Volume 1, The Pennsylvania University, University Park, Pennsylvania, pp. 205-208.

Rollins, R.R., 1978, " Nonsymmetrical Decoupling," *19th Symposium on Rock*

Mechanics, Stateline, Nevada, pp.193-198.

Sabina, A.P., 1983, "Rocks and Minerals for the Collector, Kingston, Ontario to Lac St-Jean, Quebec," Miscellaneous Report 32, Canada.

Sanchidrian, J.A. and Pesquero, 1992, "Damage In Rock Under Explosive Loading: Implementation in DYNA2D of a TCK Model," *International Journal of Surface Mining and Reclamation*, pp. 109-114.

Sanden, B., 1974, "Pre-Split Blasting," M.Sc. Thesis, Dept. Min. Eng., Queen's University.

Scoble, M., 1994, "Perimeter Blasting," Class notes, McGill University, Montreal, Canada.

Shaffer, R.J., Heuze, F.E. and Nilson, R.H., 1987, "Finite Element Models of Hydrofracturing and Gas Fracturing in Jointed Media," *Proceedings of the 28th U. S. Symposium on Rock Mechanics*, University of Arizona, pp. 797-408.

Simha, K.R.Y., Holloway, D.C. and Fourney, W.L., 1983, "Dynamic Photoelastic Studies on Delayed Pre-Split Blasting," *First International Symposium on Rock Fragmentation by Blasting*, Luloa, Sweden, pp. 97-133.

Singh, S.P. and Lamond, R.D., 1995, "Effects of Decoupling and Simultaneous Detonation on Blast Vibrations," *Proceedings of the Eleventh Symposium on Explosives and Blasting Research*, International Society of Explosives Engineers, Nashville, Tennessee, pp. 175-189.

Singh, S.P. 1993, "Damage Causing Potential of Different Explosives," *Proceedings of the Nine Annual Symposium on Explosives and Blasting Research*, International Society of Explosives Engineers, San Diego, California, pp. 325-337.

Singh, S.P., 1990, "Controlled Blasting in Quarries," *International Journal of Surface Mining and Reclamation*, pp. 119-123.

Singh, S.P. and Sastry, V.R., 1986, "Rock Fragmentation by Blasting-Influence of Joint Filling Material," *Journal of explosives Engineering*, 3(5), pp. 18-27.

Sinkala, T., 1985, "Layers in Rock Cause Unidirectional- and Not Random Drill Hole Deviations," *Proceeding of International Symposium on Large Scale Underground Mining*, Lulea, Sweden.

Smith, N.S., 1976, "Burden-Rock Stiffness and Its Effect on Fragmentation in Bench Blasting," Ph.D. Dissertation, University of Missouri-Rolla.

Smith, A.O., 1965, "Application of Controlled Blasting," *Canadian Mining Journal*, pp. 50-53.

Smith, C.W., Bass , R.C. and Tayler, L.D., 1978, "Puff'N Tuff, A Residual Stress-Gas Fracturing Experiment," *Proceedings of the 19th U.S. Symposium on Rock Mechanics*, Stateline, Nevada, pp. 137-141.

Song, J. and Kim, K. 1995, "Micro-Mechanical Modelling to Study Smooth Blasting," *SME Annual Meeting*, Denver, Colorado.

Song, J. and Kim, K. 1995, "Blasting Induced Fracturing and Stress Field Evolution at Fracture Tips," Rock Mechanics, Daemen and Schultz, Balkema, Rotterdam, pp. 547-552.

Stachura, V.J. and Cumerlato, C.L., 1995, "Highgwall Damage Control Using Pre-Splitting with Low-Density Explosives," *Proceedings of twenty-First Annual Conference on Explosives and Blasting Technique*, International Society of Explosives Engineers, Nashville, Tennessee, pp. 187-197.

Stewart, D.P., 1974, "Geology for Environmental Planning in the Milton-St. Albans Region, Vermont," Water Resources Department Montpelier, Vermont.

Stewart, D.P., 1973, "Geology for Environmental Planning in the Burlington-middlebury Region, Vermont," Water Resources Department Montpelier, Vermont.

Stewart, D.P., 1971, "Geology for Environmental Planning in the Barre-Montpelier Region, Vermont," Water Resources Department Montpelier, Vermont.

Sunu, M.Z., Reed, S.M. and Singh, R.N., 1988, "Evaluating of Rock Parameters on Surface Mine Blasting by Finite Element Analysis," *International Journal of Surface Mining and Reclamation*, pp. 209-215.

Susanszky, Z, 1978, " Direction of Shock Waves by Reflexion," *Proceedings of Fourth Conference on Explosives and Blasting Technique*, International Society of Explosives Engineers, New Orleans, Louisiana, pp. 273-279.

Sutherland, R.B., 1963, "Some Dynamic and Static Properties Of Rock," *Proceedings of the Fifth Symposium on Rock Mechanics*, University of Minnesota, pp. 473-491.

Szechy, K., 1966, "The Art of Tunnelling," Akademial Kiado, Budapest.

Tariq, S.M. and Worsey, P., 1995, " An Investigation into the Effect of Joint Frequency and Spatial Positioning on Pre-Splitting," *Proceedings of twenty-First Annual Conference on Explosives and Blasting Technique*, International Society of Explosives Engineers, vol. 2, Nashville, Tennessee, pp. 287-296.

Terzaghi, K., 1946, "Rock Defects and Loads on Tunnel Supports," Rock Tunnelling with Steel Support. Commercial Shearing and Stamping Co., Youngstown.

Trent, B.C., Young, C., Barbour, T.G. and Smith, J.W., 1981, " A Coupled Gas Pressurization Explicit Fracture Model for Oil Shale Fragmentation," *Proceeding of the 22nd U.S. Symposium on Rock Mechanics*, pp. 211-217.

Trudinger, J.P., 1972, "An Approach to the Practice of Pre-Splitting in Anisotropic Rock masses," *Bulletin of the Association of Engineering Geologists*, pp. 161-171.

Van Diver, B.B., 1987, "Roadside Geology of Vermont and New Hampshire," Mountain Press Publishing Company, Missoula.

Vutukuri, V.S. and Bhandari, S., 1973, "Some Aspects of Design of Open Pit Blast," *National Symposium on Rock Fragmentation*, Australian, pp. 55-61.

Wickham, G.E., Tiedemann, H.R., Skinner, E.H., 1972, "Support Determination Based on Geological Predictions," *Proceeding First North American Rapid Excavation and Tunnelling Conference*, AIME, New York.

Worsey, P.N., 1984, "The Effect of Discontinuity Orientation on the Success of Pre-Split Blasting," *Proceedings of the Tenth Conference on Explosives and Blasting Technique*, International Society of Explosives Engineers, Lake Buena Vista, Florida, pp. 197-217.

Yang, R., Bawden, W.F., Talebi, S. and Rocque, P., 1993, "An Integrated Technique for Vibration Monitoring Adjacent to a Blast Hole," *CIM Bulletin*, Volume 86, No. 972, July-August, pp. 45-52.

Young, C., Barbour, T.G. and Trent, B.C., 1985, "Geology Control of Oil Shale Fragmentation," Society of Experimental Mechanics, Massachusetts, pp. 93-99.

Zen, White, Hadley and Thomposon, 1968, "Studies of Appalachian Geology, Northern and Maritime," John Wiley and Sons, Inc., U.S.A.